

Low Cost, High Integrity Plasmatron Joining for Automotive Body in White Manufacture

by

Johannes Dedenbach

Dipl. Ing. (FH)

Thesis submitted to the University of Nottingham for the degree of Doctor of Philosophy

Department of Mechanical, Materials and Manufacturing Engineering

The University of Nottingham

July 2016

Abstract

Plasmatron brazing is a unique tungsten inert gas (TIG) joining process, which allows joining of thin steel panels and is an economical alternative to laser brazing. This technology is used by some car manufacturers to generate water-tight joints on outer skin panels on low volume production lines.

This study seeks to verify if Plasmatron brazing could be a new technique for high volume steel vehicle outer body skin joining, or if it would be better to concentrate on another technology.

The current state of joining technologies in body production is presented. A rating of the most suitable joining techniques showed that laser and Plasmatron brazing are both ranked highly. Laser brazing is superior in terms of brazing speed but worse in regard to the capital investment cost. Plasmatron brazing is good in investment cost but drops in brazing speed and process feasibility due to the robustness of the electrode service life. As a by-product, the current limitations of the adhesive technology were delivered in detail. There is a need to make improvements to this technology.

In a second part, a series of brazing experiments was undertaken to identify parameter influences and to improve the process window for Plasmatron joints. Findings indicate that a lateral filler wire – electrode tip misalignment of 0.3 mm resulted in marked base metal melting and unequal braze lines. Furthermore, strong evidence was found that brazing speed up to 2.5 m/min is possible only, with an energy input in the range between 74 - 84 Joule per mm. Current maximum braze speed is limited to 1 m/min. Moreover, it can be stated that the optimum joint quality can only be achieved through fine control of the input parameters and camera based control of the electrode tip settings.

The last part investigated impact on post braze processes. For example, the behaviour of the electrode tip contamination and if it is possible to clean these electrodes. Furthermore, the influence of carbon deposits next to the braze seam to the following paint process was studied.

Results show that the start stop phase during the brazing process is not associated with contaminations of the tungsten electrode tip. Also, it is possible to clean the electrode tip mechanically. Additional, carbon deposits next to braze seams must not be brushed away for the four tested zinc coat types before professional paint shop painting.

Researchers can easily understand the overall developments and why focused arc brazing is a coming method for joining of automotive outer skin panels.

Acknowledgements

Firstly, I wish to thank my academic supervisors Dr. Adam Clare and Dr. Simon Lawes for their guidance in my research. Throughout the past years, both have offered exceptional support beyond my expectation. Special thanks go to Dr. Peter Standring, my first academic supervisor, for the opportunity to carry out this research and for his valuable guidance.

The author gratefully acknowledges the support from my Ford of Europe colleagues. Special thanks go to my managers Lee Turner and Colin Levis for their willingness to support this study.
I also wish to thank my friends of the University of Nottingham. Special recognition goes to Peter Holland and Matthias Hirsch for exchanging ideas and their valuable support on the Plasmatron test cell.

I would like to extend my sincerest thanks to my family for their emotional support. Especially Nicole for her patience and continual support over the past several years that enabled me to complete this thesis.

I dedicate this thesis to my lovely children Lucy and Tim. I thank you for your love. I appreciate all your patience during the last years and the minutes where you missed me.

Contents

ABSTRACT I

ACKNOWLEDGEMENTS III

CONTENTS IV

LIST OF FIGURES VIII

LIST OF TABLES XII

LIST OF ACRONYMS XIII

1. INTRODUCTION 1

1.1 Industrial Context 1

1.2 Aim and Objectives of this Research 3

1.3 Overview of the Thesis 4

2. LITERATURE REVIEW 6

2.1 Body-in-White (BIW) 6

2.2 Classification for Body Outer Skin Panels 8

2.3 Current State of the Art BIW Joining Methods 9

2.3.1 Adhesive Bonding 10

2.3.2 Mechanical Joining 13

2.3.3 Welding 19

2.3.4 Brazing 30

2.4 TIG-Brazing Fundamentals 44

2.4.1 Electric Arc Processes 44

2.4.2 Influence of Current Types 46

2.5 Tungsten Electrode Fundamentals 47

2.5.1 Electrode Material Classification 48

2.5.2 Electrode Preparation 51

2.6 Shielding Gas Influence 54

2.7 Zinc Coated Steel Panel Fundamentals 55

2.7.1 Issues due to Zinc Coated Steel Panels 57

2.8 Seam Tracker Systems for Brazing Operations 58

2.9 Chapter Summary 61

3. METHODOLOGY, EXPERIMENTAL SETUP AND PROCEDURES 63

3.1 Research Approach 63

3.2 Test Facilities and Consumables 66
3.2.1 Brazing Test Cell at the University of Nottingham 66
3.2.2 Brazing Test Cell at the Company Inocon 70
3.2.3 Welding Test Cell at the Company Castro 71
3.2.4 Process Consumables 72
3.3 Description of Braze Imperfections, Measurements and Tests 76
3.3.1 Braze Imperfections 76
3.3.2 Requirements for Brazed Outer Skin Panels joints 78
3.3.3 External Visual Imperfections 79
3.3.4 Internal Imperfections 89
3.3.5 Braze Visual Properties Report 95
3.3.6 Non-Destructive Brazed Seam Test 96
3.3.7 Destructive Brazed Joint Test 97
3.3.8 Microscopic Examination 100
3.3.9 Black Soot Measurement 101
3.3.10 Electrode Monitoring Vision System 102

4. ECONOMIC AND LOGISTICAL MODELLING OF BIW JOINING METHODS – A ROLE FOR FOCUSED ARC PLASMA BRAZING 104

4.1 Research Process 104
4.2 Rating of BIW Joining Methods 106
4.3 Limitations of the Current Adhesive Technology 109
4.3.1 Experimental Methodology 110
4.3.2 Results 113
4.4 Laser Brazing vs. Plasmatron Brazing 113
4.4.1 Tensile Force Comparison Laser vs. Plasmatron 114
4.4.2 Cost Comparison Laser vs. Plasmatron Brazing 119
4.5 Chapter Discussion 125
4.5.1 Limitations of the Current Adhesive Technology 125
4.5.2 Laser Brazing vs. Plasmatron Brazing 126

5. PROCESS WINDOW FOR PLASMATRON BRAZING 129

5.1 Research Process 129
5.2 Torch Tilting 'Pushing - Pulling' 130
5.2.1 Experimental Methodology 131
5.2.2 Results 132
5.3 Influence of Surface Cleanliness 133

5.3.1 Experimental Methodology 133
5.3.2 Results 134
5.4 Electrode Offset 135
5.4.1 Experimental Methodology 136
5.4.2 Results 137
5.5 Influence of Electrode to Wire Gap 139
5.5.1 Experimental Methodology 139
5.5.2 Results 140
5.6 Influence of Brazing Current 144
5.6.1 Experimental Methodology 144
5.6.2 Results 145
5.7 Braze Speed 148
5.7.1 Experimental Methodology 148
5.7.2 Results 150
5.8 Chapter Discussion 153
5.8.1 Torch Tilting 'Pushing - Pulling' 154
5.8.2 Electrode Offset 154
5.8.3 Influence of Surface Cleanliness 155
5.8.4 Influence of Electrode to Wire Gap 155
5.8.5 Influence of Brazing Current 157
5.8.6 Braze Speed 157

6. PLASMATRON INTEGRATION AND IMPACT ON POST BRAZE PROCESSES 159

6.1 Electrode Service Life 160
6.1.1 Shielding Gas Chamber 161
6.1.2 Experimental Methodology 163
6.1.3 Influence of Ignition 164
6.1.4 Experimental Methodology 164
6.1.5 Electrode Cleaning 166
6.1.6 Experimental Methodology 167
6.1.7 Experimental Methodology 171
6.2 Influence of Black Soot on Paint Quality and Aesthetics 173
6.2.1 Black Soot Adhesion 174
6.2.2 Experimental Methodology Methodology 174
6.2.3 Coat Adhesion 177
6.2.4 Experimental Methodology 178

6.3 CHAPTER DISCUSSION 181
6.3.1 Shielding Gas Chamber 182
6.3.2 Influence of Ignition 182
6.3.3 Electrode Cleaning with Acid 183
6.3.4 Mechanical Electrode Cleaning Device 184
6.3.5 Black Soot Adhesion 185
6.3.6 Coat Adhesion 185
7. THESIS CONCLUSIONS AND FUTURE WORK 186
7.1 RESEARCH KEY FINDING 186
7.2 RESEARCH CONTRIBUTIONS 186
7.3 LIMITATIONS AND FUTURE WORK 192
7.4 CONCLUDING REMARKS 194
REFERENCES 196
APPENDIX A – PUBLICATIONS 213
APPENDIX B – RATING OF BIW JOINING METHODS 214
APPENDIX C – BRAZE PROPERTIES REPORT 217
APPENDIX D – ADHESIVE EXPERIMENT 220
APPENDIX E – LASER- VS. PLASMATRON BRAZING TENSILE 221
APPENDIX F - COST COMPARISON LASER VS. PLASMATRON 222
APPENDIX G - CAUSE AND EFFECT DIAGRAM 224
APPENDIX H – EXPERIMENT DECISION MATRIX 225
APPENDIX I - TORCH TILTING EXPERIMENT 227
APPENDIX J - SURFACE CLEANLINESS EXPERIMENT 227
APPENDIX K - ELECTRODE OFFSET EXPERIMENT 228

List of Figures

Figure 2-1: Uni-body design - Ford Mustang BIW [6] 6
Figure 2-2: Ford Motor Company surface classification [14] 8
Figure 2-3: List of main BIW joining methods, ... 10
Figure 2-4: Self-piercing riveting process [31] 14
Figure 2-5: RIVTAC® High-speed tack joining [38]..... 16
Figure 2-6: Tox® clinching principle [40] 16
Figure 2-7: Tog-L-Loc® process description [45] 18
Figure 2-8: Door flange hemming principle [46] 18
Figure 2-9: Resistance spot welding principle with AC power source [50] 19
Figure 2-10: Resistance roller seam welding principle [57] 21
Figure 2-11: Embossed RPW projection configuration [62]..... 22
Figure 2-12: Principle of Drawn Arc Welding; 24
Figure 2-13: Principle of ultrasonic spot welding [71]. 25
Figure 2-14: Typical sonotrode tip surface pattern 26
Figure 2-15: Principles of FSSW with fixed pin [79]..... 27
Figure 2-16: Manual brazed seam; 31
Figure 2-17: Roof design differences [90]; 32
Figure 2-18: Schematic of laser brazing principle [94]..... 34
Figure 2-19: Typical roof to body laser brazing clamping station, ... 35
Figure 2-20: The principle of the CMT process, ... 36
Figure 2-21: (a) Conventional MIG torch, (b)new CMT braze+ MIG torch 38
Figure 2-22: Schematic illustration of TIG arc process [112]. 39
Figure 2-23: ForceTig™ torch from the company EWM. 40
Figure 2-24: ForceTig™ tungsten electrode insert [115]. 41
Figure 2-25: Functional diagram of the TopTig™ process [118]. 42
Figure 2-26: Nozzle designs for Plasmatron and other plasma systems; 43
Figure 2-27: Illustration of a Plasmatron torch [121] 44
Figure 2-28: Regions of a TIG arc 45
Figure 2-29: Characteristics of different current types for TIG joining. 47
Figure 2-30: Influence of the grinding direction 52
Figure 2-31: Course of the arc if the tip is not ground centrically [143]. 52
Figure 2-32: Penetration profiles as a function of the tip angle [144]..... 53
Figure 2-33: Tungsten tip differences 54
Figure 2-34: Optical seam tracker system, ... 58
Figure 2-35: Overview of different seam tracker systems; 60

Figure 3-1: Flow chart about the main stages of the thesis 65
Figure 3-2: Plasmatron wire guiding arm [166] 67
Figure 3-3: Schematic of the Plasmatron cell 68
Figure 3-4: Plasmatron cell at the University of Nottingham 68
Figure 3-5: Test panel clamping at the Nottingham Plasmatron cell. 69
Figure 3-6: Metal clip pre clamping 69
Figure 3-7: Overview of the Plasmatron Test cell at Inocon. 70
Figure 3-8: Castro TIG welding gas chamber 71
Figure 3-9: Electrode profile for a Plasmatron torch [172] 74
Figure 3-10: Brazed seam width measurement example 80
Figure 3-11: Wavy brazed seam 80
Figure 3-12: Discontinuous seam 81
Figure 3-13: Seam with pores; 82
Figure 3-14: Two different seam pore types; 83
Figure 3-15: Braze seam with small brazing spatter [14] 84
Figure 3-16: Black soot lines next to a brazed seam 85
Figure 3-17: Example on seam surface roughness 86
Figure 3-18: Brazed seam start imperfection; 87
Figure 3-19: Defect on end section of a brazed seam; 88
Figure 3-20: Principle of panel distortion detection with a whetstone [189] ... 88
Figure 3-21: Braze joint cross section cut from an internal pore. 89
Figure 3-22: Braze joint cross section cut which shows inclusions [190]. 90
Figure 3-23: Braze joint cross section cut, ... 91
Figure 3-24: (a) shows melting of base material; 91
Figure 3-25: Joint hardness is up to three times higher in intermetallic joint . 92
Figure 3-26: Important dimensions on braze joint cross section cuts. 93
Figure 3-27: Insufficient filler adhesion; 94
Figure 3-28: Non parallel braze 94
Figure 3-29: Braze joint cross section cut, ... 95
Figure 3-30: An excerpt from the developed braze visual property report. 96
Figure 3-31: Prepared tensile test sample piece for tensile test 98
Figure 3-32: BIW roof section sawing for destructive test sections 99
Figure 3-33: Braze run with black soot lines; 102
Figure 3-34: Setup of the low cost USB microscope camera 102
Figure 3-35: User interface for the electrode tip measurement system [196] 103
Figure 4-1: Three-stage research program 105

Figure 4-2: Example of a joining method,.....107
Figure 4-3: A painted body on bodyskids,.....111
Figure 4-4: Sketch of a flange butt roof joint 111
Figure 4-5: Vehicle roof joining by adhesive bonding; 112
Figure 4-6: Cracked adhesive on a roof joint [9] 113
Figure 4-7: Tensile force results comparison 117
Figure 4-8: Cumulative histograms about the tensile force.....118
Figure 4-9: Total brazing costs per liftgate – German plant. 122
Figure 4-10: Cost per liftgate comparison laser vs. Plasmatron.....124
Figure 5-1: Plasmatron head tilting capabilities; 131
Figure 5-2: Influence of surface cleanliness. 134
Figure 5-3: Cross-section of the cleaned test panel side. 135
Figure 5-4: Cross-section of the uncleaned test panel side. 135
Figure 5-5: Schematic of the electrode tip offset. 136
Figure 5-6: Camera set-up from the wire offset experiment 137
Figure 5-7: Definition for the dimensions on the braze cross section; 137
Figure 5-8: Distance between electrode tip and filler wire surface. 139
Figure 5-9: Joint top view of different electrode to wire gap setups. 141
Figure 5-10: Cross-sections of the electrode to wire experiment. 141
Figure 5-11: Estimation of the best electrode to wire distance. 142
Figure 5-12: Correlation between the electrode to filler 143
Figure 5-13: Brazed seams of different current inputs. 145
Figure 5-14: Cross-sections of test run (1a-5a) and run (1b-5b).....145
Figure 5-15: Determination of the perfect braze current setting.....147
Figure 5-16: Effect of different braze speeds on the seam quality. 150
Figure 5-17: Cross-sections of braze speed test run (a) and (b) 151
Figure 5-18: Seam quality in relation to heat input and braze speed 153
Figure 5-19: Schematic of ‘electrode tip to wire gap’ influence 156
Figure 6-1: Illustrates the research process and lists the experiments 159
Figure 6-2: Electrode tip defects; 160
Figure 6-3: Shielding gas cover from Linde [215] 162
Figure 6-4: Advantage of the oxygen reduced glove box; 162
Figure 6-5: TIG welded lap joint on zinc coated steel panels 164
Figure 6-6: Electrode ignition experiment. 165
Figure 6-7: Photos from the electrode tip; 166
Figure 6-8: Experiment set-up for electrode cleaning with acids 169

Figure 6-9: Current electrode cleaning solutions; 171
Figure 6-10: Result of the first mechanical cleaning trial; 172
Figure 6-11: Damages on the nozzle outlet 173
Figure 6-12: Brazed specimens with special tapes 175
Figure 6-13: Top view of a brazed test panel 176
Figure 6-14: Black soot analysis on different zinc types;..... 176
Figure 6-15: Typical automotive paint shop process [224] 179
Figure 6-16: Fixing of specimen on a BIW; 180
Figure 6-17: Painted brazes after the scratch test. 181
Figure 6-18: Schematic of a nozzle shield..... 182

List of Tables

Table 2-1: Work functions of different oxides and tungsten [134]. 49
Table 2-2: Recommendations for the type of electrode 50
Table 3-1: Chemical composition of used steel grade DC06 [168] 72
Table 3-2: Used zinc coating types on DC06 steels 73
Table 3-3: Chemical composition of WLa20 tungsten electrodes [171] 74
Table 3-4: Chemical composition of $CuSi_3$ filler metal wire 75
Table 4-1: Material specification from the weakest base material 114
Table 4-2: Main parameter values used for the laser vs. Plasmatron trial. 116
Table 4-3: Tensile test results 118
Table 4-4: CAPEX comparison 120
Table 5-1: Results from the torch tilting 'pushing – pulling' experiment. 132
Table 5-2: Results of different electrode tip offsets to the braze wire axis. ... 137
Table 5-3: Parameter set up for the 'gap electrode to wire' experiment. 140
Table 5-4: Effects of the increased electrode to wire gap 142
Table 5-5: Input parameters for the influence of 'current' experiment. 144
Table 5-6: Cross section measurements and tensile forces 146
Table 5-7: Parameter set-up for the 'braze speed' experiment 149
Table 5-8: Cross section measurements and tensile forces F_{max} 152
Table 5-9: Arc energy and heat input formula contributions and results 152
Table 6-1: Input parameters for the argon chamber experiment 163
Table 6-2: Acid concentrations for the electrode tip cleaning experiment 168
Table 6-3: The electrode cleaning with acid experiment results. 170
Table 6-4: Mechanical electrode cleaning design concept 172
Table 6-5: Material details from the Plasmatron brazed specimens. 175
Table 6-6: Black soot measurements after tape removal 177
Table 6-7: Test panel details for this coat adhesion experiment 178
Table 6-8: Schematic of an improved mechanical cleaning device 184

List of Acronyms

AC	Alternating Current
ASTM	American Society for Testing and Materials
AWS	American Welding Society
ASF	Audi Space Frame
BIW	Body in White
CAPEX	Capital Expenses
Cm	Capability Machine
Cmk	Capability Machine Index
CMT	Cold Metal Transfer
Cp	Capability Process
Cpk	Capability Process Index
DIN	Deutsches Institut für Normung (German Institute for Standardisation)
DOE	Design of Experiment
DV	Disposal Value
EDM	Electrical Discharge Machining
FEA	Finite Element Analysis
FTT	First Time Through
FSW	Friction Stir Welding
FSSW	Friction Stir Spot Welding
GA	Galvannealed
GI	Galvanized
GMAW	Gas Metal Arc Welding
HAZ	Heat Affected Zone
HD	Hot-Dip
HDG	Hot Dip Galvanize
IO	Initial Outlay
ISF	Institut für Schweißen und Fügen RWTH Aachen (Institute for Welding and Joining, University of Aachen)
ISO	International Standards Organization
LHD	Left Hand Drive
LHS	Left Hand Side
LTL	Lower Tolerance Limit

MAG	Metal Active Gas
MFDC	Medium Frequency Direct Current
MIG	Metal Inert Gas
NVH	Noise Vibration Harshness
OM	Optical Microscope
PD	Product Development
PLC	Programmable Logic Controller
Ppk	Process Performance Index
R&D	Research & Development
RHD	Right Hand Drive
RHS	Right Hand Side
RPW	Resistance Projection Welding
RSW	Resistance Spot Welding
RTM	Resin Transfer Moulding
JPY	Jobs Per Year
USW	Ultrasonic Spot Welding
UTS	Ultimate Tensile Strength
VR	Volume Rate
SFW	Spot Friction Welding
SPR	Self-Piercing Riveting
TC	Total Cost
TCM	Total Cost Model
TFC	Total Fixed Cost
TIG	Tungsten Inert Gas
TVC	Total Variable Cost
VC	Variable Cost
VR	Volume Rate
1K	1 Component Adhesive
2K	2 Component Adhesive

1. Introduction

This chapter introduces the thesis and provides a rationale for this research project. Additionally, it briefly describes the methodology of this research and outlines the contents of each chapter.

1.1 Industrial Context

Outer skin panel joining by brazing presents some of the most important technical challenges for automobile manufacturing. Structural integrity, crash worthiness, aesthetics and cost must all be balanced to deliver a product that meets the expected quality metrics.

As automotive design has developed in complexity, so too must the manufacturing techniques capable of meeting these expectations. Hence, there is a clear drive to improve the associated manufacturing technologies and underlying strategies. Since there are a number of companies competing in this market, manufacturing capability continues to be driven forward rapidly.

This is exemplified in one key technical area, by outer skin panel brazing operations in the European automotive industry (Audi A5 Coupe roof joint [1], VW Golf roof joint [2], Volvo V70 ring frame [3], Mercedes Sprinter bodyside [4], Ford Mondeo roof). The structural properties and aesthetics of these are widely reported.

Increased requirements on body shell aesthetics, the permanent pressure to reduce weight plus recent advances in laser technology have led to the emergence of laser brazing, which is often cited as a potential replacement for more established techniques like resistant spot welding or gas metal arc welding.

Despite this, laser brazing is currently not suitable for low volume production of lower cost vehicles with less than ~30,000 vehicles per year as it requires high capital and maintenance investment. Ford recognized this issue a few years ago as they planned to build the Mondeo, which has a laser-brazed roof, in some low volume plants around the globe. The responsible manufacturing planning team searched for a laser brazing alternative, which required less capital investment, to continue to maintain profit in low volume plants.

At a welding technology fare, the Ford planning team discovered a new focused TIG brazing technology that proposed an alternative to the expensive laser brazing technology. Inocon Technology Ltd., based in Austria, commercialised this technology.

At that time, only one automotive manufacturer was using this technology for joining of thin steel panels, but was not willing to share their insights with Ford, which is understandable due to enormous cost competition.

The Plasmatron process, as named by the inventor, was a new technology where no publications had been detected, except for the positive reports from the supplier. Nevertheless, extensive laboratory tests from Ford indicated that this technology is capable as an alternative for laser brazing.

Currently, this technology is in use at three low volume Ford plants to braze join vehicle roofs to the body.

Despite this, until now Ford was not able to use this technology in high volume automotive production plants. The Plasmatron system suffers from serious drawbacks, having been recognised in production plants during the last few years of operation. One of the main obstacles is the short lifetime of the tungsten electrodes during brazing of zinc coated steel panels. There is a distinct lack of published work in literature regarding tungsten electrode contamination during brazing of zinc coated steel panels and how to maintain electrodes. Another key issue which was found is that brazing speeds higher than 1 m/min are not possible without significant negative effects on seam quality. For these reasons, it would be beneficial to conduct research to find the conditions to optimise the Plasmatron brazing process.

To ensure that the focus on Plasmatron brazing is the correct approach, it should be investigated if brazing is really the best joining solution for the next 12 years or if there are other alternative joining methods that might be more promising (the twelve year timespan reflects two vehicle lifecycles).

For example, it is important to understand if roof joining in the bodyshop by adhesive bonding could be a technically functioning low cost alternative to brazing. The car line managers often raise the question why it is not possible to bond a steel roof into a body, similar to a windscreen or glass

roof assembly, instead of considering expensive laser cells. There is no literature available that is able to answer this question. Arising out of this, it would be very beneficial to investigate if adhesive roof joining would be feasible for a high volume manufacturer.
Therefore, this research seeks to develop a low cost, high integrity method for automotive body in white joining.

1.2 Aim and Objectives of this Research

The aim of this research is as follows:

To assess the viability of Plasmatron brazing as a cost effective method for high integrity joining in automotive body in white manufacture.

The outcome should enhance our knowledge of low cost joining technologies, especially about low cost outer skin panel Plasmatron brazing in the automotive industry.

Specific objectives are as follows:

- Summarise and benchmark all automotive BIW joining methods currently available.
- Investigate where Plasmatron brazing stands in comparison to the other joining methods.
- Detect Plasmatron brazing bottlenecks and practical difficulties
- Characterize the influence of the main parameters of the Plasmatron brazing process.
- Improve the current process tolerances.
- Lay down possibilities to tackle the current difficulties.
- Present recommendations for future work.

1.3 Overview of the Thesis

This final section of the introduction describes how the thesis is structured chapter by chapter. It shows the major components of the research and shows how the various threads are woven together.

Chapter 2 - Deals with the theory and literature relevant to this research and has the task to familiarise the reader with the area of interest and to explain the basic theory of the different topics used in the thesis. The literature as sourced from academic journals, specialist books and industrial sources. Also the merits of Plasmatron brazing for low volume production are presented.

Chapter 3 – Describes the general apparatus that was used in experimental work, as well as other consumables. Furthermore, the utilized measurement equipment, procedures and methods to capture the results are introduced.

Chapter 4 – Presents an economical and logistical model of body in white joining methods to gain an overview about where focused arc brazing stands in comparison to other body in white joining methods. The limitations of the adhesive technology by joining of outer skin panels were examined in detail. Furthermore, a tensile force comparison and a systematic total cost model were developed to compare laser brazing versus Plasmatron brazing.

Chapter 5 – Characterizes the influence of the main Plasmatron brazing parameters. Six experiments were performed to identify the sensitivity range and effect of parameter setting differences.

Chapter 6 – Deals with the process integration and impact on post braze processes. The results from the tungsten lifetime and black soot related experiments were presented.

Chapter 7 - Presents conclusions of this research and recommendations for the future work that can be undertaken. Furthermore, the key findings are placed in the industrial context based upon the author's experience as an automotive production engineer.

2. Literature Review

This chapter presents an overview of the relevant literature considered as part of this research. It allows the reader to understand the stage of low cost arc brazing in comparison to other automotive joining practices. A summary about the main findings is outlined at the end of this chapter. These findings were used to consider and establish a research plan.

2.1 Body-in-White (BIW)

The term 'Body-in-White' (BIW) is used in the automotive industry to describe the structural body of a vehicle onto which various components (engine, chassis, suspension, interior trim etc.) are subsequently mounted. The BIW is made up of the closures (doors, hood, tail-gate) and the frame. The frame can be of a uni-body design, a body-on-frame or a space frame. The uni-body design features stamped panels [5]. The space-frame is made up of light metal extrusions and cast parts normally that will be planked with metal or plastic panels. The end product of a body shop is referred to as BIW, which means an unpainted body. Figure 2-1 shows a BIW (uni-body design) out of stamped steel panels.



Figure 2-1: Uni-body design - Ford Mustang BIW [6]

Currently, the high volume vehicle manufacturers are mainly using steel for the construction of their BIWs. Only the premium vehicles and the Ford F150 can justify the use of more expensive materials like aluminium, magnesium alloys and carbon fibre.

The automotive journal, Supplier Business [7] highlights that Magnesium costs about 75 per cent more than steel and 33 per cent more than aluminium, which has been a major reason behind its limited use in the non-premium automotive industry.

To produce carbon fibre body panels, very long curing cycles with high energy consumption and large capital investments for pre-forming dies and autoclaves are required, where the cost increases dramatically by the growth in part size. The limitation of autoclaves is one of the great challenges to large-scale automotive polymer composites. Researchers and industries still research low cost out-of-autoclave composite fabrication methods. Studies on different curing alternatives are continuing, including X-ray, ultraviolet, electron beam and microwave [8]. The use of microwaves has often led to significant benefits compared to conventional heating in laboratory experiments [9], but is still not good enough for industrial usage. The US Company Plasan, which produces the body panels for the Chrysler Viper, has started to use an induction process where infrared head is used instead of an autoclave. This cuts the part cycle time to 17 minutes. BMW uses for their electric vehicle i3 body carbon parts that were manufactured with the RTM (Resin Transfer Molding) process. Woven carbon fiber mats where hereby placed in a die, filled with resin and hardened by applying heat and the pressure of a press. This method reduced the curing time to 4 to 8 minutes [10]. This is still not fast enough as current high volume plants produce a vehicle every 60 seconds. However, mass-carbon parts could become one of the greatest growth segments in the automotive industry in the second half of this decade [11] if the cycle time and the cost could be reduced further. Currently, it is not possible for mass vehicle producers to manufacture carbon fibre car bodies in the required volume output and cost range. Therefore, this thesis is concentration on uni-body design BIW, made out of steel. The construction of a steel BIW for a medium-sized vehicle typically involves the need to join approximately 300 stamped sheet metal components together to form a ‘body shell’. These are made of new lightweight steels. This body shell, when assembled, represents the heaviest single component of a vehicle and has the largest influence on many of its key characteristics, including vehicle handling and crash

performance [12]. The vehicle's BIW makes up approximately 35 per cent of the total vehicle mass. This makes the BIW a prime candidate for weight saving, thereby maximising performance and increasing the efficiency of the vehicle [13].

The primary factor influencing automotive BIW development practices has traditionally been the desire to achieve stiff yet light-weight structures. However, in recent times BIW structures have also been required to meet additional demands for lighter and more stylish designs with improved crash performance [12]. Aesthetics are now key.

2.2 Classification for Body Outer Skin Panels

The automotive industry defines class-A outer skin panels as all visible outer surfaces. The following illustration (see Figure 2-2) shows the surface classification of Ford Motor Company.

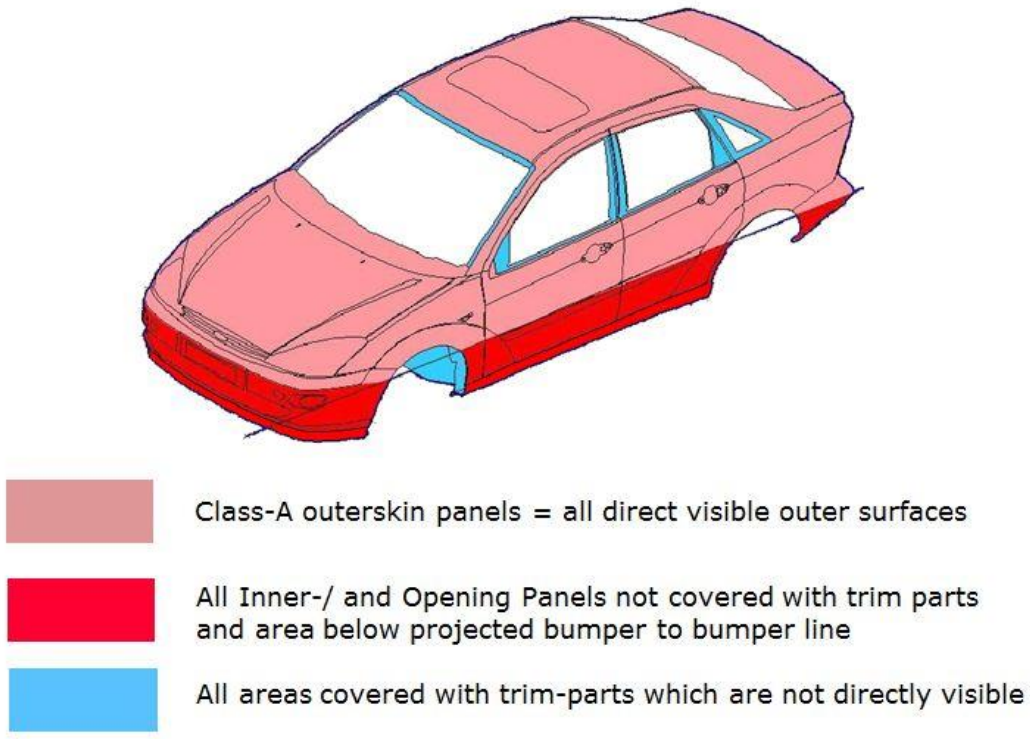


Figure 2-2: Ford Motor Company surface classification [14]

Class-A panels have to fulfil the highest quality standard, which means absolutely no scratches, dings, dents, pores or waviness, according to current customer expectations, as these failures will be visible on the

painted body too. The average surface roughness parameter Ra on class-A panels is at Ford specified with Ra 1.0 – 1.7 µm (2.5 mm cut-off).
Ford assesses the surface quality on finished BIWs and on the finished painted vehicles under intensive illumination in so called light tunnels. This is a common industry practice shared by most automotive manufacturers. Surface imperfections are classified by into three concern types:

A-Defects = unacceptable for most of the customers
B-Concerns = annoying and disturbing issue to customers
C-Concerns = will be noticed by trained customers only

Class-A surfaces should be free from A or B type defects.

2.3 Current State of the Art BIW Joining Methods

Joining is an important part in the process chain of vehicle manufacturing. This chapter provides the theoretical framework to understand the current bodyshop joining methods for BIWs in the automotive high volume industry.
Today, joining technology in general covers about eighty different modern techniques that are in use worldwide [15]. There are several ways of grouping these joining technologies. The German norm DIN 8593 [16] classification splits the joining techniques very detailed and is therefore not practical enough for bodyshop related joining study. Grote and Antonsson [15] recognized that the BIW joining methods can be broken down into three main categories, which assist to analyse the BIW joining complexity closer.
The first category is joining with thermally dependent changes of component properties and the second category is joining without thermal influence of the component properties. The third category is hybrid joining which means a usage of a minimum of 2 joining techniques for one joining purpose. The following chart Figure 2-3 shows these three categories, including some of their related joining methods.

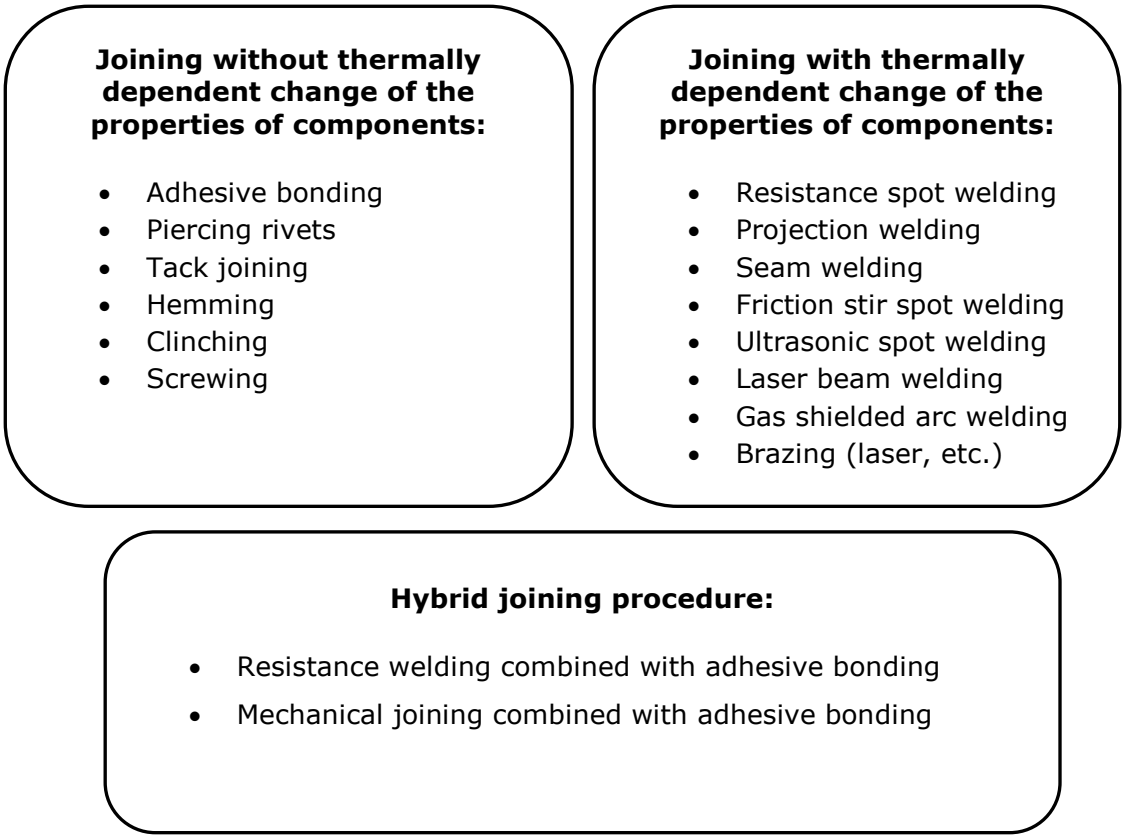


Figure 2-3: List of main BIW joining methods, adapted from Grote and Antonsson [15].

The succeeding sub-chapters describe the most important BIW joining technologies for volume vehicle manufacturer.

2.3.1 Adhesive Bonding

Adhesive bonding is a proven joining technology, widely used in the body shops to improve stiffness and reduce Noise Vibration Harshness (NVH) through damping. It is an effective method of joining structures made up of different materials having complex design [17] as well. Nowadays, the automotive industry is offered a complete portfolio featuring different adhesives by the adhesive suppliers. For metal to metal structural bonding, body shops use mainly epoxy-based adhesives [18] because they provide high strength (10-30 MPa) and low elongation.

The adhesive can be applied robotically in bead, swirl or jet spray using standard industrial equipment. The adhesive can also be applied manually from dispensing systems or cartridges.

Body shops normally only use 1K epoxy based adhesives. 1K stands for "one-component" adhesives, which require a heat source to complete the curing process. The required heat for the curing is supplied by paint shop ovens that are used to dry the electro-coated BIWs. It is very important that the structural adhesive can cure in the given temperature and time window to reach the required quality. 1K adhesives are preferred in the body shop because this adhesive type reaches stronger tensile, shear and peel strengths than a 2K adhesive (two component epoxy adhesive - hardener and binder). Additionally, the 1K adhesive is less sensitive to dirt and oil contamination on the metal panels to be joined. The 2K adhesive requires a longer curing time to reach the maximum strength and is more expensive in Europe than 1K adhesives. It is also all automotive manufacturers' target to minimize the number of adhesive types used within the body shops worldwide to simplify and to standardize processing requirements.

The presence of epoxy adhesive in a modern car body structure is considering common and increasing. For example the Focus 2014 MY BIW using 3 meter adhesive and the S-Max 2015 MY (model year) BIW use 25 meter adhesive. The Mercedes E-Class MY 2009 use 110 meter adhesive seam where the predecessor model used 70 meter adhesive. Some of the aluminium BIWs even have over 150 meters of adhesive in their bodies. For example, the Jaguar XJ MY 2010, increased the adhesive bond length by 50 % from his predecessor to a total of 154 m [19].

Due to the larger bonding areas associated with adhesive methods, the local stresses can be reduced and therefore the fatigue strength is increased. These improvements in stiffness and fatigue strength are important factors to consider in the design stage [20].

An additional advantage of adhesives is that they often perform a sealing function simultaneously. One good example is the inner and outer door panel joining where the adhesive improves the stiffness, taking over the sealing function to prevent corrosion in the clinched flanges as well. These kind materials are termed adhesive-sealants. As the primary purpose of a

sealant is to prevent air, water and other substances from entering or exiting a structure or assembly while permitting a certain amount of movement of mating partners [21]. Sealants typically have lower strength and higher elongation than adhesives [22].

Other fastening methods, including self-piercing rivets, clinches, or rolled hem joints, are used in conjunction with adhesives for the joining in critical areas. Purely adhesively bonded joints show limited strength in peel and cleavage in the case of overload (e.g. crash). The combination of the assembly methods ensures high fatigue strength and offers economic benefits because there is no need for fixtures during the polymerisation of the adhesive [23].

Only low volume vehicle manufacturers are able to glue a roof into a body before painting because their low vehicle output allows for a long fixing time during the adhesive hardening process. The Aston Martin Vantage is one of these low volume produced vehicles. During production, the aluminium roof is glued with a 2K adhesive to the aluminium bodyside.

It is important to know that the lubricants for the stamping process and the zinc layer coating quality and type from the steel panels greatly affect the adhesive bonding characteristics. Furthermore, it is also important to know that the long-term stability of adhesive joints, especially the fracture behaviour of adhesive joints after hot-wet exposure, can be significantly affected [24]. Therefore, it is necessary to expose adhesively bonded joints to various tests to simulate actual service conditions. The American Society for Testing and Materials (ASTM) is the organization that has assumed the responsibility for the deployment of these adhesive testing specifications to validate mechanical and environmental performances. The testing specifications of other organizations often parallel those specified by ASTM [25].

2.3.1.1 Hybrid Structural Joining

In addition to the adhesive, another fastening method may be used simultaneously. For example, spot welding or mechanical joining methods like self-piercing rivets, clinches or hemmed joints are all commonly used together with adhesives. Manufacturers use the term “Hybrid Joining” to

describe this technique. They compensate disadvantages of one joining method with the advantages of another joining technique. Multiple design requirements, such as stiffness, static and dynamic strength and energy absorption, can often be met through a proper combination of adhesive bonding and traditional joining techniques, such as spot welding, riveting or clinching [26]. Hybrid joining techniques that involve adhesives can also compensate for difficulties posed by the materials being joined. The difficulties associated with joining aluminium can often be circumvented by using adhesives. For example, the second generation of Audi TT (build between 2006 – 2014) using 97 meter adhesive bonding, supplementary to 172 clinched and 1,606 self-piercing rivets in order to improve joint strength. The 2013 automotive manual from the European Aluminium Association highlights also the rivet-bonded aluminium Audi A6/A7 from 2011, the 2012 aluminium-steel body from the Porsche 911 and the Range Rover L405 from 2012 [19]. The new Ford F-150 body from 2015 using more than 106 meter of structural adhesive per body to supplements the 2,500 rivets and the 350 flow-drill screws [27].
However, some disadvantages have to be highlighted. The increased risk of crevice corrosion in case of joining of different materials [28] and the increased joining cost. It is important to recognize that hybrid joining techniques need to be adapted to each individual case if maximum reliability is to be achieved.

2.3.2 Mechanical Joining

The technical term "permanent mechanical joining" is used for manufacturing connections between two or more work pieces by transforming at least one of the work pieces or an additional fastener. Fasteners are additional parts needed for producing a connection with form or force closure between two or more work pieces [15]. A common "non-permanent mechanical joining" method is the usage of nuts and bolts. However, this approach is not used for joining of body panels because it requires drilling and matching holes which needs processing time to generate. Compared to spot weld joining, it would take too much

time to bolt parts together [29]. Normally, only closures and fenders are bolted to the body to allow quick replacements after damage.
Common examples of BIW mechanical joining with fasteners are punch riveting, self-piercing riveting and blind riveting. Mechanical joining without fasteners are for example crimping, hemming, lock forming and joining by expanding.
The following sub-sections describe the current most used mechanical joining methods in the automotive industry.

2.3.2.1 Self-Piercing Riveting

Self-Piercing Riveting (SPR) is a key production process used to join aluminium body structures in the automotive industry, but it can be used as well to join steel sheets and sheets of dissimilar materials, such as steel and aluminium. This cold forming technology has many advantages, such as no pre-drilled hole requirement, capability to join a wide range of similar or dissimilar materials and combinations of materials, no fume emissions etc. [30].
Additionally, this joining process provides very strong and reliable joints, without changing the properties of the material around it.
A punch and die are used to complete the joining operation in a single step. The punch drives the rivet that pierces the top sheet and is set into the work piece by partially piercing the bottom layer. A shaped die (or anvil) on the underside reacts to the setting force and causes the rivet tail to flare within the bottom sheet. This produces a mechanical interlock that includes the added rivet-joining element and creates a button in the bottom sheet [31]. The complete joining process is illustrated in Figure 2-4.

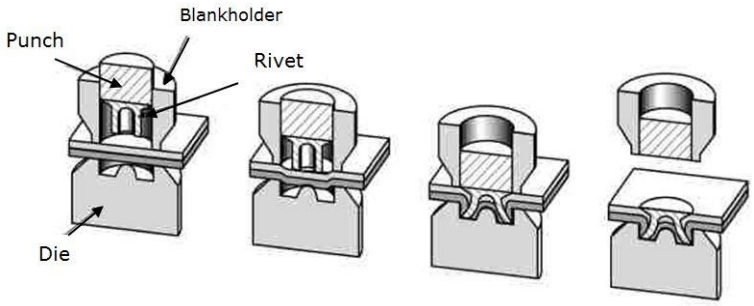


Figure 2-4: Self-piercing riveting process [31]

Since SPR does not require a pre-drilled hole unlike the conventional riveting, the joining speed is in the same level with that of spot resistance welding [32]. To avoid galvanic corrosion, coated steel rivets are used primarily on aluminium-intensive vehicles [33]. However, the combination of steel rivets and aluminium components makes vehicle recycling a challenge. Therefore, a couple of reports [30] [34] indicate that researchers working on aluminium rivets to avoid this recycling issue. As well, the car weight could be reduced further by the usage of aluminium SPRs.

A disadvantage of this joining technique is the rivet gun used, which is larger and heavier than a comparable spot welding gun. This creates a need for robots with a minimum payload of 200 kg. In addition, the process is limited by the inability to change process parameters such as rivet size or die configuration "on the fly" between successive joint positons on a vehicle structure [30]. The ability to join high strength steel panels is limited, too. For example, SPR is effective in combining aluminium with high strength steel panels having a tensile strength below 590 MPa only [32]. SPR requires double-sided accessibility and piercing to the upper sheet layer as well and can have an impact to the joint strength since it can grow into cracks [35].

2.3.2.2 High-Speed Tack Joining

In this mechanical joining process, a nail-like auxiliary joining part is accelerated to high speed by a pneumatic accelerated piston into the work pieces alt speeds between 20 and 40 m/s [36]. Due to the high speed, there is no need for predrilling or piercing. This process requires only a one side-accessibility and it is possible to join multi-layer up to 6 mm thickness [37]. The pointed tack displaces the material without forming punching's. The high speed reduces temperature diffusion in the metallic sheets. The high deformation gradient generates heat, which reduces material strength locally during penetration [35]. As a result, a high form fit can be achieved. Figure 2-5 demonstrates this high speed nailing method, the material displacement caused by the tack can be observed in the different steps.

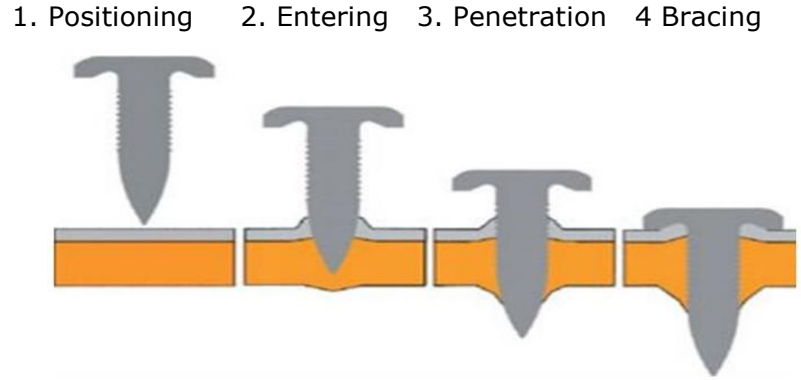


Figure 2-5: RIVTAC® High-speed tack joining [38]

Mercedes Benz is the world's first automaker that is using this new joining process [39]. The first implementation was launched on the SL (R231) rear floor in 2012. Their second BIW with this technology, where they join steel and aluminium rear floor parts together, is their new C-class estate, which was launched just recently in May 2014.
However, Mercedes-Benz highlighted as well disadvantages like local deformations of the joining spots and that a noise protection cabinet is necessary [37]. As well, it is applicable for consumer not visible areas only as the nail heads does not look good.

2.3.2.3 TOX® Clinching

The mechanical interlock with the application of the TOX® clinching technique (TOX Pressotechnik GmbH & Co. KG, Weingarten, Germany) is shown schematically in Figure 2-6. The mechanical joining of two or more metal sheets is based only on the accurate movement of the punch into the die.

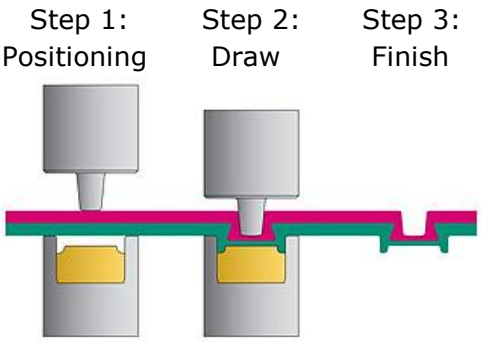


Figure 2-6: Tox® clinching principle [40]

This clinching method is a push-button style, positive, non-detachable connection of two or more layers of sheet metal by cold forming. A simple punch presses the materials to be joined into the die cavity. As the force continues to increase, the punch side material is forced to spread outwards within the die side material as shown in Figure 2-6 [40].
A disadvantage has to be highlighted that the clinched joint is 50-70 % weaker than a resistant spot welded joint. Mota and Costa [41] found this out as they compared the strengths of TOX® clinched joints and spot welded joints on similar steel sheet. However, this technology is used by some OEMs to join outer and inner closure panels. As well, there are ongoing investigations to improve the strength of this join type by increasing the undercut and the neck-thickness of the upper sheet by optimising the clinching tools and other process parameters as Chan-Joo Lee et al. highlights [42].

2.3.2.4 Tog-L-Loc® Clinching

Since the 1980s, Tog-L-Loc® has assisted in the assembly of vehicles by clinching a wide range of components, which include aluminium, pre-painted metals, dissimilar metal combinations and galvanized steel.
Tog-L-Loc® is BTM (Bending Tools & Manufacturing) Corporation's patented sheet metal clinching process. Tog-L-Loc® clinching using an expanding die where TOX® clinching using a fixed die. A special punch and die is used to form a strong interlocking joint within the metals themselves (see Figure 2-7). The figure shows that the moving blades encompass the die anvil. An elastomeric ring is located around the moving blades. This ring allows the blades to move outward while applying a straining force, which causes the blades to pinch the sheet material [43]. The result of the process is a round, button-shaped extrusion on the die side of the assembly, and a small cylindrical cavity on the punch side. The joint is comprised completely of the sheet metals that were joined. No additional fasteners or welding is required [44].

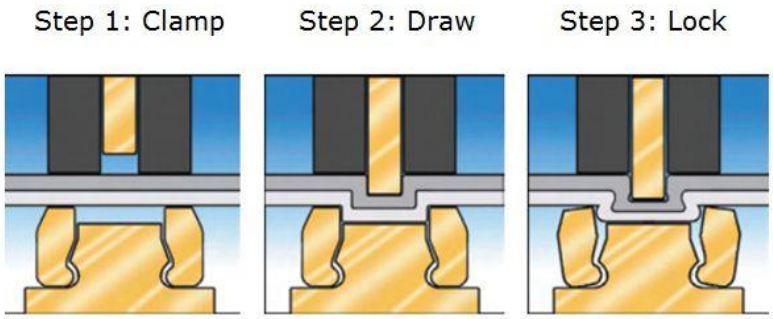


Figure 2-7: Tog-L-Loc® process description [45]

2.3.2.5 Hemming

A common example of joining in the automotive manufacturing is hemming. This is a joining method without any fastener. A linear joint is formed by plastically folding one piece of sheet metal over and around another to create a seam [46]. Figure 2-8 depicts a typical closure hemming process, which consists of three sequential steps: flanging, pre-hemming and final hemming. In order to avoid flange corrosion and to increase the closure strength, all closure flanges have adhesive applied before hemming.

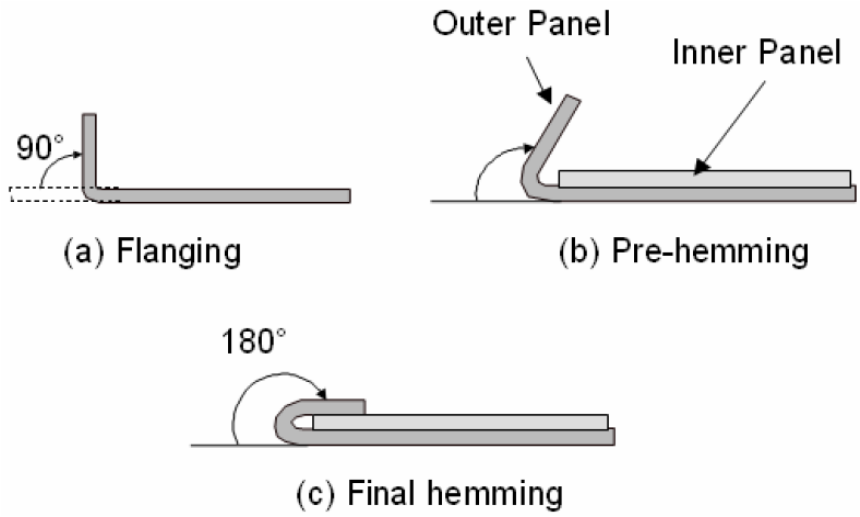


Figure 2-8: Door flange hemming principle [46]

Sheet thicknesses of work pieces joined by hemming should be lower than 2 mm because of the high forming degrees [15]. As well, hemming requires a counter support in form of a die or minimum of a robust steel beam with the wanted hemming contour.

2.3.3 Welding

The AWS (American Welding Society) defined welding as "a joining process that produces coalescence of materials by heating them to the melting temperature with or without the application of pressure or by the application of pressure alone and with or without the use of filler material [47]."

Since welding is a central technology for automotive BIW manufacturing the different most used body welding techniques are explored in the following sections.

2.3.3.1 Resistance Spot Welding

Resistance welding is the type of welding where the necessary heat is generated through the resistance of the parts to be welded to the flow of an electric current [48]. The main difference between resistance welding and other types of welding is that no filler metal or fluxes are used [48]. This process was invented in 1877 by Elihu Tomson [49].

Resistance spot welding (RSW) is by far the most common material joining process for mass vehicle manufacturer due to its high economic efficiency. Typically, a midsize steel BIW includes around 4,000 spot welds. Figure 2-9 shows the most used BIW joining case for steel bodies – the RSW overlap joining configuration.

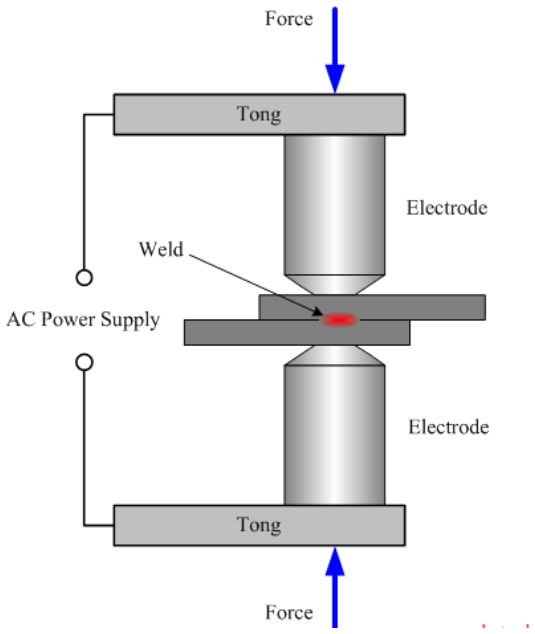


Figure 2-9: Resistance spot welding principle with AC power source [50]

The electrodes conduct the welding current and apply the welding force. The welding current is disconnected after the welding process and when the welding spot is solidified, electrodes unblock their mechanical force [49].

Weld spots should not be too close together due to the risk of shunt. A minimum distance of 15 mm has to be taken in account when spot welding 0.75 – 1.0 mm steel sheets [49].

Alternating Current (AC) power source is primarily used in North American automotive industry. These procedures use a very high electric current up to 100 kA, the voltage used is low (~ 20 V). The welding time takes just 0.1 second [49].

The new Median Frequency Direct Current (MFDC) power source is commonly used in Europe and Japan [51]. Compared to AC, MFDC has a faster response time of the feedback control at the millisecond level [51]. This permits a quicker process control [49]. As well, each spot can be programmed separately [49]. This improves the weld quality, especially for thick-to-thin stack-ups, zinc coated material, and high-strength steel RSW welding. MFDC sources have a more effective energy usage (37 % efficiency compared to AC on 26 %) [52]. A negative point that should be mentioned is the higher acquisition cost for MFDC sources. Modern weld controllers are capable of delivering control on the major process variables including welding current, force and time.

Only electrode wear is not controlled and can cause variation in the weld quality [53]. The spherical or flat shaped electrodes are made from either a precipitation strengthened copper, chromium and/or zirconium alloy or a dispersion strengthened copper alumina system [34]. These electrodes are wearing parts and have to be sharpened or replaced. The frequency depends on the joint configuration, the spot location, the joined material and the coating type of the joined material.

Another negative is that the electrodes require a minimum of 16 mm panel overlapping of the joined material for access reason. In the past, this was negligible but nowadays the car manufacturer must save every gram to make the vehicle lighter.

2.3.3.2 Resistance Roller Seam Welding

Resistance roller seam welding (RRSW) offers similar advantages as spot welding but has the additional benefit of being capable of producing continuous, leak tight welds [54]. RRSW uses rotating electrode wheels from copper that maintain contact force during a succession of welds along a seam. The rollers above and below the sheets to be welded press the sheets together and simultaneously transfer the weld current [55]. In *continuous-motion welding*, the electrodes (or work pieces) are driven at a constant speed. The welding current either is interrupted or flows continuously. In *intermittent-motion welding,* rotation of the electrode wheels is automatically stopped to make a spot weld [54]. When a welding spot has been produced again a current flow can be started. Adjustment of timing can be made to produce not a continuous seam but a series of individual welds [56]. Figure 2-10 shows the resistance roller seam welding principle.

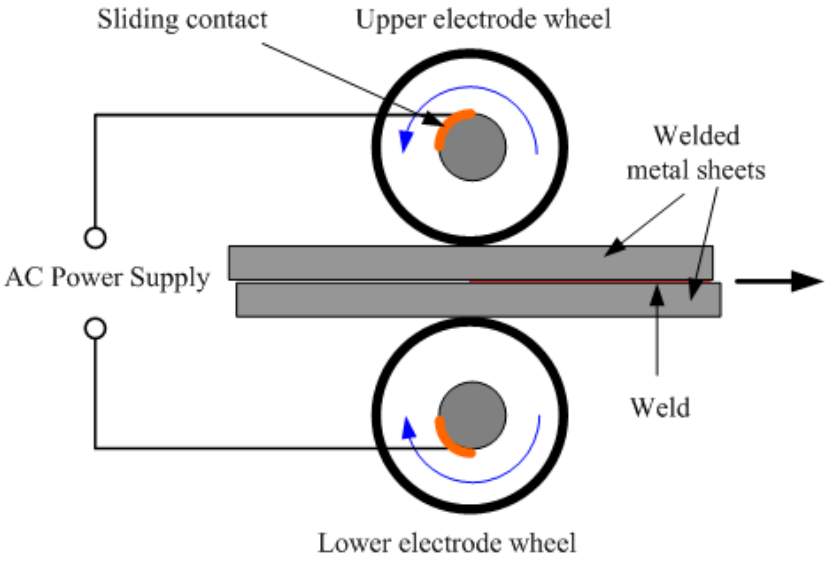


Figure 2-10: Resistance roller seam welding principle [57]

Usually, seam welds are made on overlapped panels but it is possible to generate butt joints as well. The resulting weld is extremely durable due to the length of the contact area. Applications are often gas or liquid-tight joints on sheet metal tanks and mufflers.

The typical welding speed is 1.5 m/min for thin sheets [58]. The electrode wheels are usually from copper alloy in 10 mm to 16 mm thickness and have a diameter between 150 mm to 230 mm [59]. Welding can be done only along a straight or uniformly curved line [60].

2.3.3.3 Resistance Projection Welding

Resistance Projection Welding (RPW) is a resistance welding process in which the force and current to make the weld are localized by the use of a projection raised on one or more of the sheet surfaces. This process is commonly used to attach mechanical fixings to the auto body structure, e.g. weld nuts and weld studs [61]. Projections are formed on at least one of the work pieces at the points where welds are desired. The projections – small, raised areas – can be any shape, such as round, oval circular, oblong or diamond. They can be formed by embossing, casting, stamping or machining [59]. Figure 2-11 shows an embossed projection configuration.

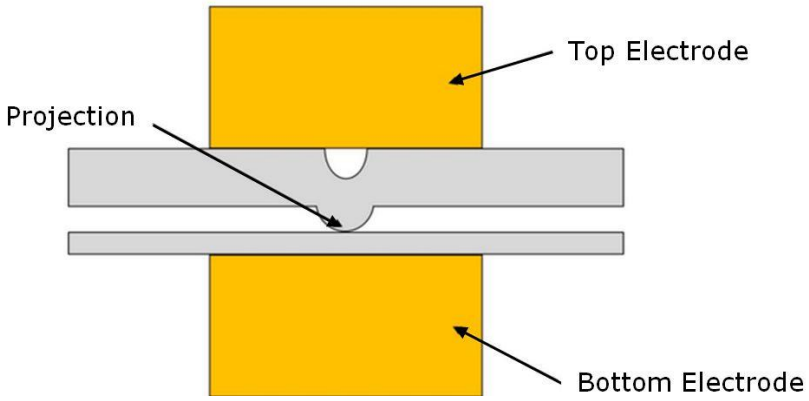


Figure 2-11: Embossed RPW projection configuration [62]

In RPW, high current (peak current is about 20 kA for steel [63]) and short weld time are used. When the current is turned on and pressure is applied, nearly all of the resistance is in the projections which heat up rapidly, flatten and result in fusion of the work pieces. With the exceptionally short weld time (~ 0.5 sec.) not only is process throughput

improved, but also welding energy is saved [51]. Additional advantage of the short weld time is the reduced chance of shrinkage and distortions around the weld zone.
As disadvantage has to be noticed that metals that are not strong enough to support projections cannot be projection-welded satisfactory [60]. Another negative is that if the shape, dimension and structural integrity of the projections are not 100 per cent according the standards, the risk is that the melting of the projection does not take place in a controlled way. This may result in inadequate weld connections, but may also cause structural damage to the work piece [64]. Therefore, the most important variables of this assembly technique are the quality of the projections and the response of the cylinder as the projection collapses during the welding time [65].

2.3.3.4 Drawn Arc Welding

Drawn arc welding is a joining process not requiring welding wire, solder or electrodes. The automotive industry uses this welding technology to join fastening components like cables, hoses or trim parts to a steel body.
The weld area needs to be accessed only from one side in contrast to resistance spot welding. The welded components do not need additional angle brackets. This allows it to reduce the part size, which means a reduction in weight and material consumption.
The drawn arc techniques requires a DC power supply to create the arc, a weld gun and a disposable ceramic ferrule, which concentrates the heat and contains the molten pool of metal [66]. The weld times range from 50 milliseconds to 1.5 seconds [66].
In the automotive industry, the fastener is usually loaded by an automatic feeder system to the weld head, which functions as a gripper, the components are positioned and welded in a single step. Figure 2-12 demonstrates the difference between a conventional weld-fastening component and a drawn arc weld-fastening component. The weld-on elements can be placed, flush, with their weld-on end onto the metal sheet (b) [67]. The conventional fastening bracket (a) weights 44 grams

and the drawn arc bracket (b) only 9 grams. Both brackets have the same performance in their area of application [68]. In this case, to hold a brake fluid hose clip in position.

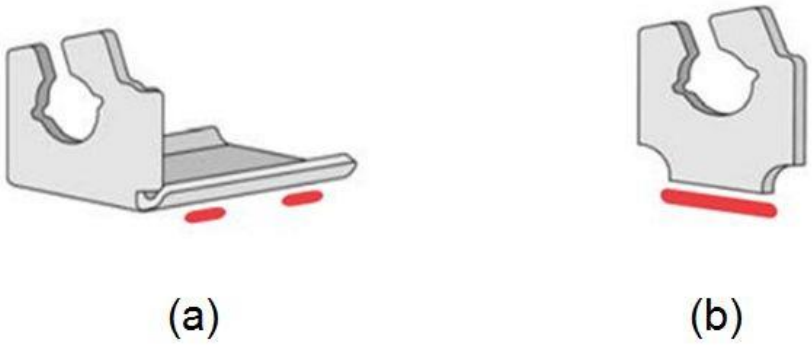


Figure 2-12: Principle of Drawn Arc Welding;
(a) conventional fastener bracket; (b) drawn arc bracket is lighter and can be placed flush, with their weld-on end onto the panel.

The conventional brackets have to be spot welded early in the production because they need access of both sides of the metal sheets to produce the weld spots. The drawn arc brackets require only single-sided access. This has the advantage that the brackets can be joint to the almost finished BIW. This is more exact and avoids bracket bending during handling of sub-assemblies.

2.3.3.5 Ultrasonic Spot Welding

Ultrasonic metal welding equipment was developed in the 1940s and 1950s and was first patented in the United States of America in 1960 (U.S. Patent 2946119) [69]. Traditional applications for ultrasonic metal welding include tube sealing, wire bonding and thin foil joining.

Ultrasonic spot welding (USW) is a promising joining technique for light weight automotive body construction applications. This technique involves an ultrasonic high-frequency vibration to generate localized heat to soften the material at the weld interface [70]. It is an attractive point joining method for light alloys as it is far more efficient than RSW, using only 0.6 - 1.5 kJ per weld instead 50 - 100 kJ (RSW) [71]. This very low energy process, forming effective welds less than a second, particularly for difficult dissimilar material combinations such as aluminium to steel joints

[72]. USW systems consist of a transducer, booster and sonotrode assembly, or stack. A controller, often with an integrated power supply, delivers the high frequency (15 - 40 kHz) to the stack. Most transducers today consist of a stack of piezo-electric crystals [73]. When a voltage is applied at ultrasonic AC frequencies, the transducer produces a corresponding high frequency mechanical vibration motion. The transducer is connected to the booster and sonotrode, which modify the vibration amplitude to meet the weld requirements [73]. Figure 2-13 shows the principle how USW works.

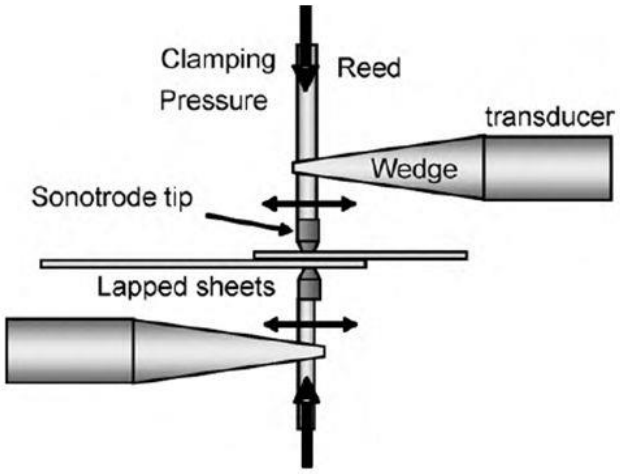


Figure 2-13: Principle of ultrasonic spot welding [71].

Material properties are especially significant with ultrasonic welding. Generally, the harder the material, the more difficult it is to weld. Softer metals, such as aluminium are easily welded. In addition to hardness, the material surface conditions, such us roughness, oxides, coatings and contaminants, also significantly influence the weld quality [73].

The tool material also needs to be considered regarding its ability to resist bonding to the work, as sticking between the tooling and the work is traditionally a significant issue [73]. Also, it has to be considered that the sonotrode tips are consumables and require replacing with time. Figure 2-14 shows typical sonotrode tip gripping surface patterns.

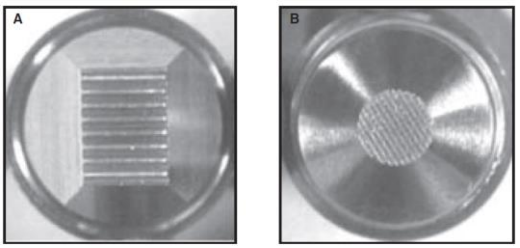


Figure 2-14: Typical sonotrode tip surface pattern
(a) Flat row gripping pattern, (b) flat axisymmetric pattern [69].

Ford Motor Co. and three joint venture partners — Branson Ultrasonics Corp., Edison Welding Institute, and Sonobond Ultrasonics Inc. - have recently concluded a four-year National Institute of Standards and Technology (NIST) Advanced Technology Program (ATP) to develop ultrasonic metal welding capability for aluminium closure and structural welding applications [69].

2.3.3.6 Friction Stir Welding

Friction stir welding (FSW) was invented (Patent EP0615480) by Wayne Thomas and his team at the Welding Institute (UK) in 1991 [74]. It is a joining technique that has expanded rapidly since its development and has found applications in a wide variety of industries [75].

This type of welding process uses a pin tool, requires no filler metal and no shielding gas. During FSW, the pin tool runs the length of the required weld area, stirring and forging the two pieces together through heat and force. The rotational speed of the pin varies from a few hundred revolutions per minute to several thousand. The welding tool then spins while force is applied. This creates the frictional heat required to melt the metal [76]. Ford uses continues FSW to lap join the aluminium central tunnel from two aluminium extrusions on the 2004 Ford GT. The latest Mercedes-Benz SL (R231) BIW using 8.1 m length FSW joining on the aluminium parts [19].

Friction stir spot welding (FSSW) is a relatively new joining application of the FSW process [77]. FSSW has many more potential applications in automotive body applications than FSW since in a typical BIW construction; there are numerous spot welds and very few long, linear

joints. FFSW is more suitable than resistance spot welding for joining of aluminium body panels [29]. Mazda Motor Corp. is the first automaker that used FSSW for production aluminium body assemblies. The technique is used for hem flanges on aluminium rear doors and hoods of the 2004 Mazda RX-8 [76].

In FSSW, the joint is created by plunging a rotating tool into a weldment until the welding tool's shoulder reaches a desired penetration depth. It will remain at this plunge depth for a specified length of time. The two tools are retracted after a spot weld is created [78]. The process is schematically illustrated in Figure 2-15.

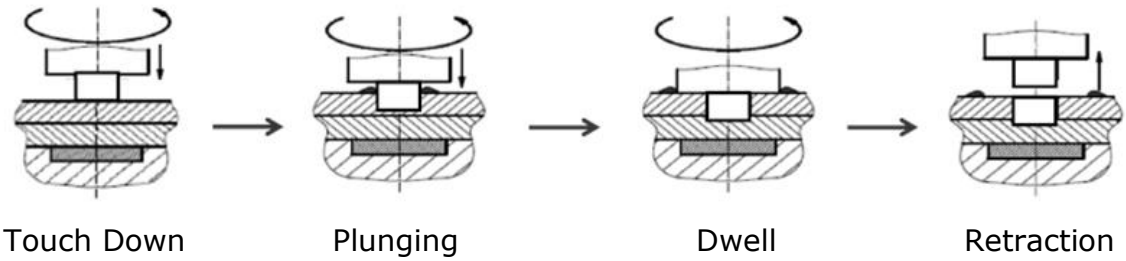


Figure 2-15: Principles of FSSW with fixed pin [79].

The process eliminates the need for the large current and coolant/compressed air that conventional resistance welding requires. The process also produces no weld spatter, which makes for a cleaner and safer assembly line [80].

So far, the majority of the research and development efforts on FSSW have been on aluminium alloys. Because Al alloys are easy to deform at relatively low temperatures (below about 550 °C) they are relatively easy to friction stir weld [79]. The FSW tools are not yet robust enough to be employed to join steel panels in industrial production environment due to the required higher mechanical loading. Also, FSSW requires two-sided access.

2.3.3.7 Laser Beam Welding

During the last two decades, laser welding has developed into a key assembly technology in the automotive industry for some OEMs, in particular in BIW fabrication. It is an accepted technology for applications such as joining of roof and joining of closure-, bodyside- and underbody flanges for some OEMs already.

The laser beam can provide a localized high power density (of the order of 1 MW/cm² or more), allowing for narrow, deep welds and high welding speeds. The metal absorbs energy from the laser beam and melts, creating a weld pool in a small area and then freezes behind the welding spot. This process takes only a couple of thousandths of a second [49]. Therefore, the localized heat input in laser welding leads to small heat-affected zones and results in high heating and cooling rates [81].

The OEMs that use laser joining in their bodyshops use currently mainly solid-state laser sources. Especially the Nd:YAG (neodymium-doped yttrium aluminium garnet) sources are widely accepted because of their power efficiency in comparison to the previous used CO2 sources. Nd:YAG laser has a near-infrared wavelength of 1.06 µm, while the CO2 laser is in the far-infrared at 10.6 µm. The shorter wavelength ND:YAG laser is absorbed well for most metals. Thus, less power is required than CO2 laser with equivalent welding speed and quality [51]. In addition, the ND:YAG near-infrared radiation allows light transmission via flexible laser light cables and therefore permits the usage of robots and low weight optical heads.

One of the main benefits of laser welding is that it only requires single-sided access to the joining location, as opposed to classic resistance spot welding, which operates with upper and lower electrodes. This creates possibilities for completely new design solutions [18] like shorter weld flanges. Laser welding also provides higher work piece accessibility than resistance and arc welding processes [82].

Laser welding of zinc coated steel sheets is known to present problems due to weld porosity caused by the expulsion of zinc present in the coating at the sheet-to sheet interface, which causes blow-outs and porosity in the weld seam since zinc boils at 906 °C and steel does not melt until about

1,500 °C. If no gap is allowed between the sheets to evacuate the zinc gas will be trapped in the weld pool, producing defects such as spattering, pinholes and porosity [83]. As well, rapid vaporization of zinc increases fluctuation of plasma cloud that expands above metal surface.
Meanwhile, it enlarges heat-affected zone and debases weld stability. Inner stress cracks and gas holes can appear and the quality of welding seam decreases. The adoption of side-blown protective gas can control the percentage of zinc in welding seams as Qiang Wu et al. showed [84]. Davies reported [48] that techniques are being developed to overcome this inherent problem, either through new beam technology or technologies to maintain a controlled gap at the interface in order to allow the zinc vapour to escape.
In comparison to resistance spot welding, laser welding does not require electrodes to be in contact with the panels. Therefore, LBW requires higher part matching quality in comparison to spot weld joints. This is because the to be joined panels must close fit-up at the joint interface. During spot welding, the gun electrodes push the panels together. When laser welding, clamps have to push the panels together. This requires more complicate and therefore more expensive panel holding fixtures. As a consequence, the investment costs for the parts clamping equipment are higher. As well, the to be joined press panels have to be more accurate at the flanges due to the higher part matching requirements which leads to higher die cost.
Additionally, the important personnel safety by laser usage requires huge eye safety housing around the clamping fixtures, which are costly and not required when spot welding or arc joining.
Furthermore, laser welding power sources are still very expensive in comparison to weld transformers.
These additional capital investments are the main obstacle for a fully replacement of resistance spot welding in the bodyshops.

2.3.3.8 Gas Metal Arc Welding

Gas Metal Arc Welding (GMAW), also known as Metal Inert Gas (MIG) welding, is a semi-automatic or automatic process that uses a continuous

wire feed as an electrode and an inert or semi-inert gas mixture to protect the weld from contamination [85].

GMAW was a standard process for attachment of steel brackets (fender holding brackets, brake fluid pipes holding bracket, etc.) to vehicle bodies. Nowadays, the automotive industry uses drawn arc welding to join fastening components due to the lower weight of the brackets, which was explained in Chapter 2.3.3.4 already. Audi uses GMAW for joining their aluminium tubular space-frame. The biggest advantages of GMAW are the low investment and the one-sided application. The disadvantage is that it is not possible to weld class-A panels since localised heat input can deform panels.

2.3.4 Brazing

According to DIN ISO 857-2:2005 [86], brazing is defined as a joining process in which a molten filler material is used that has lower liquidus temperature than the solidus temperature of the parent material(s), that wets the surfaces of the heated parent material(s) and that, during or after heating, is drawn into the narrow gap between the components being joined.

Brazing produces stronger joints than soldering, primarily because of the higher filler melting temperature and, generally, stronger fillers are employed [46]. Opposed to soft soldering, the filler material having a liquidus above 450 °C. These processes are generally carried out with metals but they can also be carried out with non-metallic materials. In this thesis, the term brazing is used only for metal brazing. The filler material always has a different chemical composition from the components being joined. This process can be carried out with or without the use of a fluxing agent.

The strength of the brazed joint relies on the diffusion of the liquid filler metal on the hot surface of the base sheet metal. Its composition and quality upon cooling is crucial for the strength of the bond. It is therefore

important to choose a filler metal that is compatible with the parent material(s) [87].

Normally, the molten filler metal gets drawn through the joint area without any voids or gaps by capillary actions. This action is a result of surface tension between base metal(s), filler metal, flux or atmosphere and the contact angle between base metal and filler metal. In practice, filler metal flow characteristics are also influenced by dynamic considerations involving viscosity, vapour pressure, gravity, and metallurgical reactions between filler metal and base metal [88].

2.3.4.1 Brazing on Automotive Panels

Brazing on automotive outer skin panels has been in place for low volume production for decades, mainly on convertibles and coupes. For example, on convertibles the front header will often be braze joined with the A-pillar and on coupes often the C-pillar (see Bentley Coupe, Figure 2-16). These kind of brazes cannot be thought of as representative class-A panel brazes because they always have to be ground post joining, which is not typical of large volume techniques. Grinding is needed to obtain a smooth surface for the following painting process.

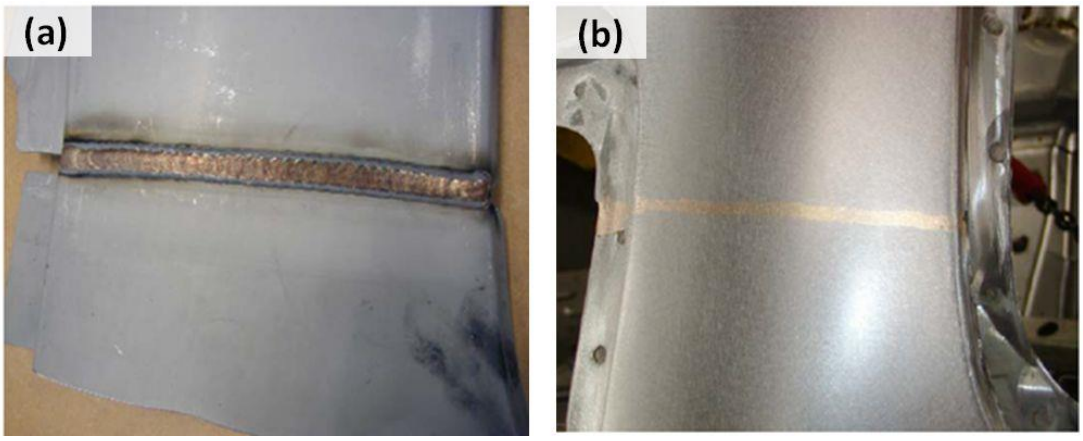


Figure 2-16: Manual brazed seam;
(a) outer skin braze joint on a C-pillar Bentley Coupe before manual grinding,
(b) after manual grinding [89].

As a relatively new method, some OEMs have begun to braze outer skin panels together without the need for grinding processes. This was possible due to improvements in the laser brazing technology.

In comparison to conventional spot welding, a brazed roof does not require PVC sealer, roof plastic moulding and the related fixing clips to create a watertight seal. In addition to the component number and material savings, there is also less finishing work required to complete the operation. The seam itself seals both body parts and delivers a good aesthetic appearance. Ford began using this brazed roof joining method for the first time on the Mondeo models in 2008. Figure 2-17 shows a spot welded roof (previous Ford Mondeo) and a laser brazed Mondeo roof (latest Mondeo).

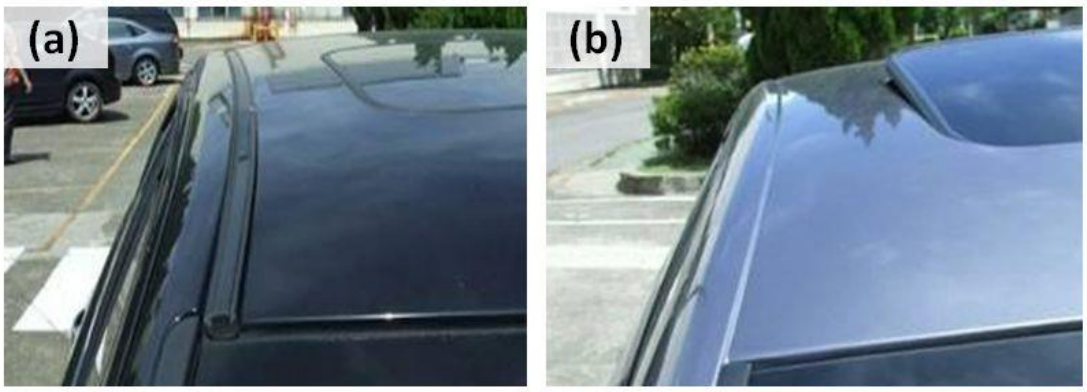


Figure 2-17: Roof design differences [90];
(a) spot welded roof, covered with plastic ditch moulding and
(b) brazed roof which does not require the joint sealing and plastic covering.

Brazing of Class-A panels has many advantages over other metal joining techniques such as welding. Since brazing does not melt the base metal of the joint, it allows much tighter control over tolerances and produces a clean joint without the need for a sealing operation. Brazing also produces less thermal distortion than welding due to the lower heating of the panels.

Another aspect is that it would be following the consumer trend. Ford consumer surveys show that customers like smooth vehicle body shell joints. A brazed roof is visually better than a spot welded or laser welded roof and points to an aesthetically higher quality vehicle [91]. Therefore,

brazed roof panels can improve the customer satisfaction, which increase the sales volumes, market share and earnings. As well it proves technical competences.

One other advantage offered by brazing versus traditional resistance spot welding is in the reduction of flanges that are found in various areas on vehicles such as between roof and bodyside. The spot welding flanges, which are generally on the order of 16 to 18 mm in width, are sized to accommodate the tip of the spot welding gun. The spot weld point itself has a diameter of 4.5 mm bur further space is needed to allow the weld gun to access the flange to be bonded [92].

This dimension can be reduced by approximately 10 mm through the use of brazing. The exact minimum flange width has to be investigated case by case and depends on the application. However, shorter flanges result in savings of raw material and therefore savings on weight, money and time.

Laser beam brazing and MIG brazing are currently widely used when joining body panels. Recently, TIG brazing technology jointed this group because it has more favourable investment cost than laser brazing and shows better joint quality than MIG brazing when joining thin steel panels.

The following sections describe the basics about these three brazing methods and highlight why brazing is a coming joining technology in automotive body manufacturing as well.

2.3.4.2 Laser Beam Brazing

Laser beam brazing (LBB) uses a laser beam as the source for the energy required to melt the filler metal wire and to heat up the base sheet metal. The molten wire flows into the seam and creates the braze joint. The benefits of laser brazing in general are the rapid and minimal heating of the surrounding metal and the ability to precisely control the process [88]**.**

Only a few OEMs use this state of the art joining technology already, mainly to attach the roof to body sides, for the drain channel in the trunk

lid opening, and for the split skin panel of the trunk lid. Figure 2-18 shows the schematic representation of the laser brazing process [93].

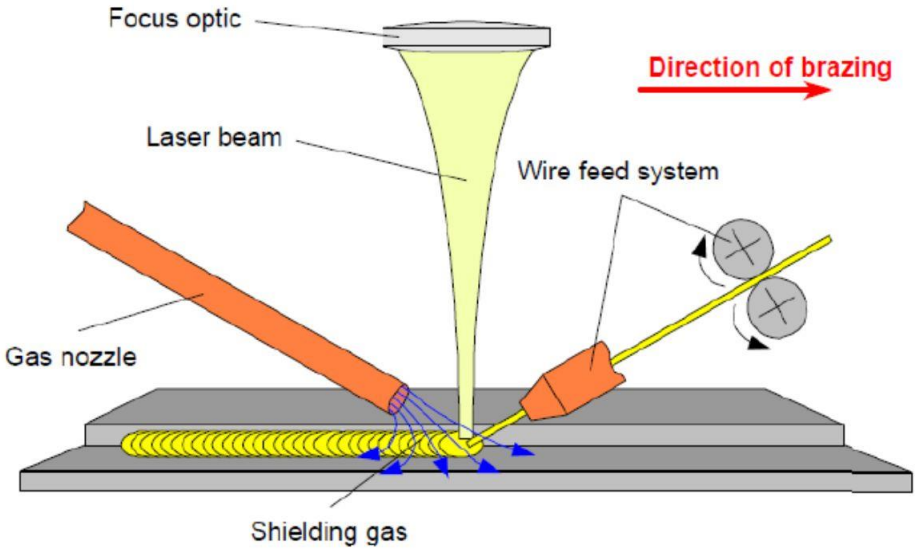


Figure 2-18: Schematic of laser brazing principle [94].

Typical process demands on the laser beam source for brazing are: laser power from 2 to 4 kW, a laser spot size of from 1.5 to 3.0 mm at a working distance of about 150 to 250 mm. The solid-state Nd:YAG lasers and the newer diode laser types fulfil these demands [95]. However, the automotive industry has started to use more direct diode laser sources for laser brazing applications because they have several benefits in comparison to the older Nd-YAG solid state technology, which are a much smaller footprint and increased system efficiency compared to Nd:YAG and CO2 lasers. The small size of the laser head allows for access into tight areas, and therefore eliminates the need for fiber-optic delivery that is commonly used with Nd:YAG lasers. The ability to weld directly reduces power loss and therefore supports the system efficiency [96].

Laser brazing requires, similar to laser welding, good part matching quality in comparison to resistance spot welding. This dictates the use of more complicated part clamping. Furthermore, this requires close tolerance stamping dies to get better part matching, which increases the stamping die quantity and thus the press die cost. These additional investments have to be considered in the planning for the use of LBB in the production environment. Like laser welding, the investment costs for

the laser equipment and the required eye safety housing around the clamping fixture are quite high. A more detailed assessment of capital and process cost is strategically very important and therefore part of this thesis (see Chapter 4.4.2). Figure 2-19 shows a typical roof to body laser brazing cell.

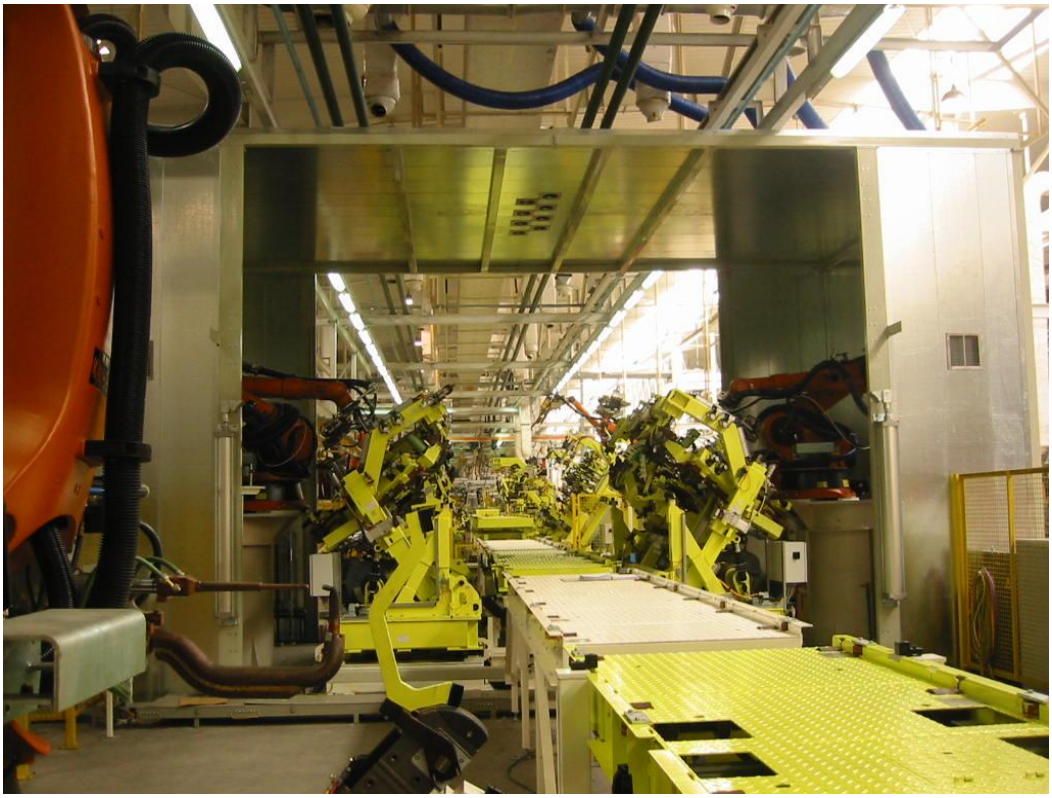


Figure 2-19: Typical roof to body laser brazing clamping station, including eye safety housing with open swing gates [97].

2.3.4.3 MIG Brazing

Metal inert gas (MIG) brazing was developed because of its lower heat input in comparison to MIG welding when it comes to joining metals. The copper based filler wire electrodes used for MIG brazing have a lower melting point (between 900°C and 1,100°C, depending upon the alloy used) than typical steel wire electrodes used for MIG welding of steel in bodyshops. The base metals fusion temperature (around 1,500 °C, when brazing steel) is not reached in contrast to GMA welding [98]. Conventional MIG brazing has the disadvantages of spatter and heat distortion often requiring rework making it unsuitable for automotive

joining operations on outer skin panels. Even so, MIG brazing is still in use for joints, which the consumer cannot see, for example on underbody related joints.

2.3.4.3.1 Cold Metal Transfer Brazing

A relatively new process for the automotive industry is Cold Metal Transfer (CMT) brazing [99], which was patented (EP1901874A1) by the company Fronius in 2006 [100]. This process is classified as a Metal Inert Gas (MIG) process and of its predominant advantage is reduced heat input, which is ideal for minimizing the distortion of sensitive joint configurations.

The basic operation mode of CMT is characterised by an arcing phase during which a molten droplet is formed on the end of the wire electrode and a weld pool created. After a set duration, the wire electrode is fed forward to make contact with the weld pool/base material creating a short circuit. During this phase, material transfer is initiated and the arcing current substantially reduced. After a defined period, the electrode is mechanically retracted, this rearward motion aiding in pinching the molten globule into the weld pool. The arc is then reignited and the cycle repeats [101]. This hot cold, arc on arc off cycle is repeated up to 70 times per second as it is shown in Figure 2-20. When the wire is drawn back, the movement supports the metal transfer due to the surface tension of the molten material. Therefore, the current during the short circuit can be kept very low and the heat input is also very small [102].

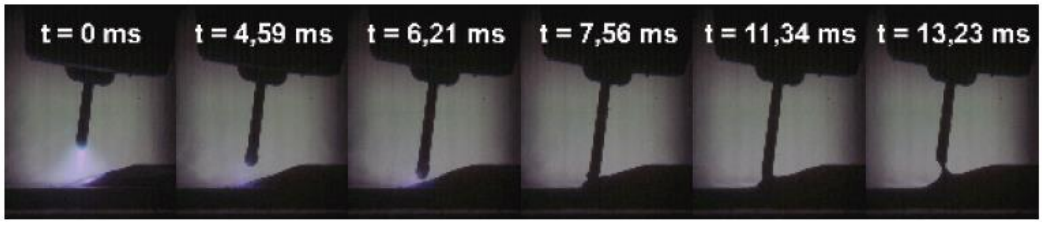


Figure 2-20: The principle of the CMT process, where an oscillating wire feeding is performed with an average oscillation frequency up to 70 Hz [102].

The resultant brazes experience less heat input into the work piece than standard MIG brazing [98]. The heat effected zone (HEZ) for welding is about 1,500 °C and for MIG brazing near 910 – 1,025 °C. The HEZ temperature for CMT brazing is on the lower temperature side [103].

In joining situations with large gaps (around 0.5 – 2.0 mm) where resistance welding will not work, CMT is suitable because normal arc welding would be too hot, causing spatter, material distortion and damage to the zinc coating [104]. In many areas of automotive BIW production, the CMT brazing machines have replaced the conventional MIG brazing process because of the nearly spatter free process that reduces the need for rework.

However, for outer skin panel joining, the brazing heat caused by the standard CMT equipment is still too high and results in shape distortions, which were previously investigated by the author but not published yet.

The company Fronius presented end 2013 their new CMT Braze+ system. CMT Braze+ is a new development of the normal CMT process. The narrow conical shape of the gas nozzle causes the shielding gas to constrict the arc, resulting in a more localised energy provision. Figure 2-21 shows a conventional MIG torch (a) and the new CMT braze+ torch with narrow conical shape of the gas nozzle (b).

The shielding gas consumption is reduced to sixty per cent of the standard CMT process [105], but most important for the automotive industry is that CMT Braze+ should be able to deliver high quality brazed seam on automotive outer skin panels.

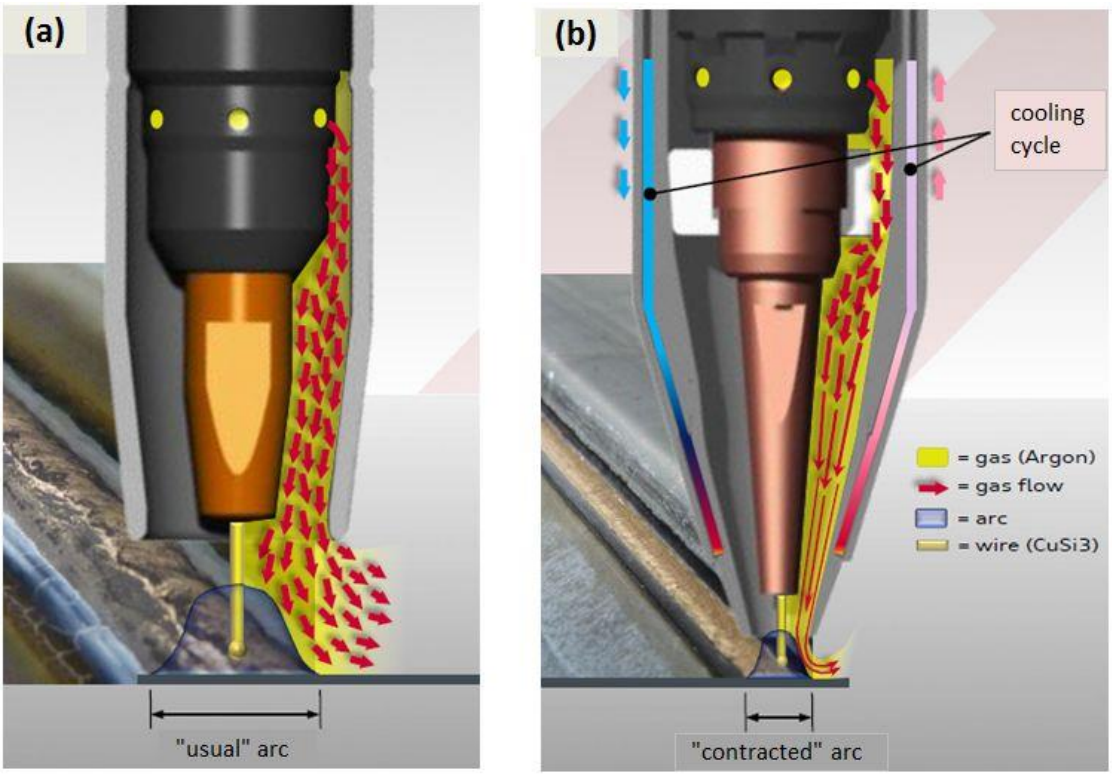


Figure 2-21: (a) Conventional MIG torch, (b)new CMT braze+ MIG torch with narrow conical shape of the gas nozzle and integrated cooling cycle leads to a constricted arc [106].

2.3.4.4 Tungsten Inert Gas (TIG) Brazing

Tungsten-inert-gas brazing is one of the most important joining technologies in joining of thin sheets in the automotive industry.

This process was developed for the aircraft industry back in early 1940s [107] to join hard to weld lightweight metals such as aluminium, magnesium and titanium [108]. The melt pool, the tungsten electrode and the filler wire are protected from atmosphere by a shield of inert gas to prevent oxidation of the seam and surrounding heated metal. The process commonly uses argon but other inert gas mixtures can be used for shielding.

The process is named after the type of electrode material (tungsten) and the shielding gas used (inert). The non-consumable tungsten electrode does not melt due to the high melting point of tungsten (3,380°C) when the process is used correctly. Non-consumable means that the electrode is not intentionally melted as in conventional arc welding. However, the tungsten will erode and become contaminated in use [109]. The shielding

gas is emitted from the shielding gas nozzle and surrounds the electrode concentrically, protecting the electrode and the metal underneath it from the atmosphere [110].

The filler metal gets struck from the arc end and does not have to run through the arc length as it does in MIG brazing [111]. As the electrode is not consumed during brazing, as in the MIG brazing process, brazing can be practised without the need of continual compromise between the heat input from the arc and the deposition of the filler metal. Key parameters of the TIG process can be independently controlled in contrast to MIG joining. The degree of melting of the filler wire is determined by the brazing current with respect to the brazing speed, whilst the degree of the molten pool is determined by the rate at which the filler wire is added to the braze pool. Visually good brazing joints without spattering are achievable with this fine-tuning capability. Figure 2-22 shows the schematic illustration of the TIG arc process. The HF (high-frequency) unit produce the arc that provides the required initial conducting path through the shielding gas.

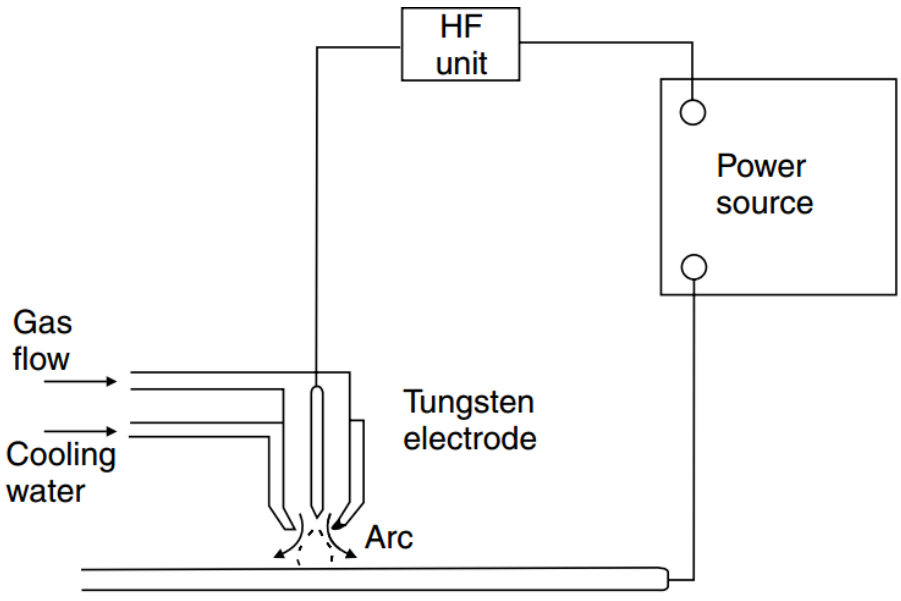


Figure 2-22: Schematic illustration of TIG arc process [112].

The TIG brazing torch carries the tungsten electrode in an adjustable clamp arrangement. There has been little change in brazing torch design since the inception of the commercial TIG process [94]. The literature

distinguishes only two main types of TIG torches: water-cooled and air-cooled torches [113]. An official classification for TIG brazing torches does not exist yet.

For TIG welding, recent innovations have included the introduction of dual shield TIG, keyhole TIG and laser GTAW hybrid processes [114].

For TIG brazing, three TIG system suppliers developed improved TIG torch designs that are able to deliver a more focused arc. This allows brazing of thin steel panels (< 1.0 mm thickness) as well, without following panel distortions. The following sections introduce these three torch developments.

2.3.4.4.1 ForceTig™ Brazing

The company EWM offers a brazing torch called ForceTig™, which they presented for the first time in 2009 (patent no. EP2008750A1 from 12/2008). EWM promised that it is possible to braze class-A panels with this TIG head (see Figure 2-23).



Figure 2-23: ForceTig™ torch from the company EWM.
With the large nozzle (22 mm diameter) it is not possible to braze in small channels and curved seam paths.

Of interest is the nozzle design. A 6.4 mm diameter tungsten electrode is pressed in a copper carrier, which allows a high head runoff to the water cooled nozzle body. This cooling system allows the nozzle to change the electrode without the normally used electrode setting gauges due to the defined, calibrated geometry. Easy-to-change electrode means reduced

non-value added time which is a benefit in mass production. Figure 2-24 shows a ForceTig™ electrode insert and the related electrode holder.

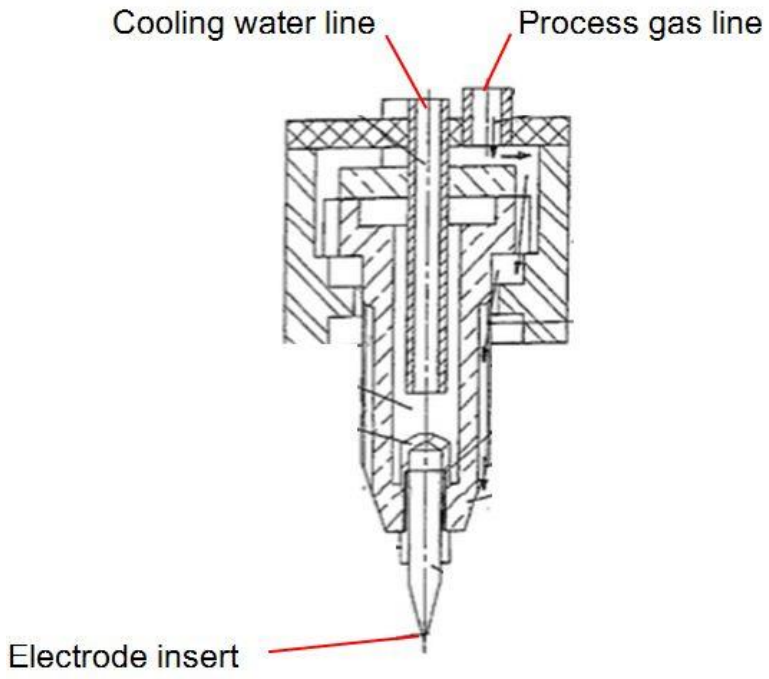


Figure 2-24: ForceTig™ tungsten electrode insert [115]**.**
The electrode insert can be screwed in the ForceTig™ holder,
which reduces the electrode changing time**.**

However, EWM was not able to announce an introduction in the automotive industry for outer skin panel brazing at any volume vehicle manufacturer to date. A main negative has to be highlighted that the nozzle diameter (22 mm) is quite large and as such it is not possible to braze in small joint channels, which is a typical requirement for vehicle manufacturers. It is also clear that brazing of curved seam paths will be difficult using a nozzle of this size. Before usage a CAD simulation should be conducted to ensure that the joint design delivers enough access for the bulky ForceTig™ torch.

As well, it needs to be reviewed if an electrode change would cause seam quality issues like nonparallel filler flow. This could be generated due to little repeatability inaccuracies of the electrode tip position. The author was not able to find any report that has studied these important subjects.

2.3.4.4.2 TopTIG™ Brazing

The French company Air Liquide Welding developed a new TIG torch called TopTig™. The difference to conventional TIG nozzles is that the filler metal is fed through the nozzle directly into the arc zone with an angle of 20° to the electrode, where the temperatures are higher resulting in 'continuous liquid-flow' transfer. This configuration also offers the advantage of reduced overall dimensions and greater accessibility of the torch for robotic welding of complex geometries [116]. Figure 2-25 describes the function of the TopTig™ process. Air Liquide developed an automatic electrode change device for their TopTig™ nozzle that contains 6 electrodes in a revolver head, which does not require an operator for change and can be fully automated. The automotive industry currently uses this system for welding brackets to steering columns and to join muffler parts but not for joining of automotive outer skin panels [117].

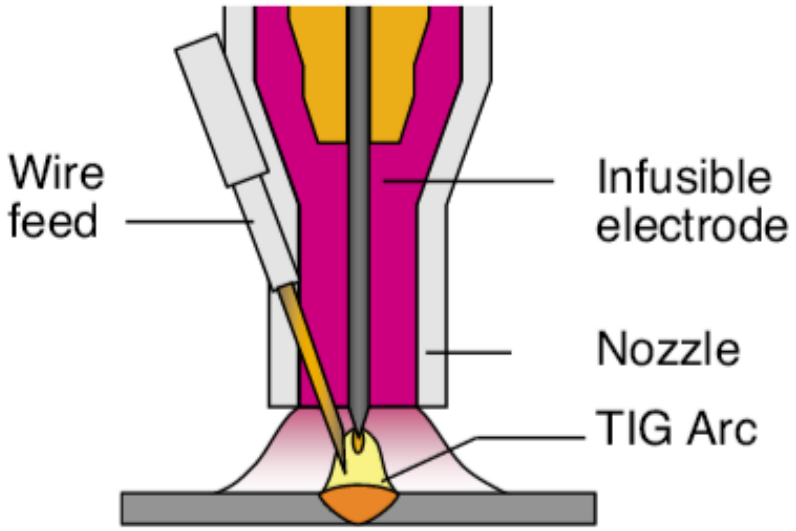


Figure 2-25: Functional diagram of the TopTig™ process [118]**.**
The filler wire is fed through the nozzle directly in the arc zone.

2.3.4.4.3 Plasmatron Brazing

The Austrian company Inocon developed a TIG brazing torch that Audi used as the first OEM to braze an automotive roof to a body on their A4 and Q7 in 2006. Ford used this brazing technology for the first time to braze a roof to a vehicle in their Taiwan low volume plant in mid-2008. Two further Ford low volume plants in Vietnam and Russia then introduced the same technology because the capital investment on setup was lower than a laser brazing system.

The key difference of Plasmatron brazing to other plasma systems is the unique nozzle design feature that differs from conventional arc plasma systems (see Figure 2-26). This enables an elongated and more direct energy plasma at the filler wire and parent metals when compared to conventional arc plasma systems. The pointed nozzle design optimises the arc shape and therefore improves the filler flow characteristics resulting in a smooth braze filled joint.

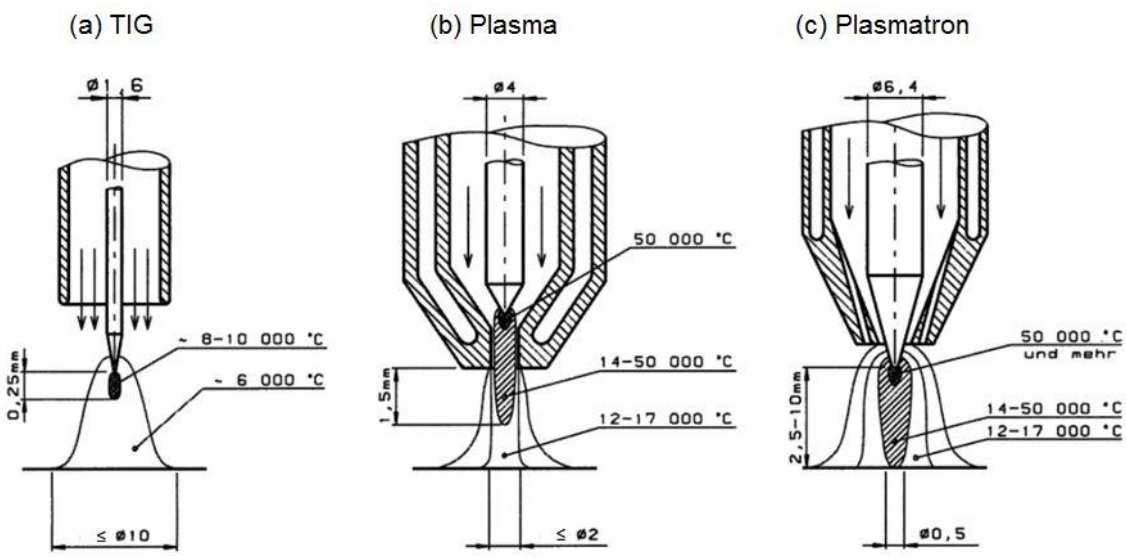


Figure 2-26: Nozzle designs for Plasmatron and other plasma systems; (a) shows a standard TIG nozzle, (b) a plasma nozzle and (c) the focused Plasmatron nozzle [119].

The Plasmatron torch includes a tungsten electrode, which is located in a water-cooled copper nozzle. The copper nozzle that holds the electrode has a small opening at the point with the electrode protruding slightly. The nozzle is designed to allow inert gas through the orifice to the electrode to

generate an arc. During the brazing, the nozzle is supplied with cooling water to cool down the electrode and nozzle casing to prevent softening. Figure 2-27 illustrates the nozzle design. The electrode tip stands 1.2 mm proud of the nozzle face [120].

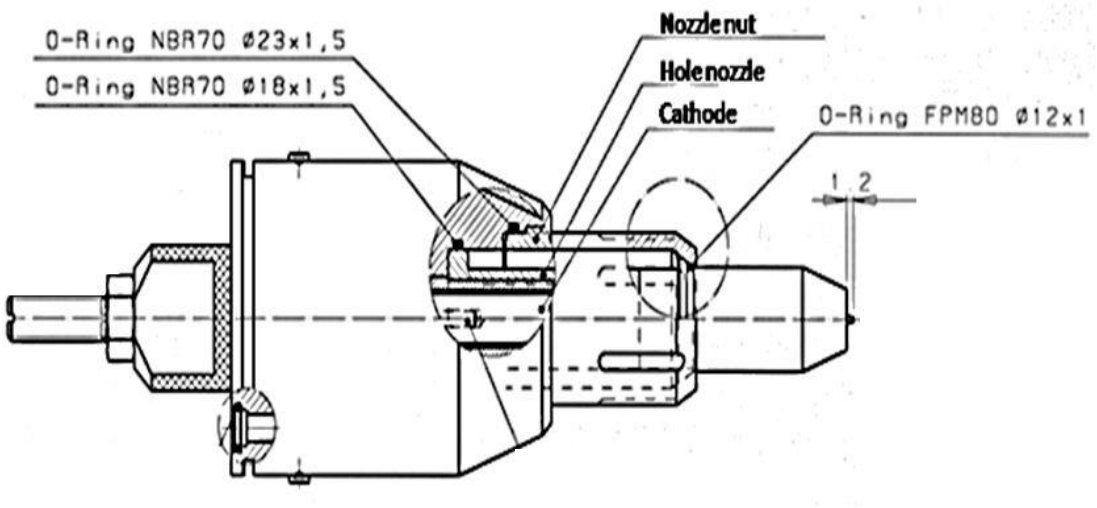


Figure 2-27: Illustration of a Plasmatron torch [121]

2.4 TIG-Brazing Fundamentals

In a typical TIG brazing process many different input parameters can influence the braze quality. To understand the influence logic of these input parameters it is important to understand the electric arc basics and the forces acting on the arc. This chapter presents fundamentals of electric arc processes and tungsten electrodes and their significance in arc TIG brazing.

2.4.1 Electric Arc Processes

The TIG brazing arc can be broken up into five distinct regions: anode spot, anode drop zone, arc plasma column, cathode drop zone, and cathode spot. The basic schematic of a TIG arc is shown in Figure 2-28.

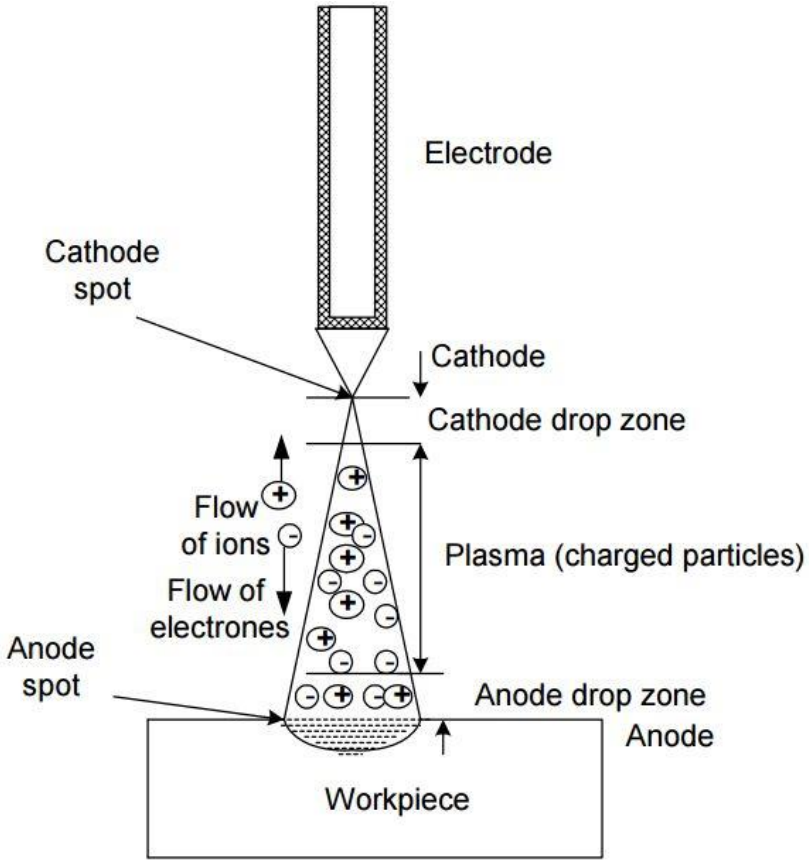


Figure 2-28: Regions of a TIG arc (electrode negative polarity) [122].

During EN (electrode negative) polarity, electrons flow from the tungsten cathode to the anode (here braze wire and base metal) by means of the arc plasma. The anode spot is the localized positive part of the anode that attracts the negative electrons. Condensation of electrons at this region leads to intensive heating of the anode substrate. The small arc region adjacent to the anode spot is termed the anode drop zone [123]. A very sharp drop in voltage takes place in this region due to the cooling effect of the anode [122]. The cathode spot is the location of electron production by thermionic emission. The cathode drop zone is the electrical connection between the cathode and the arc column [123]. The arc column is defined as that part of the arc, which is located between the cathode fall and the anode fall. It is occupied by a 'thermal plasma' composed of ions, electrons and atoms of the shielding gas [124]. An important aspect of the arc column is its electrical neutrality. At atmospheric and higher pressures, each volume unit of the column contains equal numbers of positive and negative electric charge carriers [125].

The voltage drop in the arc column depends on the length of the arc and, in particular, on the composition of the shielding gas. Argon plasma has a voltage drop of about 6 V/cm, while helium plasma has a voltage drop of 42 V/cm. Helium also gives higher temperature in the plasma due to its higher ionisation energy [113].

2.4.2 Influence of Current Types

The polarity of the electrode also plays a part, as there is greater heat evolution at the anode than at the cathode. This due to the fact that the input of energy to release electrons at the cathode is recovered at the anode in the form of heat as the electrons are absorbed by the anode. It is therefore standard practice, when performing TIG brazing, that the tungsten electrode should be connected to the negative pole of the power source. This Direct-Current Electrode Negative (DCEN) polarity will mean that there will be less heat load (~ 1/3 heat) on the electrode, with the heat being concentrated on the filler wire (~ 2/3 heat) [113].

Direct-current electrode positive (DCEP), in this polarity electrons leave the work and accelerate as they make their way through the ionised gas to the electrode under the influence of the voltage across the arc. Their impact on the electrode generates intense heat that will melt the electrode if not removed. It provides a cleaning effect on the base metal within the arc area. Positive ion bombardment onto the work produces cathodic etching [126]. This effect can remove aluminium surface oxides and assist with aluminium welding.

Alternating current (AC) provides equal heat at the electrode and the work because each receives electron bombardment. It is used most often to weld aluminium and magnesium because its cleaning effect is essential [126]. The frequency at which the current cycles is the rate at which it makes a full change in direction [59]. Figure 2-29 summarizes the differences between the current types DCEN, DCEP and AC.

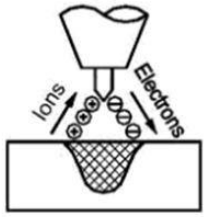
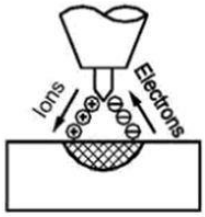
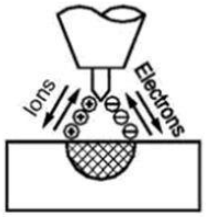
Current Type	DCEN	DCEP	AC (Balanced)
Electrode Polarity	Negative	Positive	
Electron and Ion Flow			
Penetration Characteristics	Deep, Narrow	Shallow, Wide	Medium

Figure 2-29: Characteristics of different current types for TIG joining. The schematic shows the ions and electrons flow differences [127].

2.5 Tungsten Electrode Fundamentals

The appropriate electrode material for an arc brazing application depends on several variables, including the composition of the materials being brazed, the field of application and the amperage level. The following section describes the electrode basics and highlights the state-of-technology.

While a temperature is generated in the arc during brazing, the role played by the electrode material is crucial as it must have a high melting point and it should be hardly consumable. Tungsten quickly established itself as the most suitable material.

Tungsten, atomic symbol W, has the following properties:

- High tensile strength: 3,447 kg/mm^2
- Hardness: 300 – 650 HV 30
- Highest melting point of all metals: 3,422 ± 15 °C
- Boiling point: 5,700 ± 200 °C (corresponds to the sun surface)
- Good thermal conductivity: 1.75 W cm^{-1} K^{-1} (298 K)
- Low electrical resistivity: 5.28 µΩ cm (298 K) [128]
- Density: 19.25 g/cm^3 (298 K)

Outstanding is the highest melting point of all pure metals. Another benefit is the high thermal conductivity. It allows a rapid heat flow from

the electrode tip to the water-cooled collet, which avoids the arc heat melting of the tungsten tip.

Tungsten is produced mainly by reduction of its trioxide with hydrogen. Powdered tungsten is then purified to 99.95 +%. The tungsten powder size is typically within the range of 3 - 5 µm [129]. Tungsten electrodes cannot be produced by foundry process because of the high melting point of the metal. Therefore, it is produced through powder metallurgy methods. Which means, compressed, followed by sintering (heated to a temperature below melting where grain growth can occur) is commonly used to make an ingot [130]. The ingot is heated to increase ductility and then swaged and drawn through dies to produce electrodes [59].

The standardized electrode diameter lies between 0.5 and 10.0 mm according to ISO 6848:2004 MOD [131]. The most commonly used diameters are 1.6, 2.0, 2.5, 3.2, 4.0 and 6.4 mm [132]. Large diameter electrodes conduct more current because the resistance heating effects are reduced. However, excessively large sizes may result in a too low temperature for a stable arc [59]. That means the electrode load could be too small and the plasma flow will be too turbulent [133]. If the diameter is too small, the electrode tip will melt.

The electrode lengths correspond to the torch resp. the nozzle design. Standardized lengths are 50, 75, 150 and 175 mm.

The electrode surface needs to be free of impurities, undesirable films, foreign inclusions, cracks, scale and other defects to avoid arc hampering and permit a clean arc formation. The electrodes also need to be straight (100 mm ± 0.5 mm) to properly control the arc [131].

2.5.1 Electrode Material Classification

As the knowledge of arc characteristics increased, it became clear that the use of pure tungsten presented some limitations on arc initiation and arc stability. Small additions of head-resistant oxides to the tungsten showed that significant overall improvements in performance could be achieved [130].

Oxides naturally migrate from inside the tungsten to the heated outside surface at the point of the electrode, where the oxides are given off in the arc, leaving a film of the metal alloy on the tip. The oxides that are emitted at the tip serve to improve arc starting stability. Lower temperatures improve the longevity of the electrode and keep the grains within the electrode smaller for improved arc stability [134].

The energy required by an electron to escape from a metal surface is called the work function of the material [135]. This energy is a measure of how tightly a particular metal holds its electron and it is measured in electron volts (eV). The lower the work function of an electrode, the lower the voltage necessary to strike an arc, thus the easier the arc starts. The oxides added to tungsten electrode serve to promote the electron emission by lowering the work function of the tungsten at the near surface. Depletion of the electrode of these oxides naturally results in an elevated work function.

The metal work function is important, because upon emitting an oxide, the metal is left as a film on the tip. The lower the eV of the metal at the tip, the lower the temperature will be at the tip, which will decrease grain growth and provide a constant flow of oxides and longer service life [134].

Even if electrodes are the same type, electrodes of different manufacturers cannot be compared using only the electron work function and volume of oxides, because this comparison would not take account for manufacturing variables such as grain size and the structure of the oxide size and distribution. Therefore, the work function and oxide density numbers should only be used as a general guide.

Table 2-1 lists most commonly used oxides and metals and their respective work functions.

Table 2-1: Work functions of different oxides and tungsten [134].

Material	Work Function Oxide (eV)	Work function Metal (eV)
Lanthanum	2.5	3.30
Thorium	2.6	3.35
Cerium	3.2	2.84
Pure tungsten	No oxide present	4.50

According to ISO 6848, 2004 [136], tungsten electrodes have been classified into 11 types based on their chemical composition (see Table 2-2). Each type having a distinctive symbol and defined colour code.

Table 2-2: Recommendations for the type of electrode depending on the work piece [132]. Thoriated electrodes are grouped together because thorium is a radioactive substance.

Work piece	WS2	WLa 20	WLa 15	WP	WZr 8	WLa 10	WCe 20	WTh 10	WTh 20	WTh 30	WTh 40
Unalloyed steel	++	+	++	-	o	++	+	+	+	+	+
Alloyed steel	++	++	+	-	o	o	++	o	+	++	++
Copper, copper alloys	++	+	+	-	o	o	+	+	+	-	-
Nickel, nickel alloys	++	++	+	-	o	o	++	-	+	++	++
Aluminium, aluminium alloys	++	o	o	++	++	+	o	+	-	-	-
Magnesium, magnesium alloys	++	o	o	++	++	+	o	+	-	-	-
Titanium, titanium alloys	++	+	+	-	-	-	+	-	+	++	++
Zirconium	++	+	+	-	-	o	+	-	+	++	++
Tantalum	+	++	o	-	-	o	+	-	+	++	++
Tungsten	+	++	o	-	-	o	+	-	o	++	++

Suitability: ++ very good, + good, o partly, - bad

Identification is made by colour-marking each of the electrodes or by inscribing the classification marks on the surface of the electrode [131]. The most commonly used additives are thorium oxide (ThO2), zirconia oxide (ZrO2), lanthanum oxide (LaO2) and ceria oxide (CeO2).

Four of the ISO classified electrodes are based on thorium oxide (see WTh at the right side in Table 2-2). This oxide has a high melting point (3,378°C) [137]. The element thorium was named after Thor, the Scandinavian good of war by Swedish chemist Jöns Berzelius in 1815. Thorium is a natural radioactive substance. It is advised not to use thoriated electrodes since radioactive dust that can be incorporated is released during brazing as well as during grinding [132].

Lanthanum trioxide has the best plasma flow properties of any of the materials, thus, it usually ignites easiest and has the lowest temperature at the tip, which resists grain growth and promotes longer service life. Testing of tungsten with 2 per cent lanthanum oxide electrode has shown that, if not overloaded, it offers a much longer service life than thoriated tungsten cathodes and keeps better arc starting characteristics in most applications. It is also especially good at resisting the "thermal shock" of pulsing caused by rapid heating and cooling and resisting contamination.

Lanthanum is a "rare earth" material and is not radioactive. This electrode is primarily used for DC welding, but will also show good results for AC welding [134].

Cerium based electrodes were developed as replacement for thoriated electrodes because ceria is not radioactive. They will successfully operate either AC or DC [126]. However, lanthanum electrodes overtop ceria electrodes in the low current field due to their lower work function, as described before.

Zirconiated tungsten electrodes contain a small amount (0.15 to 0.40 wt %) of zirconium oxide. These types of electrodes are good for alternating current welding, which is required to break up the aluminium oxide by aluminium welding. The reason for this is that zirconium additives reduce the risk that tungsten contaminates by dropping in the melt pool. They have a higher current carrying capacity and better arc starting characteristics of thoriated tungsten electrodes [126].

2.5.2 Electrode Preparation

Different techniques have to be utilised when preparing electrodes for brazing operations, which are given below.

Since tungsten is a very hard material, electrodes must be diamond ground. Grinding with other types of wheels can create jagged edges, imperfections, or invisible poor surface finishes that contribute to arc inconsistency [138]. This grinding machine should not be used for anything other than tungsten electrodes to ensure that the wheel and hence the electrode tip will not become contaminated during the grinding operation and transfer grinding particles to the braze pool [134]. Furthermore, the electrode tip could be contaminated during the brazing process. Regrinding a contaminated tip may not remove all of the contamination, and the grinding wheel can be contaminated, only to be picked up again in future grinding operations [134].

The form of the electrode tip determines the arc flow and the quality of the braze seam. Special attention must be taken when grinding to prevent the electrode tip from breakage. This is reflected in the microstructure, where grain boundaries are weaker than the grains themselves [139].

In the grinding operation, mechanical stress may weaken the electrode, causing fractures along the grain boundaries in the tip.
The temperature of the electrode increases rapidly in the brazing start phase. With this, the fatigue strength of metals decreases with increasing temperatures (high-temperature fatigue). This can lead to grain boundary crack formations at its tip [140].
Electrode tip grinding in a circular or crosswise pattern causes the arc to be unfocused and possibly jump sidewise from the electrode rather than off the tip point [141]. With longitudinal grinding, the arc starts straight at the tip and remains narrow, concentrated, and more stable [138]. This creates an electric arc without a strayed corona (see Figure 2-30). The tungsten electrode is subjected to a lower thermal load and will therefore have a longer lifetime [142].

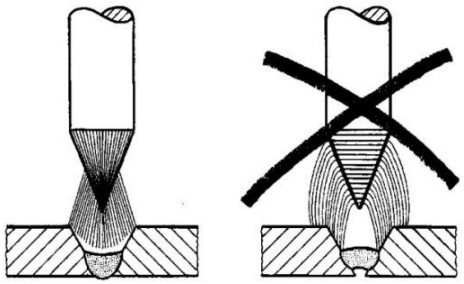


Figure 2-30: Influence of the grinding direction
on the formation of arc [143].

The tip should be ground centrically as far as possible. If this is not the case, the arc may be unstable and will not ignite at the correct point (see Figure 2-31). The arc illustrates the mirror image of the grinding angle [143].

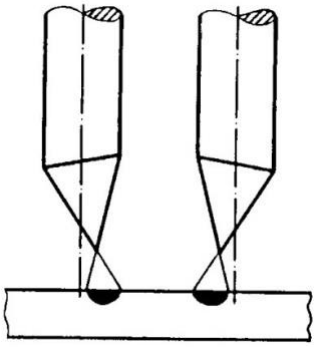


Figure 2-31: Course of the arc if the tip is not ground centrically [143].

In conjunction with the diameter of the electrode, the grinding angle has a marked effect on the plasma beam. Figure 2-32 demonstrates the relation between penetration profile and grinding angle at constant current and gas. If the electrode has a sharp tip, the full energy is concentrated on a small area, which causes a deep penetration. On the other hand, a blunt grinding angle causes the same energy to be spread over a much larger area, thus, the penetration is clearly shallower. Again, the arc and its penetration profile is a reflection of the grinding angle [144].

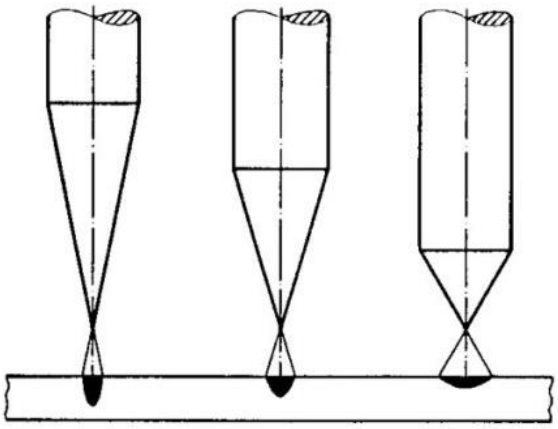


Figure 2-32: Penetration profiles as a function of the tip angle [144].

Depending on the type of tungsten electrode, preparation consists of creating one of three tip shapes: pointed, truncated or balled.

A pointed tip shape works well for welding or brazing with lower currents on thinner materials as it directs the welding current into a focused arc and helps prevent it from distorting. It is not recommended to use a pointed tungsten electrode for higher current applications since erosion would blunt the tip [126].

For higher current applications, a truncated or flat tip works well. The flat tip helps prevent the tungsten electrode from being transferred across the arc and/or from balling. To improve the service life and to reduce the tip load, it is recommended to flatten the tip of the electrode after grinding. The tip resulting from it should have a diameter of about 10 per cent of the electrode diameter; that means an electrode with diameter 4 mm should have a tip diameter of 0.4 mm [144]. The company Inocon recommends to use truncated electrodes with a 0.5 mm tip diameter for

their 4 mm and a 0.8 mm diameter for their 6.4 mm electrodes for brazing of zinc coated steel panels.

The balled electrode tip shape (see Figure 2-33, right side) is most common for pure tungsten electrodes. To ball the tungsten electrode peak, the recommended AC amperage for the electrode diameter should be chosen. The ball will then form itself. In order to reduce the risk of the tip falling off or causing arc instability, the diameter of the balled end should not exceed 1.5 times the diameter of the electrode [145].



Figure 2-33: Tungsten tip differences
(a) pointed, (b) truncated, (c) balled [146]

2.6 Shielding Gas Influence

Argon and helium are the most commonly used shielding gases for TIG joining next to hydrogen and sometimes nitrogen. All are inert gases, which mean that they do not readily combine with other elements. They will not burn or support combustion. These gases ionize when present in an electric arc.

Gas flow rate is important for generating the drawn-arc and for obtaining the proper flow rate to protect the brazing surfaces. It is crucial for the seam quality.

The inert gas flow must be dosed properly. The use of too little gas results in an insufficient inert gas coverage of brazing seam and electrode. Possible residual oxygen adhering to the material leads to oxidation and a poor braze quality. The use of too much gas leads to turbulence in the gas flow due to the high flow velocity. Thereby, small parts of the ambient air

are sucked in, which could then cause an oxidation of the seam and material as well. This can result in the formation of distinct surface deposits on the seam surface [147]. Furthermore, the electrode tip could oxidise. This is visible as a blue tinted electrode peak [133].
Also, hot tungsten is sensitive to oxygen contamination [59], a good inert shielding gas is required to keep the air away from the hot tungsten and molten braze wire.

2.7 Zinc Coated Steel Panel Fundamentals

Obtaining good quality braze joints requires an understanding of interaction phenomena of brazing filler with zinc coated steel surfaces. Therefore, it is important to study the fundamentals of zinc coating from automotive steel panels.
The vehicle's safety, especially crash parts, remains stable during the whole period of usage when using zinc coated steel panels. This will become even more important as the thickness of the steel sheets is steadily reduced, a common trend in automotive engineering. The environmental advantage is that the duration of usage and the recycling intervals will be considerably prolonged.
In this manner, the end customers of cars benefit from properties such as longer life-time and long-time maintenance of value [148].
The automotive manufacturers buy flat steels in coils that are zinc treated. These pre-treated flats can be produced either by hot-dip (HD) galvanisation or electrolytic [149].
In this hot dipping, continuous coils of sheet steel are pulled at through a bath containing molten zinc at a controlled speed. The zinc reacts with the steel and forms a bond. The excess liquid zinc sticking to the sheet surface as it exits the bath is wiped off on both the top and the bottom side of the strip by blowing pressure-controlled air or nitrogen onto the strip to achieve a controlled coating weight of thickness per unit area [150].
Galvanized (GI) zinc coatings contain pure zinc with 0.3 to 0.6 weight per cent aluminium. The term "galvanize" comes from the galvanic protection that zinc provides to the steel substrate when exposed to a corroding

medium. A galvannealed (GA) coating is obtained by additional heating of the zinc coated steel at 450 – 590 °C immediately after the steel exits the molten zinc bath. This additional heating allows iron from the substrate to diffuse in the coating. Due to the diffusion of iron and alloying with zinc, the final coating contains about 90% zinc and 10% iron. The alloying of zinc with diffused iron in the coating results in no free zinc present in the galvannealed coating [150]. The name galvannealed is formed from the two verbs, to galvanize and to anneal [151].

For quality control, steel producers measure the zinc thickness on-line after galvanising for each coil. The zinc layer applied to the steel material averages at 50 g/sqm = 7.0 – 9.8 µm thickness on galvanized sheets and 55 g/sqm = 7.6 – 10.0 µm thickness on galvannealed sheets per side for Ford [14].

Recently, various hot dip zinc coatings alloyed with aluminium and magnesium (ZnAlMg) have become available as possible alternatives to zinc galvannealed and zinc galvanized coatings, because the corrosion resistance of these ZnAlMg coatings is better than for conventional GI and GA [152]. With these ZnAlMg coating types it is possible to reduce the coat thickness without sacrificing the corrosion resistance. This would assist to reduce the car weight.

In 2013, the company Posco presented a new GI type, called GI-ACE. Posco developed a new method of solidification of molten zinc. ACE stands for aerosols charged with electrostatic. That means that the steel strips get electrostatically sprayed with water after leaving the zinc bath. The advantage is that the grain size of GI-ACE is very fine (50-60 µm) compared to conventional GI (1,000-2,000 µm). This delivers a smoother and spangle free surface, such as GA and EG surfaces [153].

However, before the implementation of these new coatings for automotive class-A panel braze joints the methods of joining them must be verified.

Electrogalvanized zinc coated steels are characterised by a very pure zinc coating without iron in the coat in comparison to hot dipped zinc coated steel. In plating cells, the metal ions that have been dissolved in the electrolyte are deposited cathodically on the passing steel strip under the influence of an externally applied voltage. The amount of the zinc deposited depends on the current density and the coating time [154].

2.7.1 Issues due to Zinc Coated Steel Panels

Research to date has tended to report only positive aspects of the brazing of zinc coated steel panels rather than study the problematic aspects when brazing zinc coated steel panels. One report [155] noticed that the melting temperatures of GMA and MIG welding wires are higher than the evaporation temperature of zinc (910°C), causing the zinc to vaporize both in and around the weld zone. Another study [156] concluded that the low heat input of the brazing process helps to reduce the width of the heat affected zone in the base metal and limits the Zn coating degradation besides the bead and backside.

On the other hand, the braze ability of the zinc coated steel panels, the amount of black soot at the panels, the amount of electrode contamination due to the vaporized zinc, the quality of the seam and the brazing process window size might be significant, depending on the chosen zinc coating types.

There is no European industry standard available that describes the brazing behaviour of different zinc coating types or that would give the industry a guidance, which zinc coating types should be preferred for brazing.

The vehicle designers have presently no guidelines that they can follow. Currently, the designer follows the stamping guidelines and the guideline to reduce the piece price as much as possible.

It is becoming increasingly difficult to ignore the lack of braze standards regarding this zinc panel coating subject.

For example, the product development engineers are encouraged to take care of every little cost saving. As bare steel material is cheaper than zinc coated steel material, the PD engineers determine to braze galvanized panels to galvannealed panels or even to braze zinc coated steel panels to bare steel panels. Afterwards, this decision can create the source for braze quality issues due to the reduced braze parameter window.

2.8 Seam Tracker Systems for Brazing Operations

For brazing high quality joints in the automotive industry, for instance the roof to bodyside connection, the use of a robot combined with a seam tracking system is indispensable. It ensures that the brazing torch and wire repeatedly follow a given joint, and that the subsequent braze is consistent. This is essential to gain and maintain control over the process. A manual joining method would not lead to a satisfying seam result. Only an automatic, seam tracker guided method can deliver the required joining quality.

Currently, two main methods exists to ensure a high quality seam – optical and tactile tracking in combination with either robot controlled seam tracking or adaptive seam tracking [157].

Optical seam trackers most often use light section sensors that utilize the triangulation principle. A laser line is projected onto the workpiece surface [158]. The light is reflected from the surface and captured with a camera. After processing, the correction data is transmitted to the robot control system [159]. Figure 2-34 shows a schematic view of a laser seam tracking head.

The advantage of optical seam tracking is that they work with no contact between the sensor and the joint, which means there is no tendency for the system to run out of the joint. In comparison to tactile sensors which cannot track all joint designs [160].

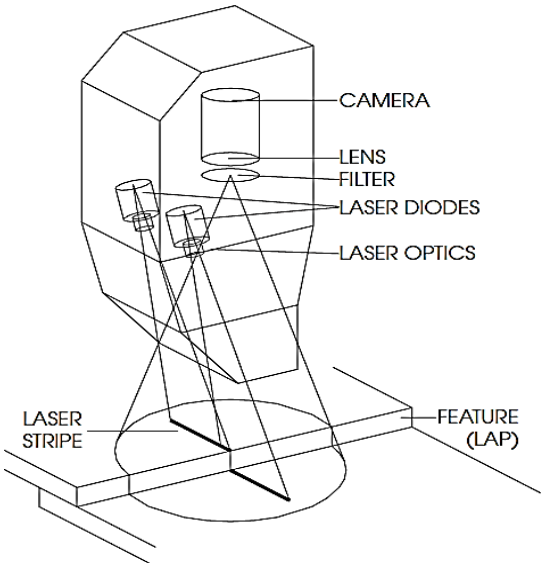


Figure 2-34: Optical seam tracker system,
which utilizes the triangulation principle with help of a laser stripe [159].

Another used optical measurement concept is grey-scale image processing. This sensor type also uses a two dimensional detector (camera) to observe the workpiece surface. Instead by a projected laser line, the joint and workpiece surface is illuminated with diffuse light. The joint position is recognized by separating areas of different reflectivity (or brightness) within the camera image [158].

In contrast, the tactile seam tracker method, where a tactile sensor running in advance of the brazing process, acting as a 'feeling' mechanism when there is any deviation between a touched edge and the original source coordinates. The sensor rides in the joint ahead of the torch and tracks the joint providing correction signals to the seam tracker system [160]. Alternatively, the filler wire can be used as tactile sensor, without running ahead of the process [161].

The conversion of the acquired process data into mechanical movements can be achieved by the brazing robot itself or a special adaptive processing head where the robot just guides an autonomous processing head. The processing head compensates here for any deviation. This can also take place with forerun compensation. This has the advantage that a separate seam tracker head works independently from the robotic controller, which guarantees a very dynamic compensation adjustment [157]. This adaptive seam tracking can either be done by pneumatic actuation or via servo mechanism or with a mixture of both. For example, pneumatic control in z-Axis and servo mechanic control in y-Axis can be used.

Permanova Lasersystem has developed a triangulation seam tracking module for their Permanova WT3 laser welding system (Figure 2-35a), where a sensor camera looks through the actual laser beam path. This allows the measuring position of the tracking to be extremely close to the joining position, typically 2 - 6 mm in front. This way, the robot variations are accounted for by the seam-tracking as well. An additional diode laser is used to project a line on the work piece for the sensor camera to read [162].

The APN1 from Scansonic (Figure 2-35b) offers another seam tracking technology for welding and brazing. A filler wire provides the material for

creating the seam and acts simultaneously as a mechanical sensing device. Utilizing force control, the tip of the filler wire is pressed into the weld/braze joint and is mechanically guided along the path of the joint. Any deviations from the programmed path of the joint are compensated for automatically [163].

Inocon also provides its MNV ('mechanical seam tracking system' in German) as seen in Figure 2-35c. The wire outlet nozzle acts as the sensor. This system, which was developed for the Plasmatron® process, enables the tracking of a seam in 3D. Therefore, robot tolerances, tolerances in the clamping device and tolerances of parts can be corrected for automatically [164]. The mechanical tracking system has the benefit of less electronics needed, making it more robust and decreasing the error probability due to the intense electromagnetic radiation emitted by the plasma arc.

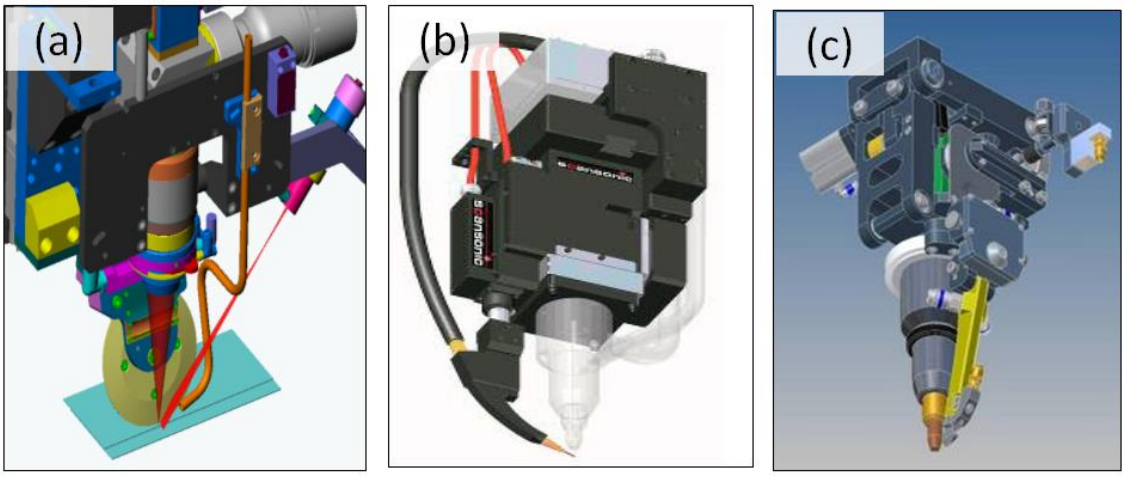


Figure 2-35: Overview of different seam tracker systems;
(a) Permanova's opctical seam tracker, (b) Scansonic's filler wire guided seam tracker, (c) Inocon's wire nozzle guided seam tracker.

Other technologies being investigated are seam tracking via eddy current sensor and with an acoustic signal. Being developed by LZH (Laser Zentrum Hannover) the eddy current technique for seam tracking is especially suited for butt joints or other seam geometries that are hard to detect with optical or tactile seam tracking systems [165].

2.9 Chapter Summary

This section summarizes the published literature and main findings in BIW joining, with special focus on TIG brazing and the related fields. Knowledge gaps are stated at the end of this section.
The main findings from this chapter are outlined as follows:

- The mass manufacturing of carbon fibre car bodies will not come in the next 10 years. It makes sense to research metal joining technologies.

- The advantages and disadvantages of the most used and coming future BIW joining technologies are identified.

- Braze joints stiffen the BIW, are aesthetic and do not require watertight PVC sealing.

- Tungsten electrodes can be classified into 11 types based on their chemical composition.

- Tungsten electrode preparation requires special knowledge.

- There are different zinc coating types for automotive steel panels.

- Seam tracker systems are essential for braze joining of thin steel panels.

From the literature survey, the information found about BIW joining, especially about the brazing process, could help the author understand the problem areas that should be investigated and understand the system capabilities and limitations. However, despite the significant findings from the screened literature, the following gaps in knowledge have been identified:

- There exists a lot of literature about the different joining techniques, which are currently in use at the automotive industry. However, a benchmark matrix about joining methods could not be found. Additionally, no report studied the most promising outer

panel joining method. There is no cost comparison available about joining methods.

- There is no industry standard available that describes which zinc coating type should be preferred for brazing.

- For the automotive industry, it is important to understand which joining method could be the most common method. No previous study has investigated this important subject.

- There is only limited insight available into focus arc brazing of thin metal sheets. Particularly, great detail about the influence of fundamental input parameters could not be found.

- There is no controlled comparison study (technique and cost) available of laser and focused TIG brazing.

- The literature review has indicated that there is no vision based electrode tip monitoring system available. Such a system is mandatory to study and to quantify electrode contaminations and electrode wear.

- There is no published classification available for braze failures on thin metal sheet joints. It might be that there is no great industrial will to lay down such insights. However, to understand the complex field of braze failures and to define problem solving strategies, it is important to have such a report.

- The influence of the cleanness grade for the soon to be joined panels is still unclear. The answer for the question ‘how clean have the panels to be before joining’ could not be found.

In light of these knowledge gaps, a research agenda was derived, which is addressed in the following chapters.

3. Methodology, Experimental Setup and Procedures

This chapter describes the approaches that have been used for this thesis. In addition, the equipment and the materials used with respect to the conducted experiments. It also describes braze imperfections and the methods for the measurements and tests performed during this project. To bring together these details in one chapter avoids repetition in the text and allows a more fluent reading of this thesis.

3.1 Research Approach

This sub-chapter describes the approaches that have been used to progress the project. To achieve the aim and objectives of this study the project was divided into six main stages.

Stage 1: Initial Project Planning

The project started by outlining the research proposal. Therefore it was important to identify current Plasmatron brazing issues and advantages. Following discussions with the supervisor ensure that the faculty is interested and has the required equipment, facilities and staff expertise to support the research on assessing the viability of Plasmatron brazing. As next step the content of relevance was narrowed down, which assisted to define the draft research aim and objectives. A proposed research methodology and proposed time schedule outlined the provisional execution plan for the project.

Stage 2: Studying the Area

The literature review assisted to find out which BIW joining methods are available and in development. Additionally, it helps to understand what research has been undertaken in the TIG joining field and what difficulties exist. Most importantly, it helps to verify the initial research ideas and assists to refine them. The literature was sourced from academic journals, books, industrial sources and interviews.

Stage 3: Organising Experiments and Investigations

At this stage of the project, a detailed planning of the experiments and investigations was conducted. First, all possible experiments and investigations were collected in a matrix. A following rating assisted to define, which experiments and investigations are the most important to conduct. Based on the results, the required experiment facility and tooling plus the related data measurement apparatuses were defined and organised.

Stage 4: Conducting Experiments and Investigations

Three steps of experiments and investigations were conducted to collect sufficient data to achieve the aim and objectives of the project.

In the first step, a brief benchmark between all BIW joining methods was conducted to get an overview about where Plasmatron brazing stands in comparison to other BIW joining methods. Additionally, adhesive and laser brazing joining studies were performed to allow a closer data comparison against Plasmatron brazing.

In a second step, experiments were conducted to collect data for exploring the influence of the main Plasmatron brazing parameters.

The third step deals with experiments for process integration and post braze processes to tackle current Plasmatron brazing difficulties.

Every experiment got its own experiment methodology, which explains which and why certain methods were used.

Stage 5: Evaluating the research

The gained probes and data of the experiments and investigations were analysed by various methods like tensile testing, microscopic examination, and statistical evaluation. Afterwards, the gained results were critically discussed.

Stage 6: Completing the project

At stage six the main findings, limitations and suggestions for future work that can be undertaken and the concluding remarks were highlighted.

The flow chart in the following Figure 3-1 illustrates the described six main stages.

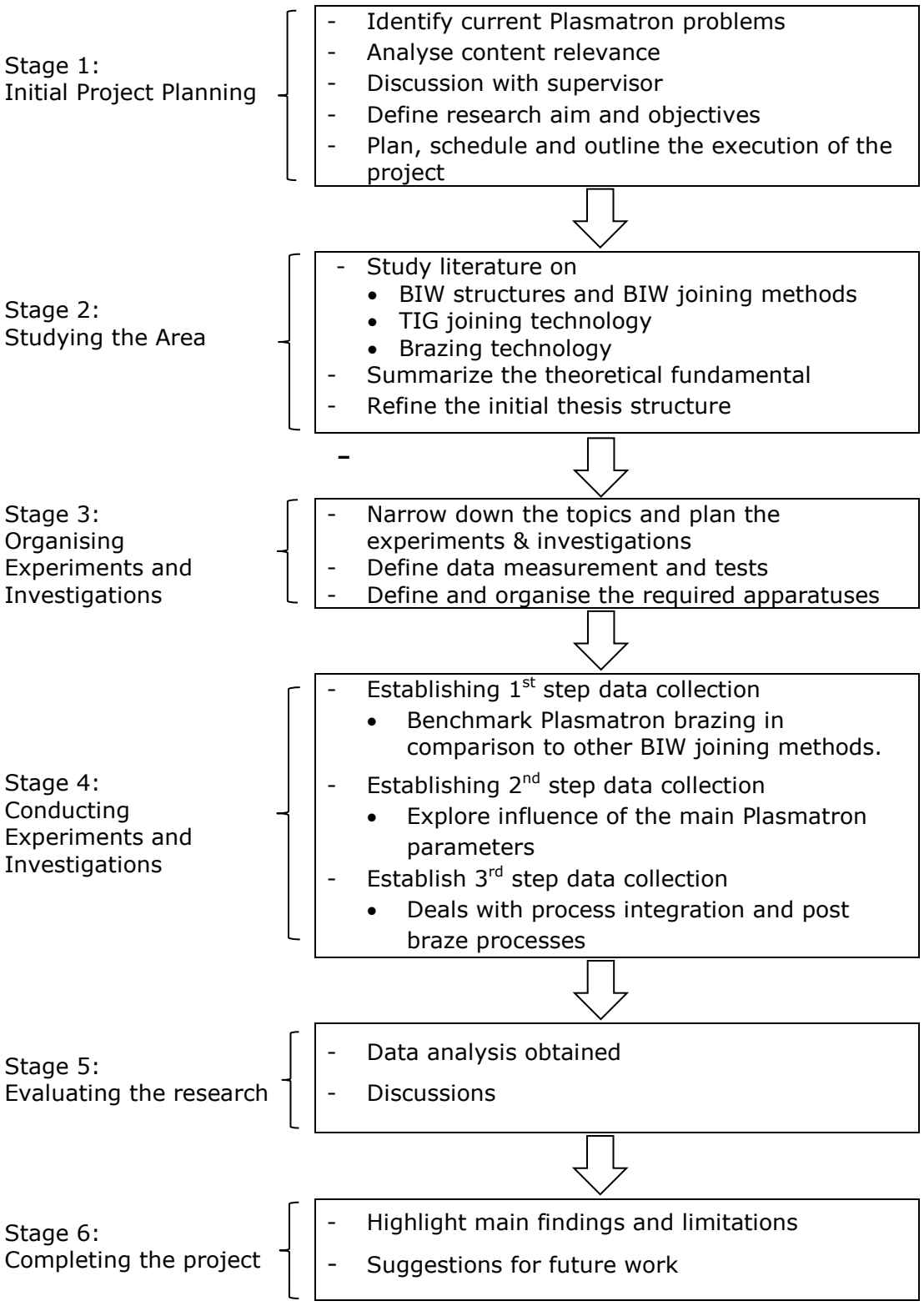


Figure 3-1: Flow chart about the main stages of the thesis

3.2 Test Facilities and Consumables

This section describes general facilities and consumables, which were used at multiple times in the thesis. Specific processes such as scratch testing are described in their own sections later.

Ford has three Plasmatron brazing facilities in use, which cannot be utilized for brazing research experiments because they are incorporated in production lines. The bodyshop managers would not permit the use of these production Plasmatron cells for braze experiments. The risk is too high that the production restart could fail due to misaligned machine parameters. Hence, a Plasmatron test cell was developed at the University of Nottingham.

Additionally, the companies Inocon and Castro supported the author with their TIG and MIG test cells. This was necessary because the University of Nottingham test cell could not always be used. In addition, the usage of other test cells widens the arc joining experience.

3.2.1 Brazing Test Cell at the University of Nottingham

The University of Nottingham brazing test cell consists of a machine frame, which has a Plasmatron head mounted on an adjustable z axis. The wire feed system is mounted with the Plasmatron head, which includes the brazing torch with a 3 mm x 6 mm oval nozzle, a wire core adapter and the wire guiding arm (Figure 3-2). It is used to adjust and direct the wire feed during the brazing process.

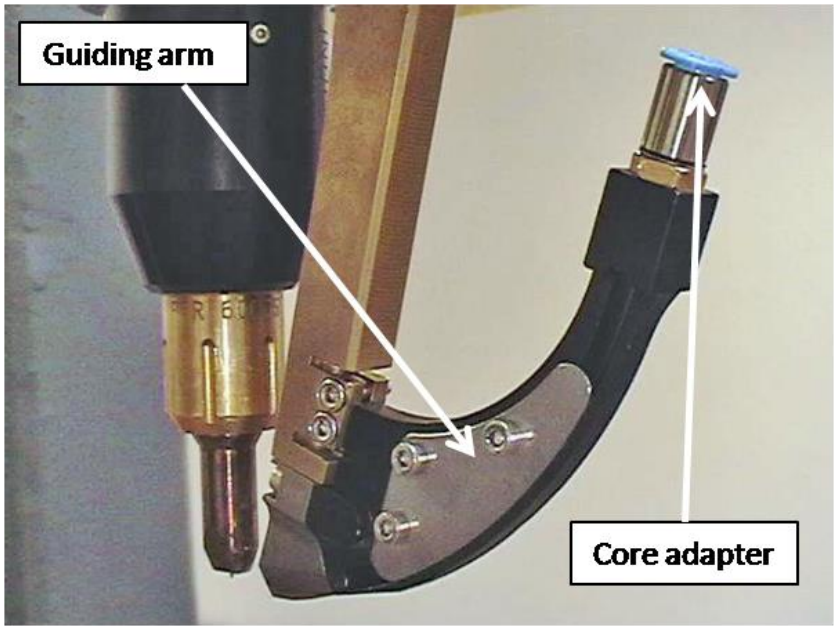


Figure 3-2: Plasmatron wire guiding arm [166]

A stepper motor driven ball screw is mounted behind the torch at the machine frame with its base vertical and its travel in the horizontal (x) direction. A set of two precision rails is mounted off the machine horizontal table parallel to the ball screw. On these a rectangular frame cradle is mounted. The cradle can travel through a maximum of one metre and the maximum traverse speed is 5.0 m/min. The Plasmatron torch connects with a power source (TIG welder) model R-Tech TIG401 by a short hose package. The TIG welder's technical details: input (volts/amps) is 415 V 3-Phase, the TIG has current range 20 A - 400 A and the arc starting mode is HF micro start. The hose package includes one welding cable, two water hoses and one gas hose. The water hoses are used to cool down the Plasmatron nozzle brazing process. The wire feeder is isolated to the ground and has a high performance wire feeder master controller.

The Plasmatron station is controlled by a Siemens PLC (Programmable Logic Controller), which is placed behind the cell. The PLC can adjust the table speed, wire feeder speed and the travel distance of the table.

The design of the Plasmatron cell at Nottingham is shown in Figure 3-3 and Figure 3-4 shows a photograph.

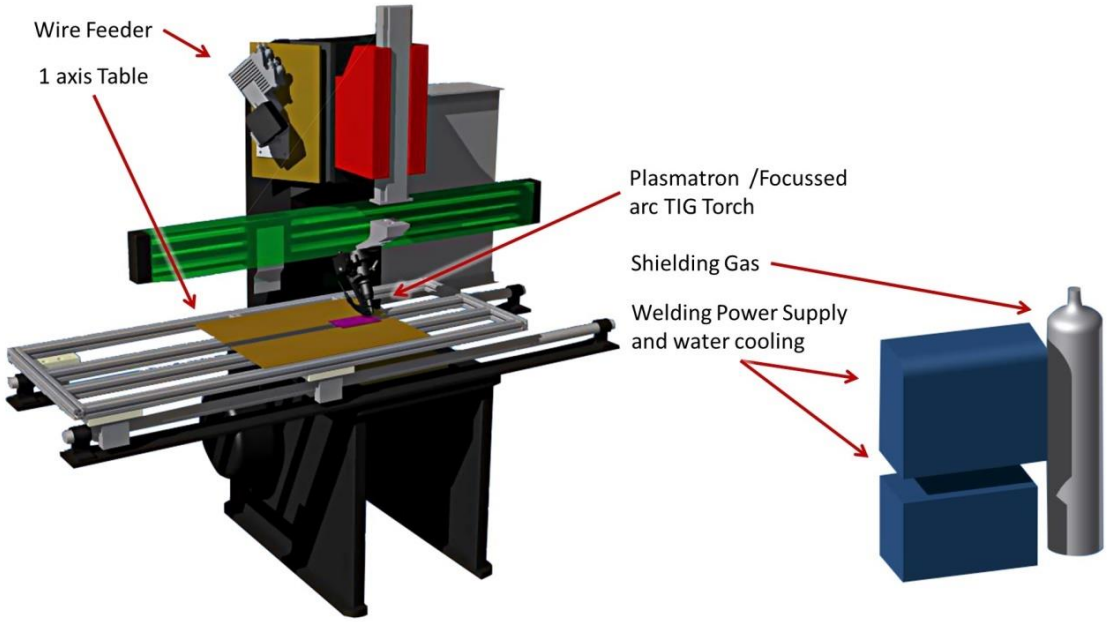


Figure 3-3: Schematic of the Plasmatron cell
at the University of Nottingham [167]

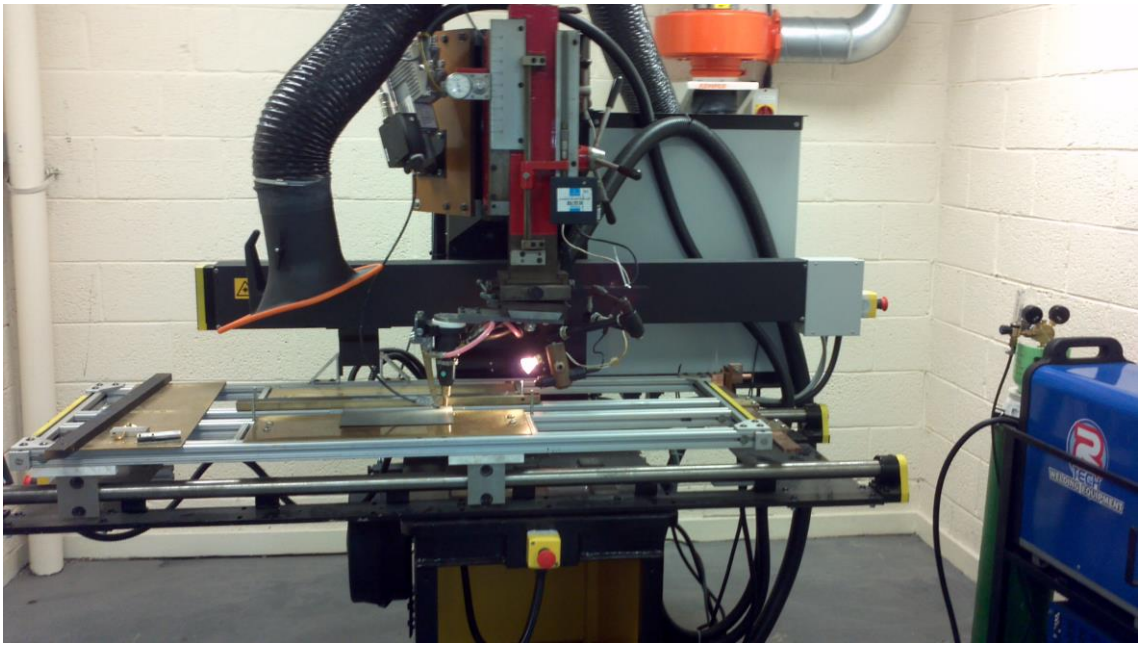


Figure 3-4: Plasmatron cell at the University of Nottingham

Dedicated test panel clamping fixtures were fabricated to simulate the production-clamping situation. The test panels to be brazed were clamped by brass bars to the table and secured by wing nuts on all four corners to a brass plate that was connected to the power source (see Figure 3-5).

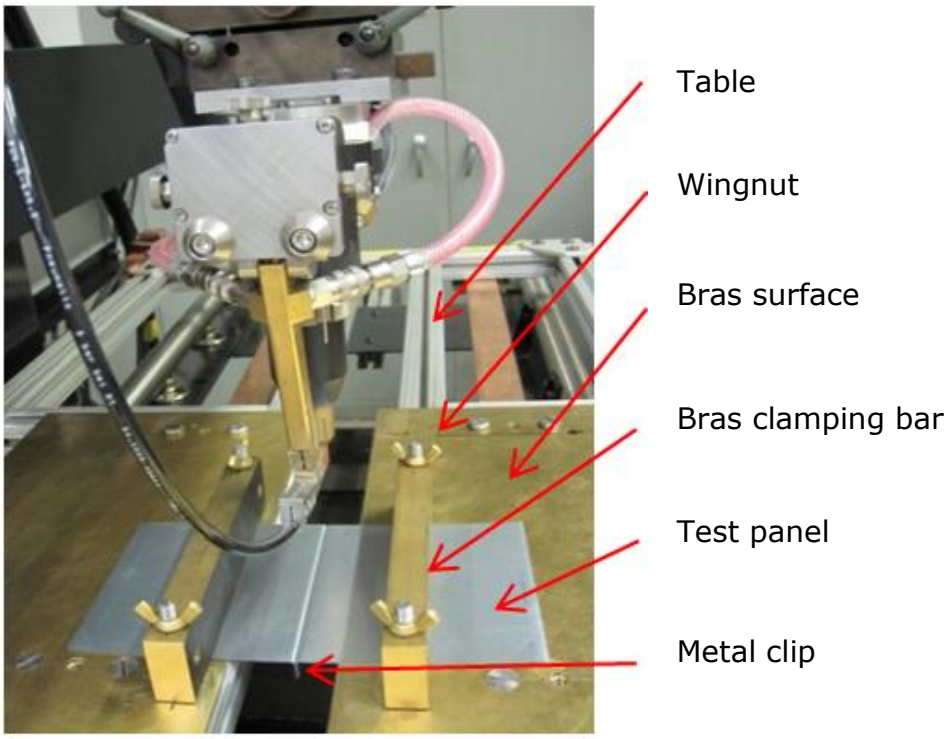


Figure 3-5: Test panel clamping at the Nottingham Plasmatron cell.

When brazing flange butt joints, the test panels were pre clamped from below with metal clips to ensure a zero gap joint before full fixing in the braze cell (see Figure 3-6).

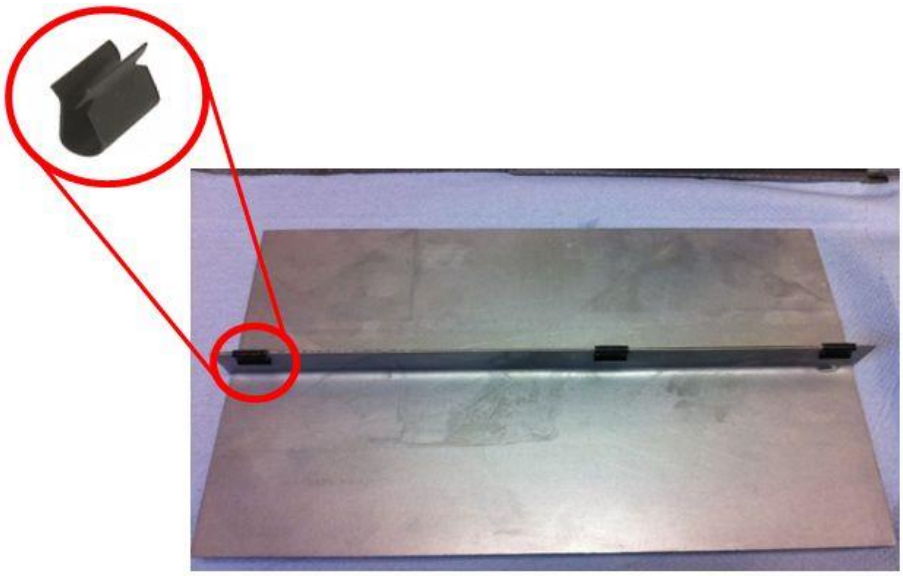


Figure 3-6: Metal clip pre clamping
to ensure zero gap on flange butt joint test panels.

In a production system, a Plasmatron torch is attached to a robot actuator and then it is used to braze across static work pieces. The approach at the University of Nottingham uses a fixed Plasmatron torch to braze moving work pieces as they pass below it. The latter approach has been chosen to eliminate variations of the robot in position and control, allowing only the Plasmatron system to be assessed. This cell was used for the experiments that were conducted in Chapter 5.

3.2.2 Brazing Test Cell at the Company Inocon

The Inocon Plasmatron test cell in Attnang-Puchheim (Austria) was used since it is able to simulate the production environment more closely than the Nottingham test cell. This is because the test cell is equipped with a six-axis jointed-arm robot instead of a movable table. The test cell as shown in
Figure 3-7 consists of a Plasmatron brazing torch with a 3 mm x 6 mm oval nozzle, an Inocon wire feeder, a Fronius MW 5000 TIG welder power supply and an integrated ABB robot with a controller.

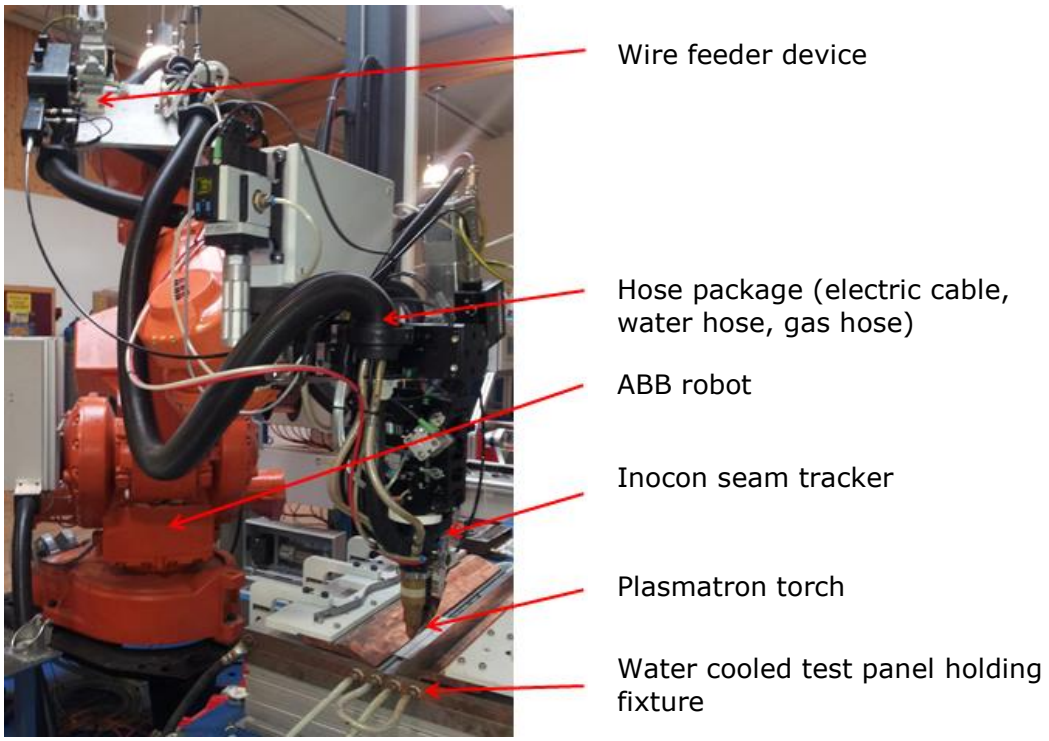


Figure 3-7: Overview of the Plasmatron Test cell at Inocon.

Furthermore, an Inocon seam tracker is integrated in the brazing head to ensure that the brazing torch and wire repeatedly follow the joint, and guarantee a consistent brazed seam. A test panel clamping fixture which simulates lap joint production part fixing holds the test panels in position during brazing. The robot was programmed to run the joint path in a manner to simulate production environment.

3.2.3 Welding Test Cell at the Company Castro

One experiment was conducted in collaboration with the company Castro in Augsburg, Germany. The reason for asking Castro to collaborate was their positive welding experience in the welding of fine seams due to their gas chamber usage. Castro stated that their key for success is the completely isolated inert gas atmosphere due to their gas chamber. Their oxygen reduced glove box welding system utilises a TIG head with a tungsten electrode like the Plasmatron system but with a standard TIG nozzle instead of an arc focused nozzle. Opposed to the Nottingham and Inocon brazing cells, the Castro cell did not utilise filler material.
Figure 3-8 shows Castro's glove box, including the Castro RB100 six axes robot.

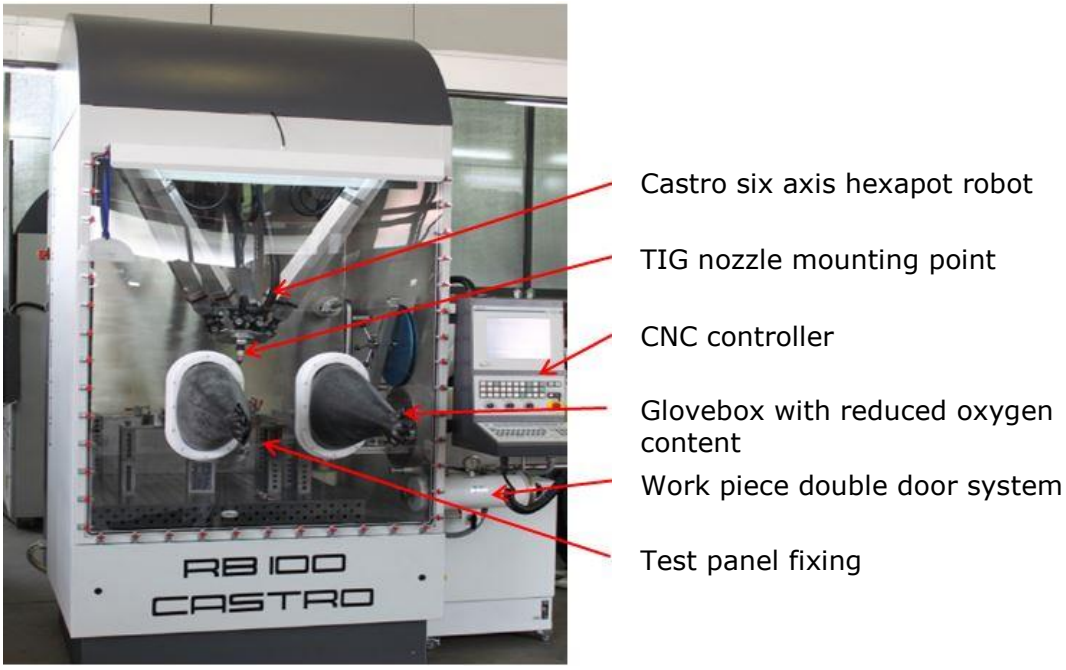


Figure 3-8: Castro TIG welding gas chamber with a Castro hexapod robot.

This cell was used to study if the glove box shows benefits regarding electrode contamination by brazing of zinc coated steel panels (see chapter 6.1.1).
The glove box is equipped with an oxygen sensor for measuring the oxygen content in the glove box from ppm (parts per million) level. In the front, two glove ports with butyl gloves give access to the inside of the glove box. At the right side wall, an airtight door is integrated for loading and unloading the goods.

3.2.4 Process Consumables

Due to the amount of experiments, it was decided to list all for the experiment important process consumables in the related experiment methodology. Following is a description of the main consumables only.

3.2.4.1 Test Panel

The test panel materials used in this research are all from cold rolled, low carbon steel for high formability that represent those typically used for outer skin panel material in the automotive industry. This steel grade was developed for extremely high cold forming behaviour requirements. In particular, for extreme deep drawing strain and for the manufacturing of complicated outer skin press parts in rapid processing and highly automated press lines. Table 3-1 shows the compositions of this steel grade, which is labelled in the European norm EN 10130 : 2006 as DC06 [168].

Table 3-1: Chemical composition of used steel grade DC06 [168]

C	Mn	P	S	Ti	Fe
max 0.02 %	max 0.25 %	max 0.02 %	max 0.02 %	max 0.3 %	rest

For these experiments, typical outer body steel panels were organized with standard automotive zinc coat types like galvanized (GI), galvannealed (GA) and electrolytically galvanized (EG) coat. In addition,

two new coating types were used: MagiZinc® from the company Tata and GI-Ace® from the company Posco. The used test panel coatings are shown in Table 3-2.

Table 3-2: Used zinc coating types on DC06 steels

Coating Type	Layer composition	Coating weight/side (g/m^2)	Coating thickness (µm)
GI: Standard hot dip galvanized, excellent formability, cost effective	Zn + < 0.50 % Al < 0.38 % Fe	57	8
GI Ace: hot dip galvanized, new development, very fine Zn grain size	Zn + < 0.5 % Al < 0.38 % Fe	57	8
GI-MagiZinc: hot dip galvanized, new development, thinner coating	Zn + 1.8 % Al 1.8 % Mg < 0.17 % FE	35	5
GA: galvannealed, presence of iron, better weldability	Zn + 10.2 % FE	41	6
EG: electrolytically galvanized	100 % Zn	36	5

MagiZinc® is an innovative new thin hot dip zinc coating alloyed with aluminium and magnesium. According to Tata [169], this coat delivers an improved resistance to corrosion and stone chipping. As well, the coating thickness, and therefore weight, was reduced.

According to Posco [170], the new GI-ACE® zinc coat has a few benefits to normal GI coat. Due to the finer spangle surface, the coat shows less flaking-off zinc particles, an increased corrosion resistance and less oil stain trace. Posco achieved these benefits due to their electrostatic water aerosols charge when the steel strip left the zinc pot.

Simple bead-on-plate brazes were used to test the equipment and the first parameter set-up. For all other experiments, special test panels were produced to simulate the currently most used outer skin braze joint types in the automotive industry. To simulate a vehicle brazed roof joint and the lift gate braze joint design, some test panels were flanged. The inside radius for these 90° bents was 3 mm ± 0.1 mm. The lap joints design was

used to simulate D-pillar drain trough joint. For several experiments real production parts or cut outs from real production parts were used.

3.2.4.2 Electrodes

WLa20 electrodes, which contain 1.8 - 2.2 wt.-% of dispersed lanthanum oxide, were chosen for all TIG joining related experiments. "La" stands for lanthanum. The advantage of this electrode type is its good ignition behaviour in the low current range and a low tip erosion rate in comparison to other tungsten electrode types [144]. Table 3-3 shows the chemical composition of WLa20 electrodes.

Table 3-3: Chemical composition of WLa20 tungsten electrodes [171]

Classification Symbol	Principal Oxide	Mass Percent	Impurities, Mass Percent	Tungsten, Mass Percent
WLa20	$La2O_3$	1.8 to 2.2	0.5 max	Balance

The Plasmatron torches in the Ford plants utilize 4.0 mm diameter WLa20 electrodes with a top angle of 20^0. These electrode settings were used for all Plasmatron brazing experiments as well. Figure 3-9 illustrates the electrode dimensions.

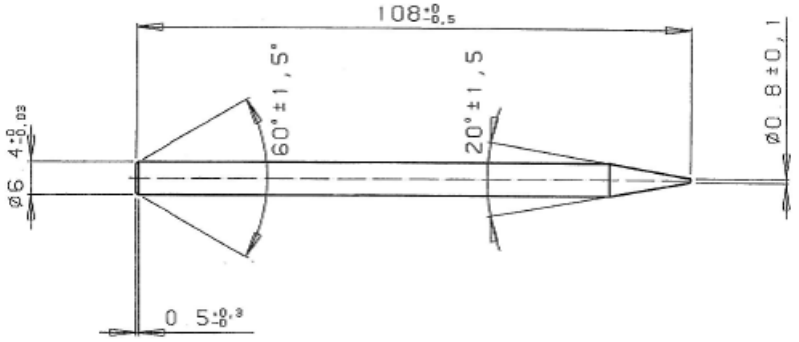


Figure 3-9: Electrode profile for a Plasmatron torch [172]

3.2.4.3 Filler Wire

SG-$CuSi_3$ wire according to ISO 24373:2008 [173] represents the standard filler metal wire which is released by most European vehicle manufacturers for braze joints on zinc coated steel panels. This wire type has excellent flow behaviour, the required strength and the required lifetime stability. The yield strength of its brazed deposits is approx. 260 Mpa. The melting range of the $CuSi_3$-alloy is between 910 and 1025°C. This wire is available in 0.8, 1.0, 1.2, 1.6, 2.0, 2.4, and 3.2 mm diameter. For the Nottingham and the Inocon brazing cell the 1.6 mm wire diameter was chosen as fixed parameter, because the Ford roof to bodyside joining process uses this diameter. Table 3-4 lists the chemical compositions of the $CuSi_3$ wire as defined in ISO 24373:2008, with the exception of the silicon content, which was reduced to maximum 3 per cent. A lower silicon level results in better paint adhesion. This is because silicon is highly hydrophobic and the modern environmental friendly automotive paint shops using water based paint.

Table 3-4: Chemical composition of $CuSi_3$ filler metal wire

Chemical Composition	Cu	Si	Sn	Zn	Mn	Fe
(%)	> 94	2.8 – 3.0	< 0.2	< 0.2	0.5 – 1.5	< 0.3

3.2.4.4 Gas

Argon is a suitable gas for arc brazing and is more suitable than helium for TIG joining in the automotive industry. Excellent arc starting, ease of use and the relative low cost make it the most desirable shielding gas for arc joining applications in the industry. Helium has a better conductivity and a high ionization potential, which results in a higher heat input [174], which is not required when brazing. Due to this fact, plus the much higher helium price, it was give up testing helium and other inert gas types or gas mixtures. Argon in the standard shielding gas purity 4.6 (*99.996* vol. %) according to DIN EN ISO 14175:2008-06 [175] was

chosen to create the plasma column and as shielding gas for all experiments.

The gas flow rate can have significant effects on the results of arc brazing. If the gas flow is too high, it might be possible that the gas deforms the melt pool [176]. Initial experiments showed that a flow rate of about 8 l/min provides good results [132]. Therefore, the gas was set up at 2.3 bar and 8 litre/min, unless otherwise noted in the experiment details. The flowrate of argon was controlled by flow meter.

The gas flow was initiated ten seconds before braze to clean the gas pipes and stopped ten seconds post braze to allowing the electrode to cool and solidification of the melt pool.

3.3 Description of Braze Imperfections, Measurements and Tests

To analyse the experiment results, it is important to get as much measurable data as possible. This increases the quality of the experiment and makes it easier to compare the results of different experiments. The author can as well identify which brazing specimen or electrode gives the optimum joint quality and trace back to find the parameters that affect the quality.

The following sub-chapters describe braze imperfections, the primarily used measurements and tests.

3.3.1 Braze Imperfections

To analyse and to improve brazing, a given brazing system is mandatory to:

1. Understand brazing imperfections and how they occur
2. Understand the best method to detect imperfections (in- offline, destructive testing like tensile test, microscope investigations etc.) in the industrial context
3. Understand how braze imperfections are to be assessed
4. Propose quality limits for brazing imperfections

Extensive work has been carried out to examine the significance of imperfections for welded joints. Barely any work has been carried out for brazed joints, and work on welded joints is rarely relevant to brazed joints due to the differences in geometry and relevant stress mechanisms [177]. For example, the significant penetration of the base materials, which is typical for welding processes, leads to several fundamental differences in comparison to brazing. These differences include the metallurgical composition, heat distribution, joining temperature and reaction times. Hence, few results are truly transferable.

The European Standard 18279 'Brazing – Imperfections in brazed joints' from 2003 [177] provides some details for classifying imperfections that can occur in brazed joints. This norm classifies imperfections in six groups as follows:

1. Cracks
2. Cavities
3. Solid inclusions
4. Bonding imperfections
5. Shape and size imperfections
6. Miscellaneous imperfections

A further distinction is made between external and internal imperfections that may occur in brazed joints [177]. The ISO labels 'surface-breaking porosity' as an external imperfection. This classification would be correct for standard brazed seams but not detailed enough for the automotive industry. A roof seam could appear to be acceptable when viewed from the exterior, but the other side of the brazed roof joint could show surface-breaking porosity. Therefore the term 'external imperfections' could be misleading. The terms 'external visual imperfections' would be clearer and more appropriate for use by the automotive industry.
This standard, however, does not describe requirements for acceptable levels of imperfection since these will differ very markedly, depending on the application. There is no published classification available for brazed automotive outer skin panels. This might be because this joining method

has only become established within the last few years. The OEMs that are using this joining technology already do not share their knowledge in order to maintain their lead.

3.3.2 Requirements for Brazed Outer Skin Panels joints

Brazed joints usually contain imperfections of various types, some are harmless like minor internal porosity and others will be detrimental. For example, imperfections that affect the structural integrity. This depends entirely on the service requirements of the joint in question. Therefore, it is important to understand the requirements that a brazed joint has to fulfil.

In the first place, it is important to understand the needs of the automotive user and the safety requirements for the brazed outer skin panel joints in the vehicle system it will be applied.

As an example, the following list shows the main requirements for a brazed roof joint.

- Sufficient strength of the brazed roof seam to fulfil the vehicle torsion and crash behaviour over the complete vehicle lifetime, as well as under increased conditions like bumpy roads, installed loads like a roof rack system and high temperature differences. Exact strength targets are based on case-by-case finite element analysis, performed during the vehicle design phase. These targets will be verified later in vehicle durability tests as part of the so called verification prototype phase (VP). The VP builds are production intent vehicles, which are manufactured in the pilot plant approximately one year before production start.

- Sufficient corrosion protection under increased conditions like heavy rain and salty winter roads. The related test procedure is a design verification method for a 12 weeks long test at Ford. This test represents 6 years in service for the worst ten per cent of vehicles in markets of northern Europe and northeast USA/Canada. The test consists of a Monday through Friday daily four hour repeated driving

program on special prepared tracks (dust, mud, grit, salt bath, etc.). For the rest of the time, the vehicle is contained in a climate chamber with a controlled humidity program [178].

- A visually pleasing seam, which means a smooth surface, no holes, no waves, nice seam start and seam end. At Ford, product deployment composes visual quality targets for every single braze joint design. The target in these specifications depends on the customer expectations for the related joint area.

- The brazed roof seam should be water proof. Under no circumstances should water penetrate into the vehicle. Ford tests their vehicles with a dynamic 5-minute long water leak inspection in a special water test booth. Every new vehicle has to run through this spray line booth before it leaves the final assembly building. In addition, randomly selected vehicles will be tested every production day in a 20-minute static water test [179].

3.3.3 External Visual Imperfections

The following sections describe braze defects that can be identified through visual examination of the seam surface.
Most of these external visual braze defects can be repaired. However, repairing brazed seams should be avoided as much as possible in a high production environment. Only with a significant effort on space, investment and headcount is it possible to repair defect seams in a high volume plant. The parts or vehicles have to be separated from the production line through special transfer stations and to be buffered in space consuming repair stations before a manual repair can be carried out. These repairs destroy the build sequence of the production shift as well. The repaired vehicles for example have to be manually inserted in the production line and in the plant vehicle scheduling system later, which always requires a large expenditure.

3.3.3.1 Brazed Seam Width

The width of the brazed seam observing from the top-view of the joint is indicated as D (see Figure 3-10). A target value for D was set at 2.5 ± 0.5 mm. This represents the quality target from a brazed vehicle roof joint. All brazed test panels were checked if they reached this target.

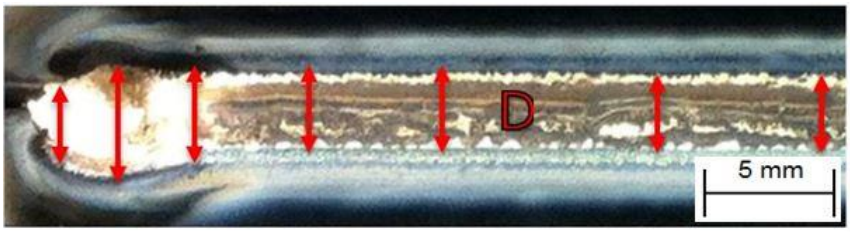


Figure 3-10: Brazed seam width measurement example

3.3.3.2 Incorrect Linearity

This failure occurs when the braze does not follow the planned seam contour. Figure 3-11 shows an example. The cause is mostly an unstable robot arm or an unstable seam tracker. The brazing cell has to be stopped and repaired as soon as possible. An uneven joint is not acceptable and cannot be reworked. If the defect is too large, this rating depends on the product development requirements; the part has to be scrapped.



Figure 3-11: Wavy brazed seam
cause due unstable robot arm or unstable seam tracker

3.3.3.3 Discontinuous Braze

Discontinuous braze, as well called "underfill imperfections", have a profound effect on the function of the seam. Apart from the poor optical appearance, the defect inhibits the distribution of loads across the affected

area. This influences the overall strength of the brazing seam. Additionally, the seam might not provide a watertight seal. As a result of these defects on the functionality of the seam, the affected seam must be repaired. If a repair is not possible or the defect is too large, this rating depends on the product development requirement; the assembly may well be scrapped.

ISO 18279 [177] does not describe underfill imperfections in detail. In the interest of the automotive industry, this failure type should be defined further.

An adhesion defect occurs when a correct filler material bridge fails to develop between the metal surfaces being joined. This type of error can occur throughout extended parts of the seam. An example can be seen in Figure 3-12. The gap between two brazed metal panels, here a flange butt joint, should be not greater than 0.3 mm. From Ford experience, it was observed that a 0.2 mm gap is the best gap size for a flange butt joint.



Figure 3-12: Discontinuous seam
occurs due to large panel gap or missing filler wire at a flange butt joint.

Another reason for an underfill defect can be characterized by insufficient braze alloy due to missing brazing filler. Generally, this defect is related to an error in the filler material feed or to high brazing speed.

Insufficient heating during the brazing process can cause a lack of melting of filler material as well and lead to a discontinuous brazed seam.

3.3.3.4 Surface Cracks

Cracks in the surface of the braze might occur due to an inhomogeneous temperature distribution through the seam during the heating and cooling phases. Every crack is a potential weak spot of the joint. Surface cracks are very rare on braze joints in the bodyshop. The Ford quality monitoring system, which collects all customer complaints, does not highlight any

customer complaints regarding a surface crack on a brazed roof during the last view years [180].

3.3.3.5 Surface Breaking Pores

Another external defect is the formation of pores on the seam. Pores that are open to the exterior decrease the aesthetic quality of the seam. Single pores caused by bubbles in the filler material for example only have marginal effect on the structural integrity of the seam but have a high disappointing effect for the customer when they detect for example pores on a brazed roof joint on his brand new vehicle. Figure 3-13 shows a section of a seam affected by pore formation.

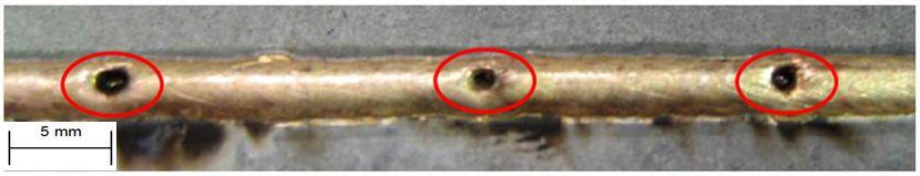


Figure 3-13: Seam with pores;
the red circles highlight surface pores in a brazed seam.

Palmquist et al. [181] estimated that between two and four per cent of the brazed joint comprise surface-breaking pores. Porosity is thought to be caused by impurities in the filler material and impurities or defects in the surfaces to be joined. By lowering the impurities in the filler material and the contamination of the surfaces, the percentage of surface-breaking pores can be lowered. Oil contaminations vaporize at approximately 350°C and zinc at 907°C. The pressure of theses vapours can generate bubbles in the molten filler material, which leads to pore formation.
Surface-breaking pores can be eliminated by finishing of the brazed joint (e.g. polishing, grinding or filling), but this technique is time-consuming and labour-intensive. Pores in the brazed joint will tend to have negative effects on the physical properties (e.g. strength) of the joint, and surface-breaking pores are a particular problem in applications requiring a smooth finish. This is especially relevant for brazed joints which are to be painted, as surface irregularities or surface-breaking pores may also be evident after painting [181], as for example a brazed vehicle roof.

A visual inspection is not able to differentiate between superficial pores and pores that extend to the interior of the seam. Pores that continue through the entire depth of the seam permit the intrusion of water, leading to corrosion.

Figure 3-14 presents two examples. Two pores are shown that are similar in appearance and size. An examination of the cross section of the seam reveals that one pore is a superficial pore while the other passes all the way through the seam. The variable size and sporadic occurrence of pores makes their detection in a high volume production extremely challenging [182].

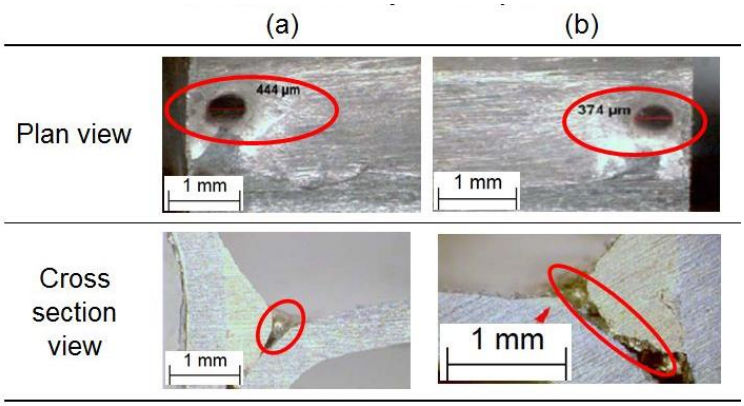


Figure 3-14: Two different seam pore types;
(a) superficial pore which does not pass completely through the seam;
(b) pore which passes all the way through the seam.

To repair brazed seams with small surface pores (for example < 0.3 mm diameter, the size depends on the specification), cosmetic repair methods can be used. As a first step, the true sizes of the pores need to be determined by using a punch or a drill in order to correctly fill the pore with a PVC sealer. However, the sealer would slightly shrink when the BIW is painted and dried in the oven but that does not affect the seam significantly if the defective area is small. For this reason, this method of repair is not appropriate to be used to repair defective seams that are above a certain length (~ 5 mm). The maximum repair length depends on the used paint shop temperature and has to be determined during testing. In general, seam surfaces should be free of pores.

3.3.3.6 Spatter

Spatter of filler material frequently leads to filler residue left on the base materials in the vicinity of the brazed joint. Since joined surfaces exclusively form part of the vehicle exterior and filler residue leads to decreased optical quality of the brazed joint, it is imperative that this type of defect is avoided. The source of spatter is usually traced back to a localized excessive energy input or material defects. Since the parameters affecting spatter can be directly controlled, it is unlikely that spatter will be a significant source of defects after process optimisation has been completed. Figure 3-15 shows a brazed seam with spatter. These minor aesthetic defects have to be ground before the vehicle moves into the paint shop.

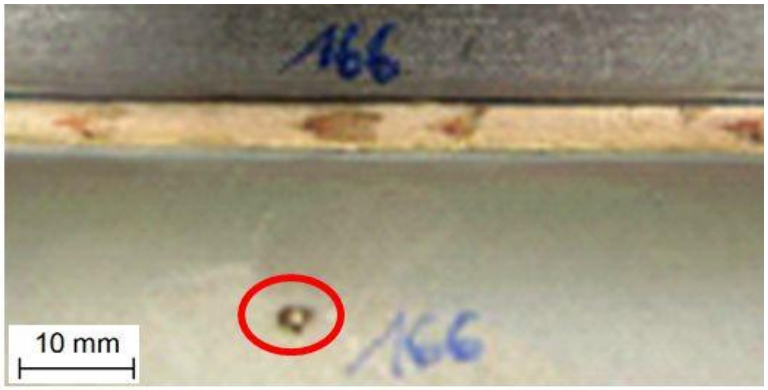


Figure 3-15: Braze seam with small brazing spatter [14]

3.3.3.7 Excessive Residues

'Soot' is an unwanted by-product from the incomplete combustion of carbon-based materials for the generation of energy or heat, or for the disposal of waste [183]. Soot usually consists of quasi-spherical particles ranging from about 10 nm to about 500 nm in size, which are often joined together in clusters. In most soots, these particles are accompanied by a poorly defined mixture of ash, polyaromtic hydrocarbon, and inorganic material [184].

A welding study in this field highlighted that in ninety-nine per cent of all cases, this unwanted black soot came from impurities, which was burned to carbon [185].

With regards to black lines next to brazed seam (see Figure 3-16, red encircled area), the usage of the term "black soot" might not be completely correct by the above mentioned definition because it does not consider the partly included zinc particles, which merge the soot during the rapid heat-up phase from the Plasmatron arc. However, this thesis uses the term "black soot" when it comes to unwanted black lines next to a brazed seam.

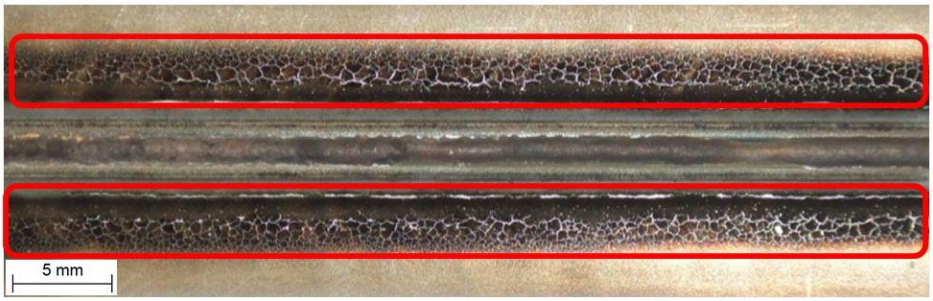


Figure 3-16: Black soot lines next to a brazed seam (see encircled areas) [90]

White residue, mainly on the reverse side along the brazed joint, is a sign for an overheated braze process. The zinc from the zinc coated steel panels tends to overheat, causing rapid oxidation with the formation of white powdery zinc oxide (ZnO). This is given off as white deposit on the work and white fumes [186].

These black and white residues on the surface of brazed work pieces around the braze bead should be minimized because they will affect the following paint processes and lead to unacceptable paint quality [187]. Especially on white painted vehicles, the black soot on the steel panels could be visible as light marking.

The reduction of residues during brazing of zinced steel panels is an interesting investigation field. Several attempts [188] have been made to avoid this kind of imperfections but until now there is no solution. Also, there is little known if black soot really has a negative effect on the paint

quality. Nowadays the black soot will be mostly brushed away in the bodyshop before the body moves to the paint shop. For the automotive industry, it would be very important to understand if this operation could be abolished, because this would save investments and work time. Residues not only affect the optical appearance of a seam, they also can interfere with optical seam quality control systems. Consequently, the occurrence of surface deposits on brazed seams should be avoided.

3.3.3.8 Rough and Rippled Seam Surface

A rippled and or rough surface of the brazed seam decreases the optical appearance of a brazed seam. Strength and functionality are often not affected by this type of defect. This defect appears more clearly after paint or clear coats have been applied, due to the increased light reflection of the coated surface. Practical experience has shown that these imperfections can easily be detected in cross section view under optical microscopy. Bodyshops usually have master reference samples to assist the go/no-go filter. Figure 3-17 shows an example of a rippled joint. This kind of imperfection can be repaired with a grinding disc in the bodyshop. Only trained operators should do this repair because too much material could easily be removed due to the low outer skin panel thickness (~ 0.7 mm). The surface roughness Ra should not exceed 1.7 µm as already mentioned in Chapter 2.2.

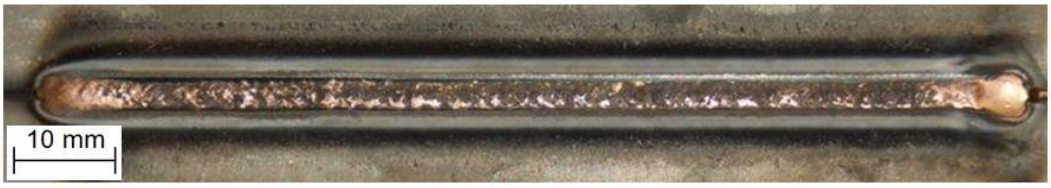


Figure 3-17: Example on seam surface roughness

3.3.3.9 Defects on Beginning or End Sections of a Seam

The beginning and end sectors of a brazing seam are especially sensitive areas in a brazing process. Since the panels being joined tend to round off at the ends, the space to be filled by the filler material becomes larger.

During brazing, a heat wave precedes the actual brazing process and pre-warms the materials. In the beginning of a seam, this pre-warming has not yet occurred and so the chance of a brazing error increases. In addition, the acceleration and deceleration of the robot/stage is a potential failure cause on a beginning or end section of a seam. Figure 3-18 shows a bad seam start from the plan view (a) and from a cross section view (b). This defect is not only a visual issue because most of the base material has melted, which can be seen in the cross section view (b).

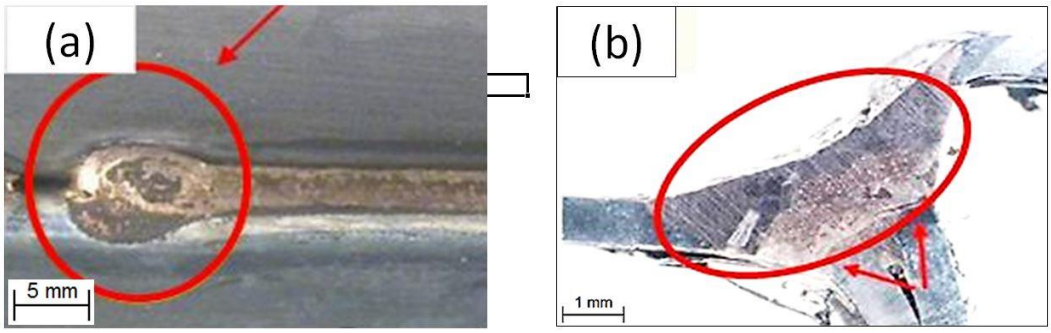


Figure 3-18: Brazed seam start imperfection;
(a) top view, (b) cross section view from this similar seam section which shows melted base material.

Towards the end of a brazed seam, the heat caused by the brazing process has no material in front of it to dissipate into, and overheating of the joining materials can occur. This effect leads to localized melting of the materials being joined at the end of the seam. Additionally, the precise clamping of the panels is very important because otherwise the robot does not locate the exact start and end point of the seam. All these interactions have to be considered from the brazing cell designer and launch teams perspective.

The roof seam quality in the beginning and end sections of the seam play an important role in creating the necessary torsional strength and rigidity of the entire vehicle. These types of defects need to be costly repaired in order to ensure that the required strength is given. Plants use manual TIG brazing equipment for this kind of repair. In contrast to a structural repair, a cosmetic repair is a repair with sealer or glue. This serves to improve the appearance of the seam without increasing the strength of the seam.

Figure 3-19 shows a seam end of unacceptable quality (a) and a seam end of quality (b).

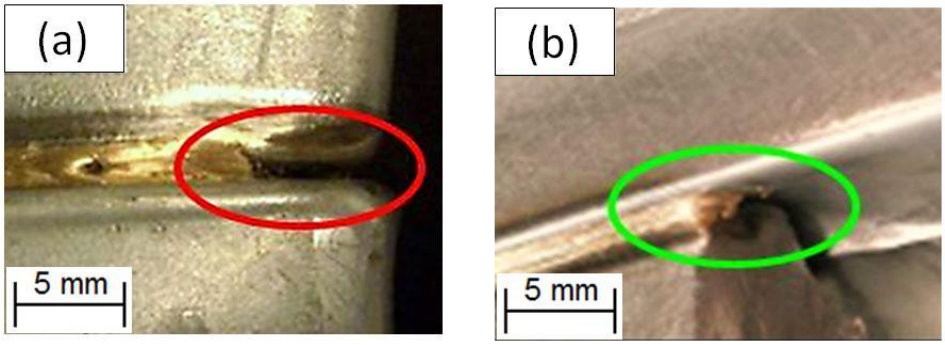


Figure 3-19: Defect on end section of a brazed seam;
(a) unacceptable brazed seam end, where the last 5 mm are not brazed;
(b) good brazed end with braze until the end of the joint.

3.3.3.10 Panel Distortion

Thermal residual stresses during the heating and cooling process from brazing temperature and after cooling can cause significant panel distortions. The main reason for this failure is excessive brazing temperature caused due to low braze speed, unsteady braze speed or too much electric power. Distortions could also occur because of mechanical tensions build up due to not proper matching panel flanges, due to incorrect panel clamping or a mixture of both. This failure can even cause incomplete joint penetration due to an inadequate joint clearance at brazing temperature. To check if there is any panel distortion, the bodyshop expert can use a special whetstone, which he strips physically over the surface. Using this method, it is quite easy to detect panel distortions due to discontinued grinding marks on the panel. Figure 3-20 describes the principle of this checking method.

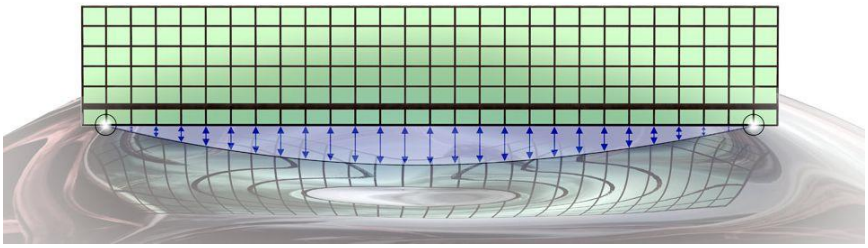


Figure 3-20: Principle of panel distortion detection with a whetstone [189]

3.3.4 Internal Imperfections

The previous chapter described defects that can be detected through external examination of the brazed seam. This section describes defects that occur internally and cannot be detected by examining the surface of the brazed seam. They are all related to the inner surface quality of the brazed seam which can only be analysed with laboratory equipment.

3.3.4.1 Internal Pores

Internal pores are gas bubbles trapped in the solidified filler material (see Figure 3-21). This type of defect can create some danger for the joint strength. Bubbles located near the surface of the brazed seam can burst during heating inside the paint drying oven. The burst bubble exposes untreated copper filler material to the exterior. This weakens the protective coating and compromises corrosion resistance. Uncontrolled accumulation of internal bubbles in a brazed seam can also decrease the structural integrity of the seam. Experience has shown that the diameter of a pore shall not exceed 0.3 mm and the upper tolerance limit for encapsulated porosity should be maximum ten per cent of the test section surfaces [190]

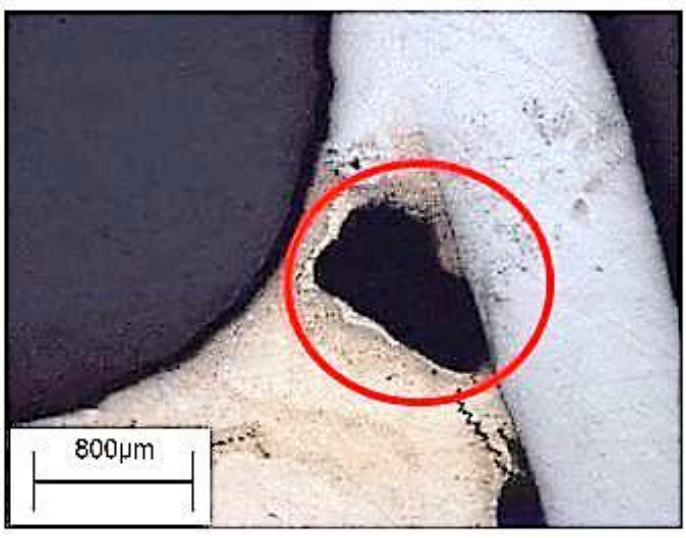


Figure 3-21: Braze joint cross section cut from an internal pore.
The seam surface is intact.

3.3.4.2 Inclusions

Base material surfaces contaminated by dust etc. can lead to inclusions in the brazed seam (see Figure 3-22). These particles can lead to a decrease in joint strength. The upper tolerance limit for inclusions depends on the specification. Generally, Ford does not allow more than twenty per cent inclusions at the cross section surface. Dust particles could lead to braze inclusions. It is important that the panels are oil free because dust could stick easily to the oily panels during storage and transportation.

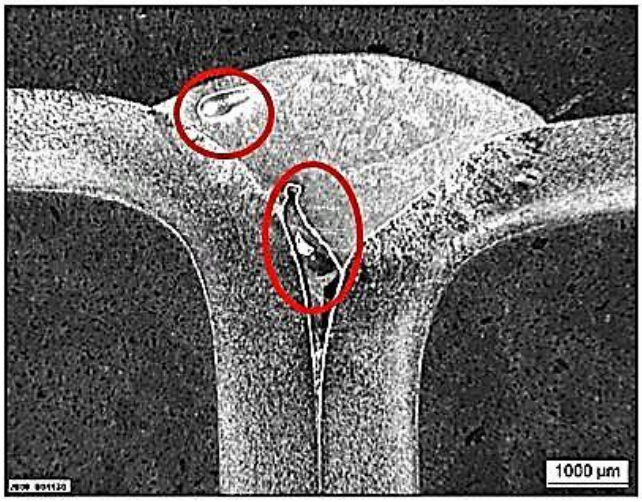


Figure 3-22: Braze joint cross section cut which shows inclusions [190].

3.3.4.3 Internal Cracking

When cracks are not visible on the seam surface, it does not provide assurance that the braze is crack free. Often they are only visible at the cut-out section.

The seam should be free of cracks either on the filler material, in the heat affected zone or in the parent material as these hinder the performance of the overall work piece as well as the possibilities to propagate further. Cracks normally occur during the solidification process due to the inhomogeneous heat distribution in the joint. Figure 3-23 shows a photo from a crack in the parent metal. Cracks can occur because of unequally distribution of heat during brazing process as well as through the cooling process.

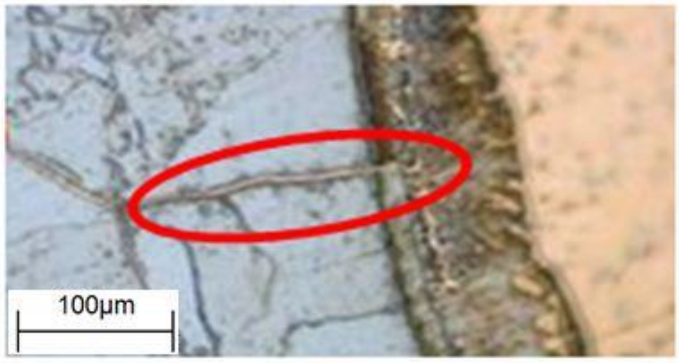


Figure 3-23: Braze joint cross section cut,
which shows stress cracking in the base metal [190].

3.3.4.4 Melting of Base Materials

Melting of the base material can occur as shown in Figure 3-24. Excessive melting of the base material can cause a change in microstructure and a loss of strength.

Additionally, a mixture of liquid base material and filler material can also lead to a loss of strength. Therefore, this kind of imperfection is very serious and has to be avoided. On some brazed joints, this is visible at the surface in the form of a blue coloured seam. Mostly, this kind of imperfection can be detected after cutting the seam and following microscopic inspection only. Figure 3-24 shows a microscope section photo where the steel base material was melted (red circled area) and a photo from a joint without base metal melting. This melt led to the formation of intermetallic phases.

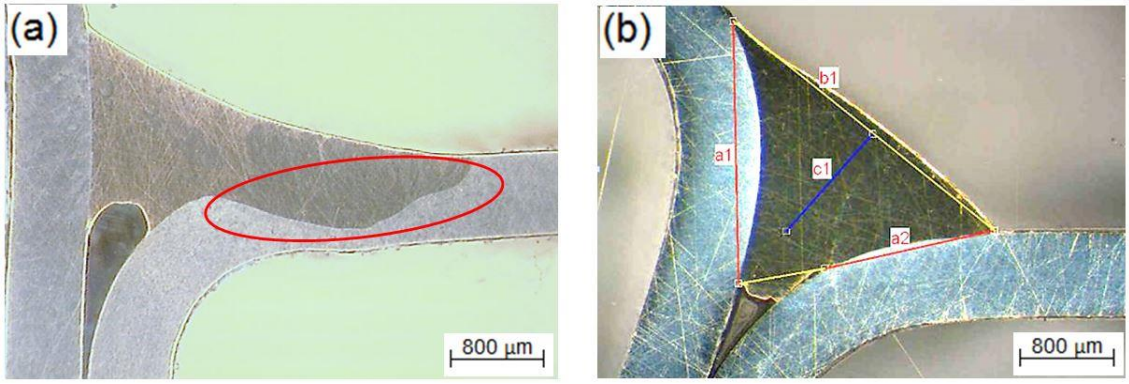


Figure 3-24: (a) shows melting of base material;
(b) as comparison, braze joint without base metal melting.

A comparative hardness measurement series (nine measurements) between the non-influenced area and the intermetallic influenced area showed that the hardness increased up to three times in the intermetallic affected area. The CuSi3 filler reached an average hardness of 115 HV 0.05 (point 2). The intermetallic influenced area showed and average hardness of 320 HV 0.05 (point 1, see Figure 3-25) [191].

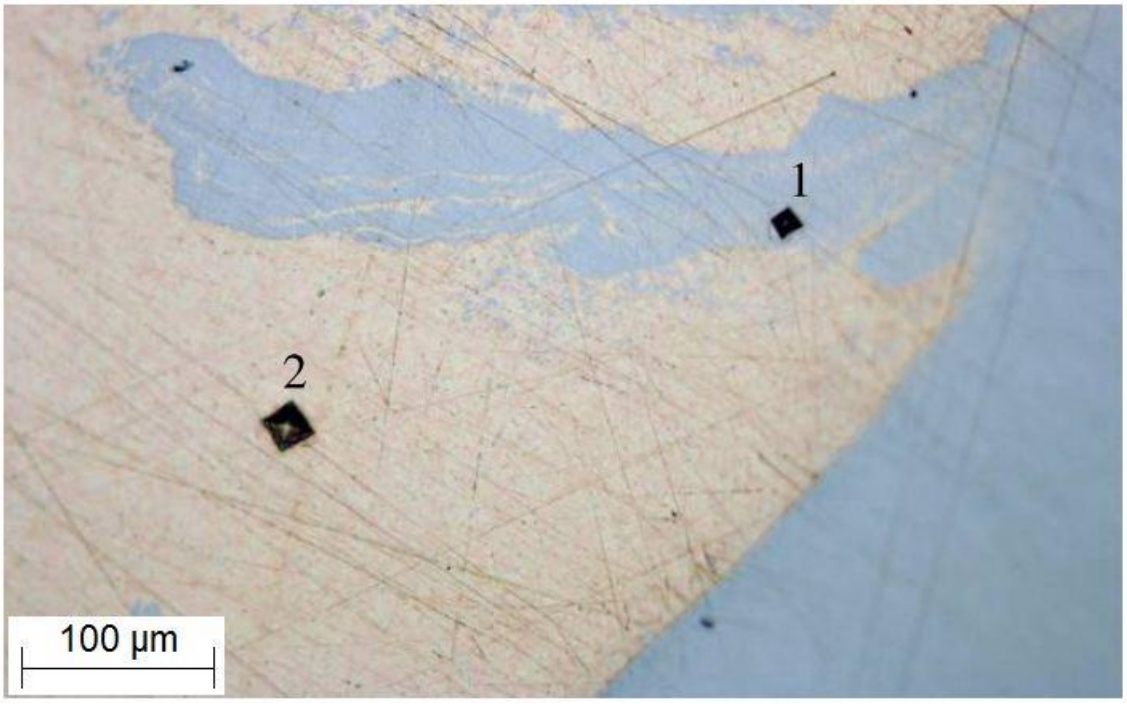


Figure 3-25: The joint hardness is up to three times higher in intermetallic joint regions. Point 1 and point 2 are indentions after a Vickers hardness test. Point 2 indention is in the filler material region and point 1 indention in the intermetallic influenced region of the braze joint.

3.3.4.5 Internal Filling Imperfections

The ISO 18279 [177] does not sub-classify internal 'filling imperfections". In the interest of the automotive industry, this failure type should be researched further.

Incorrect cross sectional geometry of the seam occurs when certain geometric requirements of a seam are not met. This failure is not detectable without cutting the seam. The section geometry of a seam is important when determining the strength of the seam and is outlined in

the engineering drawing. Figure 3-26 shows the five relevant dimensions for a typical flange butt joint section.

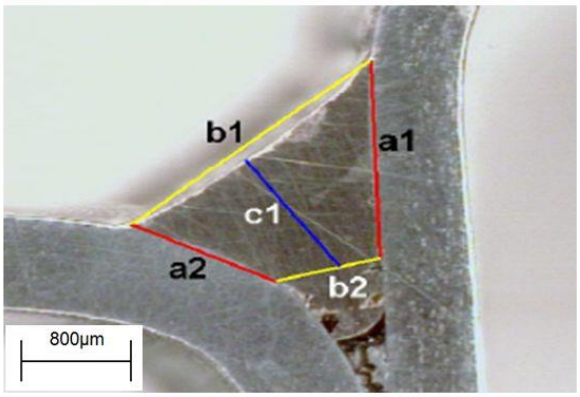


Figure 3-26: Important dimensions on braze joint cross section cuts. There are five relevant dimensions of a roof joint geometry.

The most important dimensions in this case are a1, a2 and c1. The thinnest cross section of the filler bridge is described by c1. The contact area between filler and base material of the roof or side wall should be as large as possible. Dimensions a1 and a2 refer to the contact points between filler and base and should be at least as thick as the thinnest point on the filler bridge. Furthermore, if a1 and a2 have approximately the same length, the brazed bead was positioned in the middle of the base panels and filler alloy was centrally deposited at the middle of the base metals.

An insufficient adhesion between the filler material and the parent metals could be a reason for incorrect cross section geometry. The filler metal has failed to flow through the required length of the joint. As result, the contact surface of the braze metal might not be large enough.

The adhesion of filler material to base materials only occurs during specific conditions. The base material needs to be brought up to an adequate temperature to permit the capillary action between the filler material and the base material to take place. The temperature at which this occurs is known as the working temperature of the filler material, which is above the solidus and often below the filler liquidus [192].

When using $CuSi_3$ wire, the required temperature is 950 °C. Additionally, the surfaces of the base materials should be free from dirt particles, oil, scratches and other contaminations. Large adhesion defects significantly

reduce the braze strength. The correct gap size between the base panels is an important factor as well. If the capillary gap is too large, the filler cannot flow deep enough. Figure 3-27 shows an adhesion defect in the middle of the brazed seam.

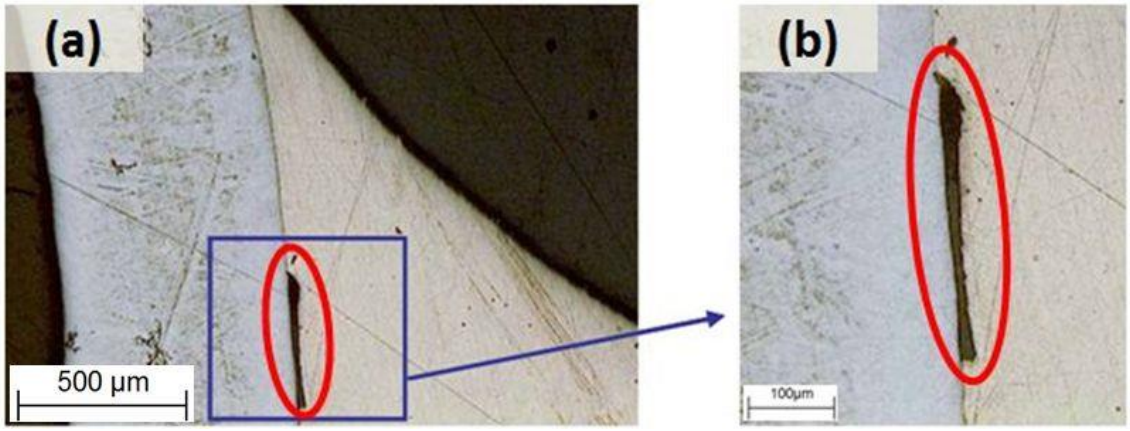


Figure 3-27: Insufficient filler adhesion;
(a) shows an insufficient filler adhesion with the base material;
(b) enlargement of this failure.

Figure 3-28 shows that a large amount of filler material has run deep into the interstitial space between the two base material pieces being joined. This area was not sufficiently warmed and did not reach the required temperature for the capillary effect to take place. This results in faulty seam geometry and also the previously described adhesion defect. The notch effect, created by these two elements of the defect, severely impacts the strength of the seam.

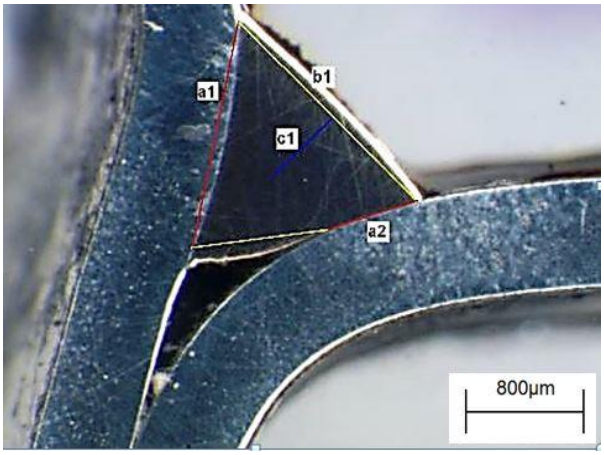


Figure 3-28: Non parallel braze.
This braze joint cross section cut shows an insufficient adhesion between the filler material and the base sheet metal. The distance a2 is much shorter than a1.

Figure 3-29 shows another example of incorrect seam positioning. The optical seam quality might not be affected by inconsistent braze line centering along the length of the seam. As a result of this, this kind of failure is difficult to detect without cutting the brazed panels. This defect type is very dangerous because it has an effect on the durability of the seam, which can be hard to determine without destructively testing the vehicle. This failure is known as "false friend" and a significant problem for every braze cell fitter.

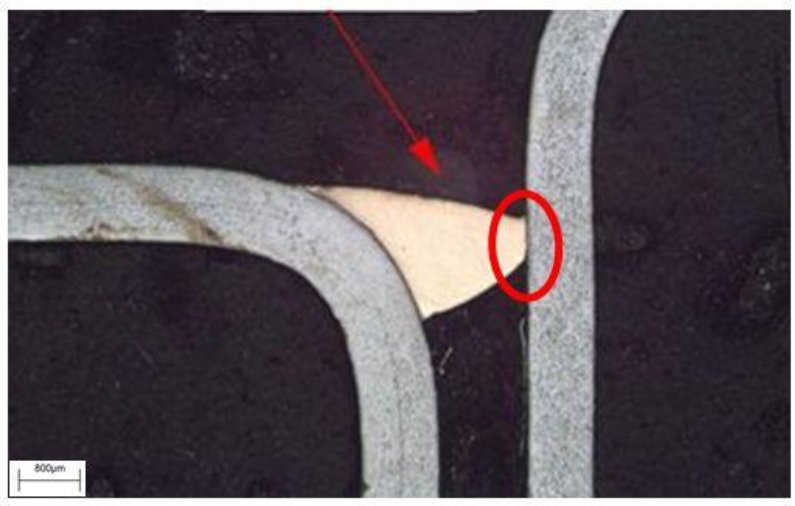


Figure 3-29: Braze joint cross section cut,
which shows an incorrect seam position caused by poor alignment.

3.3.5 Braze Visual Properties Report

Availability of published results on defects or imperfections in arc and in laser brazed seams as well is rather limited [147], especially in conjunction with possible defect causes. Therefore a properties report about all visual detectable potential braze failures was developed as part of this thesis. The purpose of this is to provide a top level descriptor of the braze properties. It is curries that it was not possible to find such an important report in the limited braze quality related literature. This was essential when attempting to understand the complex field of braze failures and when attempting to improve the failure assessment time and assessment quality. This was divided into external brazing imperfections and internal brazing imperfections. Furthermore, the matrix includes columns for the defect description, the defect cause, the defect severity

and affects if a rework might be possible and a defect image or sketch. Figure 3-30 shows a cut-out from this matrix. The complete matrix can be found in Appendix C -Braze Properties Report.

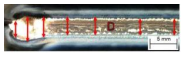
Possible External and Internal Plasmatron Brazing Imperfections on Outer Skin Automotive Panels						
No.	**Defect**	**Defect Cause**	**Defect Severity**	**Corrective Action**	**Rework Action**	**Example Defect Image / Sketch**
External Brazing Imperfections (visual surface)						
1	**Incorrect Brazed Seam Width**	Wrong braze speed, filler wire speed or current setting.	If the seam width is to small it might be that the part has to be scrapped. The assessment result depends on the product development requirements. If the seam width is to wide it might be that this can be corrected with manual grinding.	Check, robot-/table and filler wire speed setting. Check current setting.	If the seam width is to small it might be that the part has to be scrapped. The assessment result depends on the product development requirements. If the seam width is to wide it might be that this can be corrected with manual grinding.	
2	**Incorrect Linearity** Braze does not follow the planned seam contour.	The cause is mostly an unstable robot arm or an unstable seam tracker. As well it could be a magnetic field disturbances due magnetized panel clamping or panels which was magnetized because of previous weld gun operations. For example could a bodyside be magnetized from previous spot weld operations. Check if the tactile finger is loose or worn off.	An uneven joint is not acceptable and cannot be reworked.	Use non-magnetic clamping units. Use path program options from your robot supplier. Use a mechanical seam tracker because these systems have no tracking delays.	Manual or robot re-brazing on short length only.	
3	**Surface Breaking Pores**	Braze gases escaping during solidification. To large gap between the panels. Dirty panels or filling wire. Incorrect shielding gas setting. To much water in the atmosphere or shielding gas. Often porosity is caused by getting the puddle too hot.	Unacceptable as the finished joint will not be aesthetically pleasing. Holes create potential weak spots in the joint. Potential risk for water intrusion into the vehicle.	Check the shielding gas setting. Check the gap width between the panels. Check the panel cleanliness. Check braze speed and braze current.	With PVC sealer or manual brazing for a small amount of holes but not at the start or end of the seam.	
4	**Surface roughness and/or texture.**	Lack of steady state condition being achieved. Unsteady braze speed or to fast braze speed. Robot related failures (programing, installation, etc.). Seam tracker failures. Electrode wear out.	Minor aesthetic defect of slight unevenness. Strength and functionality are normally not affected by this type of defect. However, these defects may act as stress concentrations.	Check, robot/table speed setting. Check filler wire speed setting and electrode quality.	Smooth grinding.	

Figure 3-30: An excerpt from the developed braze visual property report. The complete matrix displays all possible external and internal brazing imperfection on class-A automotive panels.

The quality of brazed joints can be examined by non-destructive and destructive methods. The following sections explain the related details.

3.3.6 Non-Destructive Brazed Seam Test

The European norm EN12799 [193] highlights the following non-destructive test methods for brazed joints:

1. Visual examination
2. Ultrasonic examination
3. Radiographic examination
4. Penetrant examination
5. Leak testing
6. Proof testing
7. Thermography

Unfortunately, all of these listed common used non-destructive testing methods fail for brazed outer skin panel joint checking in the automotive industry, except the visual examination method. For instance, ultrasonic examinations in the automotive industry are the preferred non-destructive checking methods to check spot-welded joints. The huge advantage is the high possibility to find failures shown in correlation to destructive tests.

Sadly, this method does not deliver reliable results for brazed seams, which Ford testing has shown. Radiographic examinations and leak testing need bilateral seam access and this is mostly not possible for brazes on outer skin panel joints because of no access to the closed sections on the inner side. Thermography is a technology, which is increasingly used to check laser welded joints but this technology needs two side access, which is mostly not possible for brazed automotive joints.

3.3.7 Destructive Brazed Joint Test

This chapter describes destructive test techniques on brazed joints.
The European norm EN12797 [194] lists the following destructive test methods for brazed joints:

1. Shear tests
2. Tensile tests
3. Metallographic examination
4. Hardness test
5. Peel test
6. Bend tests

All these tests are costly and time consuming for the automotive industry because a vehicle body or a large component always has to be destroyed.
The following sub-chapters introduce the main destructive quality-checking techniques in the automotive industry to check brazed seams on automotive skin panels.

3.3.7.1 Durability Tests

First are the durability tests. During the vehicle prototype phase, durability tests take place on prototype vehicles and first production build vehicles. These durability tests will be executed on special pulse test stands and on real road tests, which should simulate worst-case customer scenarios. During and after the durability test, the seams will be visually checked. Due cost reason, no durability test was performed as part of this thesis.

3.3.7.2 Tensile Test

Tensile test results are one of the key outputs from quality checks on brazed parts. The results show how strong a joint is. Main influences on parameters for the tensile test results on braze joints are the panel material, the used filler wire and the brazing parameter. For all tensile tests, the European tensile testing standard EN 10002-1 [195] for metallic materials from December 2001 was considered.

Specimen tensile tests are the preferred plant check because they are much faster than vehicle durability tests and they deliver exact values. In the plant, the minimum force depends on the finite element calculation results, on the prototype or on the first production durability results. Often, the requested strength should meet the strength of the thinnest or lowest grade parent sheet metal.

For production, brazed joint strength tests have to be regularly performed to ensure that the joint meets the required strength. The frequency of the tests has to be so selected that not OK vehicle can be detected before they leave the plant. The required strength is a result from crash test calculations.

For this thesis, the brazed test panels were prepared by band-saw cut, milling or EDM (Electrical Discharge Machining) in tensile test coupons as seen in Figure 3-31 to represent the currently used Ford roof joint specimen design.

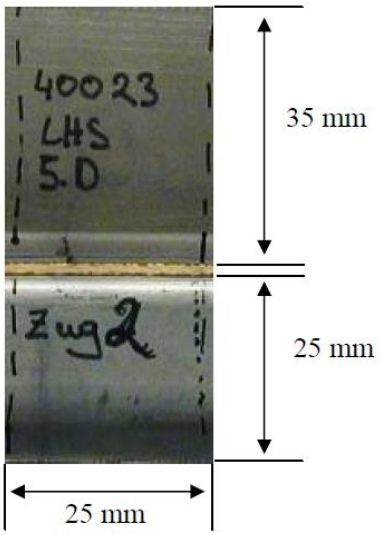


Figure 3-31: Prepared tensile test sample piece for tensile test

The usually used dog bone structure was not used because the coupons should simulate the automotive industry situation. The automotive industry cannot use the standard dog bone structure due to not enough material availability. The flanges are simple not long enough from BIW obtained specimen. Additionally, it would be very difficult and time consuming to cut the dog bone shape in a curved panel.
Each test piece has a unique test piece number so that they are traceable. The maximum tensile force (F max in kN) and the different failure modes were recorded. The UTS (Ultimate Tensile Strength) value was not measured for this thesis. This is because the UTS is measured as force per unit area and the unit area size is not known on brazed test specimen. On braze specimen, the unit area size varies with the size of the wetting area. It would not be correct to use the unit area size of the base metal.
The lower limit tensile force ($F_{Lower\ Limit}$) was calculated by the minimum tensile strength (R_m) of the weakest base metal multiplied with the panel thickness (G) and the specimen width (W).

3.3.7.3 Destructive Test Example on Brazed Roof Seam

The following section describes an exemplary destructive quality check of a brazed roof seam.
A complete vehicle body which represents the body mix is taken from the production line before going into the paint shop. The whole roof seam from this body will be sawn out as shown at Figure 3-32.



Figure 3-32: BIW roof section sawing for destructive test sections

This seam roof sample will be further cut in into different sections. For a four-door vehicle roof in five sections. The beginning and the end specimens play a bigger role for the durability and therefore one section from the roof front and one from the end part of the roof. Additionally, three sections from the middle roof area. These sections will be cut into further sections because fifty per cent will be used for tensile strength tests and the other fifty per cent sections will be used for microscopic investigations.
Only the tensile force comparison experiment between laser and Plasmatron in sub chapter 4.4.1 used real vehicle section cuts. The other experiments used test panel section cuts due cost save reasons.

3.3.8 Microscopic Examination

It is necessary to review the joint quality under a microscope to check if the brazed joint fulfils the internal joint requirements. Only with this checking method, it is possible to detect the internal seam imperfections and the pool geometry. To inspect the inner details of the seam, it is necessary to prepare proper specimen. This includes documentation, sectioning and cutting, compression mounting, planar grinding, polishing and etching.
Microscopic analysis has to be used to measure cross sections and to assess the microstructure of brazed joint test samples. This is necessary to check the influence of different braze parameter settings. The following list highlights the main inspection characteristics;

- Filler material penetration and position
- Material mixing and base metal melting
- Zinc coating damage
- Damages on the parent materials

The analysis of samples with destroying the material requires preparation of the samples. The following list describes the five sample preparation processes.

1. Cut work piece (cross section braze probes or electrode probes)
2. Mounting (hot mounting with conductive resin in a mounting press)
3. Grinding (with 240, 400, 800 and 1200, rotating coarse paper)
4. Polishing (by 6 µm and then 1 µm diamond wheel, wash with soap)
5. Etching (applying alcoholic ferric chloride, wash with water and finish with alcohol)

By using optical microscopy (OM) it is possible to examine the quality of the brazed seam in detail and to detect micro hardness, molten base material, internal pores and other internal seam imperfections. Images from the OM are transferred into an image analysis software so that cross sectional measurements can be taken (distances, circles, ellipses, angles, polygons). This methodology is used along certain points of interest, which are described in the method section of the particular experiment.

3.3.9 Black Soot Measurement

The area size contaminated by black soot is an important value because black soot might have a negative effect on the paint quality. To study the effect of different input parameters, it is necessary to measure the area contaminated by black soot on the specimens. Images from brazed seams were analysed with ImageJ. This powerful public domain image analysis program was developed at the National Institute of Mental Health, Maryland, USA.

A threshold feature allows the user to select the black soot contaminated area only. Figure 3-33 shows an image with a black soot area which was threshold coloured red to easily calculate the black soot amount in certain areas. Important to note is that the hue and saturation were adjusted to full. The brightness bar and the saturation bar are then fine-tuned to the point at which all black areas are selected. This red marked area can then be calculated by the software.

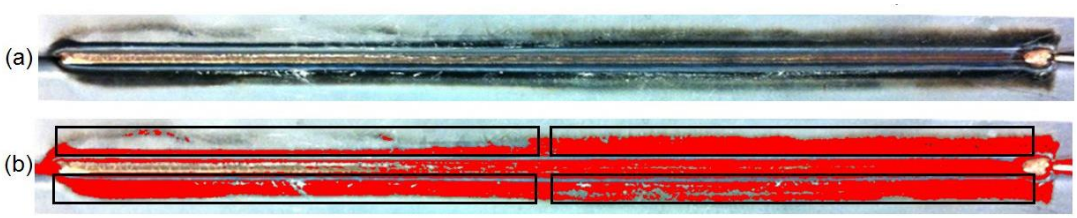


Figure 3-33: Braze run with black soot lines;
(a) normal image; (b) threshold red coloured image with marked areas to measure the black soot amount.

It is important that all the pictures are taken with consistent conditions. That means always using the same camera, the same magnification, the same light and the same braze seam length. In addition, the black soot was measured from the left and the right seam side separately. This method avoids miscalculation because the seam surfaces where partly marked red too as these surfaces were darker than the black soot free test panel surfaces.

3.3.10 Electrode Monitoring Vision System

A low cost flexible vision system has been developed for this thesis [196]. This system can automatically measure the electrode tip geometry, the electrode alignment to the wire & nozzle and the electrode cleanliness. This vision system is designed to operate as an add-on system to TIG brazing cells.

The monitoring system consists of a low cost USB digital camera microscope (20x magnification, 0.3 megapixel imaging sensor) which is mounted next to the Plasmatron torch as seen in Figure 3-34.

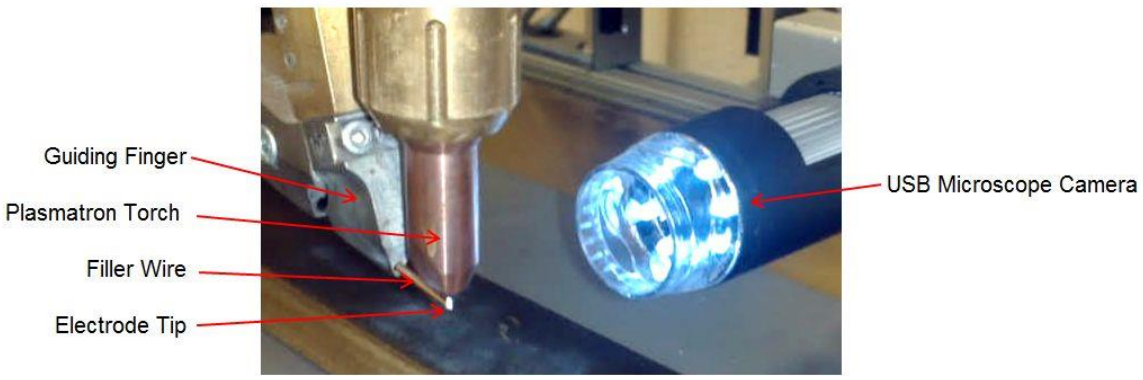


Figure 3-34: Setup of the low cost USB microscope camera

The camera is controlled by a host computer, which performs the picture analysis from the captured pictures automatically, based on predefined algorithms. The vision analysis software used is based on National Instruments LabVIEW. An Arduino microcontroller was used to provide input/output connectivity and act as an interface between the host computer and the industrial hardware from the brazing cell.
Figure 3-35 shows the LabView front end user interface. It is designed for ease of use with the key information clearly displayed [196].

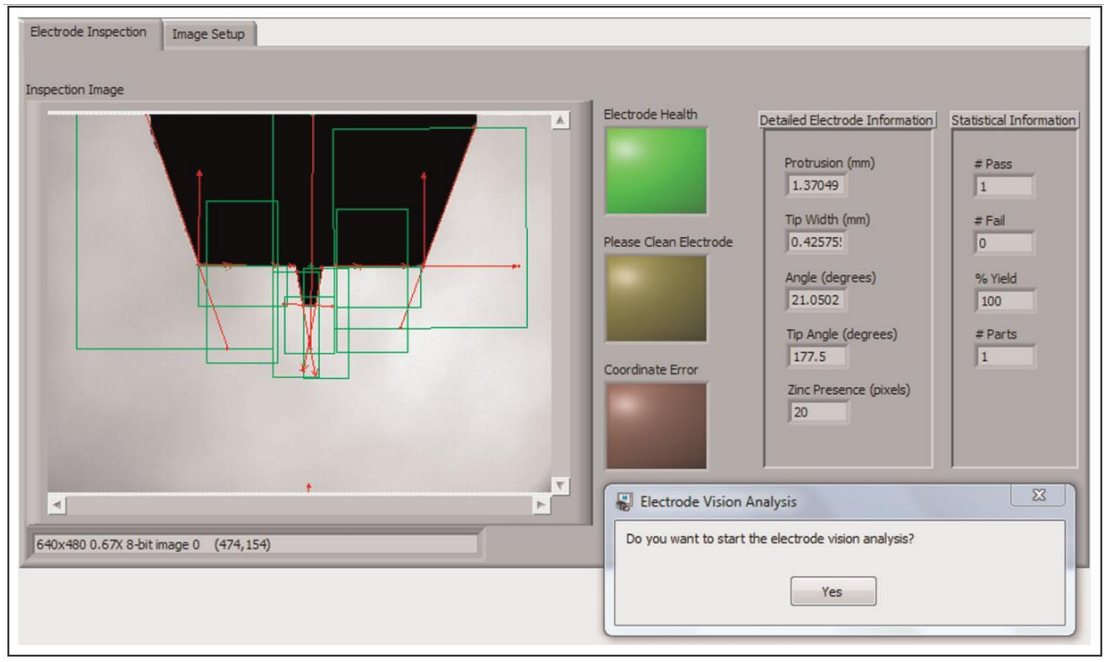


Figure 3-35: The user interface for the electrode tip measurement system [196]

The measurements collected are:

- Electrode tip protrusion out of the torch
- Electrode width on the tip point
- Electrode tip angle
- Distance from electrode tip to filler wire
- Filler wire offset to electrode axis

These measurements are important to capture because they are essential for the following electrode tip offset experiment (detecting the influence of the electrode to wire gap). In addition, this monitoring system should capture the electrode wear and electrode contaminations during the different brazing experiments.

4. Economic and Logistical Modelling of BIW Joining Methods – A Role for Focused Arc Plasma Brazing

The purpose of this chapter is to verify if Plasmatron brazing can be an upcoming high volume outer skin panel joining technique for steel vehicle bodies or if it would be better to concentrate on another joining technology.

The bodyshop manufacturing engineers would welcome it to focus on as few as possible different joining technologies in their bodyshops. Every additional joining method in a high volume automotive plant drives the complexity up and therefore the production cost as well. This is mainly because of larger part stock requirements for the different joining equipment. More joining methods in the bodyshop require a larger maintenance specialist pool because every production shift has to hold all required maintenance specialists available to maintain and repair the joining equipment as fast as possible. Additionally, every joining type has different quality control methods, which is another cost driver due to the increased quality control of complexity. Another important aspect is the increased risk for downtimes due to introduction of new joining technologies in bodyshops.
To minimize the quantity of joining methods as much as possible is also an important requirement for more flexible bodyshops. Nowadays, a bodyshop line has to be highly flexible. That means it should be possible to produce completely different vehicle types on the same line without change time delays between the vehicle types. It is not uncommon to produce three or more different vehicle types on one bodyshop main line. This strategy only works by minimizing the BIW joining methods in a plant as much as possible.

4.1 Research Process

The task to verify if Plasmatron brazing can be the upcoming high volume outer skin panel joining technique was accomplished by dividing it into

sub-stages, which are described within this section. Figure 4-1 shows how the stages are aligned.

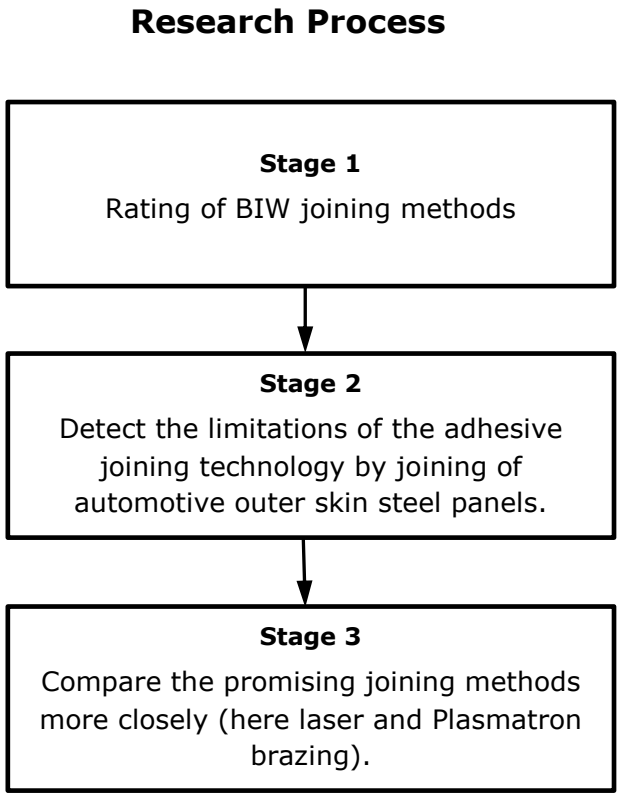


Figure 4-1: Three-stage research program to verify if Plasmatron brazing can be the upcoming high volume outer skin panel joining technique.

Stage 1: Rating of BIW Joining Methods

As contribution for this chapter, a value analysis of where Plasmatron brazing stands in comparison to other BIW joining methods was conducted. The most used and promising BIW joining technologies were rated on carefully selected rating criteria.

Stage 2: Detect the Limitations of Adhesive Joining

The limitations of the adhesive technology by joining of automotive outer skin steel panels were examined in detail, exploring why new products do not consider adhesive joining instead of weld or braze joining.

Stage 3: Compare the Most Promising Joining Technologies

The final stage of the research process was to compare the nearest and promising joining methods from the value analysis exercise (stage 1). Here laser brazing and Plasmatron brazing were compared more closely, with particular focus on the joint strength and the joining costs in dependence to the production volume. These preliminary investigations were very important for establishing the correct focus points for manufacturing planning.

4.2 Rating of BIW Joining Methods

With help of a mind map diagram, the following strategy was developed to gain an overview of where Plasmatron brazing stands in comparison to other BIW joining methods when joining BIW outer skin panels.

- List all current and potential future BIW joining methods
- Identify important joining criteria
- Identify which BIW joining methods are not suitable for outer skin panel joining
- Rate the identified criteria for each joining method
- Benchmark the best outer skin panel joining methods

For the rating of the joining criteria, personal experience and the findings based on the literature research about the BIW joining methods (Chapter 2.3), was used. The value analysis method was used without additional rating factors because for a preliminary rating it is not necessary to make the rating matrix too complicated. As well this rating exercise is only a contribution to get an overview where Plasmatron brazing if it makes The following benchmark factors were detected via the mind-map method as the best rating factors:

Require Double-Sided Access

Some joining methods require double-sided access to apply a specific force at the joining point in the moment of joining. These requirements

increase the vehicle design cost because the designers have to spend additional work time to define the access hole locations and sizes. As these access holes reduce the strength of the structure, the designer often has to compensate the reduced strength through thickening of the steel panels or the usage of larger cavities, which increases in both cases the vehicle weight. Figure 4-2 shows as an example a joint design which requires double-sided access – here resistance spot welding.

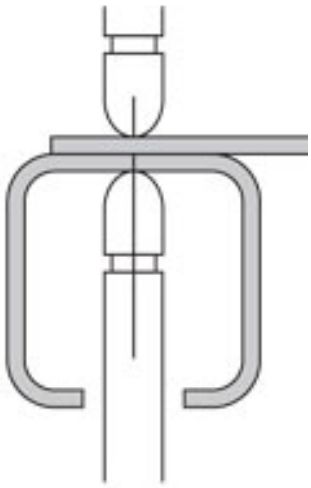


Figure 4-2: Example of a joining method,
which requires double-sided access, here 'resistance spot welding' [197].

Vehicle Weight Effective

Weight saving is an important approach to reduce the vehicle mass and therefore petrol consumption. Large flanges increase the vehicle weight and the material consumption; therefore it is a negative factor. For example, a spot welded connection usually requires a 20 mm wide flange to guarantee accessibility for the spot welding guns. Laser welded and laser brazed joints require only 8 mm wide flanges.

Cycle Time Influence

High cycle times are production bottlenecks. If stations have to be doubled, then the facility, tooling and launch costs increase as well. Additionally, two stations require more space and deliver two product charges. This increases the part matching risks for follow operations. For example, an exact rear lamp setting is difficult to achieve if the liftgate assembly comes from two different joining stations and the rear lamp

comes just from one production station. The customer is then able to detect rear lamp gap and flushness issues in the liftgate to rear lamp area.

Require Sealer Operation

Some joining methods require a following sealer operation with PVC to make the joint waterproof. This additional process increases the investment, the piece cost, the vehicle weight and the vehicle build time.

Joint Aesthetic

Ford consumer surveys show that customers like smooth vehicle body shell joints. A brazed roof is visually better than a spot welded or laser welded roof and points to an aesthetically higher quality vehicle. Currently, the vehicle designer prefers the so-called 'invisible joints' [14].

Joint Strength

Each joining method delivers a different joint strength. For example, joining methods like 1K and 2K adhesive joining deliver less strength than laser welding or brazing with $CuSi_3$ filler per square millimetre joining area by joining of zinced steel panels. The required joint strength depends on the usage. When both base sheets are from the same material, the strength of the thinnest base sheet is in general the required joint strength. It is foreseeable that the required joint strength will increase in the future due to the greater use of high strength panels for outer skin panels as well.

Feasibility for Outer Skin Panel Joining

Some joining methods are more suitable for outer skin panel joining than other joining methods. The rating of this deliverable is an indicator for the robustness of the joining process and how high the confidence is to deliver the required quality and the required production smoothness for volume production outer skin panel joining.

Cost Effectiveness

Automotive manufacturers are always striving to reduce cost. This report estimates the total cost for each joining method under the assumption that the method runs for a 6-year production cycle. The total cost view

includes tooling, fixture, headcount, energy and the consumable cost. As well, the flexibility to adopt a joining process to another vehicle type plays a role for a better cost effectiveness.

Contribution Outcome

The outcome of this contribution rating (see Appendix B) found that two brazing methods are of preference: Laser brazing and Plasmatron brazing. Therefore, it is important to compare these two methods closely. As well, this study has shown that it is useful for the industry to gain more knowledge on the Plasmatron system to improve it further.

The 1K adhesive joining method was also rated highly. The automotive management often raises questions why the bodyshop engineers are not willing to join the vehicle roof to the body with adhesive. To give a qualified answer to this question, the following described adhesive experiment was conducted.

4.3 Limitations of the Current Adhesive Technology

For the automotive industry and for this study, it is important to understand if roof joining in the bodyshop by adhesive bonding without additional fastening method like rivets could be a future joining method, analogous to a windscreen or glass roof assembly in the trim area on already painted bodies. This question came up during the search for a low cost laser brazing alternative. It is important to understand that most of the consumers nowadays prefer smooth roof joints without additional plastic mouldings, as described in sub-chapter 2.3.4.1. Unfortunately, this roof design does not allow the use of additional fastening methods along the roof to bodyside joint due to missing tooling access. Only adhesive bonding might be a feasible solution because this process does not require access to both sides.

Adhesive bonding is used for various applications in the automotive industry. For example, glass panels like windscreen and glass roofs are currently bonded to the painted body in the trim area. Also, bodyshops already use adhesives, but mainly as hybrid structural joints in underbody

areas and as hemming adhesives in the hem flanges between outer and inner closure panels like doors, hoods trunk lids or tailgates [95].
Most bodyshop related studies in the field have focussed on anti-flutter bonding, spot-weld sealing, joint sealing and hem flange sealing. There is no report published which covers bonding of vehicle roof panels in bodyshops. There are only two car manufacturers (BMW [198] and Aston Martin) that use a roof to body adhesive process in their bodyshop, but only for some of their low volume models. In order to better understand the viability of adhesive joining for roof joining, a simple but meaningful experiment was performed, described in the following section.

4.3.1 Experimental Methodology

The aim of this experiment was to show if it is possible to adhesive join a zinc coated steel roof to zinc coated bodysides inside a 10 minutes cycle time. This cycle time was chosen because it represents a yearly vehicle production of ~ 26.000 units per year in a two shift production, which reflects a medium volume production.
The experiment was conducted in the Ford Plant Genk because it is very difficult to simulate a production paintshop on a test rig. This is because a BIW passes a couple of process and transport steps in the paintshop. It starts with e-coating where the BIW gets dipped in a phosphor bath. This dipping process can create torsional stress to the not yet final cured roof adhesive. The following e-coat, base coat and final paint ovens could add additional torsional stress due to different thermal expansions from the different steel grades in the BIW during the heat up and cooling down phases. Additionally, the bodies will not be transported gently through the paintshop. The bodyskids, which are locked on the underbody from each body, often bump together heavily, which could have an influence to the adhesive joint. This is because the bodyskids sit loosely on the transport steel chains. At each line pass the bodies get a certain distance from each other. On the next coming pass the bodyskids bump together because they have to wait until the next chain has a free space. Figure 4-3 shows painted bodies on bodyskids.



Figure 4-3: A painted body on bodyskids,
which sits on transport chains [199].

Rather than use test panels for this experiment, it was decided to use unpainted Mondeo bodies with disjoined roofs to get more meaningful data. Due to cost reasons, only two bodies were used for this experiment.

The Mondeo has a flange butt roof joint design (see Figure 4-4) which will be joined in the high volume production by laser brazing.

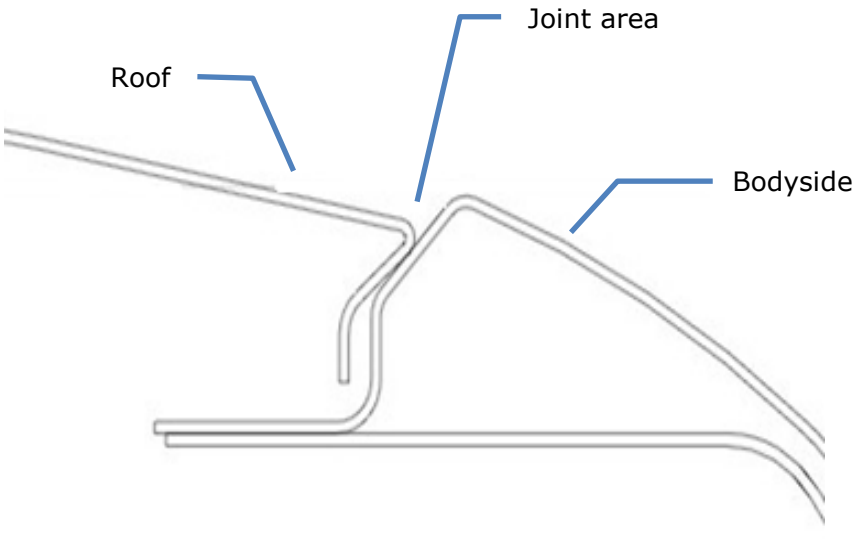


Figure 4-4: Sketch of a flange butt roof joint

The joint area was manually cleaned with propanol. The 60°C warmed adhesive Terokal-5074 (1K with 100 µm glass pellets in a cartridge) from the company Henkel was manually applied on the two roof flanges with a heatable cartridge air gun (40 psi pressure). The glue beat diameter was approximately 3 mm. 1K adhesive was used because 2K is more sensitive against dirt and humidity. As well, 1K reaches higher tensile forces as stated by Henkel [200].

The roof was then carefully located into the vehicle by hand. Additional clamping units guaranteed that the roof was sitting in the correct position and did not move during the pre-curing process (see Figure 4-5).

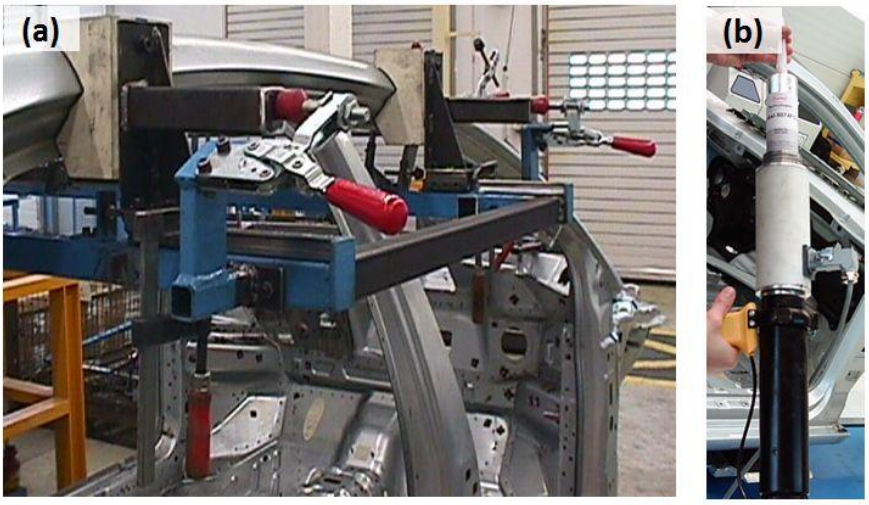


Figure 4-5: Vehicle roof joining by adhesive bonding;
(a) BIW with roof holding & clamping jig-;
(b) heatable adhesive cartridge hand gun.

The glue seam was stripped off with a scraper. The seam was heated up with infrared heaters from the company GH Induction to 180°C for 10 minutes per side to get a pre-curing as suggested by the adhesive supplier.

Afterwards, the body was painted in a production paint shop like a normally produced BIW. It was planned that the 1K adhesive joint gets the final cure in the paint oven (~ 200°C).

The joint quality of the bonds for example, visual quality and tensile force was assessed every 200 mm of the seam as described in sub-chapter 3.3.3. and sub-chapter 3.3.7.2. The related section cuts were obtained as described in sub-chapter 3.3.7.3.

4.3.2 Results

No roof panel distortions and no bodyside distortions were observed along the roof joint areas after the two bodies left the paint shop ovens. However, regrettably all four joints showed fine adhesive cracks near the roof start and the roof end. Figure 4-6 shows one of these adhesive cracks, which all looked quite similar.

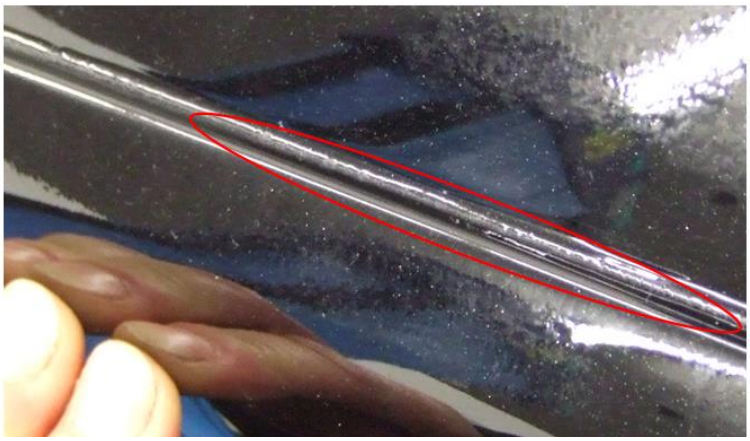


Figure 4-6: Cracked adhesive on a roof joint [9]

The following conducted tensile tests on the roof joint seam specimens showed maximum tensile forces between 380 – 740 Newton. As reference, similar sized laser brazed and Plasmatron brazed specimen reach tensile forces around 6,300 Newton on similar sheet combinations [14]. The tensile force results did not show any correlation, trend or anomalies. It should only be noted that two tensile test specimen broke during the roof cutting phase for the tensile test specimen extraction. This might have happened because of the vibration or the entrapment of the saw during the specimen cut out phase. The detail tensile test result can be found in Appendix D – Adhesive Experiment.

4.4 Laser Brazing vs. Plasmatron Brazing

Within this section, the major focus is to compare laser brazing and Plasmatron brazing with each other to understand similarities and differences between these brazing methods. The chosen dimensions for

this benchmark were consistency of braze tensile force, visual appearance and cost because these are the most important factors in this case for the automotive industry.

4.4.1 Tensile Force Comparison Laser vs. Plasmatron

This section should give the answer if there are differences between laser brazing and Plasmatron brazing joints regarding the maximum tensile force (F_{max}).

The tensile force results are very important within the quality tests for brazed seams. For example, the automotive manufacturer cannot tolerate that a brazed roof peels off during a traffic collision.

Therefore, to identify the tensile force differences between two brazing methods is very important. Most significant for the tensile test results of a brazing method are the used parent metals, the applied filling wire and the brazing parameters.

To compare the two brazing techniques realistically with each other it was decided to use the vehicle roof brazing process. Therefore, three identical roofs where joined with laser brazing and three identical roofs with Plasmatron brazing in identical produced bodies.

The lower limit tensile force ($F_{Lower\ Limit}$) was calculated by the minimum tensile strength (R_m) from the weakest base metal multiplied with the panel thickness (G) and the specimen width (W). Table 4-1 shows the weakest material grade details.

Table 4-1: Material specification from the weakest base material

Lowest Grade Material in Joint	Min. Tensile Strength Rm (N/mm^2)	Gauge (mm)	Zinc Coat Type
DC05	270	0.75	Galvanised (50G 50G Z)

The specimen width (W) was determined with 25mm. The following formula was used to calculate the tensile strength ($F_{Lower\ Lmit}$) from the weakest steel panel:

$$F_{Lower\ Limit} = R_m * G * W \quad 4\text{-}1$$

Then the lower limit tensile force for the used roof joint section as calculated is 5.1 kN. This limit was chosen because it reflects the best possible joint strength due to the consideration of the lowest grade material strength as the lowest possible joint strength.

For their PPAP (Production Part Approval Process), the automotive OEMs typically expect a Ppk (Process Potential Capability) level equal or greater to 1.67 and a Cpk (Capability process index) equal or greater than 1.33 for significant characteristics [201]. A Cpk = 1.33 corresponds to a 30 ppm (parts per million) defect rate. A higher Cpk amount indicates that the process is closer to the target. This definition is for a centered target case only and does not fit in this tensile strength characteristic case, because of the single specification limit only. Here the definition would be that the Cpk shows if the process meets the established specification.

The Cp (capability index), often mentioned as process potential index as well, could not be calculated due to the unilateral tolerance from the tensile strength attribute. The vehicle designer knows that the tensile strength has some variation and has therefore not defined an upper specification limit for the tensile strength.

The Cpk index was analysed as an example so as to detect the process efficiency differences of laser and Plasmatron within the tolerance limit. This limit is used as an indication in this investigation only and does not follow the standard statistical process control (SPC) rules. Normally, before calculating a Cpk index, a Cm (capable machine) and a Cmk (capability machine index) have to be calculated. A Cmk requires at least fifty parts (n = 50) but one hundred (n = 100) are preferred. These parts have to be produced consecutively without changing settings. To fulfil this request and to conduct the following required measurements would overrun the available resource here. Additionally, due to the confidential obligation from Ford, it was not allowed to show a larger size of in-house quality data here. Therefore, it was decided only to calculate the Cpk example, to deliver an indication of the process performance differences.

The lower specification limit (LSL) force was calculated at 85%, where 85% is a self-defined recommendation by the author of the lower limit force ($F_{Lower\ Limit}$) from the weakest parent material. The formula is then:

$$F_{LSL} = F_{Lower\ Limit} * 85\ \% \qquad 4\text{-}2$$

The lower specification limit is then 4.3 kN.

The main brazing parameter values that were used in this experiment are shown in Table 4-2. These values are similar to currently running automotive production lines.

Table 4-2: Main parameter values used for the laser vs. Plasmatron trial.

Parameter	Laser	Plasmatron
Speed of Robot	2.4 m/min	1.0 m/min
Wire Speed	2.9 m/min	1.3 m/min
Gas Flow type & rate	No gas required	Argon, 8.0 l/min
Filler wire type	$CuSi_3$, Ø 1.6 mm	$CuSi_3$, Ø 1.6 mm

The complete roof seams were sawn out from all six bodies. From each roof seam, four uniformly chosen sections were cut out as described in Chapter 3.3.7.3. Each section cut-out had a 25 mm width. The cross section area size is unknown as the contact areas varied from braze to braze. The section cut-outs were prepared and analysed by the tensile strength method as described in Chapter 3.3.7.2.

4.4.1.1 Results

It is apparent from the experiment results shown in Figure 4-7: Tensile force results comparison that the tensile test differences between laser and Plasmatron brazing are minor. The point clouds look very similar. As well, the best-fitting trend lines from both joining methods are nearly identical. The almost horizontal lines show that the process is, for the

amount of taken data, quite robust. The tensile force specification limit (4.3 kN) was exceeded in every tensile test sample. As well the minimum tensile strength (5.1 kN; see the dashed yellow line at Figure 4-7), which was calculated by the minimum tensile strength from the weakest base metal, was not once reached or passed through. The lowest tensile force result from laser brazing was 5.55 kN and the lowest tensile force from Plasmatron brazing was 5.53 kN. These results are very close together and were ~ 28 % higher than the required specification limit.

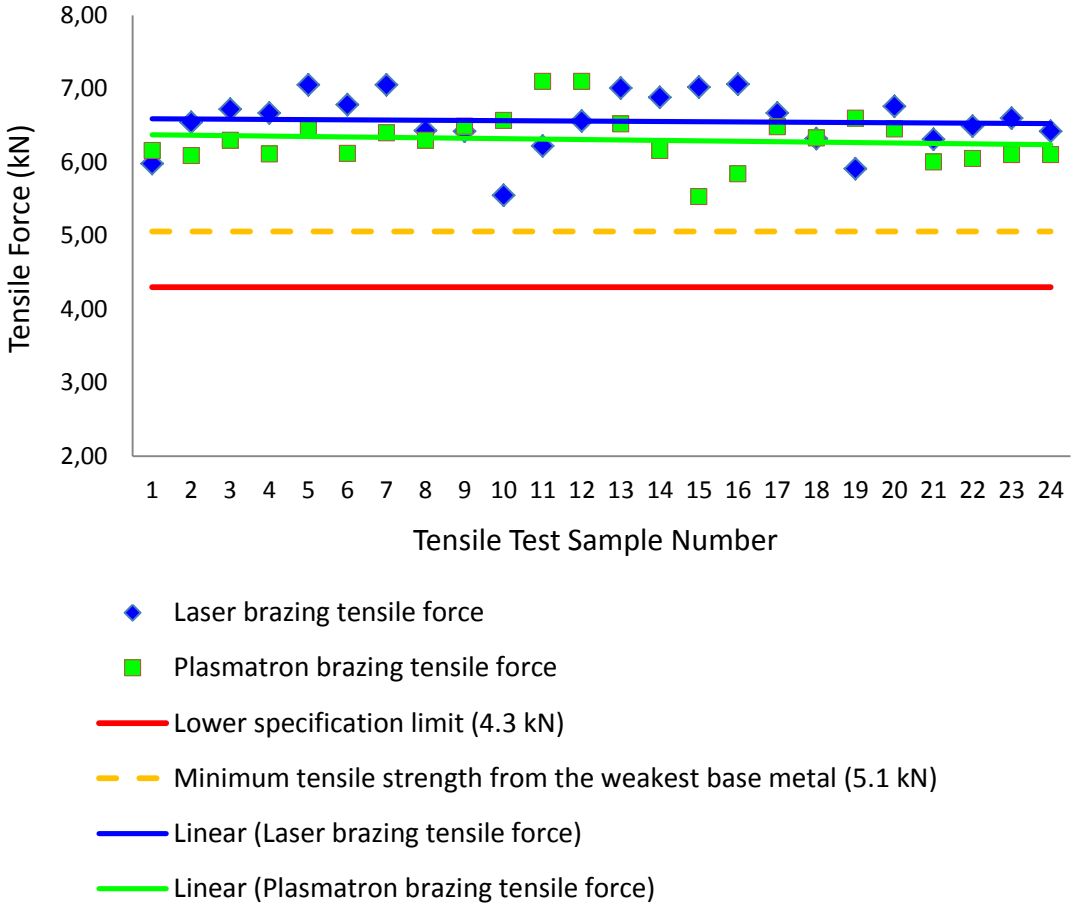


Figure 4-7: Tensile force results comparison
Laser vs. Plasmatron brazing.

The following cumulative histograms as seen in Figure 4-8 show the tensile force distribution differences between laser and Plasmatron brazing.

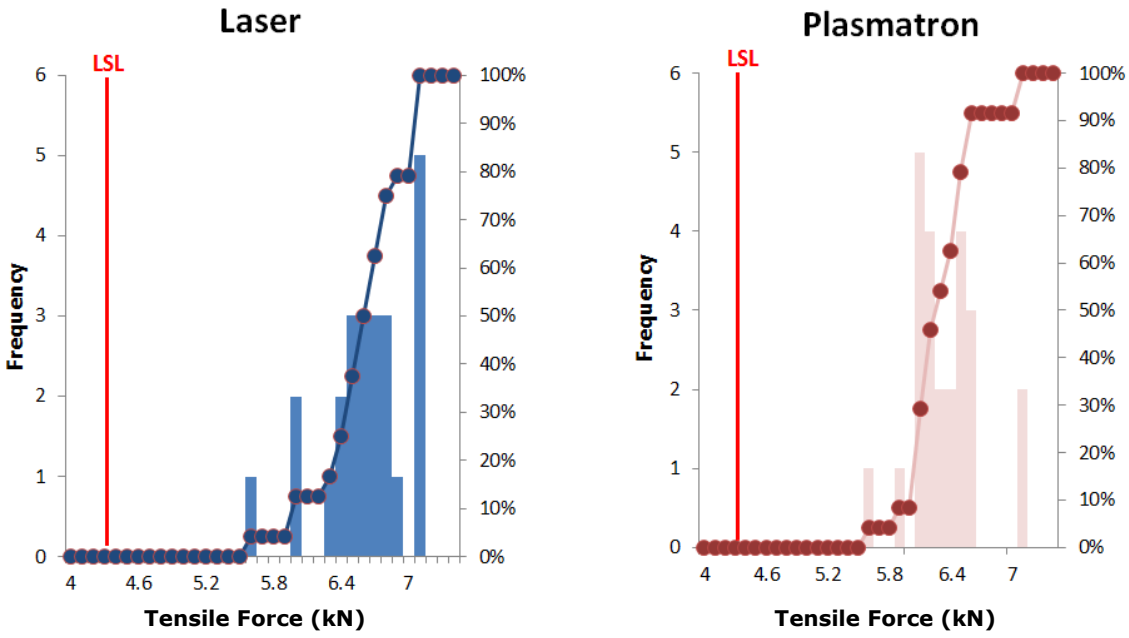


Figure 4-8: Cumulative histograms about the tensile force results of laser and Plasmatron brazing

The cumulative histograms graphically display the tensile force variation differences between laser and Plasmatron brazing. Laser brazing shows a tendency to higher tensile force results and to a left skewed histogram.

The Cpk value as shown in Table 4-3 was exemplary calculated from the average value of the specimens ($\emptyset V$), the lower specification limit (LSL) and the standard deviation (σ) for each brazing technique.

$$C_{pk\,LSL} = \frac{\emptyset V - LSL}{3 * \sigma} \qquad 4\text{-}3$$

Table 4-3: Tensile test results

Braze System	Average value ($\emptyset V$) kN	Lower specification Limit (LSL) kN	Standard deviation (σ) kN	Cpk
Plasmatron	6.31	4.30	0.35	1.93
Laser	6.57	4.30	0.39	1.95

Plasmatron brazing had a Cpk of 1.93 and laser brazing a Cpk of 1.95. That means both joining methods have shown that they are able to produce brazed seams within the required PPAP ranges.

However, it has to be noted that the calculated Cpks have to be seen as provisional Cpks only. As highlighted before, the analysed roof seam quantities were far too low for valid Cpk calculations. Also, the data collection time span does not meet the Cpk calculation requirements because the data should be collected after at least one month of robust production [202].

4.4.2 Cost Comparison Laser vs. Plasmatron Brazing

Within this section, the major focus is to compare Plasmatron and laser brazing costs with each other to understand which joining method is more cost effective. To determine which volume of each brazing method makes more sense, the seam of a two piece liftgate was chosen as a practical automotive example. The cost analysis can be used to gain a detailed cost overview of both brazing methods. Therefore, the productions of two different countries were compared. This is important due to salary differences between countries and in this abstract to analyse the impact of the different brazing speeds and production volumes on the costs. In addition, a weakness analysis was completed to determine the major aspects of possible improvements.

To compare laser and Plasmatron brazing with each other, a capital expenses (CAPEX) comparison was created. Thereby the different cost segments of the techniques were the focus. Table 4-4 shows the CAPEX calculation of the base investments for each brazing technique and the required areas of the investments (power source, safety, brazing head and others). It can be realised that the laser brazing unit is in general more expensive, the power source and safety units are also cost-intensive. Nevertheless, it has to be mentioned that these CAPEX do not include the purchase of additional clamping fixtures or other production related support units because those have the same independent values and have therefore no impact on the individual joining methods.

Table 4-4: CAPEX comparison
Laser vs. Plasmatron brazing facility and tooling costs

No.	Item	Qty.	Unit Costs (US $)	Plasmatron Brazing (US $)	Laser Brazing (US $)
1	Power source				
2	- Braze transformer, max 500 A, 400V	1	11,305	11,305	
3	- Laser source, max 4.0 kW, 400V	1	319,410		319,410
4	Safety				
5	- Tinted plastic curtain (arc protection)	1	10,480	10,480	
6	- Laser safety housing	1	152,100		152,100
7	- Exhaust system	1	13,500	13,500	13,500
8	Brazing head				
9	- Plasmatron head	1	60,750	60,750	
10	- Laser head	1	108,000		108,000
11	Documentation				
12	- Plasmatron head	1	665	665	
13	- Laser head and laser source	1	1,900		1,900
14	Accessories (electrode grinder, gas control)	1	13,300	13,300	
15	Wire cutter	1	1,862	1,862	1,862
16	Wire feeder	1	28,728	28,728	28,728
17	Seam tracker	1	34,048	34,048	34,048
18	Tools (nozzle pull-off tool, adjust gauge for cathode, tool set…)	1	9,450	9,450	
19	Hose package (ground cable, hose package)				
20	- Plasmatron head	1	8,606	8,606	
21	- Laser head	1	17,755		17,745
22	Climate house for brazing wire storage	1	7,000	7,000	7,000
	Total			**199,694**	**684,293**
				29%	100%

To make the correct production decision, the total costs (*TC*) have to be determined. Economists and accountants often define *TC* as the sum of two components [203]. Total variable costs (*TVC*) and total fixed costs (*TFC*). As a formula:

$$TC = TFC + TVC \qquad 4\text{-}4$$

TVC consist of costs that are zero when output is zero and vary as output varies [204]. For example, operator wages, energy and raw materials.
TFC are the sum of the costs that do not vary with output. These costs will remain unchanged when output rises or falls in the short run [205].

For example, a firm's insurance premiums, its property taxes. As *TFC* are generated by adding all costs which are volume independent. Therefore other fixed costs (*oFC*; here costs of the first investments) are added to the depreciation (*DC*) and the interest (I) of the machine as shown in this formula:

$$FC = oFC + DC + I \qquad 4\text{-}5$$

For the depreciation, the facility and tooling costs have to be divided by six, the quantity of years of the regarded depreciation to get the right value. Thereby six is the standardized lifetime of a vehicle in production. High tech equipment, like laser systems, is worn out and no longer corresponds to the state of the art after those six years, usually. Furthermore, the Disposal Value (*DV*) is subtracted from the Initial Outlay (IO), has to be divided by two and multiplied with the interest rate (i) to calculate the Imputed Interest (I). In this special case, the system will be scrapped after the 6 years and this means that there is no income by reselling the brazing system (*DV* = zero USD).

$$I = \frac{IO - DV}{2} * \qquad 4\text{-}6$$

$$I = \frac{IO}{2} * i \qquad 4\text{-}7$$

In addition to the TFC, are the variable costs (*VC*) that increase with rising production volumes (*V*). Electric energy, water, gas and filler wire consumption, as well as the maintenance and labour costs, can belong to those variable unit costs (*vUC*).

$$VC = vUC * V \qquad 4\text{-}8$$

The production volumes for each year are defined by the Marketing Department and are based on three different procedures. Those methods are the qualitative procedure (expert discussions), development of an explanatory model (socio-economic influences) or the quantitative procedure (time series analysis).

4.4.2.1 Analysis

Based on the described formulas and the related calculations (see Appendix F), the following Figure 4-9 shows the impact of the variable costs within a simulated production of liftgates. It has to be mentioned that the calculation is based on a production plant located in Germany with German labour costs (56 US $/h). When the production is located in countries with lower salaries like Thailand (18 US $/h), there will be a deviation.

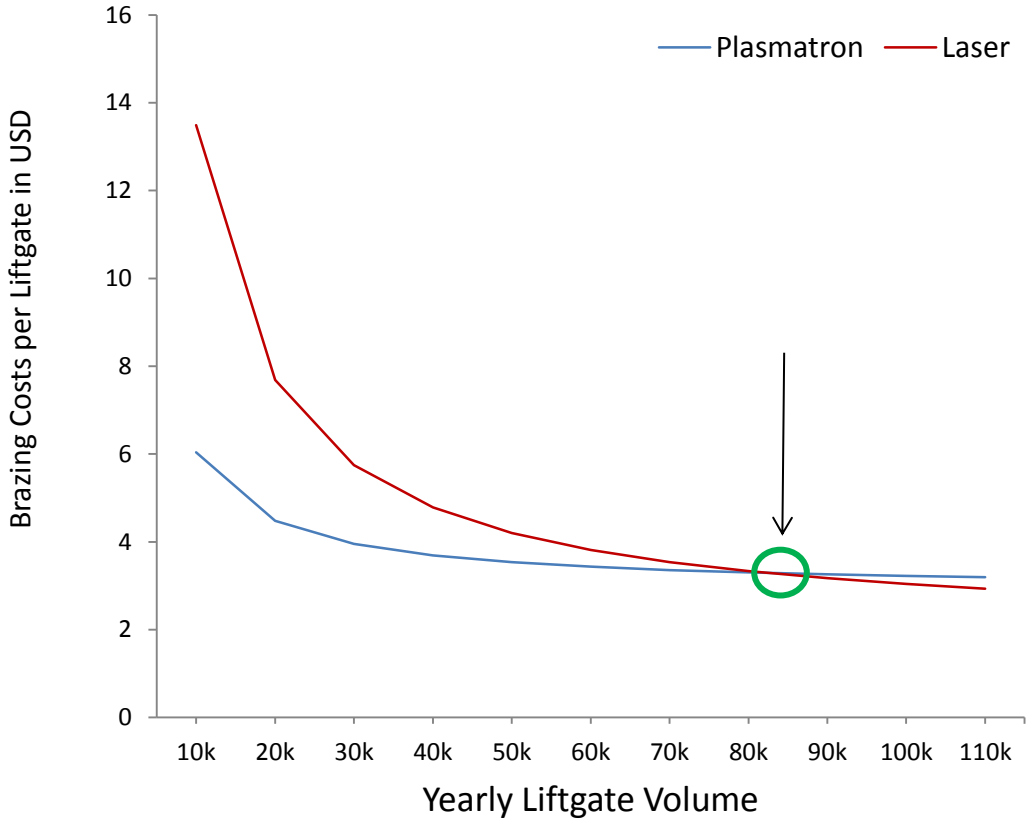


Figure 4-9: Total brazing costs per liftgate – German plant.
The green circle marks the break-even point.

In business, "breakeven" is defined as the point where income just covers the associated cost. In engineering economics, the breakeven point is more precisely defined as the point where two alternatives are equal [206]. The Break-Even-Point (green circle; see Figure 4-9), the volume rate (*VR*) when both brazing methods have the same production price per

liftgate, can be taken from the graph or calculated exactly by the following calculations:

$$TC_{Laser} = TC_{Plasmatron} \quad 4\text{-}9$$

$$TC_{Laser} = FC_{Laser} + VC_{Laser} \quad 4\text{-}10$$

$$TC_{Plasmatron} = FC_{Plasmatron} + VC_{Plasmatron} \quad 4\text{-}11$$

$$FC_{Plasmatron} + VC_{Plasmatron} = FC_{Laser} + VC_{Laser} \quad 4\text{-}12$$

$$FC_{Plasmatron} + (vUC_{Plasmatron} * VR) = FC_{Laser} + (vUC_{Laser} * VR) \quad 4\text{-}13$$

$$(vUC_{Plasmatron} * VR) - (vUC_{Laser} * VR) = FC_{Laser} - FC_{Plasmatron} \quad 4\text{-}14$$

$$VR = \frac{FC_{Laser} - FC_{Plasmatron}}{vUC_{Plasmatron} - vUC_{Laser}} \quad 4\text{-}15$$

$$VR_y = \frac{684{,}293\ US\ \$ - 199{,}694\ US\ \$}{6\ \text{years} * (2.44\ US\ \$ - 1.38\ US\ \$)} \quad 4\text{-}16$$

$$VR_y = 85{,}612\ (liftgates) \quad 4\text{-}17$$

With the required values, a Break-Even-Point volume of 85,612 liftgates can be calculated and emphasises the results in Figure 4-9.

4.4.2.2 Results

The CAPEX for the laser brazing system are more than three times higher than the Plasmatron brazing system. However, that is not the most important information. More important is to include the variable costs of each method to figure out the total costs related to the production volume as shown before.

Therefore, it can be realised that it is preferred to use the Plasmatron brazing system in Germany up to a production volume of 85,612 liftgates and the laser brazing system afterwards. For Thailand it would be 128,478 liftgates before the purchase of a laser system is preferred. This is due to the lower labour rate in Thailand and because the Plasmatron method needs much more maintenance time than the laser, which

increases the variable costs significantly. Furthermore, as displayed in Figure 4-10, it can be analysed by the required brazing and working time at which volume rate an additional brazing system is needed.

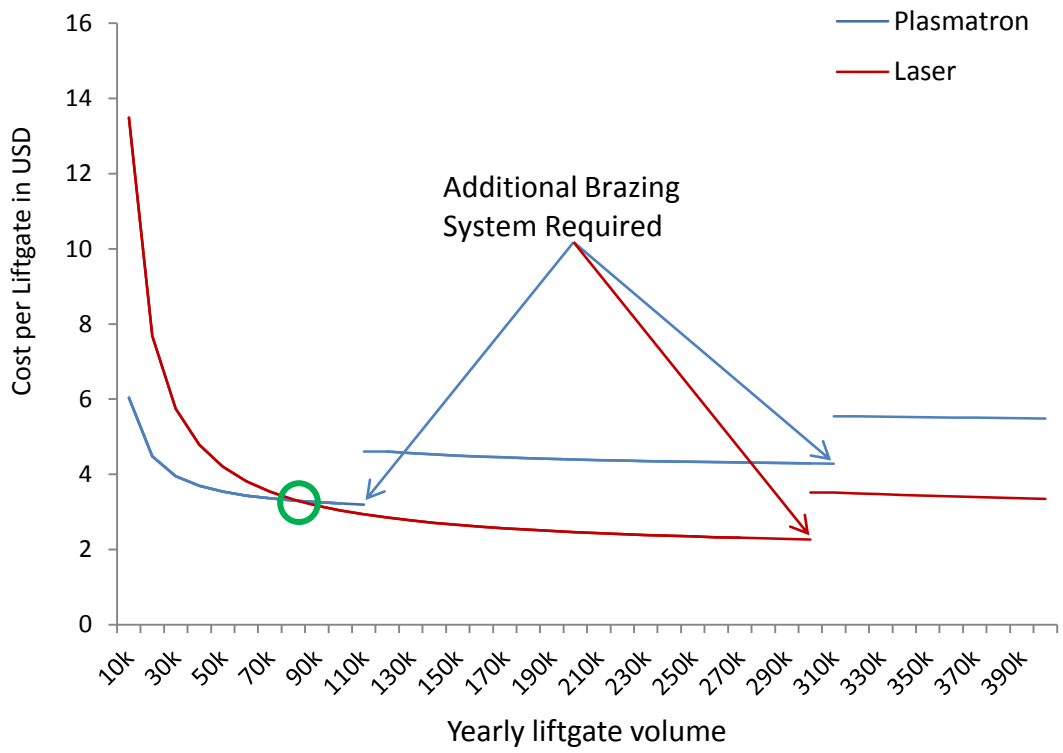


Figure 4-10: Cost per liftgate comparison laser vs. Plasmatron and detection of points for additional brazing systems – Germany.

The laser method requires a second unit at a volume of about 300 thousand liftgates. Contrary to this, the Plasmatron needs additional systems twice at a volume rate of about 110 and 310 thousand liftgates per year. Therefore, the total costs of the Plasmatron production rise dramatically and are always higher than the laser brazing systems (after the volume of ca. 85k liftgates per Year). Accountable for those higher costs are the labour and maintenance costs of the Plasmatron system because the electrode has to be changed or ground after 20 braze cycles each time. Additionally, the lower Plasmatron brazing speed also has a huge cost impact.

In the calculated example, the labour and maintenance costs of the Plasmatron (1.63 USD/liftgate) are fifty-two per cent higher than the labour and maintenance costs of the laser brazing method

(1.07 USD/liftgate). Besides the higher amount of required maintenance time, the major cost driver is the lower brazing speed of the Plasmatron method. This system is working with a brazing speed of 1 m/min compared with the two times higher brazing speed of the laser system 2 m/min.

4.5 Chapter Discussion

In this section, the results obtained from the chapter are discussed and analysed. The findings below are based on the literature research, on the benchmark of the current and future BIW joining technologies and on previous brazing and adhesive joining experiments. Additionally, a systematic total cost model for brazing methods was developed to verify where Plasmatron brazing cost stands in comparison to the laser brazing cost.

4.5.1 Limitations of the Current Adhesive Technology

For the automotive industry and for this study, it is important to understand if roof joining in the bodyshop by adhesive bonding could be a future joining method. To answer this important question, an experiment was conducted.

The experiment results have shown that an adhesive joining process is not feasible in a medium- and high volume bodyshop due to appearing cracks in the adhesive after the test vehicles left the paint shop.

Increasing panel distortions during the rapid paint oven heat-up and following cooling phase might be the reason for the seam cracks. The different body parts expansion rates stemming from the different thermal expansion coefficients are difficult to control during the heat-up and cooling phases. This then leads to the observed adhesive cracks.

The short paint drying times in the paint ovens at high volume paint shops make this an especially important point to consider. Ford's high volume paint shops use high temperature ovens where the BIWs can reach temperatures of up to 210°C. As well, to reduce the paint oven

temperature is not manageable because otherwise the paint ovens would have to be extended in length, which would need enormous space and further investments.

A roof positioning jig for every vehicle to be painted holding the roof in position when the vehicles pass through the paint shop would be too complicated and too expensive for high volume vehicle production plants.

The adverse effects of suboptimal heating and cooling highlight the importance of combining adhesive use with other joining techniques.

Perhaps a hybrid joining design with spot welds, self-piercing rivets, etc. would be the best possible solution.

Another important subject is the so-called wash-off risk of the adhesives during the various cleaning steps preceding the paint and curing processes. If the product improvements achieved by the adhesives are to be maintained, it is important to ensure that the adhesive remains in place in the time before the curing process.

Moreover negative are the low breaking joint force (between 380 – 740 N) from the taken adhesive roof joint specimen, which are much lower in comparison to a brazed seam joint (average 4,500 N) on the same joint design.

The experiment results clearly highlight the limitations of the current adhesive technology. Without panel fixing (self-piercing rivets, spot welding, etc.) it is currently not possible to conduct bonded roof joints in high volume bodyshops. Consequently, it is the right decision to concentrate on the improvement of the Plasmatron brazing method.

4.5.2 Laser Brazing vs. Plasmatron Brazing

The compared tensile test results between laser and Plasmatron brazing have shown that the differences between these two brazing methods are minor. The laser and Plasmatron histograms about the tensile force results are not symmetric, which may be for the reason that the measurements are just from six brazed roofs. This sample size quantity is far too low for a serious SPC study. The variance differences between laser and Plasmatron brazing are just minor as well and the results of this study did

show that both Plasmatron and laser brazing perform a good reproducibility per brazed vehicle. Both brazing methods fulfil the requirements within the tensile tests for the lowest grade material and are appropriate for joining of outer skin automotive panels. These results were expected because only the heating method to melt the filler wire are different but not the filler wire material. Important for both heat up methods was that the main heat was fine enough just to hit the filler wire and not the parent panels. Would the main heat hit the parent sheets a distortion of the to be brazed panels would be unavoidable.
A long-term reproducibility study could not be conducted as part of this thesis due to the resources required and Ford confidentiality requirements.

In a second step, a TCM (Total Cost Model) was set up to fully understand and quantify the cost structure of laser and Plasmatron brazing in different automotive plants and at various production volumes. The results show that the CAPEX for the laser brazing system are more than three times higher than the Plasmatron brazing system.
Under consideration of the total cost calculation approach the picture looks different. For a German based production, Plasmatron brazing cost per liftgate is higher than laser brazing when the yearly liftgate volume passed the 85k mark. Accountable for higher costs are the labour and maintenance costs of the Plasmatron system because the electrode has to be changed or ground after 20 braze cycles each time, which was an important finding. This high impact of the labour cost was not expected. This finding corroborates that it is important to find a method or a combination of methods to improve the electrode lifetime, which would reduce the maintenance cost. Several influence factors should be studied in detail. For example, it is important to understand the influence of different brazing parameter settings to the electrode tip lifetime. As well, the development of an effective electrode tip cleaning process would be beneficial. Additionally, it has to be emphasised that the calculated break-even point is based on a German labour rate. Therefore it is clear, that the break-even point moves to a higher liftgate volume, when the brazing station would be located in a low-wage country.

Besides the higher amount of required maintenance time, the major cost driver is the lower brazing speed of the Plasmatron method. Plasmatron brazing is working with a brazing speed of 1 m/min compared with the two times higher brazing speed of the laser system 2 m/min. Priority for future improvement studies should be the brazing speed of the Plasmatron system, because the cost model has shown that this has the highest negative influence on the total cost. This was the second important finding.

Another finding that was detected during the detail cost study was the floor space difference in the plant for the brazing facilities. Laser systems need a specific laser enclosure to prevent injury, for example eye injuries. The Plasmatron system needs no specific safety devices, except a cheap tinted welding curtain in some cases. Due to these geometries, Plasmatron facilities use 50 sqm, whereas laser brazing facilities use 80 sqm for a standard vehicle body. The difference of 30 sqm can require plant rearrangements or even trigger an expensive building extension. Therefore, this factor should not be underestimated. The lower space requirement is a positive aspect for Plasmatron brazing. Moreover, as the Plasmatron system does not need a closed safety booth, it can be moved more easily if a rearrangement in the plant is required.

In this way, the cost efficiency of the Plasmatron brazing process can be enhanced to gain an advantage on the laser brazing.

This cost study led to the development of systematic Total Cost Model to support a total cost driven decision making approach to decide if laser or Plasmatron brazing is the best choice. This spreadsheet based model includes all important cost items. Every specified production volume can be accurately simulated very early in the planning phase with this new framework. This is useful to select the most cost effective joining method for coming projects. Additionally, this cost calculation program assists to identify the financial influence of weak points of the Plasmatron system.

The outcome from this chapter strengthens the assumption that it is important to increase the knowledge about fundamental input parameters of the Plasmatron brazing process.

5. Process Window for Plasmatron Brazing of Automotive Panels

This chapter presents an experimental investigation of the effect of brazing parameters on seam quality and electrode lifetime.

The motivation to study this objective was conceived because Plasmatron brazing is a multivariable and sensitive joining process. It involves a high number of process parameters, which all might have an influence on the seam quality and the electrode lifetime. This sensitivity is particularly pronounced in the brazing of thin metal sheets as the author has learned during the setup of Plasmatron brazing cells at Ford plants in different locations.

As the Plasmatron brazing process is much more sensitive when comparing with traditional automotive sheet metal joining methods like spot welding, it requires an increased knowledge regarding parameter-setting effects. It is therefore very important to study the influence of key input parameters to the Plasmatron brazing process. The production plants cannot do this because their primary objective is to produce vehicles. They cannot afford to change parameter set-ups because of the production stop risk.

5.1 Research Process

This section describes the research process to meet the stated research objective. The following four process steps describe the method used.

Step 1: Cause and Effect Diagram

The initial step of the research process was the development of a Cause and Effect Diagram (see Appendix G – Cause and Effect Diagram). This diagram provides an overview of probable root causes for Plasmatron braze defects. In a production process the traditional categories are: machines, methods, materials and people [185], which were applied here as well. This diagram is intended to be used as an aid for production engineers.

Step 2: Experiment Decision Matrix

To get an overview about the planned experiments and to analyse which experiments are most important or might be combinable with other experiments, an "Experiment Decision Matrix" (see Appendix H – Experiment Decision Matrix) was developed. For each experiment suggested, it was noted if the result would have an influence on the electrode lifetime, on the seam quality or on machine set-up time. The suggested experiments were then sorted to their importance and to their combinability. As well, the experiment duration time, the likelihood of success, the required resources (budget, head count, material, consumables, etc.) was estimated and rated.

Step 3: Conduct Experiments

Based on the weighting results from the decision matrix, six braze experiments were chosen to understand how sensitive the Plasmatron braze process is to variation of these parameters. The important input parameter sets from each experiment are shown in the experiment method section. The remaining input parameter can be found in the related Appendix.

The experiments in this chapter were conducted with the Plasmatron cell from the University of Nottingham. The cell details was described in sub-chapter 3.2.1.

Step 4: Evaluating Findings

The final step is to analyse the obtained results and to discuss the findings. The discussions from all experiments were summarized at the end of this chapter.

The following sub-chapters present the conducted brazing experiments.

5.2 Torch Tilting 'Pushing - Pulling'

In this experiment the effect of different brazing head tilting directions on the braze quality is analysed. The experiment should answer the question of which torch direction would deliver the best braze behaviour, seam quality and lowest black soot. Additional, the electrode tip contamination behaviour should be observed. Figure 5-1 shows the different tilting directions of the brazing head.

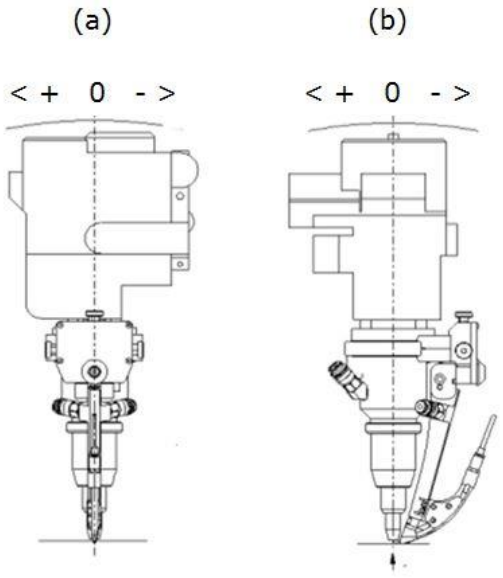


Figure 5-1: Plasmatron head tilting capabilities;
(a) Torch tilting 'left – right'; (b) torch tilting 'pushing – pulling'.

Currently it is not known what effect the torch direction pushing or pulling has on the braze quality. Inocon recommended a centred angle to the baseline arrangement. However, it would be interesting to understand if a torch tilting in pushing or pulling direction would show a difference in the seam quality.

5.2.1 Experimental Methodology

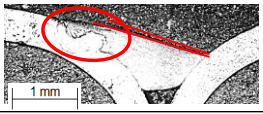
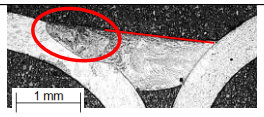
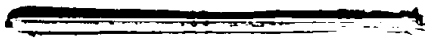
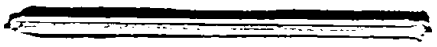
The Plasmatron cell from the University of Nottingham allows a 'pushing – pulling' tilting only in the range of 2° pushing and 4° pulling. Therefore, only four different torch tilting set-ups were used, which are 2° pushing, 0°, 2° and 4° pulling. For the accurate tilting adjustment, a digital protractor was used. The flange butt joint bended test panels were made

of galvanized steel with a material thickness of 0.8 mm. The brazing speed and wire speed were both 1.2 m/min. The current 120 ampere. The brazing length for all four specimens was 240 mm.

5.2.2 Results

The following Table 5-1 shows the experiment results.

Table 5-1: Results from the torch tilting 'pushing – pulling' experiment.
The amount of black soot shows only marginal changes.
The red circles marking the base metal melting.

Torch Tilting Direction (degree)	Cross Section View	Wetting Angle (degree)	Black Soot from the Brazed Seam (top view, tresholded)	Black Soot Area (cm^2)
0°		3.5°		20.9
2° pulling direction		2.9°		21.3
4° pulling direction		0°		18.4
2° pushing direction		0°		19.9

Each microscopic cross section showed base metal melting on the left side of the joint. Nearly half of the base metal thickness was affected. This indicates that the torch was not correctly aligned to the test panel gap direction during the brazing process.

In addition, it was observed that the 2° pushing and the 4° pulling torch directions showed the best filler sinking with a flat filler surface (zero degree wetting angles). The seams with 0° and 2° pulling direction both showed a slightly convex surface with wetting angles around 3°.

The top view of the seam indicated no seam quality issue. All seams were free of visual brazing failures. The black soot area measurement indicated only minor differences (six per cent from the largest to smallest black soot

area size). The electrode tip showed no contamination and size differences before and after the four brazes.

5.3 Influence of Surface Cleanliness

The automotive industry would welcome not to clean the panels with deoiling solvent before brazing. This would save cost because panel cleaning at the seam area with solvent requires the installation of an expensive fume extraction and an automatic or manual cleaning process. Moreover, the usage of solvent increases the health risk for the employees in the plant.

It is currently best practice in the automotive industry that the steel mills apply a thin lubricant film to the metal sheet before coiling, so-called "prelubes". They provide corrosion protection and reduce the friction during the stamping process.

For brazing, clean metal surfaces should provide better braze qualities when compared to contaminated surfaces as they are free of oil and any undesired contaminants. Oxide layers and surface contaminants can impede the wetting and flow of liquid braze filler metals and must be removed for successful brazing [207]. Only then can uniform capillary attraction be obtained.

The aim of this experiment is to investigate if pre cleaning from the to be joined zinc coated steel panel surfaces has an advantage on the quality of the brazed seam. Additionally, it is interesting for industrial users to understand if a panel pre cleaning would reduce the amount of black soot produced during brazing.

The answers to these questions are interesting because currently it is not yet understood if solvent panel cleaning from the slightly oiled automotive steel panels would deliver great, minor or even no advantage to the seam quality. To be on the safe side, production plants currently clean the joint areas with solvent before brazing.

5.3.1 Experimental Methodology

The variable investigated here was the surface cleanliness of the to be joined zinc coated steel test panels. The remaining input parameter can be found in the Appendix J - Surface Cleanliness Experiment. The interdependence with other variables was not explored because only the affect from the surface cleanliness without disturbance should be gained.
A pair of 220 mm long base metal sheets was prepared for a flanged butt joint. Half of the surfaces were cleaned with a rag soaked in alcohol. The other half side of the test panel surfaces were left as received and contaminated with oil and dust particles. To eliminate chances of contamination of dust particles transferring from unclean to clean surface area, the brazing direction ran from the clean to unclean area. Following microscopic investigations on a cross-section sample from the cleaned panel in comparison to a cross section sample from the uncleaned test panel were prepared for microscopic investigations to highlight seam internal quality differences.

5.3.2 Results

The brazed Plasmatron joint on the cleaned test panel side presented a slightly better aesthetic appearance compared to the uncleaned side, seen from the top. Additionally, it was observed that the cleaned surfaces showed thirty-five per cent less black soot contaminations than the as received area (see Figure 5-2).

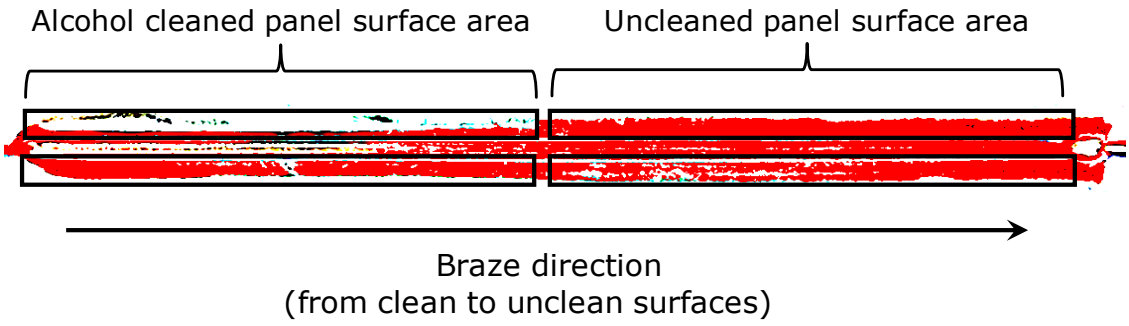


Figure 5-2: Influence of surface cleanliness.
Threshold coloured top view photo with red marked area to measure the black soot amount. The cleaned surfaces showed thirty-five per cent less black soot contaminations than the uncleaned surfaces.

The contact quality from the filler material to the galvannealed panels was observed under the microscope. The section picture from the cleaned test panel side (see Figure 5-3) shows that the contact lengths from the left and right seam sides are of different lengths. The left contact length is 0.9 mm and the right contact length is 1.9 mm. The reason for this was that the joint lines were not perfectly aligned to the braze direction. However, this panel misalignment does not undermine the observations that are relevant for this experiment. The section cut from the cleaned panel side showed only one section with a 0.1 mm short insufficient contact length.

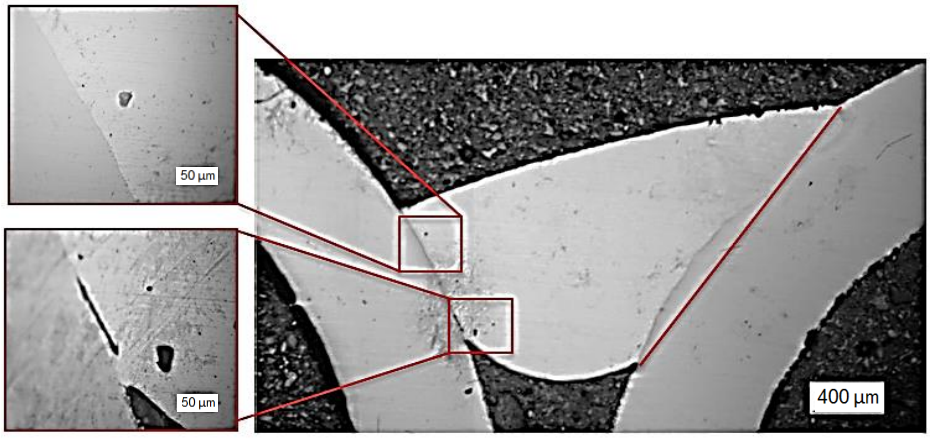


Figure 5-3: Cross-section of the cleaned test panel side.
The enlargement shows only one small unsteady joint area.

The joint section picture from the uncleaned test panel side (see Figure 5-4) showed 15 interruptions between the base metals and the filler material. One section (on the right side) showed a 0.3 mm long unsteady connection between the filler and the base metal.

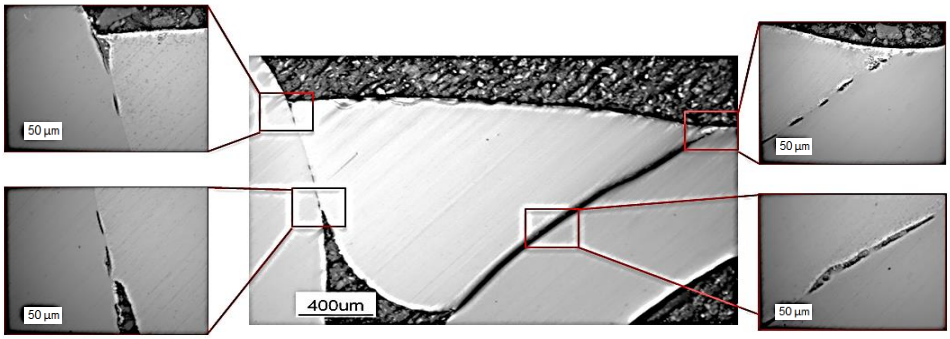


Figure 5-4: Cross-section of the uncleaned test panel side.
The inset images on the left and right side show a higher magnification image of insufficient filler adhesion in the braze interface.

5.4 Electrode Offset

It is important for the Plasmatron brazing cell set-up to understand how misalignment between the wire and the electrode tip affects braze quality. Figure 5-5 shows an illustration of electrode tip offset.

This experiment gives an essential insight of how a plasma arc reacts when the electrode is moving laterally out of the filler wire centre line.

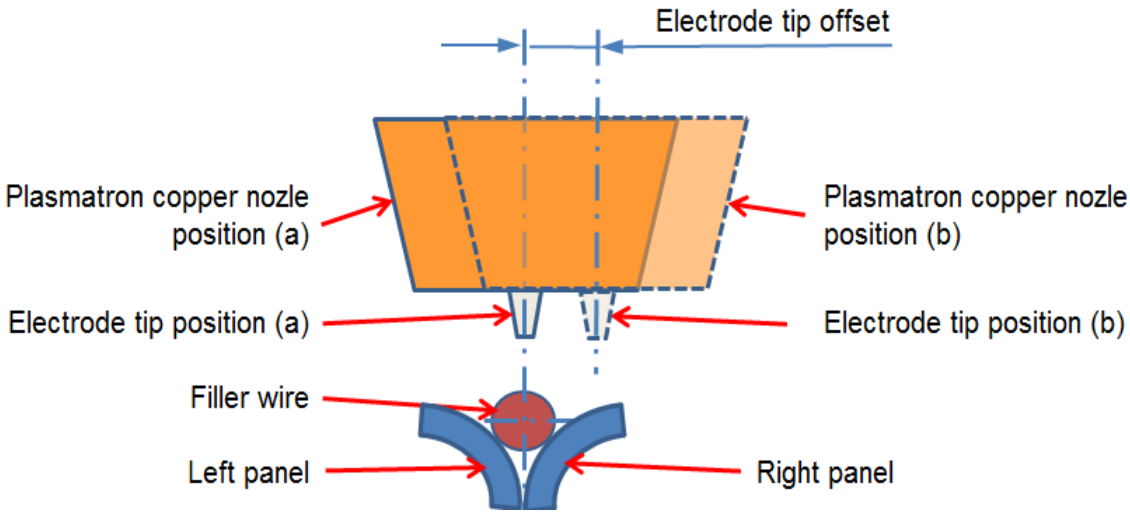


Figure 5-5: Schematic of the electrode tip offset.
Position 'a' shows an aligned electrode tip,
position 'b' an lateral electrode tip offset from the wire axis.

5.4.1 Experimental Methodology

Seven flange butt joint brazes (100 mm long) were conducted with varying wire offset positions. The range was from 0 mm offset to 1.8 mm offset in 0.3 mm steps. The remaining input parameter can be found in Appendix K - Electrode Offset Experiment.

To ensure an exact offset adjustment between the filler wire and the electrode tip, the microscope camera based electrode monitoring system as described in chapter 3.3.10 was used. The following picture shows the camera setup for this experiment (Figure 5-6).

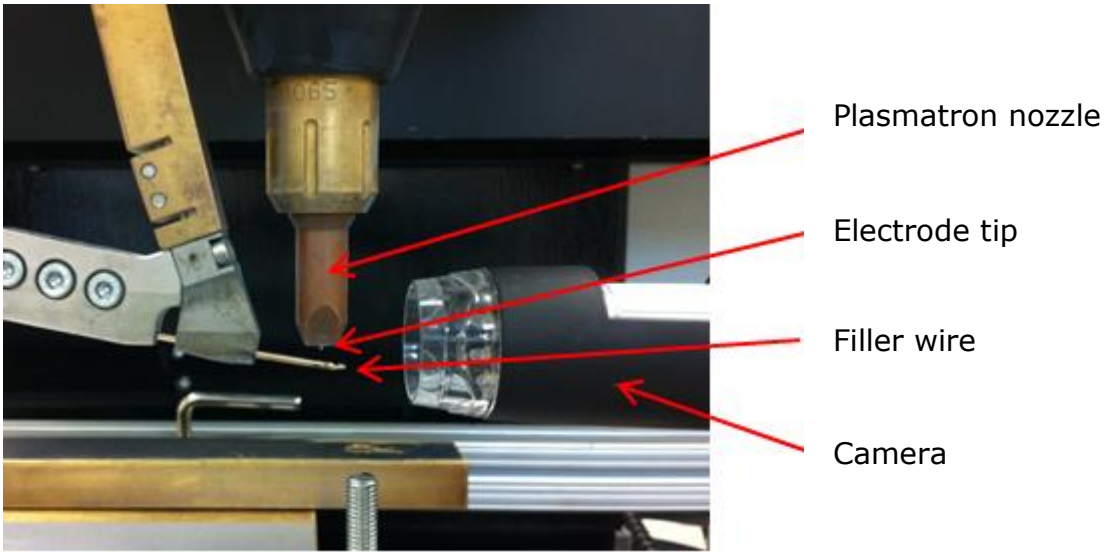


Figure 5-6: Camera set-up from the wire offset experiment

The effects of these different electrode offset settings were checked and measured using microscopic analyses on the prepared cross sections. Figure 5-7 describes which dimensions were captured from the cross sections.

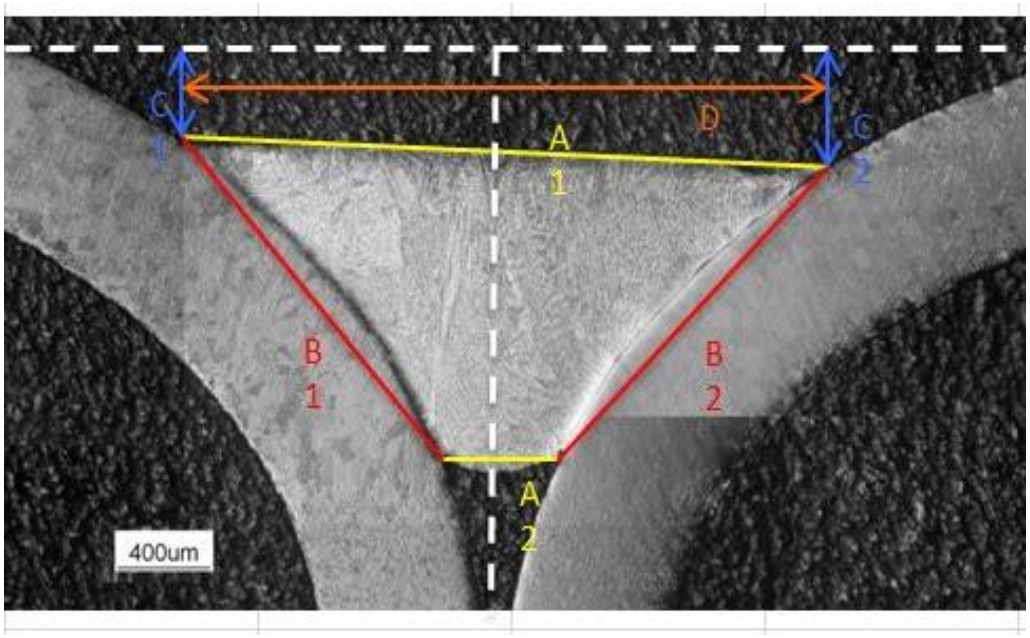
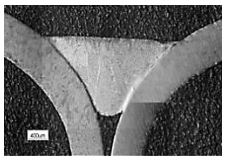
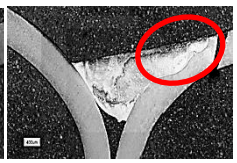
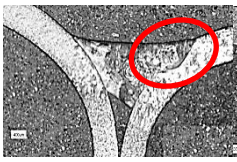
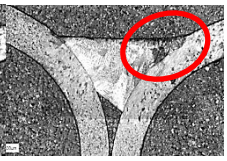


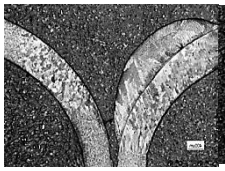
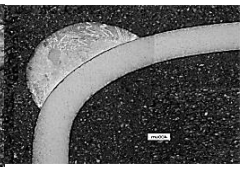
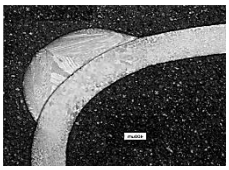
Figure 5-7: Definition for the dimensions on the braze cross section;
(B1) left adhesive length, (B2) right adhesive length and (D) the seam width were measured for this experiment.

5.4.2 Results

The recorded data from the filler wire offset experiments are shown in following Table 5-2.

Table 5-2: Results of different electrode tip offsets to the braze wire axis. The red circles marking the base metal melting.

Wire Offset (mm)	**0.0**	**+0.3**	**+0.6**	**+0.9**
Cross sectional image				
B1) Left contact length (mm)	1.71	1.04	1.56	1.49
B2) Right contact length (mm)	1.59	2.79	2.31	2.20
Ratio between left and right contact length	1.08	0.37	0.68	0.68
D) Seam width (mm)	2.81	3.73	3.59	3.17
Base metal melting area (mm^2)	0	1.06	0.76	0.59

Wire Offset (mm)	**+1.2**	**+1.5**	**+1.8**
Cross sectional image			
B1) Left contact length (mm)	0	0	0
B2) Right contact length (mm)	3.45	4.48	3.03
Ratio between left and right contact length	0	0	0
D) Seam width (mm)	0	0	0
Base metal melting area (mm^2)	0	0	0

The braze line top views with electrode offsets between 0 mm and 0.9 mm show visually acceptable seam surfaces without any imperfections like waviness or lack of adhesion. The measured seam width with an electrode offset between 0.0 mm – 0.9 mm was between 2.81 mm and 3.73 mm.
The braze lines with electrode offsets of 1.2 mm, 1.5 mm and 1.8 mm showed a complete lack of filler adhesions on the left side of the flange butt joint.
The cross section inside views on the specimen, which was brazed with an electrode offset between 0.3 mm – 0.9 mm, showed significant base metal melting. On the specimen with the 0.3 mm and 0.6 mm offset, the base metal melting depth was greater than half of the sheet thickness. The specimen with the 0.9 mm offset showed less base metal melting than the 0.3 mm and the 0.6 mm off set specimens. The seams with an offset between 1.2 and 1.8 mm showed no base metal melting.
With increasing offset, the filler material had no chance for a symmetrical capillary flow to both parent metals anymore. The filler flowed the shortest way to the nearest parent metal when the offset was ≥ 1.2 mm.

5.5 Influence of Electrode to Wire Gap

The effect of distance between electrode tip to the filler wire (see Figure 5-8) was investigated to assess the sensitivity of the process to variation in setup. The sensitivity of this parameter and the previous electrode tip off parameter is essential for the industry Plasmatron setting because it is important to understand how sensitive the process reacts to variations of these parameters.

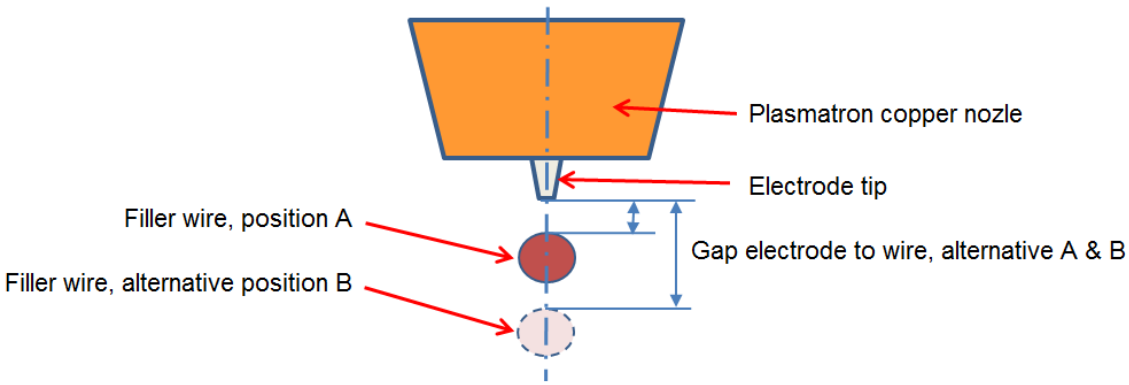


Figure 5-8: Distance between electrode tip and filler wire surface.
This schematic shows two different distances as example.

5.5.1 Experimental Methodology

The gap size between the electrode tip and the filler wire surface were the only variable input parameters in this experiment. The braze speed and the table speed was reduced to 1 m/min, which simulates the setting of the Ford Plasmatron production cell. The other settings were copied from a running Plasmatron production cell, which is in use for the same steel panel pairing. The braze trial consists of 220 mm long test panel pair for each parameter setting. Table 5-3 provides those parameter set up details.

Table 5-3: Parameter set up for the 'gap electrode to wire' experiment. The 'electrode to wire gap' was the only variable in put parameter.

No.	Main Input Parameter	Runs (a)	(b)	(c)	(d)
1	Current (A)	100			
2	Braze speed (m/min)	1.0			
3	Wire speed (m/min)	1.0			
4	Electrode to wire gap (mm)	0.6	0.8	1.6	2.0
5	Gas flow (l/min)	7.5			
6	Torch angle from side (degree)	0			
7	Torch angle from front (degree)	3.0			
8	Electrode type	WL20, ø 6.4 mm, 20° tip angle			
9	Zinc coating type	galvannealed			
10	Joint type	flanged lap joint			

It has to be mentioned that the distance between the electrode and the filler wire was increased in uneven intervals. This was done to save samples because variance between the first two stages were not recognisable.

5.5.2 Results

The visual inspection of the seams did not show any seam discontinuity, surface cracks, surface porosities or spatters at the surface. The measured results of each parameter set-up were averaged. The larger electrode to

wire gaps result in larger black residue areas from both sides of the seam as shown in Figure 5-9. The 0.6 mm electrode to wire gap generates a 1.9 mm black wide residue strip on both sides of the seam. The 2.0 mm electrode to wire gap causes a 3.6 mm black residue line width.

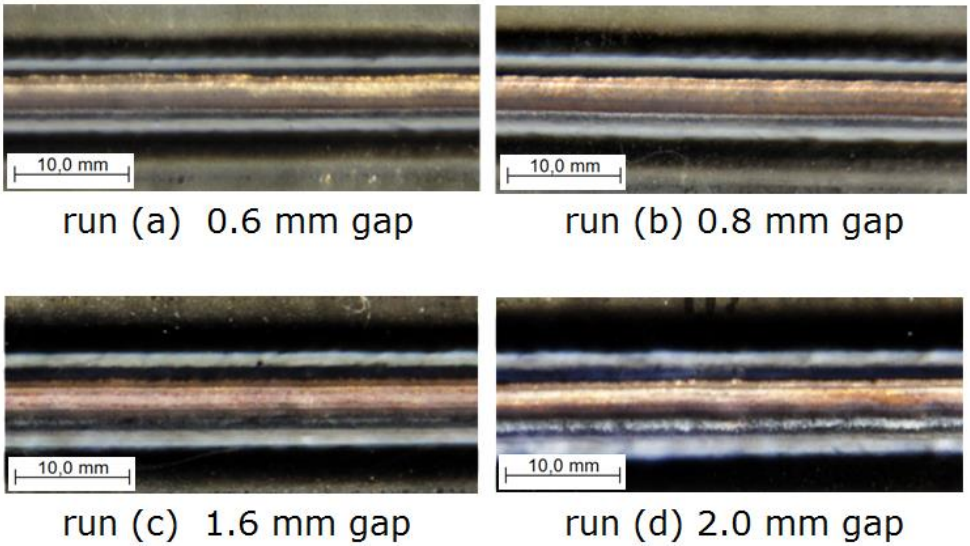


Figure 5-9: Joint top view of different electrode to wire gap setups.
The greater the distance between electrode tip and the wire,
the larger the black residue amount.

Figure 5-10 shows the cross sections of the brazed specimens exemplary for each parameter set-up. The left and right filler contact length of each cross section was measured. Additionally, the top radius of each seam was measured with ImageJ.

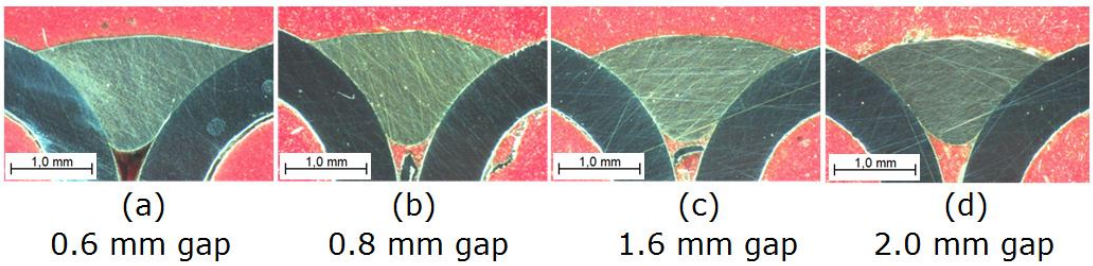


Figure 5-10: Cross-sections of the electrode to wire experiment.
The greater the distance between electrode tip and the wire, the smaller the braze radius and the contact lengths.

Table 5-4 presents the cross-measurement results. Furthermore, the table shows the results of the black soot width measurements, the tensile test results and the positions where the specimens broke.

Table 5-4: Effects of the increased electrode to wire gap to the seam cross section size, black soot width and the tensile force.

Label	Electrode to filler wire gap (mm)	Braze radius (mm)	Contact length left (mm)	Contact length right (mm)	Black soot width (mm)	Tensile force F_{max} (kN)
(a)	0.6	4.31	1.59	1.73	1.9	7.22
(b)	0.8	3.60	1.63	1.35	2.2	8.06
(c)	*1.6*	*3.36*	*1.26*	*1.37*	*2.5*	*7.71*
(d)	2.0	2.73	1.14	1.31	3.65	6.87

To illustrate the correlation between the 'electrode to wire' distance changes and the measured effects on the cross sections and on the black soot width, the following line graph was created (see Figure 5-11).

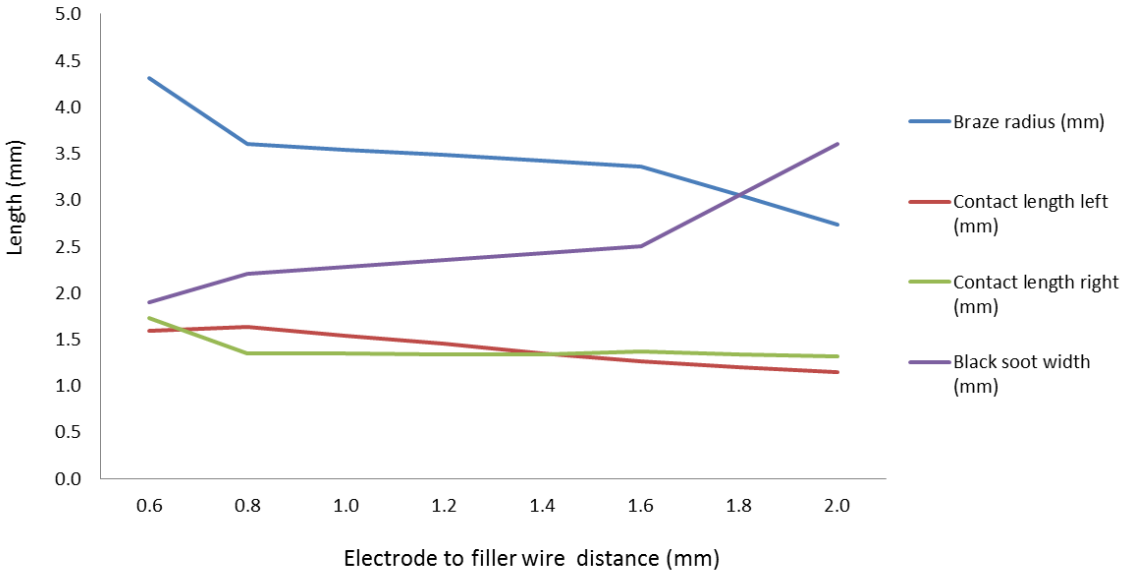


Figure 5-11: Estimation of the best electrode to wire distance. The contact lengths do not change significantly. Only the black soot width started to increase stronger at 1.6 mm electrode to filler wire distance.

In reference to Figure 5-12 it has to be mentioned that the maximum tensile force shows only small variation for the different electrode to wire gaps. All measured tensile forces were far above the required minimum tensile force limit (here 4.3 kN, see Chapter 4.4.1 for more details).

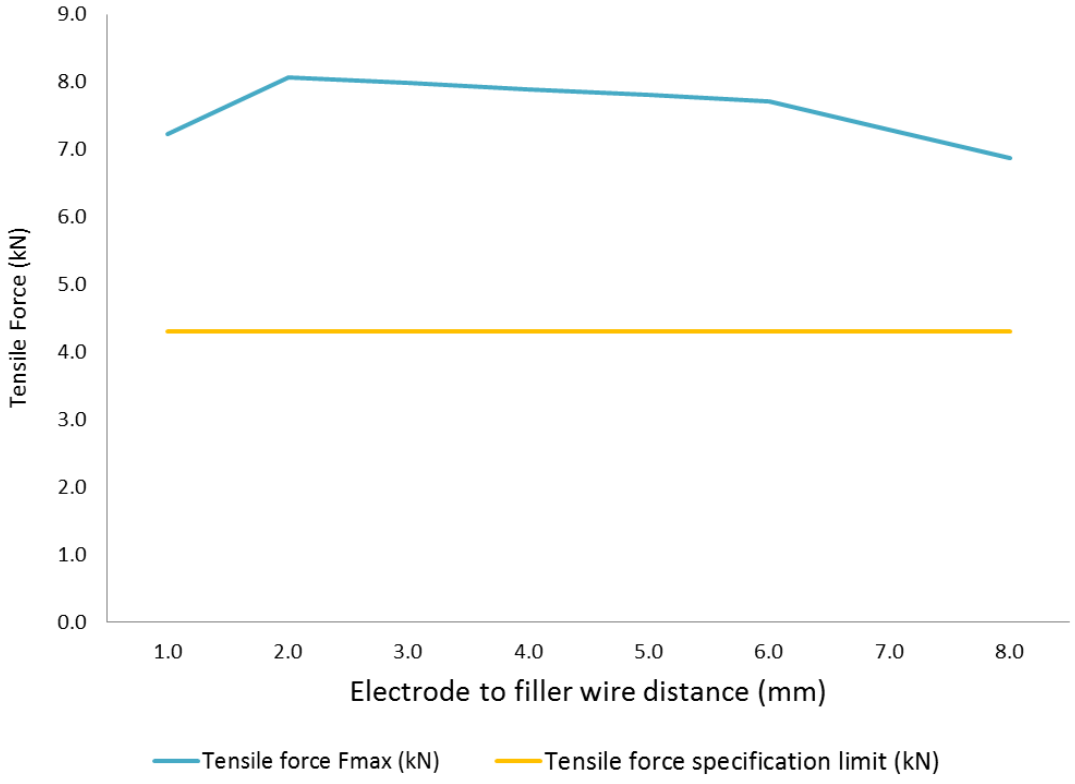


Figure 5-12: Correlation between the electrode to filler wire distance and the tensile force F_{max}.

The contact lengths from the filler to the parent metals decreased slightly when the 'electrode to wire gap' increased. Simultaneously, the braze radius is gradually reduced from 4.3 mm to 2.7 mm when the distance between the filler wire and electrode increases. When adjusting the electrode to wire gap from 0.6 mm to 2 mm, the brazed radius is reduced by 37 %. This proves that the gap size between electrode tip and filler wire shows a significant influence on the seam radius.

In addition, the black soot area is enhancing during the tests. The black soot stream from the last test panel was 3.6 mm width and was almost twice as high as the soot stream from the first test panel, which had a width of 1.9 mm.

5.6 Influence of Brazing Current

The aim of this experiment was to determine the influence of the current setting of the Plasmatron brazing process on the quality of a Plasmatron brazed seam. It is clear that a higher current would create higher process heat with all other factors constant, which could result in undesirable intermetallic phases (see chapter 3.3.4.4), base metal erosion or would even burn holes in the base panels. Otherwise, too little current could lead to incomplete filler flow, which would weaken the joint.

5.6.1 Experimental Methodology

The current was the only variable input parameter in this experiment, which was changed 5 times and run two times from 80 A to 120 A with an increment of 10 A for each step. The other settings were copied from a running Plasmatron production cell, which is in use for the same steel panel pairing. No other input parameters were changed during the experiment. Table 5-5 shows the used main settings.

Table 5-5: Input parameters for the influence of 'current' experiment. The 'current' was the only variable input parameter.

No.	Main Input Parameter	Runs									
		1a	1b	2a	2b	3a	3b	4a	4b	5a	5b
1	Current (A)	80		90		100		110		120	
2	Braze speed (m/min)	1									
3	Wire speed (m/min)	1									
4	Electrode to wire gap (mm)	0.6									
5	Gas flow (l/min)	7.5									
6	Torch angle from side (degree)	0									
7	Torch angle from front (degree)	3									
8	Electrode type	WL20, ø 6.4 mm, 20° tip angle									
9	Brazing length	220 mm									
10	Zinc coating type	galvannealed									
11	Joint type	flanged lap joint									

One cross-section sample was prepared of each brazed joint. This was undertaken to capture optical microscope images of each seam cross-section, which were measured with ImageJ afterwards. These cross-section measurements should then give an indication of how the current influences the seam quality. Additionally, each brazed joint was subject to tensile testing in order to understand how the current setting influences the tensile force.

5.6.2 Results

The joint surfaces were subject to an initial visual inspection. All seams were free of seam discontinuities, surface cracks, surface porosity or spatters. However, the surface roughness of the seams gradually changed with increased input current. Moreover, the nearby areas of the brazed joints showed black residue areas, which increased significantly by a higher current (see Figure 5-13).

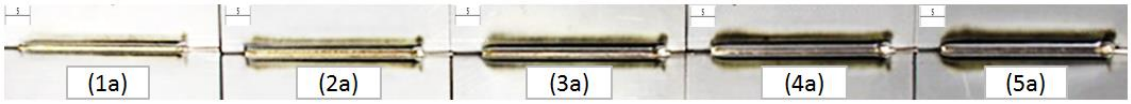


Figure 5-13: Brazed seams of different current inputs.
The black residue areas increased by higher current.
(1a) - 80 A, (2a) – 90 A, (3a) – 100 A, (4a) – 110 A, (5a) – 120 A

Figure 5-14 shows the cross section of all braze specimens. The left and right filler contact lengths of each cross section were measured. The top radius of each seam was also measured.
Surprisingly, the cross sections 4b (110 A), 5a and 5b (both 120 A) already showed base metal melting on the right side of the seams as seen in
Figure 5-14. This might be the result of a misalignment from the test panel clamping.

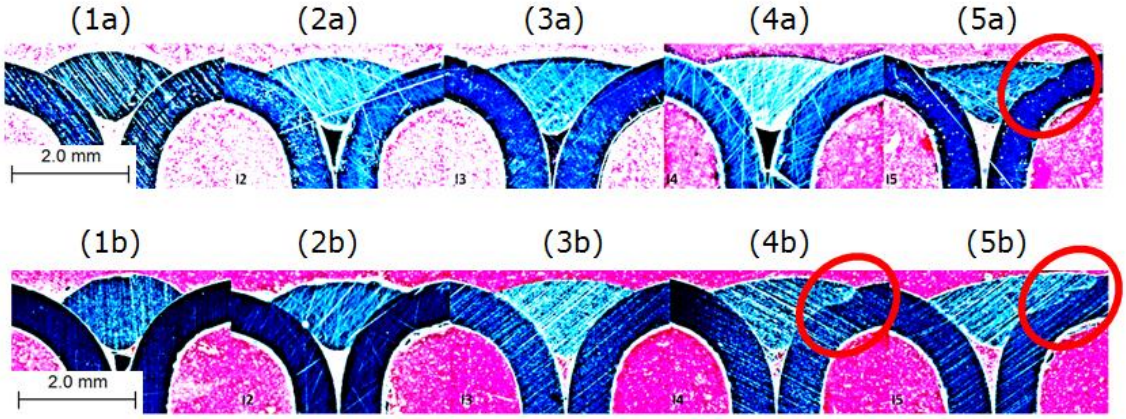


Figure 5-14: Cross-sections of test run (1a-5a) and run (1b-5b).
The red circles (5a, 4b, 5b) indicate the joint areas where
base metal melting occurred.

Table 5-6 presents the cross-section measurement results. Furthermore, the table shows the results of the tensile test (F_{max}) and the position where the specimen broke during the tensile test.

Table 5-6: Cross section measurements and tensile forces of the 'influence of brazing current' experiment.

Label	Current	Braze	Contact length		Melted	Tensile force
		radius (mm)	left (mm)	right (mm)	base metal (mm)	Fmax (kN)
1a	80 A	2.03	0.99	1.09	no	4.70
1b	80 A	1.65	0.94	1.08	no	5.80
1$\bar{x}$		1.84	0.97	1.08		5.25
2a	90A	3.02	1.51	1.39	no	6.30
2b	90A	3.09	1.12	1.53	no	8.20
2$\bar{x}$		3.05	1.32	1.46		7.25
3a	90A	4.31	1.59	1.59	no	7.20
3b	90A	3.70	1.39	1.64	no	8.70
3$\bar{x}$		4.01	1.49	1.62		7.95
4a	90A	4.95	1.59	1.45	no	9.10
4b	90A	4.02	1.39	1.73	0.12	8.30
4$\bar{x}$		4.49	1.49	1.59		8.70
5a	90A	8.21	1.17	1.73	0.21	8.40
5b	90A	6.23	0.92	2.33	0.23	8.80
5$\bar{x}$		7.22	1.05	2.03	0.22	8.60

The following plot as seen in Figure 5-15 shows the results of tensile testing and morphology against current.

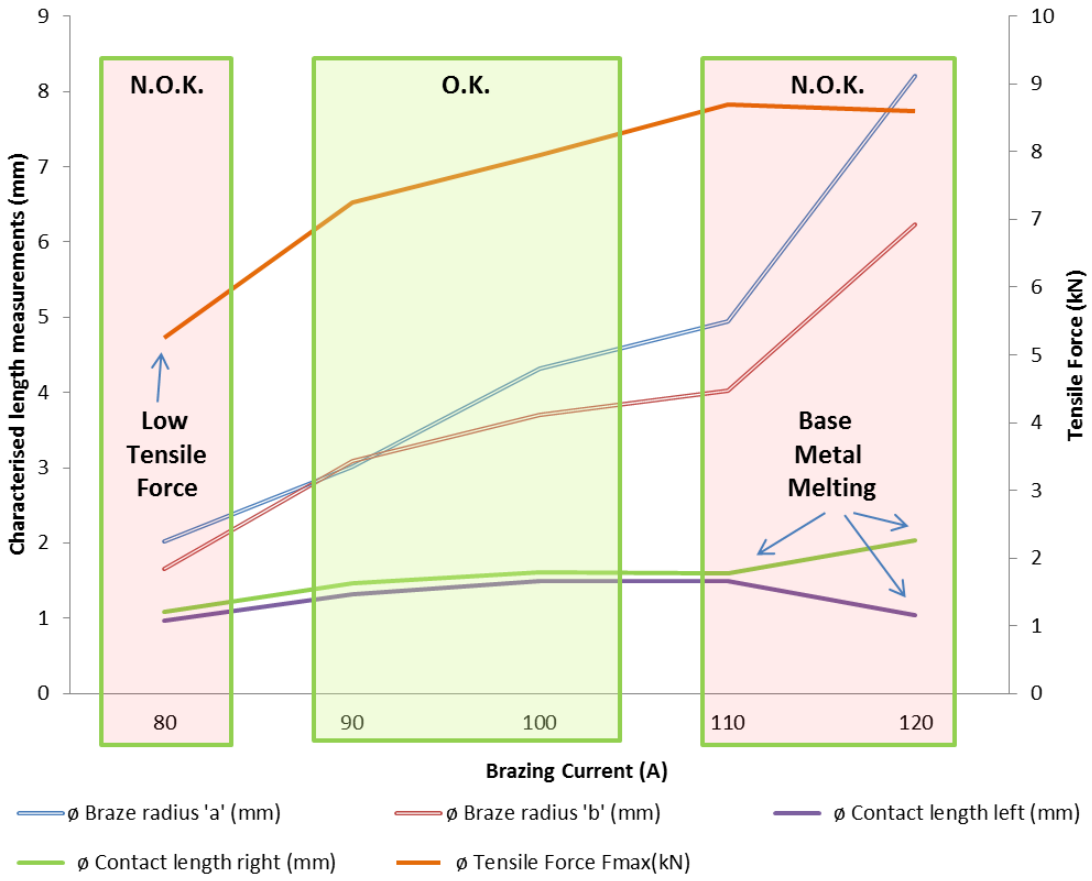


Figure 5-15: Determination of the perfect braze current setting.
The green area shows the currents with good seam quality.

The graph shows that the joint strength increases with a higher input current. However, at a current of 110 A to 120 A, the trend of joint strength seems to be stable. Although at high currents the base metal melting on the contact zone has occurred. The joint strength is still high, even higher than the joint without melted base metal. Additionally, the graph shows that with an increasing currency the braze radius increases too. The impact to the contact length is not significant.

At a value of 80 A, the current input seems insufficient to melt the filler wire completely. It leads to an inefficient adhesion length and to less strength in the joint. Thus, the joint strength is slightly above the boundary strength required from Ford for a roof joint (>4.5 kN at 25 mm braze length).

On the other hand, the 110 A value shows evidence for excessive energy input to the brazed joint which leads to base metal melting.

To conclude, when the current is between 90 A and 100 A, the quality results are O.K.

5.7 Braze Speed

The running costs of brazing depends highly on the productivity. The key parameter here is the brazing speed. As highlighted in Chapter 4.3.2, the lower Plasmatron brazing speed in comparison to the faster laser brazing speed (based on benchmarking trials [208]) has a significant negative cost impact for high production manufacturing when using Plasmatron joining. The ability to introduce the Plasmatron brazing processes in high volume plants would create an enormous cost saving for the automotive industry due to a reduced requirement for more expensive laser cells.

5.7.1 Experimental Methodology

Goal of the experiment was to increase the braze speed of 1.0 m/min (current Ford standard) as much as possible without compromising the seam quality, which means no external and internal imperfections like pores, surface roughness, seam waviness, etc. This is consistent with a continuous seam as described in chapter 3.4.2.

The current, the brazing speed (here table speed) and the wire speed were the only input parameters varied in this experiment. The brazing speed and the wire speed were set to always be equal.

It was necessary to vary both the braze speed and current for these experiments. If current is kept constant as braze speed increases, the heat input becomes inadequate to form a joint with only small changes in braze speed. Each incremental change of the braze speed was associated with specific current settings in order to gain a set of statements on the impact of different heat inputs. The chosen test material was galvannealed steel panels with a flanged butt joint, which simulates a brazed vehicle roof joint. Table 5-7 shows the parameter selected. Six different settings were brazed twice. In order to obtain a simple comparable factor for the

energy input, it was decided to divide the current through the braze speed (E).

Table 5-7: Parameter set-up for the 'braze speed' experiment

No.	Main Input Parameter	Trials					
		1 a-b	2 a-b	3 a-b	4 a-b	5 a-b	6 a-b
1	Current (A)	100	120	125	150	150	175
2	Braze speed (m/min)	1.0	1.0	1.5	1.5	2.0	2.5
3	Wire speed (m/min)	1.0	1.0	1.5	1.5	2.0	2.5
	E = Ratio Current to Braze speed	100	120	83	100	75	70
4	Electrode to wire gap (mm)	2.0					
5	Gas flow (l/min)	7.5					
6	Torch angle from side (degree)	0					
7	Torch angle from front (degree)	3					
8	Electrode type	WL20, ø 6.4 mm, 20° tip angle					
9	Brazing length	220 mm					
10	Zinc coating type	galvannealed					
11	Joint type	flanged lap joint					

More precise is the *arc heat energy* value, simplified to *arc energy*. This value cannot be measured directly. It can only be calculated from other available parameters. Industrial users are applying the arc energy equation as primary method for quantifying the heat energy of welds [209]. The arc heat energy is typically calculated as the ratio of the power to the velocity of the heat source [210]. The power is here the product of voltage and electric current. The arc heat energy equation is therefore as follows:

$$Arc\ Heat\ Energy\ \left(\frac{kJ}{mm}\right) = \frac{60 * I_A * V_A}{1000 * BS} \qquad 5\text{-}1$$

I_A is the arc current in milliamps (mA), V_A is the arc voltage in kilovolts (kV) and BS is the braze speed in meter per minute (m/min). The braze speed was set on the motor controlled movable frame cradle. The other values were captured from the transformer setting and derived from value tables, which the transformer manufacturer provided.

One obvious limitation of the standard heat energy equation is that the radiant heat energy, lost from the arc to the atmosphere, is not considered. This inaccuracy is managed by multiplying the arc heat energy

by an arc efficiency factor [209]. Each arc welding process has a different efficiency rating. For TIG welding, the efficiency factor is appropriate to $\mu_A = 0.6$ [211]. The heat input equation with arc efficiency factor is then:

$$Heat\ Input\ \left(\frac{kJ}{mm}\right) = \frac{60 * I_A * V_A}{1000 * TS}\ \mu_A \qquad 5\text{-}2$$

Digital images of the brazed seams were captured. One cross-section sample was prepared of each brazed joint to capture optical microscope images, which were measured afterwards. These cross-section measurements should then give an indication of how the different braze speeds influence the seam quality. Additionally, the tensile force F_{max} of each braze sample was measured to determine whether the braze speed changes shows a tensile strength change.

5.7.2 Results

First, the joint surfaces were visually inspected. All seams were acceptable and did not show any seam discontinuities, surface cracks, surface porosity or spatters. Only the panels number two and four on run a and b showed minor seam waviness (see Figure 5-16).

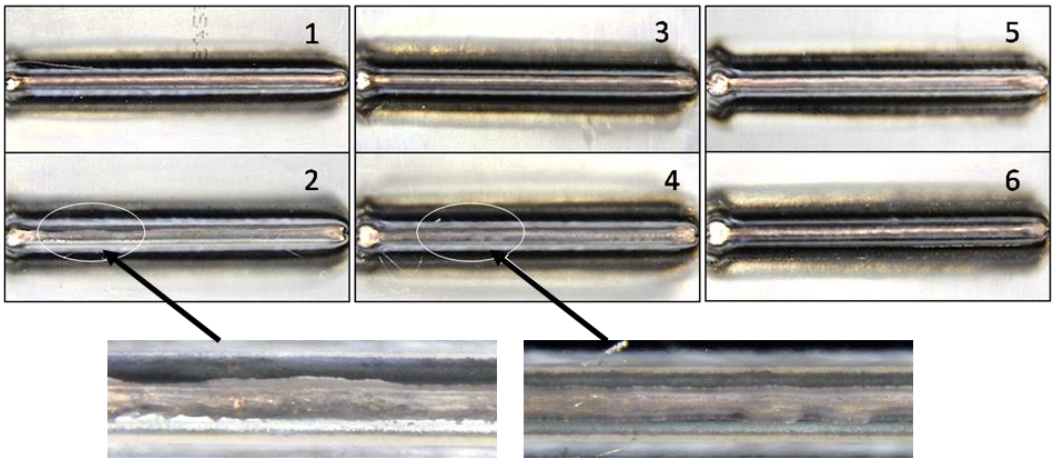


Figure 5-16: Effect of different braze speeds on the seam quality. Top views of all braze seams of run (a). The braze speed increased from 1.0 m/min (1) to maximum 2.5 m/min (6). Panels (2) and (4) show minor seam waviness.

Figure 5-17 shows the cross section of all braze specimens. The left and the right filler adhesion lengths of each cross section were measured. In addition, the top radius of each seam cut was measured. The cross sections of 2a, 2b and 4b showed base metal melting on the right side of the seam.

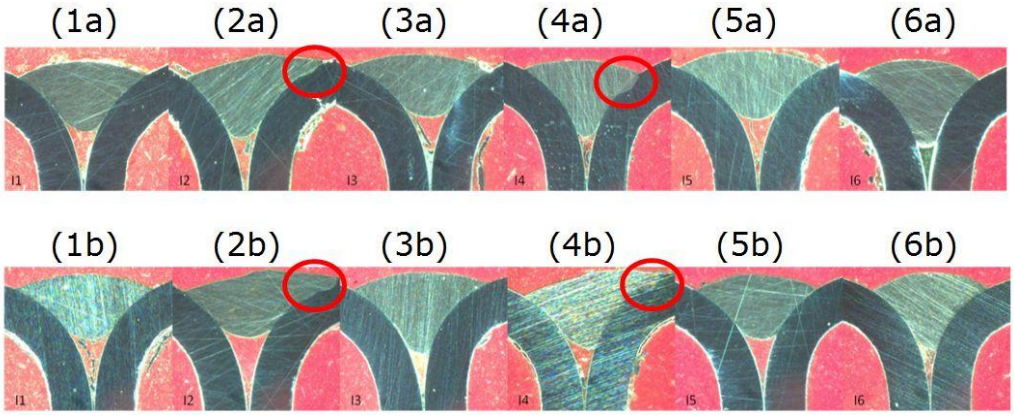


Figure 5-17: Cross-sections of braze speed test run (a) and (b)
The red circles mark base metal melting.

Table 5-8 presents the cross-section measurement results. Furthermore, the table shows the measured tensile force F_{max} and the position where the specimen broke during the tensile test.

The braze lines with the lowest energy input E (here 70 to 75 on the specimen 5a, 5b, 6a and 6b) have not shown any base metal melting. Additionally, these specimens have shown the smallest braze radius size in average (2.98 mm and 2.21 mm). These results indicate that the braze heat was lower on these braze specimen than on the other specimen. Another important finding was that the specimens with the highest braze speed (here 2.5 m/min) have shown the longest contact lengths on both braze sides. This result demonstrated that Plasmatron brazing with higher braze speed can deliver reasonable braze quality.

Table 5-8: Cross section measurements and tensile forces F_{max}

Label	Current (A)	Braze and wire feeder speed (m/min)	Energy input E (A/(m/min)	Braze radius (mm)	Contact length		Melted base metal (yes/no)	Tensile Force F_{max} (kN)	Tear down position
					left (mm)	right (mm)			
1a	100	1	100	2.73	1.14	1.31	no	6.90	on seam
1b	100	1	100	3.28	1.41	1.15	no	8.80	on seam
1 $\bar{x}$	100	1	100	3.01	1.28	1.23		7.85	
2a	120	1	120	3.59	1.23	1.76	yes	9.00	on seam
2b	120	1	120	5.89	1.01	1.72	yes	8.60	on panel
2 $\bar{x}$	120	1	120	4.74	1.12	1.74		8.80	
3a	125	1.5	83.3	3.44	1.40	1.11	no	7.50	on seam
3b	125	1.5	83.3	3.13	1.56	1.80	no	6.00	on panel
3 $\bar{x}$	125	1.5	83.3	3.29	1.48	1.46		6.75	
4a	150	1.5	100	3.22	1.75	1.43	no	7.30	on seam
4b	150	1.5	100	4.14	1.02	1.92	yes	7.30	on panel
4 $\bar{x}$	150	1.5	100	3.68	1.39	1.68		7.30	
5a	150	2	75	3.08	1.41	1.22	no	6.20	on seam
5b	150	2	75	2.88	1.18	1.24	no	5.80	on panel
5 $\bar{x}$	150	2	75	2.98	1.30	1.23		6.00	
6a	175	2.5	70	2.26	1.79	1.52	no	7.60	on seam
6b	175	2.5	70	2.16	1.29	1.60	no	6.00	on panel
6 $\bar{x}$	175	2.5	70	2.21	1.54	1.56		6.80	

Table 5-9 shows the arc energy and heat input calculation contributors, as well as the calculation results.

Table 5-9: Arc energy and heat input formula contributions and results

Label	Current I (A)	Voltage U (V)	Braze Speed (m/min)	Arc Energy (kJ/mm)	Process Efficiency	Heat Input (kJ/mm)
1	100	20.7	1.0	124.0	0.6	74
3	125	25.8	1.5	129.2	0.6	78
5	150	31.0	2.0	139.5	0.6	84
6	175	36.2	2.5	151.9	0.6	91
2	120	24.8	1.0	178.6	0.6	107
4	150	31.0	1.5	186.0	0.6	112

To assess the correlation between heat input and braze speed to the brazed joint measurements and the tensile strength, the results of the twelve specimens, two for each set of values, were captured in a line chart as shown in Figure 5-18. For the braze radius, the adhesion radius lengths left and right were measured and the average values of the two specimen sets were taken for the diagram. Additionally, the braze speed was plotted in the x-axis.

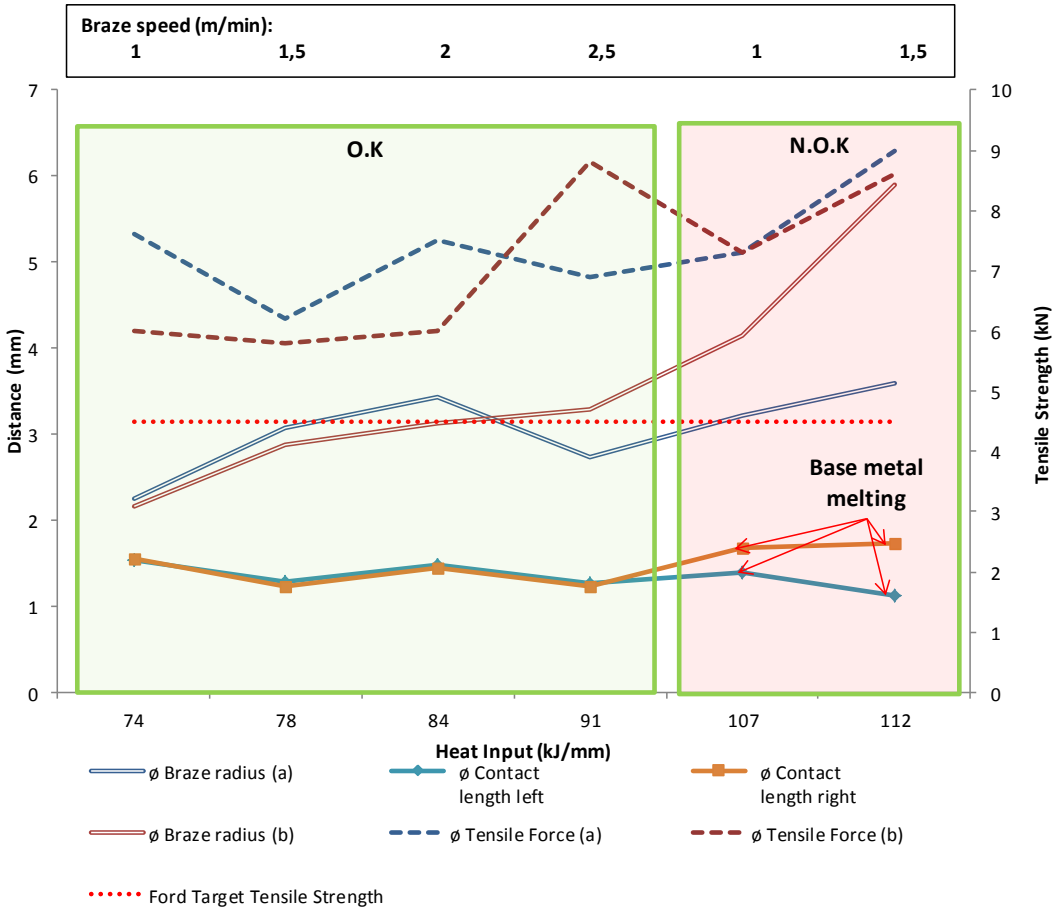


Figure 5-18: Seam quality in relation to heat input and braze speed

The line chart shows that there is an interaction between heat input and joint quality. The tensile strength increased with rising heat input. Base metal melting starts at higher heat inputs as well (here: 107 J/mm). The braze radius also increased with rising heat input, which was predictable due to the enhanced flow of the molten filler. The maximum braze speed without quality issue on the brazed joint was 2.5 m/min.

5.8 Chapter Discussion

In this section, the results obtained from this chapter are discussed and analysed. The findings below are based on the results of the previous brazing experiments, which were done to identify the influence of fundamental input parameters.

5.8.1 Torch Tilting 'Pushing - Pulling'

The results showed that torch tilt angles between 2° pushing and 4° pulling have only a minor effect on the braze quality and black soot observed. All braze seams on the test panels showed similar good filler surface qualities without any waviness or lack of adhesions. Each section cut from the brazed test panels shows massive base metal melting on the same base metal side only. This failure had nothing to do with the torch tilting. It indicates that the test panel clamping on the movable table was not hundred per cent aligned to the table travel path before brazing.

However, the recognition that a minor braze direction offset leads in base metal melting is an important finding. A small braze path misalignment to the electrode tip position should never be underestimated.

As the 'Pushing – Pulling' torch tilting experiment has shown only minor influence on the braze quality, it was decided not to repeat this experiment with an improved test panel alignment. Only a long-time observation during production with different torch tilting angles might be able to deliver new findings regarding avoidance of electrode contamination due to improved zinc vaporization behaviour. At pushing direction a preheating could generate an earlier zinc vaporization, which might produce less electrode contaminations.

5.8.2 Electrode Offset

The electrode tip offset experiment highlighted an unexpected and significant influence on seam quality when the electrode moves laterally away from the wire centre line.

Two major internal seam imperfections were observed. Melting of base material due to overheating and an acentric braze line along the length of the seam. Both failure types are problematic because they can be easily overlooked as they cannot be detected with visual surface detection methods. The failures were visibly detectable only on the cross section specimen.

It was observed that a lateral filler wire – electrode tip misalignment of 0.3 mm resulted in marked base metal melting and in an unsymmetrical

seam contact length of filler material. This sensitivity was not expected and highlighted how accurate the electrode tip needs to be aligned above the filler wire during the brazing cell setup.

5.8.3 Influence of Surface Cleanliness

It was discovered that the solvent cleaned panel surfaces showed thirty-five per cent less black soot contamination on the panel than the slightly oiled automotive steel test panels, after brazing. Additionally, it was important to observe that the filler material shows a considerably better filler contact on the cleaned test panel side than on the non-cleaned panel side. The detected insufficient filler adhesion on the not pre cleaned panel side reduces the mechanical joint strength, which could potentially lead to a seam crack. It looks as if the zinced steel panel treatment with prelubes obstructs a proper filler wetting. This might be because the lubricant is sitting in the zinc coat pockets and/or in the pockets from the temper rolling process. These temper rolling treatments are performed at the steel mills directly at the hot-dip line after the zinc coating. The automotive manufacturers require a steel panel surface that is more topographically uniform than obtainable directly off hot-dip coating lines. This is so that the underlying surface does not show through paint coatings used for such appearance critical applications as exterior automotive body panels [212]. A temper roll, which has less deep texture pockets, might be beneficial for brazing of zinc coated panels.
However, the aesthetic surface appearance of the solid filler does not highlight significant quality differences. This is an important observation as well because it could lead non-trained people to the conclusion that the seam quality is acceptable, even when it has serious filler adhesion issues inside.

5.8.4 Influence of Electrode to Wire Gap

The larger ‘electrode to wire’ gap leads to less energy input into the filler wire because the increased arc funnel can now flow on the left and on the

right side of the wire directly to the parent panels (see Figure 5-19). This leads to an increase of the black soot width on the parent panels (from 1.9 mm to 3.6 mm black sooth width as the electrode to wire gap increased 1.4 mm).

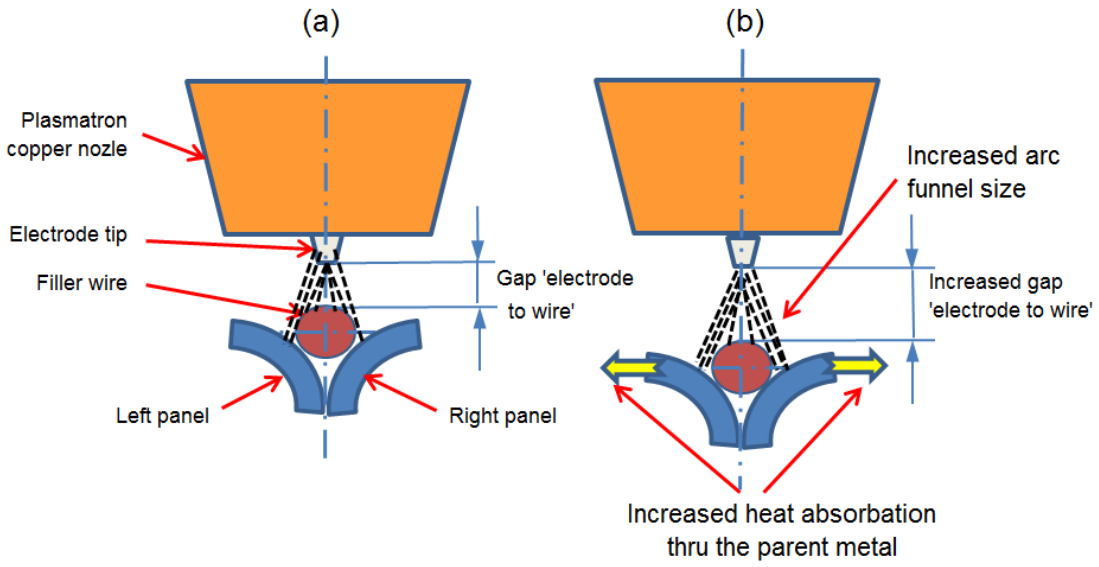


Figure 5-19: Schematic of 'electrode tip to wire gap' influence with (a) minor electrode to wire gap; (b) larger electrode to wire gap, where the arc hits the parent metals.

The parent metals absorb some of the arc energy, which then shrinks the capillary flow of the filler material. The results from the contact length measurements underscore this assumption.

The most important finding of this experiment is that the Plasmatron brazing process is not hugely dependent upon on the gap size between the electrode tip and the wire. Since this is the case, the industrial setting of this input parameter is not critical and does not need tight control.

If there is no serious impact on the quality, an increased distance between the electrode and the filler wire might be more favourable for the Plasmatron nozzle and the electrode. Through this bigger gap, electrode contamination from braze spatter or vaporized zinc could be reduced. As a result of this, the lifetime of the nozzle and the electrode may be increased when using a larger 'electrode to wire' gap. This has to be analysed by endurance tests at the production side.

The layer of black soot gained nearly double in size during the tests. Therefore, it is important for industrial users to understand that an increased black soot amount would show a negative effect on the paint quality. This has to be investigated through tests.

5.8.5 Influence of Brazing Current

It is observed that, although a higher current seems to increase the tensile strength, the highest acceptable current value is 100 A for brazing speeds of 1 meter per minute. At higher currents, the energy input starts to melt the base metal and alloy with the $CuSi_3$ filler. This is undesirable because the mechanical properties of such joint are unpredictable due to the formation of intermetallics.

To find the right balance between current and braze speed is one of the key influencing factors for a braze joint without base metal melting.

The increasing current increases the seam radius. This can be explained by the higher energy input, which leads to a flatter filler material flow.

Conversely, this means that the seam radius size could assist to draw a conclusion if a base metal was melted during brazing or not.

It would be a great benefit if the seam radius measurement could assist to detect this danger of base metal melting failure without destroying the joint. For example, with a camera system the seam width could, or better, should be controlled directly after brazing in the braze cell. This would assist detection of 'false friends'. These are serious braze failures, which can normally not be detected without destroying the joint.

5.8.6 Braze Speed

The quantity of test runs does not allow large statistical analysis. However, strong evidence was found that brazing speed higher than 1 m/min is possible without significant effects on seam quality.

This experiment highlighted that the heat input equation is an important tool to control the braze quality and much more accurate than the 'E'

factor equation, which the weld cell fitters often use. The experiment has shown that it is possible to perform excellent brazes with 2.5 m/min braze speed. Determining for this success was that the energy input was in the range between 74 -84 kJ per mm.

The findings further suggest that for an industrial brazing cell set-up a more accurate parameter measuring and control procedure is required. This means an online feedback system, which permanently monitors and controls the voltage, current, filler wire and braze speed during the brazing process. This system should instantaneously calculate the heat input. Similar systems have already been successfully deployed for spot welding process control, but not yet been adopted for focus TIG brazing. Industrial manufacturing planning teams have not yet recognized the need for such a TIG brazing online feedback system.

6. Plasmatron Integration and Impact on Post Braze Processes

This chapter deals with the process integration and impact on post braze processes.

There is a distinct lack of published work regarding avoiding of tungsten electrode contamination during brazing of zinc coated steel panels. Likewise, there is no literature available about how to clean contaminated electrodes. Furthermore, the black soot influence to the following paint process was studied. For the aforementioned reasons, this study wants to conduct research to discover the conditions to optimise the current condition. Based on the decision matrix that was presented in the previous chapter, six experiments were chosen.

Figure 6-1 describes the research process and lists the experiments that were conducted to meet the stated research objectives.

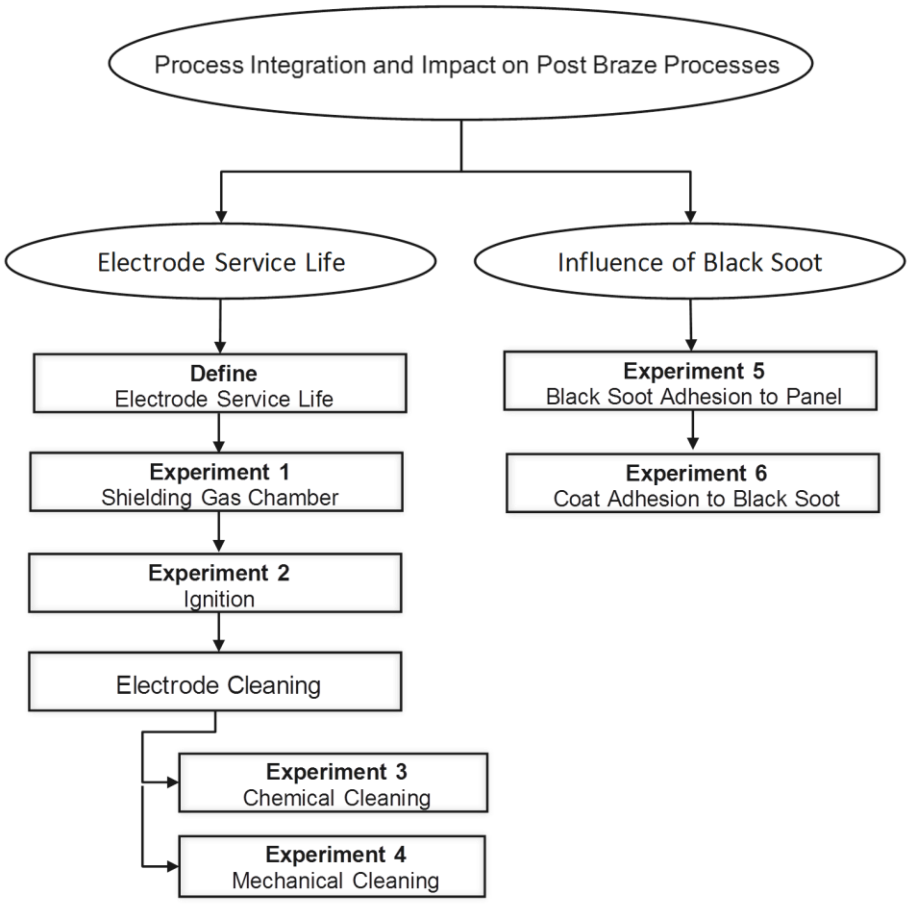


Figure 6-1: Illustrates the research process and lists the experiments that were conducted to improve the electrode service life and to review the influence of black soot.

6.1 Electrode Service Life

This section aims to define electrode service life, explain the related industrial issues and describes the conducted experiments to find a method to increase the electrode service life.

Electrode Service Life Definition

Little attention has been paid to the electrode service life problems by TIG brazing in the literature. As well, there is no definition available about what service life could mean by TIG brazing. These hinder an accurate determination of the electrode service life issues. Therefore, the author has tackled this lack and defined the electrode service life as follows:

The TIG brazing electrode service life can be defined as the braze length an electrode is in use for in a brazing application that fulfils acceptable previously defined quality standards.

In principle, that means until the electrode tip geometric shape is no longer present due to wear marks, peak erosion or other defects that impair the tip shape and hence the braze quality.

Figure 6-2 shows some examples of damaged Plasmatron electrodes. Figure (a) shows an eroded tip and (b) a tip with sediments. Both defects worsen the operating life and the braze quality. These defects modify the form of the electrode, which in turn causes a change to the plasma arc profile.

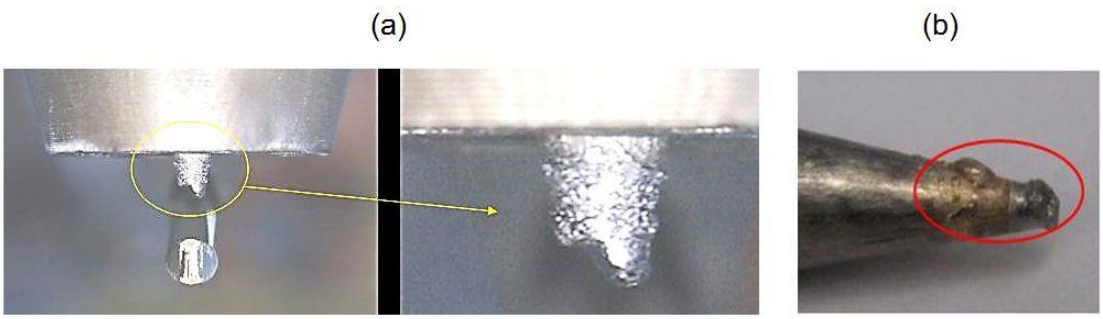


Figure 6-2: Electrode tip defects;
(a) shows an eroded electrode tip and (b) a tip with sediments.

Related Industrial Issues

Ford internal studies highlighted that after 30 m braze length the seam quality drops (lack of filler adhesion, etc.) due to electrode tip defects. This is not long enough for a high volume car manufacturer. Ten times more (300 meter) would be acceptable due to reduced production interruption. Only when the electrode tip condition can stay in good physical shape, TIG brazing is economical for higher volume production.

The following sub-chapters present the conducted experiments to this end. The discussion was summarized at the end of this chapter.

6.1.1 Shielding Gas Chamber

This experiment should show if the usage of a gas chamber would avoid electrode tip contaminations.

The extension of electrode service life for focused TIG brazing has not been explored in the literature currently available. Some investigations ([213], [214]) on tungsten electrode service life extensions for TIG welding are available, but in practice not applicable to focus TIG brazing. This is because this research studied the electrode erosion mechanism only. This is currently not an issue at focused TIG brazing. The main concerns are the electrode tip contaminations. Mainly, zinc coating from the parent metal causes contamination on the electrode tip by ZnO (white dust). It also affects the joint quality, such as porosity, discontinuity seam, lack of adhesion.

In a symposium [215], the company Linde has shown a shielding gas cover (see Figure 6-3) which isolates the nozzle and the seam from an oxygen atmosphere. It would be interesting to understand if this kind of shielding would reduce the electrode tip and black soot contaminations during Plasmatron brazing of zinc coated steel panels.

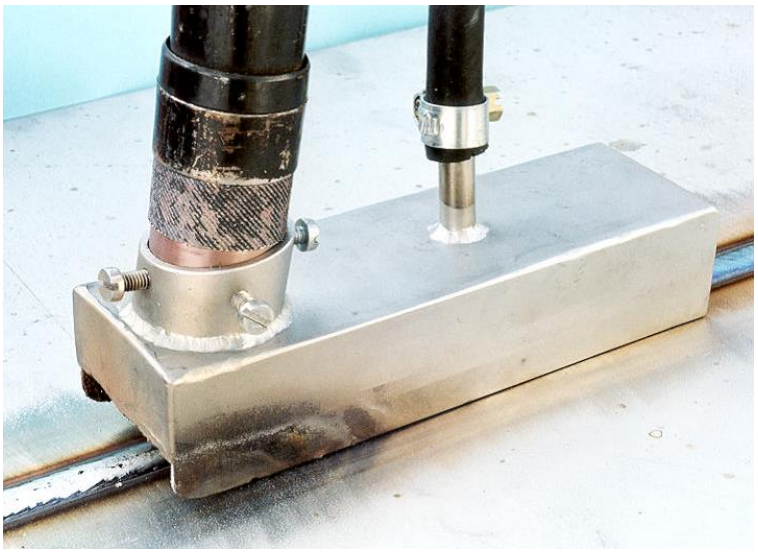


Figure 6-3: Shielding gas cover from Linde [215]

To simulate the best possible argon shielding environment, it was decided to contact a company that has experience with joining metal parts via TIG welding in an inert gas floated chamber. This process delivers very fine welds seams without heat tinting and black soot. Figure 6-4 shows an example from their TIG joined parts. One part (a) was joined in an argon floated box and the other (b) under normal circumstances.

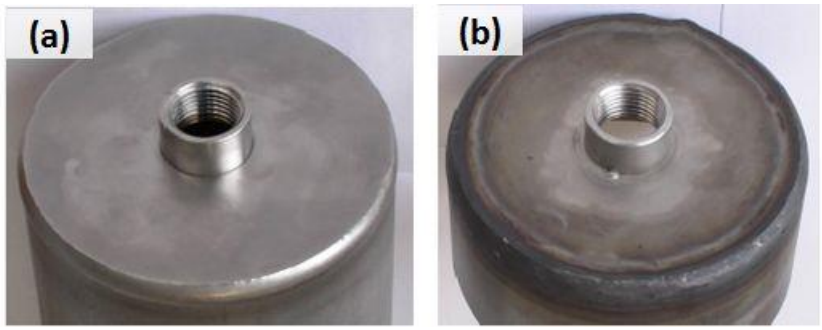


Figure 6-4: Advantage of the oxygen reduced glove box;
(a) TIG joined work piece welded in an oxygen reduced glove box,
(b) work piece welded without glove box shows black soot and heat tinting.

Castro also highlighted that, due to the oxygen reduced glove box welding process, a higher tungsten electrode lifetime has been observed [216].
The idea came up to check if these positive characteristics like black soot free panels and low electrode contamination would also appear when TIG welding of thin zinced automotive steel panels in the argon floated environment.

6.1.2 Experimental Methodology

This experiment was kindly supported by the company Castro in Augsburg, Germany. Their oxygen-reduced glove box, which was used for the experiment, is described in chapter 3.2.3. Due to resource and time shortage, it was not possible to connect the Plasmatron brazing head for this experiment with the Castro six axes robot.

Several TIG weld lap joints (120 mm long) on 0.8 mm thin alcohol cleaned zinc coated steel panels were executed inside the Castro glove box in a completely isolated inert gas atmosphere.

The inert gas used for this experiment was argon with a 99.998 % minimum purity. The oxygen level in the chamber during the experiment was 2.9 ppm (parts per million). This could be measured because the glove box was equipped with an oxygen sensor for measuring the oxygen content in ppm level. The following Table 6-1 shows the input parameters for this experiment.

Table 6-1: Input parameters for the argon chamber experiment

Current (A)	Welding Speed (m/min)	Electrode Gap (mm)	Electrode Type	Gas Shielding	Oxygen Content
80	0.36	1.4	WS2	Argon box	2.9 ppm

Weld length (mm)	Coating Type	Steel Grade	Joint Type
120	galvanized	DC06	Lap

6.1.2.1 Results

It was visually detectable that the zinc coat extensively disappeared around the seam area on the welded test panels. During the welding process, the generation of a lot of fume in the argon chamber was also observed. In comparison, previously conducted weld seams on stainless steel panels have not generated any visual fume at all in the argon chamber. This observation underlines that the zinc coat vaporises during

the welding process as there was no other element that could generate this amount of fume. Interesting is the no longer occurring of black soot at the seam area, which was expected by brazing in a nearly oxygen free environment (see Figure 6-5).
The two burned holes indicate excessive heat input, even as the current was reduced as much as possible during previous test runs. This proves that TIG welding of 0.8 mm thin steel panels in comparison to focused TIG brazing is quite difficult without damaging the panels.

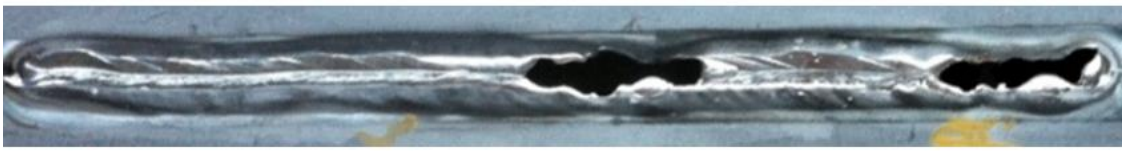


Figure 6-5: TIG welded lap joint on zinc coated steel panels
in an argon flooded chamber. The zinc vaporized during welding,
but the seam is black soot free.

The outcome of the experiment shows that an argon gas chamber with nearly complete removal of oxygen atmosphere did not show a great impact on avoidance of zinc vaporisations by joining of zinc coated steel panels.

6.1.3 Influence of Ignition

It is not fully understood if the electrode ignition process of the Plasmatron brazing system has a major influence on the electrode lifetime. This experiment should provide important information to understand if the Plasmatron electrode ignition process by brazing of zinc coated steel panels has a major influence on the electrode lifetime.

6.1.4 Experimental Methodology

This experiment was conducted in the Plasmatron test cell at the University of Nottingham (see chapter 3.2.1). For the purposes of identifying the influence of the electrode ignition process to the electrode lifetime, it was decided to braze 80 short runs in a type of on-off modus

on zinced steel test panels. Eighty ignitions simulate the brazing start phase of 40 brazed vehicle roofs (40 left + 40 right roof joints = 80 ignitions). To remind, Ford currently has to change the electrode after every 10 brazed roofs to avoid seam imperfection. The Plasmatron nozzle was equipment with an ø 6.4 mm WL20 electrode. The braze speed and the wire speed were both set to 1.2 m/min. The gas flow was 8 l/min and the direct current was set to 120 ampere. Ten test panel sets were used in total. Therefore, twenty galvannealed coated steel panels where cut and bent to simulate a flange butt roof joint. Eight 20 mm long runs were brazed per test panel set. The runs were only 20 mm long because longer braze runs would require much more test panels. As well, the plan was just to check the influence of the start phase regarding the electrode contamination.
The electrode monitoring system, as previous described in chapter 3.3.10, was used to capture the electrode protrusion and the electrode tip diameter after each braze step.

6.1.4.1 Results

All 80 brazed steps did not show any visual braze imperfections at the top view. Figure 6-6 shows one of the test panel sets with the eight 20 mm short braze runs.



Figure 6-6: Electrode ignition experiment.
Specimen with step brazes to simulate electrode ignition on zinc coated steel panels. The step brazes do not shows seam imperfections.

The electrode tip size did not change significantly after 80 step brazes. The electrode protrusion distance (tip to nozzle surface) from the fresh electrode to the electrode condition after 80 ignitions changed from 1.35 mm to 1.33 mm only as seen in Figure 6-7. The electrode tip angle and the tip width have not shown any measurable differences. On the tip

surface, no visual contaminations were identifiable after 80 ignitions. Only the nozzle surface showed some minor reposited material.

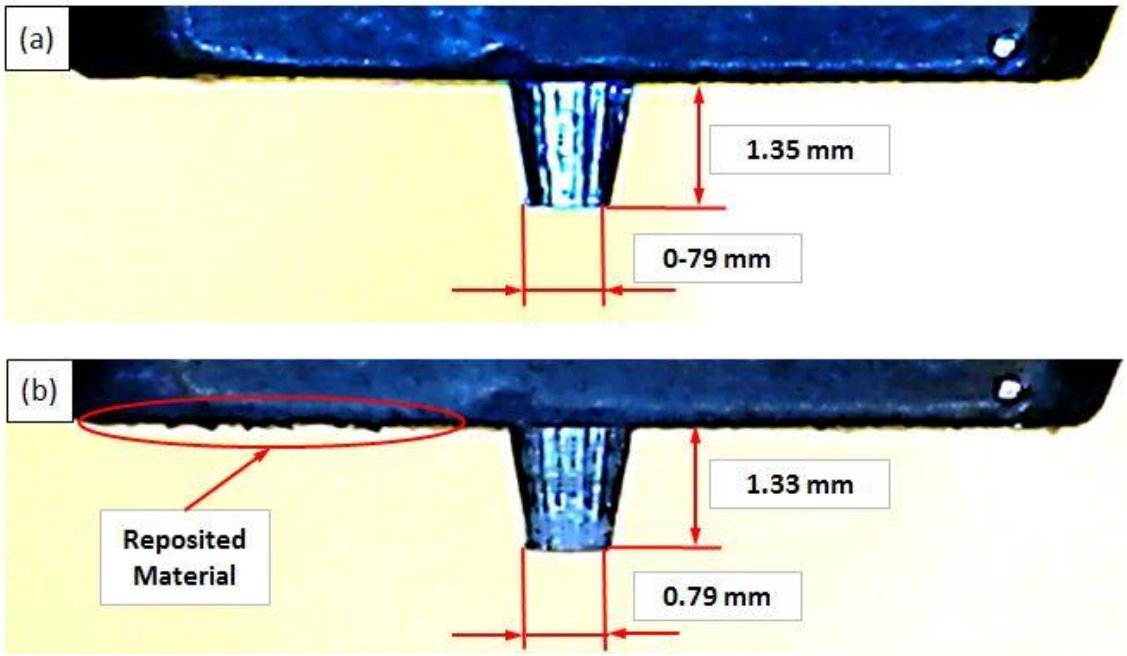


Figure 6-7: Photos from the electrode tip;
(a) electrode tip before first ignition,
(b) electrode tip after 80 ignitions.

6.1.5 Electrode Cleaning

In industrial applications of Plasmatron technology, it is important to understand if it is possible to clean a tungsten electrode in the assembled condition in the Plasmatron brazing system. Currently, there is no cleaning method available to remove zinc contamination and the $CuSi_3$ residue from the electrode. The Plasmatron brazing system supplier recommends only two methods, i.e. electrode regrinding or usage of a brand new electrode. Both methods disturb production because the torch has to be removed from the brazing system to change the electrodes. As well, the electrode change time should not be underestimated. For an electrode change, which includes unclamping the torch, disconnecting the electrode, grind electrode, connect electrode, clamp torch and align filler wire to electrode, a cycle time of 23 minutes has to be calculated. Therefore, a fast electrode cleaning method would decrease the maintenance down time and the brazing system could operate faster. Consequently, it is important to

check if it is possible to clean an electrode when it is still mounted in the brazing head.
With help of a mind-map diagram, five electrode-cleaning methods were proposed. Three of these five electrode-cleaning methods were chosen to study in more detail: ultrasonic cleaning, mechanical cleaning and chemical cleaning.
Cleaning in an ultrasonic bath was tested and did not show any cleaning effect. Cleaning with dry ice grains was not considered because of the tight space between the electrode and the nozzle. Cleaning with heat was also not considered because the tungsten electrode already reaches over 1.000°C during a normal brazing process. Only the chemical and mechanical cleaning methods remained for testing.

6.1.5.1 Electrode Cleaning with Acid Etching

The objective of this experiment was to investigate if it is possible to use a specific acid for the cleaning of a contaminated tungsten electrode tip. Important is to understand if it would be possible to clean electrodes with chemicals in direct contact with the assembled torch. In addition, it should be checked if the acid damages the tungsten electrodes. Another not to be underestimated factor is the assessment if this wet-etching process is applicable in a bodyshop. Wet-etching execution requires consideration of operator health and safety rules. Exposure to chemical etchants can cause burns, rashes, eye damage, lung problems, and chronic health issues [217].

6.1.6 Experimental Methodology

The tungsten electrode with the $CuSi_3$ and zinc contaminations was dipped in specific acids with the aim of testing if some acids are able to clean the tungsten electrode in a 60 sec. cleaning cycle (30 sec. dip cycle plus 30 sec. acid removal and drying cycle). The 60 sec. cycle would reflect the average operation of an unloading and loading process of an automatic brazing cell.

Acidic cleaners typically use hydrochloric acid, nitric acid or sulfuric acid [218]. For this experiment, nitric acid and hydrochloric acid in varying concentrations were used. The plan was to run the different tests one by one from low to high acid concentrations. Hydrogen peroxide was added in some of the hydrochloric acid test runs to accelerate the cleaning reaction. Mildly acidic cleaners like citric acid, gluconic acid or phosphoric acid were not considered because they would not be sharp enough to dissolve the contaminations in the required 30-second cleaning cycle time. The acid concentrations for the different tests can be found in Table 6-2.

Table 6-2: Acid concentrations for the electrode tip cleaning experiment

	Variable Test Inputs		
Test No.	Acid Type	Acid Concentration	Acid Dip Time
1.	Nitric acid	5 [%]	0.5 [min]
2.	Nitric acid	65 [%]	0.5 [min]
3.	hydrochloric acid	8 [%]	0.5 [min]
4.	hydrochloric acid	16 [%]	0.5 [min]
5.	hydrochloric acid plus hydrogen peroxide	16 [%] + 1 drops hydrogen peroxide	0.5 [min]
6.	hydrochloric acid plus hydrogen peroxide	16 [%] + 2 drops hydrogen peroxide	0.5 [min]
7.	hydrochloric acid plus hydrogen peroxide	16 [%] + 5 drops hydrogen peroxide	0.5 [min]

The cleaning effects from the different acid concentrations were filled in different test tubes, then set up in water at an ultrasonic bath to increase the cleaning effect. The with $CuSi_3$ spots and zinc depositions contaminated tungsten electrodes from type WL20 were dipped in the acid for 30 seconds and then cleaned with distilled water and dried by hot air stream. High-definition photos of the tungsten tips were taken with a digital camera before and after the cleaning process to analyse the effect of the cleaning. Figure 6-8 shows the experimental set-up.



Figure 6-8: Experiment set-up for electrode cleaning with acids

6.1.6.1.1 Results

The test showed that only the nitric acid with a concentration of 65 % (no. 2) and the hydrochloric acid with a concentration of 16 % plus five drops hydrogen peroxide (no. 7) were able to partly remove the copper and zinc oxide particles from the tungsten electrode tips.

Unfortunately, the tungsten electrode surfaces were in both cases etched too and showed micro pores from pitting. The other five acid concentrations were not sharp enough to dissolve the interfering particles in the required 30 seconds dipping cycle. The following Table 6-3 summarizes the test outputs.

Table 6-3: The electrode cleaning with acid experiment results.
Only tests no. 2 and no. 7 were able to remove the contaminations partly from the electrode peak but etched the electrode tip surface too.

Test No.	Variable Test Inputs	Test Outputs			
	Electrode Photo Before Trial	Electrode Photo After Trial	Results	Electrode Cleaning Effect	Effect to Tungsten Surface
1.			No Changes	The contamination was not removed	The tungsten electrode was not damaged
2.			Changes	The contamination was partly removed	The tungsten electrode was damaged
3.			No Changes	The contamination was not removed	The tungsten electrode was not damaged
4.			No Changes	The contamination was not removed	The tungsten electrode was not damaged
5.			No Changes	The contamination was not removed	The tungsten electrode was not damaged
6.			No Changes	The contamination was not removed	The tungsten electrode was not damaged
7.			Changes	The contamination was partly removed	The tungsten electrode was damaged

6.1.6.2 Electrode Cleaning with Mechanical Cleaning Devices

It was analysed if it is possible to improve the currently available mechanical electrode cleaning solutions.

The maintenance teams in the Ford plants currently clean contaminated electrodes manually with plastic scrapers and robot guided processes with wire brushes after each brazing cycle (see Figure 6-9). This works partly but is not a robust process and could therefore be optimised.

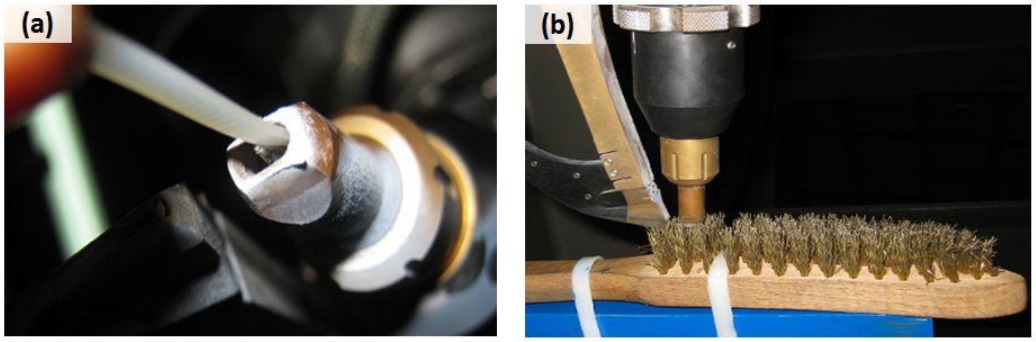


Figure 6-9: Current electrode cleaning solutions;
(a) manual electrode cleaning with a plastic stick,
(b) robot guided nozzle cleaning with a wire brush.

The author was not able find any report about mechanical cleaning of tungsten electrodes but there are some patents in this field [219], [220], [221]. Unfortunately, all these inventions are related to mechanical nozzle cleaning of MIG welding torches and not against cleaning of tungsten electrodes. The patents describe systems which mill or scrap off weld splatters that have been deposited on the nozzle by revolving blades or special reaming tools. Unfortunately, these processes might not work for the Plasmatron torch because of the sensitive electrode and the slim nozzle design. However, these patents gave some inspiration on how to develop an approach for Plasmatron torch systems.

6.1.7 Experimental Methodology

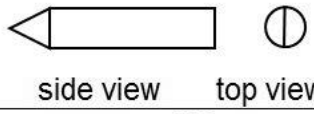
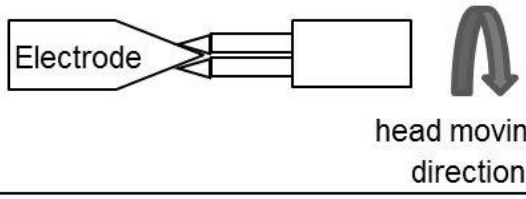
With help of a mind-map diagram and assistance from the company Thielmann Automation Technology, the following strategy was developed and tested.

From a 2.5 mm diameter spring steel wire six 16 mm long pieces were cut. The spring steel, here material code Ck75, should have a minimum hardiness of 700 Vickers. The spring steel wire pieces were sharply ground at one end to fit into the space between the electrode and the nozzle. The lower ends of the spring steel wires were fixed with 2K adhesive in 8 mm deep drilled holes (2.6 mm diameter) at the front side of a 20 mm long round steel with 10 mm diameter.

This electrode cleaning head was clamped to an electronically driven motor, which could guarantee a smoothly driven rotation movement to

clean the electrode tip. The schematic of this first electrode cleaning trial set-up is shown in Table 6-4.

Table 6-4: Mechanical electrode cleaning design concept

Blade design	
Blade configuration - top view -	
Electrode cleaning head configuration - side view -	

6.1.7.1.1 Results

The first build of the electrode-cleaning prototype was able to clean the electrode partly as can be seen in Figure 6-10.

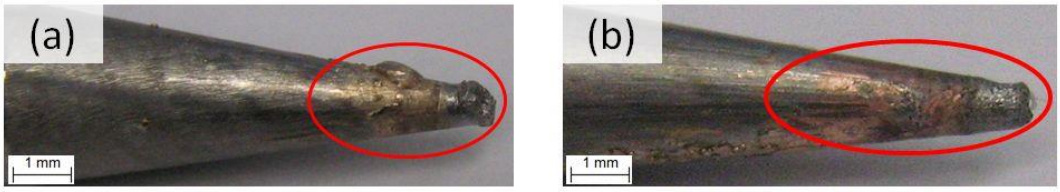


Figure 6-10: Result of the first mechanical cleaning trial;
(a) electrode before mechanical cleaning trial,
(b) electrode after mechanical cleaning trial.

However, the following concerns were observed in the first cleaning trial:

- Not all particles could be removed
- Sometimes the spring steel got stuck between the nozzle and electrode
- The electrode tips showed radial scratches
- The electrode tips showed residues from the steel blades
- The nozzle outlet showed damages from the spring steel blades as seen in Figure 6-11.



Figure 6-11: Damages on the nozzle outlet
from the steel blades on the first mechanical electrode cleaning trial.

6.2 Influence of Black Soot on Paint Quality and Aesthetics

This section deals with the influence of black soot created by Plasmatron brazing to an automotive production paint process. As highlighted in section 3.3.3.7, the black soot area on the steel panels on both sides next to the brazed seam is a by-product from oil and dust combustion, which originates during the $CuSi_3$ brazing process.

Nowadays the black soot will mostly get brushed away with a robotised wire brushing system in the bodyshop before the body moves to the paint shop. For the automotive industry, it would be very important to understand if they could forgo this brushing operation while maintaining the required paint quality through modifications to the brazing process. The removal of an automatic brushing cell represents a one-off acquisition cost saving of approximately EUR 300k for a high volume plant plus the ongoing costs of operating. As yet, this has not been explored in the literature.

To identify which influence different zinc coating types and the related black soot amount have on automotive paint quality, it was decided to produce arc brazed specimens using the range of different zinc coating types.

With this strategy, it was possible to compare different coating types and to evaluate the paint quality of these different coating type braze probes. Two batches of test panels were prepared for the experiments. The first batch to identify the bonding between the black soot and zinc surfaces. The second batch to detect if the different black soot shows paint quality differences for the pre-coat and the final automotive coat.

6.2.1 Black Soot Adhesion

The black soot on the surface of brazed work pieces around the braze bead should be minimized as much as possible because they can affect the following vehicle paint process and painting quality, as previously described in section 3.3.3.7.

This experiment was conducted to investigate if there is variation in the black soot adhesion strength amongst different zinc coated steel panels. For the automotive manufacturer it is also important to understand if there are adhesion strength differences between different zinc coating types because black soot with low adhesion might be easier to remove from arc brazed panels, for example by washing. Black soot with high adhesion might just be removable with more complicate and more expensive cleaning methods like brushing or grinding.

Another outcome could be that the black soot sticks to the panels so that a removal might not be required before painting.

6.2.2 Experimental Methodology Methodology

The lap jointed braze specimens for this experiment were produced with assistance from the company Inocon. From each zinc coat type four specimens with 160 mm long lap joint braze runs were prepared. All specimens were brazed with the same input parameters. The braze and wire speed was set to 1 m/min and the argon gas flow to 7.5 l/min.

Table 6-5 shows the panel details from these different zinc coated brazed specimens.

Table 6-5: Material details from the Plasmatron brazed specimens.
Four different zinc coat types were used for the black soot adhesion experiment.

Label	Zinc Coating Type	Zinc Coating Type Description	Zinc Layer Thickness two-sided (µm)	Zinc weight/area two-sided (g/m²)	Layer Composition	Layer Production Standard	Steel grade and Thickness (mm)	Brazed Joint Details
a	Electrolytically zinc coated	50G50G-EL	5/5	36/36	Pure Zn	DIN EN 10152:2009-07	DC06 0.75	Lap joint, CuSi3 filler
b	Hot-dip Galvanized-ACE®	50G50G Ace	7/7	50/50	Pure Zn	DIN EN 10346:2009-07	DC06 0.75	Lap joint, CuSi3 filler
c	Hot-dip Galvanized	50G50G (Z)	7/7	50/50	Pure Zn	DIN EN 10346:2009-07	DC06 0.75	Lap joint, CuSi3 filler
d	Hot-dip Galvanized MagiZinc® (ZnAlMg)	MZ 70	5/5	35/35	ZN + 1.6%Mg + 1.6%Al + remain Zn	DIN EN 10346:2009-07	DC06 0.75	Lap joint, CuSi3 filler

To evaluate the black soot adhesion of the different zinc coated brazed specimens to their zinced surface, a special tape (adhesion strength is greater or equal to 80 N/mm, here Scotch 898, 25 mm wide) was applied with a uniform load over the black soot from each brazed line according to EN ISO 2409 [222] as shown in Figure 6-12.



Figure 6-12: Brazed specimens with special tapes
before applying over black soot from brazing.

The tape was then rapidly removed, as close to the panel as possible. After removal of the tape strips, the remaining amount of black soot on the panels was measured on the related digital images with assistance of the ImageJ software as described in Subchapter 3.3.9.

6.2.2.1 Results

Black soot was easily removed with the adhesion tape from all tested zinc types. The following Figure 6-13 shows one specimen image. The yellow-circled areas mark the black soot and the blue-circled area indents the panel area where the black soot was before removal with the tape strip.

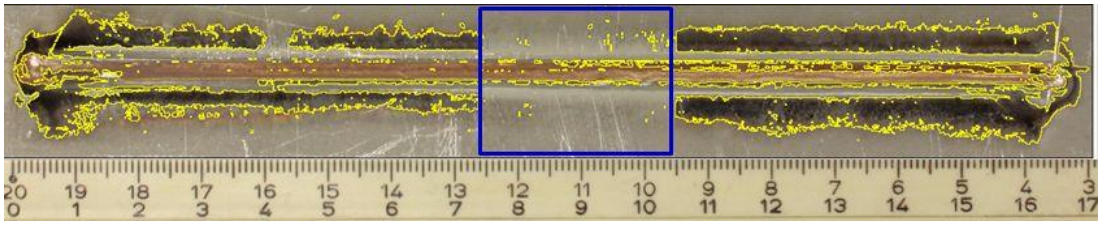


Figure 6-13: Top view of a brazed test panel
with marked black soot area (yellow-circled area). The blue circled area indicates the area where the tape strip was. Only minor black soot particles got stuck at this area.

With the tape adhesion test and the following black soot measurement of the rest black soot particles on the test panels inside the blue marked boxes (see Figure 6-14) it was not able to detect significant black soot removal differences between the four tested zinc types.

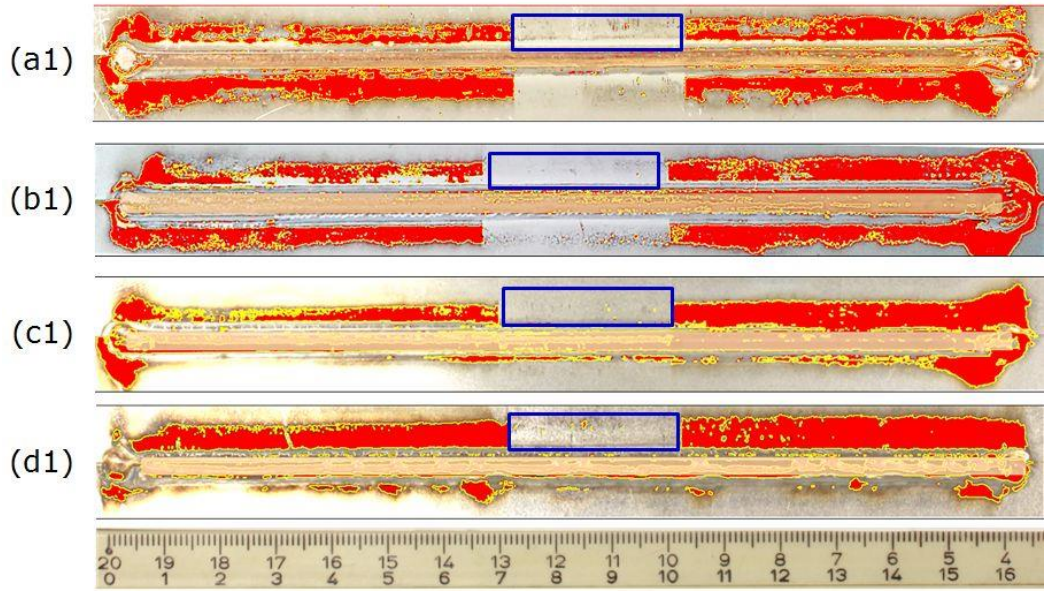


Figure 6-14: Black soot analysis on different zinc types;
(a1) Electrogalvanized, (b1) HD Galvanized ACE®, (c1) HD Galvanized, (d1) HD Galvanized MagiZinc®. The black soot was coloured red. The blue circled areas indicate the measured area where the tape removed the black soot.

Only minor black soot removal differences could be measured (see Table 6-6). With the tape strips, it was quite easy to remove 95 % - 97 % of black soot from all brazed specimens. The measured removal differences are in the range of tape application differences.

Table 6-6: Black soot measurements after tape removal

Label	Zinc Coating Type	Measured Area (cm^2)	Area with noon soot (cm^2)	Area with none soot (%)
a1	Electrogalvanized	1.2	1.178	98%
a2		1.2	1.175	98%
a3		1.2	1.169	97%
a4		1.2	1.172	98%
b1	HD Galvanized ACE®	1.2	1.173	98%
b2		1.2	1.167	97%
b3		1.2	1.161	97%
b4		1.2	1.169	97%
c1	HD Galvanized Standard	1.2	1.142	95%
c2		1.2	1.144	95%
c3		1.2	1.164	97%
c4		1.2	1.153	96%
d1	HD Galvanized MagiZinc®	1.2	1.142	95%
d2		1.2	1.167	97%
d3		1.2	1.179	98%
d4		1.2	1.155	96%

6.2.3 Coat Adhesion

As highlighted in the previous black soot experiment, the question came up if a finished automobile coat would show quality concerns like paint peel off when directly painted above black soot contaminated areas. The paint might not adhere properly to the surface areas contaminated with black soot.

Therefore, an experiment should identify if black soot from brazing on zinc coated steel panels has an influence on automotive paint quality or not. The answer to this question is important because significant warranty claims and reputation loss could occur when customers detect paint issues around brazed areas.

6.2.4 Experimental Methodology

Experimental To identify if the black soot has an influence on automotive paint quality, it was decided to produce Plasmatron brazed joint specimens from different zinc coated steel panels, as described in the previous experiment. With this strategy, it was possible to check four different coat types and to compare the paint adhesion quality of these different coat types. The following table shows the technical material details of the used specimens.

Table 6-7: Test panel details for this coat adhesion experiment

Label	Zinc Coating Type	Zinc Coating Type Description	Zinc Layer Thickness two-sided (µm)	Zinc weight/area two-sided (g/m²)	Layer Composition	Layer Production Standard	Steel grade / Thickness (mm)	Brazed Joint Details
a	Electrolytically zinc coated	50G50G-EL	5/5	36/36	Pure Zn	DIN EN 10152:2009-07	DC06 0.75	Single coach joint, CuSi3 filler
b	Hot-dip Galvanized	50G50G (Z)	7/7	50/50	Pure Zn	DIN EN 10346:2009-07	DC06 0.75	Single coach joint, CuSi3 filler
c	Galvannealed	55A55AHDC	7/7	50/50	Zn + 11%Fe	ASTM A 653/ A 653M	DC06 0.75	Single coach joint, CuSi3 filler
d	Hot-dip Galvanized MagiZinc® (ZnAlMg)	MZ 70	5/5	35/35	ZN + 1.6%Mg + 1.6%Al + remain Zn	DIN EN 10346:2009-07	DC06 0.75	Single coach joint, CuSi3 filler

A simulation of a production paint process is very elaborate. Therefore, it was decided to use the Ford Cologne production paint shop. This allows examining the black contamination effect on the various painting steps directly. To remind, the automotive painting process includes various steps. The first step consists of degreasing and phosphating. The main purpose of this step is to protect the substrate material from corrosion. The second step consists of primer coating and top coating. The main purpose of the second step is to improve the appearance and to give the colour [223].

A typical automotive paint shop process is shown in Figure 6-15.

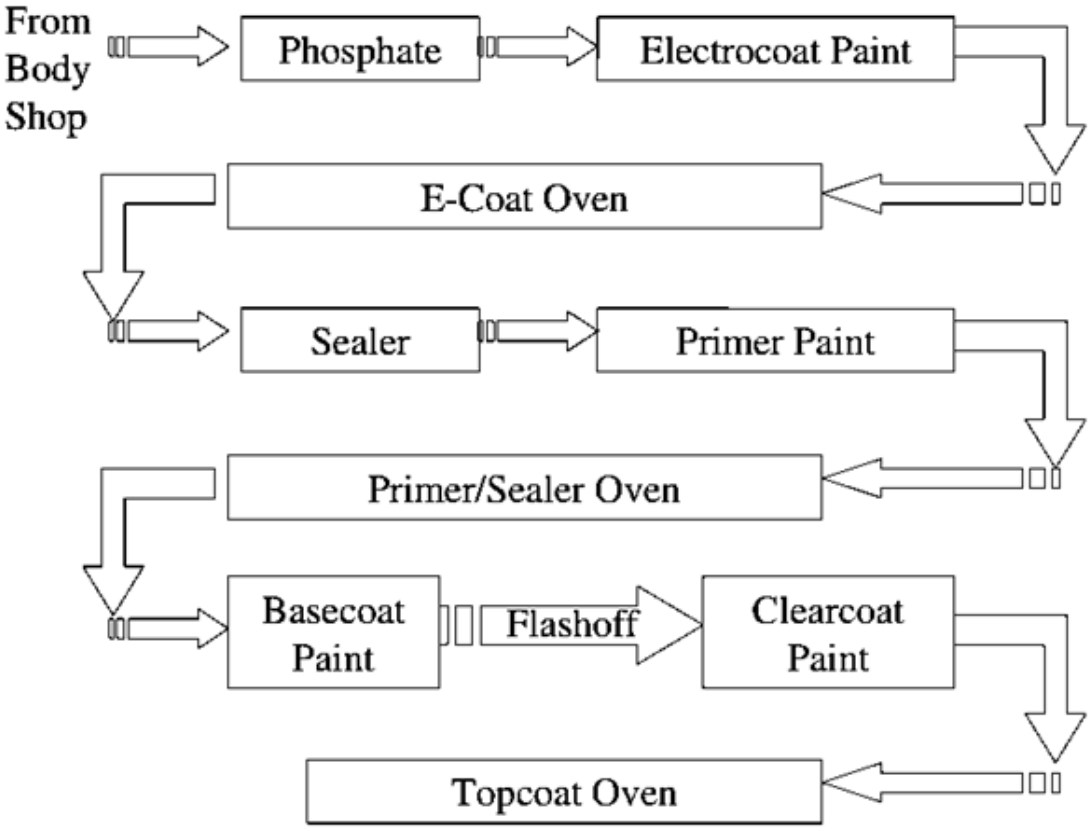


Figure 6-15: Typical automotive paint shop process [224]

The easiest way to perform the complete automotive paint process was to use a BIW as a carrier though the production paint shop. Therefore, the brazed test panels were fixed with a thin steel wire to an unpainted body (see Figure 6-16a). The wire fixing of the test panels was necessary because otherwise the specimens would be lost in the body washing station or in the electro coating dip tanks that the body has to run through. The test panels were relocated after the body passed the electro coating tanks to the hood (see Figure 6-16b). This was required to guarantee a correct paint application. White colour base coat was chosen because on white it is easy to detect if the black soot would be visible through the paint.



Figure 6-16: Fixing of specimen on a BIW;
(a) wire fixed paint specimens before running through the phosphate tanks;
(b) specimens were later removed to the hood before running over the paint line.

The electro coat and the final paint coat adhesion to the zinc coated steel panels which had black soot around the brazed seams were evaluated according to EN ISO 2409 [222] with a cross cut test. This destructive adhesion test method was used to measure the semiquantitative adhesion of an automotive coat to the black soot area on brazed zinc coated steel panels.

The knife blade was drawn diagonally over an unmarked section of a brazed test panel as long as possible, with sufficient pressure to cut through the coating down to the base material. At least five further parallel lines were drawn 1 mm apart in the same way. A minimum of five additional diagonal lines was drawn until a grid arose.

To evaluate the coat adhesion, a special tape (adhesion strength greater or equal to 80 N/mm; Scotch 898, 25 mm wide) was applied over the drawn lines. The tape was rapidly removed, as close to the panel as possible.

Observed chipping, flaking or general poor paint adhesion differences from the different test panels were noted.

6.2.4.1 Results

The observed eight painted braze specimens and the related tapes do not show any abnormal paint chipping, flaking or general poor paint adhesion differences (see Figure 6-17). The samples a1 to d1 show scratches on the e-coat and the samples a2 to d2 show scratches on the final white coat.

On all samples, the coat was not removed. It can be noted that on no specimen the black soot shimmers through the electro coat or the white final paint layer.

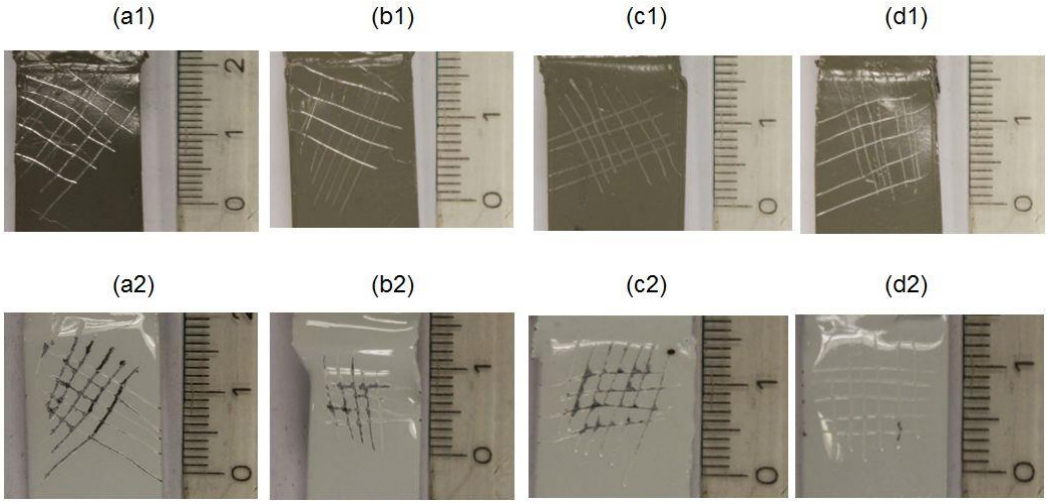


Figure 6-17: Painted brazes after the scratch test.
All probes do not show abnormal paint chipping.
Electro coat(a1) – (d1), final automotive coat (a2) – (d2).

It should be noted that the scratch test is only a semiquantitative technique because the applying load and dragging forces as input variable for this test was probably not constant due to the manual application. The following tape peel test is an effective test but gives only a go/no go type of result and just indicates whether the coat adhesion is acceptable or not acceptable. This test does not give quantitative results and can be used as heuristic analysis only. However, this combined scratch and tape test is easy, fast and useful. It is not without reason currently a standard quality check in the automotive paint shops.

6.3 Chapter Discussion

In this section, the results obtained from the experiments in this chapter were discussed and analysed.

6.3.1 Shielding Gas Chamber

The shielding gas chamber experiment demonstrated that zinc starts to boil and vaporise even in a complete argon flooded chamber with minimized oxygen concentration.

Consequently, a better argon shielding at the Plasmatron nozzle with a special developed nozzle shield to flood the seam with argon gas during brazing (see Figure 6-18) would not generate a great benefit to avoid zinc vaporisation. The zinc vaporizes because the plasma arc heats up the zinc surface above its boiling point of 907°C. However, the amount of black soot could be minimized by usage of a nozzle shield due to the improved argon gas coverage of the braze area, which minimizes the lubricants combustion.

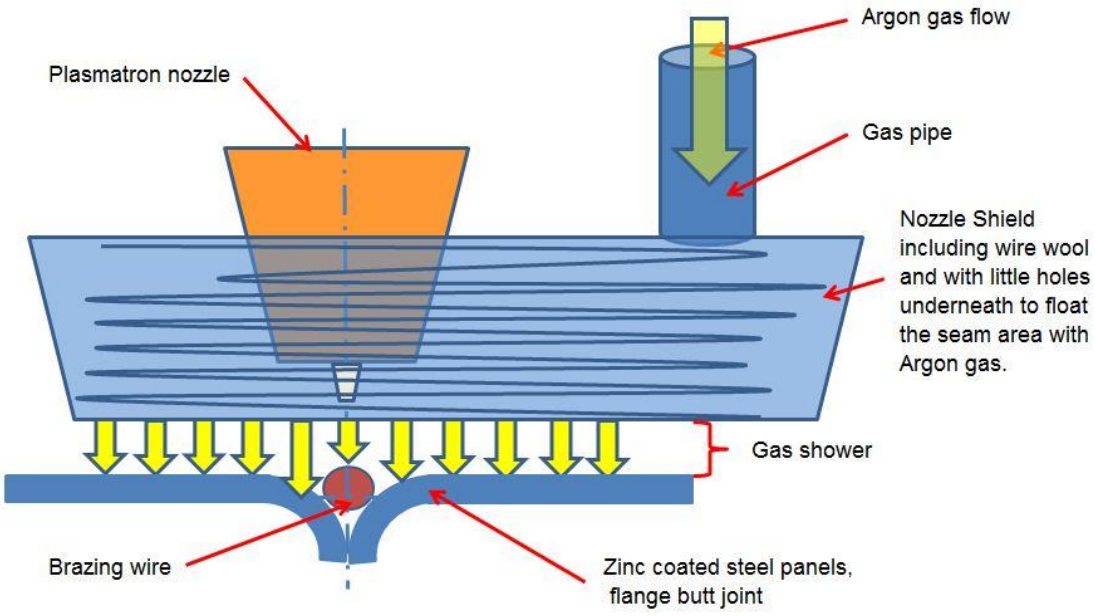


Figure 6-18: Schematic of a nozzle shield
to flood the seam area with argon gas

6.3.2 Influence of Ignition

The electrode tip shape did not change after 80 step brazes. It was interesting to observe the minor formation of sediments on the nozzle surface. It appears that vaporized zinc particles condense more easily on

the nozzle surface than on the electrode tip. The reason might be that the electrode is much hotter than the nozzle and therefore burns or vaporizes directly most of the zinc particles.
It is apparent from these results that the ignition process does not have a huge influence on the electrode lifetime.
Eighty ignition cycles simulate the brazing start phase of 40 brazed vehicle roofs. This stands for a 400 % electrode lifetime increase to the current situation at Ford. To remind, Ford currently has to change the electrode after every 10 brazed roofs.

6.3.3 Electrode Cleaning with Acid

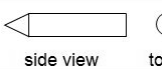
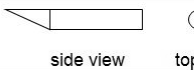
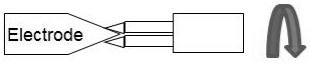
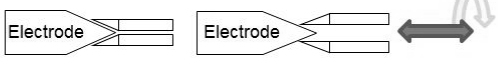
The electrode cleaning with specific acids experiment has shown that it is feasible to clean contaminated electrodes with acid. However, a number of limitations were detected for the possible introduction of this cleaning method in a bodyshop.
A specific acid concentration and type needs to be developed to make sure that only the $CuSi_3Mn$ and zinc contaminations are etched away and the tungsten electrode and nozzle do not get damaged. This would require the nozzle material to be changed because currently the nozzle is made from copper, the same material as the majority of the contaminations.
The pH value of the acid has to be controlled and automatically adjusted to keep the agent constantly in the perfect condition to fulfil the requested cleaning time and quality. Expensive control equipment may be required to fulfil this task. Another parameter that needs to be considered is the holding time in the acid; this parameter has to be automatically controlled when introduced into a production environment. The cleaning of the electrode from the acid leftovers (with distilled water) has to be very accurate because micro acid spots on body panels could lead to corrosion issues of the finished vehicle due to acid contamination.
Wet-etching execution also requires consideration of operator health and safety rules. Adequate exhaust systems must be provided in the area where the cleaning operations are being conducted. The operators need protective clothing, gloves and footwear. Additionally, special training is required to avoid accidents and pollution of the environment.

Taken together, these findings plus the health and safety concerns connected with dangerous acids currently do not support further research in this field.

6.3.4 Mechanical Electrode Cleaning Device

The first mechanical electrode cleaning prototype only partly removed the contaminations. Residues from the steel blades and radial scratches at the electrodes surface might impact brazing operations after several cleaning rounds. Especially the radial scratches might have a negative influence on the braze quality and the electrode lifetime. Bowers [138] highlights that if electrodes are ground circumferentially, skin effects result in high surface heating. The electrode becomes overheated and wears out more quickly.
To avoid these negative effects, a short distance pneumatic or electric driven linear up and down movement from the cleaning head could be tested to shed the contaminations from the electrodes when it is still installed at the torch. This would avoid the undesired radial scratches on the electrode tips as well. The quantity of the blades should be increased to nine blades as well to make the cleaning head more stable against blade sticking. As a next step, it is planned to build a second prototype with these improvements. The following Table 6-8 summarizes the suggestions.

Table 6-8: Schematic of an improved mechanical cleaning device to clean Plasmatron electrode tips. Additional blades and optimised movement improve the cleaning effect.

	1st Concept	Improved Design Concept
Blade design		
Blade configuration - top view -	 6 Blades	 9 Blades → higher pressure
Electrode cleaning head configuration - side view -		

6.3.5 Black Soot Adhesion

No significant black soot adhesion differences were found between the four tested zinc types. The interpretation of the result data can give a semiquantitative estimate only because the tape peel test can include a couple of failure modes. For example, the adhesive from the tape or the manual tape applying pressure can have variances from test to test.
However, it can be stated that the soot could be surprisingly easy and nearly completely removed with the tape strips from all brazed specimens. As the black soot adhesion to all tested zinc coated steel panels is not greater than the tape adhesion strength (here 80 N/mm, 25 mm tape wide), the question came up if a finished automobile coat would show quality concerns like paint peel off or sags when painted above black soot contaminated areas. The test results showed as well that the black soot can be easily removed without any aggressive cleaning process after brazing. Potential danger grinding methods are not required to clean the braze lines from black soot. Danger, because for example roof panels are usually only 0.7 mm thin and could get further thinned through grinding.
Also, there is the risk that the black soot contaminates the e-coat tanks when it falls off on the way through the dip tanks. Therefore, shorter tank cleaning cycles might be required.

6.3.6 Coat Adhesion

The combined scratch and tape test has not shown any abnormal paint chipping and flaking on all the eight probes. This positive test result gives a good indication that it is possible to delete current seam brushing processes after arc and even laser $CuSi_3$ filler brazing for the four tested zinc coat types in the automotive industry. Surprisingly, the electro coat adhered well to the black soot. This is contrary to the results from the black soot tape experiment, where the tapes easily removed the black soot from all brazed steel panels.
To be careful, the author recommends to always perform an adhesions experiment before not considering a black soot elimination station in the bodyshop planning. This is necessary because the automotive paint shops are all slightly different due to local regulations and local paint suppliers.

7. Thesis Conclusions and Future Work

This chapter summarizes the thesis. It is divided into four sections. Section one summarizes the key finding. Section two lists the significant contributions from this research. Section three highlights the limitations and recommendations for future work and section four delivers the concluding remarks.

7.1 Research Key Finding

Plasmatron brazing has the potential to replace laser brazing as well in high volume bodyshops for joining of automotive outer skin panels. The conducted research has proven that it is possible to deliver higher braze speed and an improved electrode lifetime if certain parameter settings would be set and controlled during the brazing process.
An important prerequisite for this is that the joint design delivers sufficient access for the Plasmatron nozzle and the related filler wire guiding finger along the joint line.

7.2 Research Contributions

The significant contributions from this research were:

Electrode Monitoring System
A special vision system has been developed to automatically monitor and measure the electrode tip geometry. Such a system is mandatory to study and to quantify electrode contaminations and electrode wear directly in the braze cell at the assembled torch. Without this system, it is not possible to monitor the electrode status properly. The author strongly recommends that such a system should always be installed when applying Plasmatron brazing because this system assists to avoid braze failures.

Braze Visual Properties Report
A properties report about all visual detectable potential braze failures in panel joining was developed as part of this thesis because it was not possible to find such a report in the literature. This report was essential

when attempting to understand the complex field of braze failures and when attempting to improve the failure assessment time and assessment quality.
It might be that there is no published classification for brazed automotive outer skin panels available because there is no great industrial will. However, this thesis delivered a classification and is aimed at serving as a guideline for the automotive industry.

Economic and Logistical Modelling of BIW Joining

The literature research identified and described 21 current and potential future BIW joining methods, which were benchmarked to identify the joining methods with the highest potential for the future (next 12 years) of outer skin panel joining in high volume plants. The outcome of this rating exercise found that two brazing methods are of preference: Laser brazing and Plasmatron brazing. The 1K adhesive joining method was rated quite high as well. However, a following adhesive experiment on BIWs has revealed a lot of cracks and low joint strengths in the adhesive joints after the BIWs left the paint shop. Panel distortions due to thermal expansion coefficient differences during the paint oven heat-up and following cooling phase were detected as reason for the cracks. Only a hybrid joining design with spot welds, self-piercing rivets, etc. would overcome this situation. This would assist to overcome the low joint strengths from a purely adhesive joint roof as well. However, as a roof with rivets or weld spots does not fulfil the changing customer requirements, it was the right decision to concentrate on the improvement of the Plasmatron brazing method in this study.

Laser Brazing vs. Plasmatron Brazing

The tensile test comparison between laser and Plasmatron brazing has shown that the tensile test differences between laser and Plasmatron brazing is as just minor. As well, both joining methods allow repeatability with good results and fulfil the strength requirements.
A Total Cost Model was set up to fully understand and quantify the cost structure of laser and Plasmatron brazing at various production volumes

and different countries to assess the effect of wage differences. The capital investment comparison shows that the laser brazing system investments are more than three times higher than those of the Plasmatron brazing system.

Under consideration of the total cost calculation approach, the picture looks different. For a German based production, Plasmatron brazing cost per typical liftgate is higher than laser brazing when the yearly liftgate volume passed the 85k mark. Accountable for those higher costs are the labour and maintenance costs of the Plasmatron system because the electrode has to be changed or ground after 20 braze cycles each time. Besides the higher amount of required maintenance time, the major cost driver is the lower brazing speed of the Plasmatron method.

Another point to consider is the floor space needed in the plant for the facilities. The Plasmatron system needs no specific safety enclosure and requires therefore ~ 35 % less floor space than a laser brazing cell.

This research led to the development of the systematic Total Cost Model to support a total cost driven decision-making approach. This is useful to select the most cost effective joining method for coming projects and serves to identify weak points in the Plasmatron system.

Influence of Fundamental Input Parameters –
Torch Tilting 'Pushing - Pulling'

The results showed that minor torch tilting angle differences (between 2° pushing and 4° pulling) have no effect on the braze quality and black soot observed. All braze seams on the test panels showed similar good filler surface qualities without any waviness or lack of adhesions. This is good for production because it gives more braze head setting freedom in braze line direction, which assist to braze curved parts, for example.

Influence of Fundamental Input Parameters – Surface Cleanliness

It was discovered that the solvent cleaned panel surfaces showed thirty-five per cent less black soot contamination on the panel than the slightly

oiled automotive steel test panels, after brazing. Additionally, it was important to observe that the filler material shows a considerably better filler contact on the cleaned test panel side than on the non-cleaned panel side. The detected insufficient filler adhesion on the not pre cleaned panel side reduces the mechanical joint strength. However, the aesthetic surface appearance from the solid filler does not highlight significant quality differences. This is an important observation as well because this could lead non-trained people to the conclusion that the seam quality is acceptable, even when it has serious filler adhesion issues inside.

Influence of Fundamental Input Parameters – Electrode Offset

It was observed that a lateral filler wire – electrode tip misalignment of 0.3 mm resulted in marked base metal melting and unequal braze lines. This sensitivity was not expected and highlighted how accurate the electrode tip needs to be aligned above the filler wire during the brazing cell setup.

Influence of Fundamental Input Parameters – Electrode to Wire Gap

The important finding was that the Plasmatron brazing process is not hugely dependent upon on the gap size between the electrode tip and the wire. If there is no serious impact to the quality, an increased distance between the electrode and the filler wire might be more favourable for the Plasmatron nozzle and the electrode. Through this bigger gap, electrode contamination from braze spatter or vaporized zinc could be reduced. This has to be analysed by endurance tests at the production side.

The only thing that has to be mentioned negatively is that the layer of black soot gained nearly twice the size during the tests.

Influence of Fundamental Input Parameters – Brazing Current

At higher currents, the energy input starts to melt the base metal and alloy with the $CuSi_3$ filler. This is undesirable because the mechanical properties of such joint are unpredictable due to the formation of intermetallics, which act as stress concentrators.

The increasing current increases the seam radius. This can be explained by the higher energy input, which leads to a flatter filler material flow.
Conversely, this means that the seam radius size could assist to draw a conclusion if a base metal was melted during brazing or not.
It would be a great benefit if the seam radius measurement could assist to detect this danger of base metal melting failure without destroying the joint. For example, with a camera system the seam width could, or better, should be controlled directly after brazing in the braze cell. This would assist to detect 'false friends'. These are serious braze failures, which can normally not be detected without destroying the joint.

Influence of Fundamental Input Parameters – Braze Speed

The experiment has shown that it is possible to perform excellent brazes with 2.5 m/min braze speed. Determining for this success was that the energy input was in the range between 74 -84 Joule per mm. This experiment highlighted that the heat input equation is an important tool to control the braze quality. The findings further suggest that for an industrial brazing cell an accurate parameter measuring and control procedure is required. This means an online feedback system, which permanently monitors and controls the voltage, current, filler wire and braze speed during the brazing process.

Electrode Service Life Definition

The author has tackled the lack of a missing electrode service life definition for TIG brazing and defined one as follows:

> The TIG brazing electrode service life can be defined as the braze length an electrode is in use for a brazing application that are of acceptable previously defined quality standards.

Electrode Service Life - Shielding Gas Influence

The shielding gas chamber experiment demonstrated that zinc starts to boil and vaporise even in a complete argon flooded chamber with minimized oxygen concentration. Consequently, the proposal of better

argon shielding at the Plasmatron nozzle with a special developed nozzle shield would not generate a great benefit to avoid zinc vaporisation. However, the amount of black soot could be minimized by usage of a nozzle shield due to the improved argon gas coverage of the braze area, which minimizes the lubricants combustion.

Electrode Service Life - Influence of Ignition

The electrode tip shape did not change after 80 step brazes. It is apparent from these results that the ignition process does not have a huge influence on the electrode lifetime. Eighty ignitions simulates the brazing start phase from 40 brazed vehicle roofs. This stands for a 400 % electrode lifetime increase to the current situation at Ford. Currently, after every 10 brazed roofs the electrode is changed. This represents a marked improvement.

Electrode Cleaning with Acid

The electrode cleaning with specific acids experiment has shown that it is feasible to clean contaminated electrodes with acid. However, a number of limitations were detected which makes the introduction of this cleaning method inappropriate. The pH value from the acid has to be controlled and automatically adjusted to keep the agent constantly in the perfect condition to fulfil the requested cleaning time and quality. Expensive control equipment may be required to fulfil this task. The cleaning of the electrode from the acid leftovers has to be very accurate because micro acid spots on body panels could lead to corrosion issues of the finished vehicle. Wet-etching execution also requires consideration of operator health and safety rules. Based on these findings, the author currently cannot recommend further research in this field.

Mechanical Electrode Cleaning

The first mechanical electrode-cleaning prototype only partly removed the electrode tip contaminations. However, the study showed that such a system could be feasible, with some improvements. A short distance

pneumatic or electric driven linear up and down movement from the cleaning head could shed the contaminations from the electrodes, when it is still installed at the torch. This would as well avoid the undesired radial scratches on the electrode tips.

Black Soot Adhesion to Body Panel

No significant black soot adhesion differences were found between the four tested zinc types. The test results showed as well that the black soot can be easy removed without any aggressive cleaning process after brazing. Potential danger grinding methods are not required to clean the braze lines from black soot.

Coat Adhesion to Black Soot

The combined scratch and tape test has not shown any abnormal paint chipping and flaking on all the eight probes. This positive test result gives a good indication that it is possible to delete current seam brushing processes after arc and even laser $CuSi_3$ filler brazing for the four tested zinc coat types in the automotive industry.

7.3 Limitations and Future Work

It is apparent that the reported research has provided a significant step forward to the development of Plasmatron brazing in the industry, especially in the automotive industry. However, the outcome of the research also outlined some limitations. For example, it was not possible to run a long term test to demonstrate that the electrode lifetime could be extended significantly as researched. Additionally, it was not possible to prove that the developed brazing speed improvement suggestions delivered the expected results during long-term usage. To capture such confirmations with a small-scale test cell is practically impossible due to the required test panel and in the available time. The automotive industry

should assist this process and consider making their quality data accessible for coming researchers in this field.
In addition to the above limitations being recognized, the following future work opportunities were identified:

Braze Speed

Based on the research findings (increase electrode to wire distance, parameter monitoring, etc.), the next step should be to perform larger test runs in a production environment with higher braze speeds (> 1.0 - 2.5 m/min). In addition, the interaction with other parameters like wire speed and gas flow rate could be considered. Design of Experiment (DOE) should be used for this more complex analysis.

Torch Tilting with Larger Tilting Angles

The findings of this study suggest to run another 'pushing – pulling' torch tilting experiment with larger tilting angles in both directions and longer braze length. It would be interesting to understand if less zinc vapour would be generated if the torch would run in a push direction. This would assist to overcome the electrode tip zinc contamination issue.

Visual Control of the Electrode and the Filler Wire

For the usage of a focused TIG system in the (automotive) industry, the author strongly recommends to always control the electrode tip – filler wire alignment via a flexible vision system, similar to the one developed for this research. This camera based electrode tip alignment check has to be performed during Plasmatron brazing cell set-up and as well during production. For example, during the part change time the robot head could position the electrode nozzle in front of the microscope camera. The developed vision system can then automatically measure the electrode tip geometry, the electrode alignment to the wire and nozzle and the electrode cleanliness. The usage of a vison system is necessary because minor misalignment (0.0 ± 0.2 mm) between the electrode tip and the wire can create serious seam quality issues as the related experiment results highlighted.

Vison Based Automatic Electrode Tip to Filler Alignment System

Further, the author recommends to develop a vison based automatic electrode tip to filler wire alignment system for the Plasmatron brazing cell. The obtained electrode tip to wire measurements could be used not only to control the correct electrode tip alignment and the tip contamination level; it could also trigger a filler wire setting correction in X-direction via a servomotor if needed. This would avoid the so-called 'false friends'. These are brazing seams, which lie outside of the intended area. This defect type is very dangerous because it has an effect on the durability of the seam, which can be determined in a very limited manner. The optical seam quality might not be affected by inconsistent centering of the braze along the length of the seam. As a result of this, this kind of failure is difficult to detect without cutting the brazed panels.

Electrode Cleaning

Further research might investigate if a combinability between ultrasonic and the improved mechanical cleaning design concept, as suggested, would deliver the desired electrode tip cleaning effect. The developed electrode tip vision system could trigger an electrode cleaning process start. This would avoid quality deterioration on the braze quality. If the system recognizes that a cleaning does not work anymore, an automatic electrode change could be triggered. At best with an electrode turret magazine, which has to be developed.

7.4 Concluding Remarks

The overall results of this thesis indicate that the focused TIG brazing process is able to match the performance and appearance of the equivalent laser brazed seam for high volume manufacturing.

This research has provided a lot of insights and improvement suggestions for the industry and coming researchers. It presents a significant step forward. The focused TIG brazing process is complicated but manageable when considering the proposed improvements. It is likely that the

research will be accepted and adopted by other manufacturing organisations and industries as well. The brazing method development for thin metal joining in the preceding ten years has shown a reliance on laser brazing. The research explores for the first time how a much less expensive focused TIG brazing system can be used to support joining of thin steel panels in high volumes.

References

[1] Audi, "Der Karosseriebau des neuen Audi A5 Coupe," in *Euro Car Body Award 2007*, Bad Nauheim, Germany, 2007.

[2] Volkswagen, "Effects on Laser Brazing of Roof Seam Using Diodelasers with Adapted Beam Characteristics," in *Automotive Circle International Conference*, Bad Nauheim, Germany, 2009.

[3] Volvo, "Laser Brazing of Ring Frame," in *Euro Car Body 2007*, Bad Nauheim, Germany, 2007.

[4] Mercedes-Benz, "Mercedes Sprinter Design," in *Fachtagung Prozesskette Karosserie*, Leipzig, Germany, 2006.

[5] M. A. Omar, The Automotive Body Manufacturing Systems and Processes, Chichester, United Kingdom: John Wiley & Sons, 2011.

[6] Experi-Metal Inc., "Full Body Build – Body in White (BIW)," [Online]. Available: http://www.experi-metal.com/products/aftermarket-body-build/. [Accessed 22 03 2016].

[7] Supplier Business Journal, "Automakers exploring use of magnesium in vehicles to lower weight," *Supplier Business,* 2013.

[8] D. Abliz, Y. Duan, Y. Zhao and D. Li, "Low-energy electron beam cured tape placement for out-of-autoclave fabrication of advanced polymer composites," Science Direct, 2014.

[9] M. Komorowska-Durka, G. Dimitrakis, D. Bogdal, A. I. Stankiewicz and G. D. Stefanidis, "A concise review on microwave-assisted polycondensation reactions and curing of polycondensation polymers with focus on the effect of process conditions," Elsevier, 2014.

[10] Schuler, "Equipment for mass manufacturing of carbon parts," 12 03 2013. [Online]. Available: www.schulergroup.com. [Accessed 5 07 2014].

[11] J. McElroy, "Manufaturing advances bring carbon fiber closer to mass production," 27 11 2012. [Online]. Available: www.autoblog.com. [Accessed 4 08 2014].

[12] D. Gildea, "Development of a Design Methodology for Systemic Identification of Optimum Joining Technologies in Automotive Body-in-White Design," University College Dublin, Ireland, Dublin, 2007.

[13] E. Incerti, A. Walker and J. Purton, "Trends in vehicle body construction and the potential implications for the motor insurance repair industries.," International Bodyshop Industry Sympossium, Montreux, 2005.

[14] Ford Quality Departement, *Ford internal training material,* Ford, 2011.

[15] K. H. Grote and E. Antonsson, Handbook of Mechnical Engineering, 10 ed., Berlin: Springer Verlag, 2009, p. 656.

[16] D. I. f. Normung, Manufacturing processes joining - Part 1: Assembling; Classification, subdivision, terms and definitions, Berlin, Germany: Beuth Verlag GmbH, 2009.

[17] D. Ghosh, L. Pancholi and A. Sathaye, "Comparative Studies of Adhesive Joints in Automotive," SAE International, 2014.

[18] J. Larsson, "Laser welding, structural adhesive bonding, for body-in-white assembly," 8 05 2007. [Online]. Available: http://www.thefabricator.com/article/laserwelding/laser-welding-structural-adhesive-bonding-for-body-in-white-assembly. [Accessed 12 03 2012].

[19] European Aluminium Association, "Applications - Car body - Body structures," European Aluminium Association, 2013.

[20] World Steel Association, "Advanced High Strength Steel Application Guidelines," World Steel Association, 120 Rue Colonel Bourg, B-1140 Brussels, Belgium, 2009.

[21] K. Mittal and A. Pizzi, Handbook of Sealant Technology, Boca Raton, Florida: CRC Press, Taylor & Francis Group, 2009.

[22] Adhesives.org, "Sealant Technologiies," [Online]. Available: http://www.adhesives.org/adhesives-sealants/. [Accessed 28 12 2014].

[23] European Aluminium Association, "The Aluminium Joining Manual," 2015. [Online]. Available: http://www.drivealuminum.org/research-resources/AluminumJoiningManual.pdf. [Accessed 03 01 2016].

[24] Butkus, "Environmental durability of adhesiveley bonded joints," Georgia Institute of Technlogy, USA, 1997.

[25] A. Pizzi and K. Mittal, Handbook of Adhesive Technlogy, Revised and Expanded, New York, USA: Marcel Dekker, 2003.

[26] F. Moroni, A. Pirondi and F. Kleiner, "Experimental analysis and comparison of the strength of simple and hybrid structural joints," Elsevier, www.elsevier.com, 2010.

[27] J. Perry, "Bodyhop of the future," Automotive Manufacturing Solutions, 1 10 2015. [Online]. Available: www.automotivemanufacturingsolutions.com/technlology/bodyshop-of-the-future. [Accessed 20 03 2016].

[28] European Aluminium Association and Matter, "Hybrid Joining: Advantages and Disadvantages," [Online]. Available: www.aluminium.matter.org.uk/content/. [Accessed 18 02 2016].

[29] P. Mallick, Materials, Design and Manufacturing for Lightweight Vehicles, Woodhead Publishing, 2010.

[30] L. Han, M. Thornton and M. Shergold, "A comparison of the mechanical behaviour of self-piercing riveted and resistance spot welded aluminium sheets for the automotive industry.," University of Warwick, Warwick, Coventry, United Kingdom, 2009.

[31] Joining Technology Research Centre, "Dogma Cluster 1," 2001. [Online]. Available: http://www.dogma.org.uk/vtt/joining/joiningtechniques.htm. [Accessed 18 2 2012].

[32] Y. Abe, T. Kato and K. Mori, "Self-piercing riveting of high tensile strength steel and aluminium alloy sheets using conventional rivet and die," *Journal of Materials Processing Technology,* p. 3914, 21 04 2009.

[33] I-Car Advanced Online, "SELF-PIERCING RIVET SELF AWARENESS," 2003. [Online]. Available: http://www.i-car.com.au/html_pages/technical_ information/advantage/advantage_online_archives/2003/112403.shtml. [Accessed 10 9 2011].

[34] N. Hoang, O. Hopperstadt, M. Langseth and I. Westermann, "Failure of aluminum self-piercing rivets: An experimental and numerical study," SINTEF Materials and Chemistry, Trondheim, Norway, 2013.

[35] Y. Chastel and L. Passemard, "Joining technlogies for future automobile multi-material modules," in *11th International Conference on Technology of Plasticity*, Nagoya, Japan, 2014.

[36] G. Meschut, V. Janzen and T. Olfermann, "Innovative and Highly Productive Joining Technlogies for Multi-Material Lightweight Car Body Structures," *Journal of Materials Engineering and Performance,* vol. 23, no. 5, pp. 1515-1523, 2014.

[37] Mercedes-Benz, "Flexible material joining technology for tomorrow's innovative lightweight design," in *Fügen im Karosseriebau 2012*, Bad Nauheim, Germany, 2012.

[38] Boellhoff Germany, "RIVTAC® High-speed joining," 2011. [Online]. Available: http://www.boellhoff.de/en/de/fasteners/special_fasteners/rivtac.php. [Accessed 14 02 2012].

[39] Daimler, "New C-Class Estate Celebrates Premiere at Mercedes-Benz Plant in Bremen," 21 05 2014. [Online]. Available: www.daimler.com. [Accessed 23 08 2014].

[40] Tillmann Gruppe, "Toxen / Clinchen," 2012. [Online]. Available: http://tillmann-gruppe.de/de/technologien/toxen_clinchen.htm. [Accessed 15 4 2012].

[41] C. Mota and N. Costa, "A comparative study between the sheet joining processes by Point TOX and Spot Welding," in *Proceedings of the annual congress of the Brazilian society for metallurgy and materials*, Belo Horizonte, Brazil, 2005.

[42] C.-J. Lee, J.-Y. Kim, S.-K. Lee and B.-M. K. Dae-Cheol Ko, "Design of mechanical clinching tools for joining of aluminium alloy sheets," Busan National University, Busan, South Korea, 2009.

[43] T. Altan and A. E. Tekkaya, Sheet Metal Forming: Processes and Application, A. International, Ed., 2012, p. 295.

[44] BTM Corporation, "Introduction to Tog-L-Loc," BTM Corporation, 6 4 2112. [Online]. Available: http://www.btmcorp.com/catalog_ main.html#toglloc. [Accessed 27 05 2012].

[45] BTM Corporation, "Sheet Metal Clinching," BTM Corporation, 15 07 2007. [Online]. Available: http://www.btmcorp.com/Catalogs/BTM_TL_innovative.pdf. [Accessed 16 01 2012].

[46] R. Messler, Integral Mechanical Attachment; Asurgence of the Oldest Method of Joining, 1 ed., Oxford: Butteworth Heinemann, 2006, p. 155.

[47] R. Messler, Principles of Welding: Processes, Physics, Chemistry and Metallurgy, Weinheim, Germany: Wiley, 2004.

[48] G. Davies, Materials for Automobile Bodies, 2 ed., Elsevier, Ed., Butterworth-Heinemann, 2012.

[49] Edag, "Joining Techniques," EDAG, Fulda, Germany, 2002.

[50] D. Kopeliovich, "Resistance Welding," [Online]. Available: http://www.substech.com/dokuwiki/doku.php?id=resistance_welding_rw. [Accessed 06 2012].

[51] H. Tang, "Latest advances in joining technologies for automotive body manufacturing," Int. J. Vehicle Design, 2010.

[52] W. Li, D. Cerjanec and G. A. Grzadzinski, "A comparative study of single AC and multiphase DC resistance spot welding," ASME Transaction Journal of Manufacturing Science and Engineering, 2005.

[53] W. Li, "Modeling and On-Line Estimation of Electrode Wear in Resistance Spot Welding," Journal of Manuf. Science and Engineering, Washington, USA, 2005.

[54] R. Bakerjian and W. Cubberly, Tool and Manufacturing Engineers Handbook, Society of Manufacturing Engineers, 1998, pp. 43-16.

[55] Kuka Systems, "Roller Seam Welding," [Online]. Available: www.kuka-systems.com/en/technologies/roller_seam-welding. [Accessed 08 09 2014].

[56] E. Reeves and M. Heathcote, Newnes Electrical Pocket Book, 23 ed., Oxford, GB: Routledge Chapman & Hall, 2003.

[57] Z. Al-Sarraf and M. Lucas, "A study of weld quality in ultrasonic spot welding of similar and dissimilar metals," Glasgow, 2012.

[58] R. Rajput, A Textbook of Manufacturing Technology: Manufacturing Processes, New Delhi, India: Laxmi Publications, 2007.

[59] L. Jeffus, Welding: Principles and Applications, vol. International ed of 7th revised ed, Delmar, 2011, p. 731.

[60] K. Kale and A. Karad, Elements of Mechanical Engineering, Pune, India: Technical Publications Pune, 2006.

[61] G. Davies, Materials for Automobile Bodies, Oxford: Butterworth Heinemann, 2003, p. 171.

[62] M. Newborne, "Projection welding balance heat and extended electrode life," 07 11 2012. [Online]. Available: http://info.miyachiamerica.com/projection-welding-balance-heat-and-extend-electrode-life. [Accessed 22 08 2014].

[63] K. Pieterman, "Welding technology for small weld flanges," in *Presentation to Daimler Chrysler Welding Tech Club*, Auburn Hills, Michigan, USA, 2005.

[64] K. Pieterman, "Method and system for real-time non-destructive testing of projection welds utilizing force sensor". Patent 8153921, 05 2012.

[65] Welding Technology Corporation, "Projection Welding," [Online]. Available: www.weldtechcorp.com/welding_concepts/projectionweld.html. [Accessed 24 08 2014].

[66] J. Sprovieri, "New Technologies for Stud Welding," 01 04 2014. [Online]. Available: www.assemblymag.com/articles/92048-new-technlogies-for-stud-welding. [Accessed 22 08 2014].

[67] G. K. Dietmar Rotheut, "Welding stud having a variable, head-side functional region". USA Patent US20140064832A1, 6 03 2014.

[68] Emhart Technologies, *Tucker Weldfast. The Innovation,* Giessen, Germany: Tucker GmbH, 2010.

[69] E. Hetrick, J. Baer, W. Zhu, L. Reatherford, A. Grima, D. Scholl, D. Wilkosz, S. Fatima and S. Ward, "Ultrasonic Metal Welding Process Robustness in Aluminium Automotive Body Construction Application," *Welding Journal,* pp. 149-158, 07 2009.

[70] A. Macwan, V. Patel, X. Jiang, C. Li, S. Bhole and D. Chen, "Ultrasonic spot welding of Al/Mg/Al tri-layered clad sheets," Elsevier, USA, 2014.

[71] D. Bakavos and P. Prangnell, "Mechanisms of joint and microstructure formation in high power ultrasonic spot welding 6111 aluminium automotive sheet," Elsevier, 2010.

[72] F. Haddadi, "Rapid intermetallic growth under high strain rate deformation during high power ultrasonic spot welding of aluminium to steel," Materials and Design, Elsevier, USA, 2014.

[73] S. David, T. DebRoy, J. DuPont, T. Koseki and H. Smartt, Trends in Welding Research: Proceedings of the 8th International, Pine Mountain, USA: ASM International, 2009.

[74] W. M. Thomas, M. G. Murch, E. D. Nicholas, P. Temple-Smith, J. C. Needham and C. J. Dawes, "Improvements relating to friction welding". Europe Patent EP 0615480 A1, 06 12 1991.

[75] B. Gibson, D. Lammlein, T. Prater, W. Longhurst, C. Cox, M. Ballun, K. Dharmaraj, G. Cook and A. Strauss, "Friction stir welding: Process, automation and control," Elsevier, 2014.

[76] I-car Advantage, "FRICTION STIR WELDING - A NEW JOINING METHOD," 14 7 2003. [Online]. Available: http://www.i-car.com.au/graphics/about_icar/current_events/advantage/2003/advantage_online_0714/web_page/fig_2.jpg. [Accessed 18 3 2012].

[77] C. D. Cox, B. T. Gibson, D. R. DeLapp, A. M. Strauss and G. E. Cook, "A method for double-sided friction stir spot welding," Elsevier, 2014.

[78] T.-Y. Pan, A. Joaquin, D. E. Wilkosz, L. Reatherford, J. M. Nicholson, Z. Feng and M. L. Santella, "Spot Friction Welding for Sheet Aluminum Joining," Dearborn, 2004.

[79] Z. Feng and e. al., "Friction Stir Spot Welding of Advanced High-Strength Steels," SAE International, 2005.

[80] J. M. Hoffman, "Car bodies first to be friction stir welded," 2003. [Online]. Available: http://images.machinedesign.com/images/archive/friction1jpg_00000038081.jpg. [Accessed 14 6 2012].

[81] European Aluminium Association, *Aluminium Automotive Manual - Joiing, Beam welding,* European Aluminium Association, 2015, p. 2.

[82] E. V. Couso and J. Gomez, "Laser Beam Welding and Automotive Engineering," Springer Verlag, Heidelberg, 2012.

[83] M. Forrest, "Recent Developments on Laser Lap Welding of Zinc-Coated Steel Sheets Without gap at the Interface," in *Automotive Laser Applications Conference & Exposition*, Ann Arbor, Michigan, USA, 2003.

[84] Q. Wua, J. Gong, G. Chen and L. Xu, "Research on laser welding of vehicle body," Elsevier, Optics & Laser Technlogy, 2008.

[85] SteelConstruction.org, "Steel Construction - Welding," [Online]. Available: http://www.steelconstruction.org/resources/technical/technical-welding.html. [Accessed 02 2013].

[86] DIN ISO, *Welding and allied processes - Part 2: Soldering and brazing processes and related terms (ISO 857-2:2005),* Berlin: Beuth Verlag GmbH, 2007, p. 23.

[87] O. Sallhammar and L. Carl, "Influence of quality and productivity of laserbrazed joints by using different optical configurations and process parameters.," Goeteborg, Sweden, 2007.

[88] M. Schwartz, Brazing, 2 ed., Ohio: Material Park, 2003, p. 52.

[89] Fronius, "VW Mosel nutzt innovativen Schweissprozess," Fronius International GmbH, Wels, Austria, 2006.

[90] Ford Werke GmbH, Internal presentation, Koeln, Germany 2011.

[91] H. Trossen, Interviewee, *Ford Product Marketing, Mgr. CD-cars.* [Interview]. 19 01 2011.

[92] J. F. Klinger, *Automotive Body Structure Assembly,* Stockholm, Sweden: KTH Royal Institute of Technlogy, 2012.

[93] H. Staufer, M. Ruehrnoessl and G. Miessbacher, "State of the Art in Technology and Practice by the Examples of the Audi A8 and VW Phaeton; Fronius," Fronius, Wels, Austria, 2004.

[94] E. A. Association, *Aluminum Automotive Manual, 6. Brazing,* European Aluminium Association, 2015, p. 12.

[95] European Aluminium Association, *EAA Aluminium Automotive Manual - Joining,* vol. 6. Brazing, European Aluminium Association, 2015, p. 12.

[96] K. Howard, S. Lawson and Y. Zhou, "Welding Aluminium Sheet Using a High-Power Diode Laser," *Welding Research,* p. 1, 05 2006.

[97] J. Dedenbach, *Roof brazing station,* Cologne, 2010.

[98] Fronius, "CMT welding, Fronius International GmbH," n.d.. [Online]. Available: www.fronius.com/cps/rde/xchg/SID-77361404-884036EE/fronius_international/hs.xsl/79_9399_ENG_HTML.htm. [Accessed 12 05 2011].

[99] Henrich Publikationen, "Was ist CMT?," 11 2004. [Online]. Available: http://www.verlag-henrich.de/index.cfm?pid=0&pk=55838.

[Accessed 14 08 2012].

[100] M. Schoerghuber, "Cold metal transfer welding process and welding installation". Austria Patent EP1901874A1, 30 11 2006.

[101] C. Pickin, S. Williams and M. Lunt, "Characterisation of the cold metal transfer (CMT) process and its application for low dilution cladding," Journal of Materials Processing Technology 211, Bedfordshire, 2010.

[102] M. Potesser, T. Schoeberl, H. Antreowitsch and J. Bruckner, "The Characterization of the Intermetallic Fe-Al Layer of Steel-Aluminium Weldings," in *EPD Congress 2006*, 2006.

[103] Konstruktion.de, "Lichtbogen- und Laserlöten von Stahlblech," [Online]. Available: http://www.konstruktion.de/allgemein/lichtbogen-und-laserloeten-von-stahlblech/. [Accessed 11 2013].

[104] G. Trommer, Loeten statt Schweissen, 1 ed., Automobile Produktion, 2008b, p. 88.

[105] Fronius, "Cold Metal Transfer," 02 2014. [Online]. Available: http://www.fronius.com/cps/rde/xbcr/SID-EA22202B-73076089/fronius_international/M_06_0001_EN_CMT_leaflet_Feb_2014_aw19_low_44211_snapshot.pdf. [Accessed 26 09 2014].

[106] Audi, D. Rudolph, "Arc brazing in visible areas - an alternative to laser brazing?," in *Joining in Car Body Engineering 2014*, Bad Nauheim, Germany, 2014.

[107] TWI Ltd, "TIG Welding," [Online]. Available: http://www.twi.co.uk/technical-knowledge/job-knowledge/tungsten-inert-gas-tig-or-gta-welding-006/. [Accessed 09 2015].

[108] Y. Tarng, H. Tsai and S. Yeh, "Modeling, optimization and classification of weld quality in tungsten inert gas welding," International Journal of Machine Tools & Manufacture, 1999.

[109] R. Finch, Welder's Handbook, New York, USA: The Berkley Publishing Group, 1997.

[110] EWM, "Welding encyclopaedia," 24 01 2012. [Online]. Available: www.ewm-group.com/en/service/downloads. [Accessed 26 09 2014].

[111] Kewell Schweisstechnik, "Lehrmaterial," 2012. [Online]. Available: www.kewell-schweisstechnik.de/informationen/. [Accessed 12 11 2014].

[112] G. J. B. David J. Eyres, Ship Construction, Oxford, GB: Elsevier Ltd., 2012.

[113] K. Weman, Welding Processes Handbook, 2nd ed., Cambridge: Woodhead Publishing Limited, 2011, p. 64.

[114] N. Ahmed, New Developments in Advanced Welding, Cambridge, England: Woodhead Publishing Limited, 2005.

[115] EWM, "ForceTig - The patented high-performance TIG joining process," 10 2012. [Online]. Available: http://www.google.de/url?sa=t&rct=j&q=&esrc=s&source=web&cd=1&cad=rja&ved=0CC8QFjAA&url=http%3A%2F%2Fwww.ewm-group.com%2Fde%2Fservice%2Fdownloads%2Fbroschueren-prospekte-und-handbuecher%2F1770-forcetig%2Fdownload.html&ei=QqjhUc_RD8SH4ATQsYHwBw&usg=AFQjCNG. [Accessed 07 2013].

[116] T. Opderbeckea and S. Guiheux, "TOPTIG: robotic TIG welding with integrated wire feeder," Taylor & Francis Group, 2009. [Online]. Available: http://www.tandfonline.com/doi/abs/10.1080/09507110802543146#.UeGbfqw9WM0. [Accessed 07 2013].

[117] F. Heinrichsmeier, Interviewee, *Project Manager Automation, Oerlikon Welding.* [Interview]. 16 09 2013.

[118] Air Liquide, "TopTig - A new robot welding process for the industry," [Online]. Available: http://www.wecs-ltd.co.uk/images/stories/machine%20pdf/top%20tig%20w000260373_1light.pdf. [Accessed 07 2013].

[119] A. Elliott, "Development of Plasma Brazing Process - Phase II," Ford Research and Advanced Engineering, USA, 2009.

[120] Inocon Technology GmbH, "Plasmatron," 2011. [Online]. Available: http://www.inocon.at/cms/front_content.php?idcat=8. [Accessed 16 03 2011].

[121] Inocon Technology GmbH, *Maintenance Handbook,* Austria: Inocon Technology GmbH, 2008.

[122] NPTEL, "Physics of Welding Arc I," [Online]. Available: http://www.nptel.ac.in/courses/112107090/module2/lecture1/lecture1.pdf. [Accessed 16 05 2015].

[123] M. Yarmuch, J. Pepin, A. Bicknell and B. Patchett, "Characterization of Fusion Behaviour during Variable Polarity AC Welding of Aluminium," in *Trends in Welding Research, Proccedings of the 9th International Conference*, Chicago, USA, 2013.

[124] R. Castro-Lopez and e. al., Welding Metallurgy of Stainless and Heat-resisting Steels, Cambridge, England: University Printing House, 1975, p. 21.

[125] J. Lancaster, The Physics of Welding. International Institute of Welding, Oxford, England: Pergamon Press, 1986, p. 136.

[126] W. Galvery, Welding Essentials; Frank Marlow, vol. 2 edition, Industrial Press, 2007, p. 210.

[127] W. Galvery, Welding Essentials, USA: Industrial Press, 2007, p. 205.

[128] International Tungsten Industry Association, "Tungsten Properties," [Online]. Available: htttP://www.itia.info/. [Accessed 9 02 2015].

[129] A. A. Sadek, "Effect of Rare Earth Metal Oxide Additions to Tungsten Electrodes," Metallurgical Trasacdtions, 1990.

[130] M. Fletcher, "Gas Tungsten Arc Welding Electrodes," 2005.

[131] American Welding Society, *Specification for Tungsten and Oxide Dispersed Tungsten Electrodes for Arc Welding and Cutting,* Miami: American Welding Society, 2009.

[132] Wolfram Industrie, *Leitfaden TIG -neu FuE mit Logo EN,* Traunstein, Germany, 2011.

[133] Furtmeyr Schweißtechnik, *Wolfram Elektroden,* München, 2011, p. 20.

[134] Diamond Ground Products, *Tungsten Guidebook,* Newbury Park, 2011.

[135] E. Lassner, Tungsten, New York: Kluwer Academic Publishers, 1999.

[136] International Organization for Standardization, *ISO 6848; Arc welding and cutting Nonconsumable tungsten electrodes,* Berlin: Beuth Verlag, 2004.

[137] J. Lehr, Nuclear Energy Encyclopedia, Hoboken, New Jersey, USA: Wiley, 2011.

[138] J. Bowers, "Selecting and preparing tungsten electrodes," 15 01 2008. [Online]. Available: www.thefabricator.com/consumables/. [Accessed 01 2012].

[139] Furtmayr Schweißtechnik GmbH, "Wolfram Elektroden," 2009. [Online]. Available: http://www.furtmayr.de/Wolframelektroden.pdf . [Accessed 08 2012].

[140] ASM International, "Elements of Metallurgy and Engineering Alloys," ASM International, 2008.

[141] CPi, Welding Complete, Minneapolis: Cool Springs Pess, 2009, p. 71.

[142] AMERICAN WELDQUIP, INC. , *Why longitudinal grinding?,* Ohio: AMERICAN WELDQUIP, INC. , 2007.

[143] Wiesehahn GmbH, *Instruction manual Tungsten Electrode Grinder EAG-3,* Oststeinbeck, Germany, 2006.

[144] Wiesehahn GmbH, "Einfluss der Wolfram Elektroden auf das Schweißergebnis," Ferd. Wiesehahn GmbH, Oststeinbek, Germany, 2008.

[145] J. Sprinkle, "Tips for Preparing and Selection Tungsten Electrodes," Welding Journal, May 2012.

[146] B. Williams, "Selecting the right tungsten," 26 2 2004. [Online]. Available: www.thefabricator.com/article/consumables/selecting-the -right-tungsten. [Accessed 006 08 2012].

[147] F. Klocke and S. Frank, "Surface deposits in laser brazing," Science and Technology of Welding and Joining, 2013.

[148] Stahl-Informations-Zentrum, "Weldable Corrosion Protection Primer," Stahl-Informations-Zentrum, Düsseldorf, Germany.

[149] H. Hackl, "Mig brazing of galvanised light-gauge sheets," Wels, Austria, 2012.

[150] World Steel Association, "Advanced High Strength Steel Application Guidelines," World Steel Association, 2009.

[151] Thyssen Krupp Steel, *Hot-dip coated steel,* Duisburg, Germany: Thyssen, 2008, p. 5.

[152] Tata Steel, "Magizinc (ZnAlMg) Coatings versus galvannealed," Tata Steel, Ijmuiden, Netherlands, 2012.

[153] Posco, "Introduction of GI-ACE," Posco, 2013.

[154] Thyssen Krupp Steel Europe, *Cold-rolled sheet. Non-coated and electrolytically coated.,* Duisburg, Germany: Thyssen Krupp Stahl AG, 2009.

[155] I-Car Advantage, "Brazing as a Substitute for GMA (MIG) Welding?," Appleton, USA, 2004.

[156] C. Chovet and S. Guiheux, "Possibilities offered by MIG and TIG brazing of galvanized ultra high strength steels for automotive applications," Rom; Italy, 2006.

[157] Scansonic, "Discover the potentials of SEAM Tracking," 20 05 2009b. [Online]. Available: www.scansonic.de/files/pdf/Discover-Seam-Tracking_Scansonic_200908.pdf. [Accessed 20 05 2011].

[158] B. Regaard, S. Kaierle and R. Poprawe, "Seam tracking for high precision laser welding," *Journal of Laser Application,* November 2009.

[159] P. Bergkvist, "Seam tracking in a complex aerospace component for laser welding," University of Trollhaettan, Uddevela, 2004.

[160] Jetline Engineering, "jst-optical-laser-seam-tracker," 2006. [Online]. Available: http://pdf.directindustry.com/pdf/jet-line-engineering/jst-optical-laser-seam-tracker/27577-54403.html. [Accessed 19 2 2011].

[161] Scansonic, "Discover the potentials of SEAM Tracking," 08 2009a. [Online]. Available: www.scansonic.de/files/pdf/Discoer-Seam-TRacking_Scansonic_200908.pdf. [Accessed 20 05 2011].

[162] Permanova, "Permanova WT03 Laser Welding Tool System for All Joining Applications," 10 11 2009. [Online]. Available: http://www.permanova.se/filearchive/1/1620/WT03%20Welding%20Tool.pdf. [Accessed 19 04 2012].

[163] Scansonic, "Electric-arc joining - Scansonic APN1 Data Sheet," n.a.. [Online]. Available: http://www.scansonic.de/en/files/pdf/Scansonic_APN1_DABv1.1_en.pdf. [Accessed 12 04 2012].

[164] Inocon GmbH, "Plasmatron \ possibilities," n/a. [Online]. Available: http://www.inocon.at/cms/front_content.php?idcat=10. [Accessed 19 03 2012].

[165] M. Botts, "Wirbelstromtechnik zur Nahtverfolgung beim Laserstrahlschweißen," Laser Zentrum Hannover e.V., 26 09 2007. [Online]. Available: http://139.174.2.142/pages/en/news227368. [Accessed 15 4 2012].

[166] Inocon, *Plasmatron components,* Austria, 2009.

[167] P. Holland, "Brazing Rig," Nottingham, GB, 2010.

[168] National Technical University KhPI, 21 Frunze Str.,Kharkov, 61002,UKRAINE, "EUROPEAN STEEL AND ALLOY GRADES," [Online]. Available: http://www.steelnumber.com/en/steel_composition_eu.php?name_id=203. [Accessed 22 03 2014].

[169] Tata Steel Automotive, *MagiZinc Auto,* Umuiden, Netherlands: Tata Steel Automotive, 2013.

[170] Posco, *Introduction of GI-ACE,* Korea: Posco, 2013.

[171] American Filler Metalls, "American Filler Metalls," [Online]. Available: http://www.amfiller.com/assets/tungsten_alloys.pdf. [Accessed 06 11 2014].

[172] Inocon Technology, *Plasmatron brazing basics,* Attnang-Puchheim, 2008.

[173] International Organization for Standardization, *Welding consumables - Solid wires and rods for fusion welding of copper and copper alloys - Classification (ISO 24373:2008),* Genf: Beuth Verlag, 2008.

[174] W. G. Stapon, "A shielding gas primer for GTAW," 27 01 2009. [Online]. Available: www.thefabricator.com/article/consumables/. [Accessed 06 02 2014].

[175] DIN Deutsches Institut für Normung e. V., *Welding consumables - Gases and gas mixtures for fusion welding and allied processes (ISO 14175:2008),* Berlin, Germany: Beuth Verlag GmbH, 2013.

[176] Inocon; S. Wohlschläger, *Private communication,* 2013.

[177] European Committee for Standardization, *Imperfections in brazed joints ISO 18279:2003,* Brussels: SAI Global, 2003.

[178] K. Wolters, Interviewee, *Ford PD Materials Team Leader.* [Interview]. 22 03 2011.

[179] D. Ponthier, Interviewee, *Ford Asia Pacific Trim Final & Chassis Specialist.* [Interview]. 12 09 2011.

[180] D. Ponthier, Interviewee, *Ford Asia Pacific Trim & Final Specialist.* [Interview]. 16 07 2013.

[181] N. Palmquist, P. Lindahl, U. Todal, E. Laurila, G. Hopkins, M. Strömblad, R. Steinert and L. Jönsson, "Method for laser brazing with twinspot". Fairlane Plaza South Suite 800 330 Town Center Drive, Dearborn, MI 48126, US) Patent EP1920864A1, 14 05 2008.

[182] S. Frank, M. Ungers and R. Rolser, "Coacial control of aluminium and steel laser brazing processes," Elsevier, 2011.

[183] A. Watson and P. Valberg, "Carbon black and soot: two different substances," US National Library of Medicine, USA, 2001.

[184] L. R. Radovic, Chemistry & Physics of Carbon, New York, USA: Marcel Dekker, 2003.

[185] J. Mosch, A. Hoffmann and M. Hopp, "Metallische Fügetechniken - eine Uebersicht," Dental Dialogue, Fuchstal, Germany, 2005.

[186] N. Parkin and C. Flood, Welding Craft Practice: Oxy-Acetylene Gas Welding and Related Studies, Oxford, England: Pergamon Press Ltd., 1979.

[187] F. Schneider, Interviewee, *Paint Specialist.* [Interview]. 12 06 2013.

[188] L. Engelbrecht, "Effects of Laser Brazing of Roof Seam Using Diodelaser with Adapted Beam Characteristics," Volkswagen , Wolfsburg, Germany, 2009.

[189] INB Vision AG, "3D surface inspections in automotive manufacturing," [Online]. Available: http://www.inb-vision.com/technologie/Evaluation_process/index.html. [Accessed 15 02 2015].

[190] J. Dedenbach, *Specification for Brazed Seams,* Koeln, Germany: Ford GmbH, 2010.

[191] J. Dedenbach, "Evaluation of test panel seam," Cologne, Germany, 2010.

[192] P. Roberts, Industial Brazing, Practice, Second Edition, vol. 2, Boca Raton, FL, USA: CRC Press, 2013, p. 13.

[193] Deutsches Institut fuer Normung, *Non-destructive examination of brazed joints, EN 12799,* Berlin Germany: Beuth Verlag GmbH, 2000.

[194] Deutsches Institut für Normung, *Destructive tests on brazed joints; EN12797,* Berlin, Germany: Beuth Verlag, 2000.

[195] European Committee for Standardization, *Metallic Materials - Tensile testing,* Brussels: CEN, 2001.

[196] M. Hirsch, J. Dedenbach, S. Lawes and A. Clare, "In situ low-cost and adaptable braze tool evaluation system with vision analysis," Sage, 2014.

[197] M. Bea, R. Brockmann and D. Havrilla, "Remote laser welding in automotive production," *Industrial Laser Solutions,* 9 1 2011.

[198] BMW Group, Der neue BMW 7er (The new BMW 7), Wiesbaden: Vieweg-Teubner, 2009.

[199] Canadian Fabricating & Welding, "Union condemns EDC for lending Volkswagen $526 million," 27 04 2015. [Online]. Available: http://www.canadianfabweld.com/wp-content/uploads/sites/43/2013/02/QualityCheckPaintShop.jpg. [Accessed 06 03 2016].

[200] G. Holdmann, Interviewee, *Key Account Manager, Henkel Germany.* [Interview]. 04 06 2012.

[201] Ford Motor Company, *Q1,* 2nd ed., Dearborn: Ford, 2003.

[202] Ford Motor Company, *Ford Vehicle Operations SPC Manual,* 2001.

[203] G. Veena, Comprehensive Basic Mathematics, Band 2, New Delhi, India: New Age Publishers, 2005.

[204] I. Tucker, Survey of Economics, South Western Educ Pub, 2010.

[205] J. Gwartney, R. Stroup, R. Sobel and D. Macpherson, Economics: Private and Public Choice, Stamford, USA: Cengage Learning.

[206] D. g. Newman and E. Wheeler, Study Guide for Engineering Economics, vol. 2, New York, USA: Oxford University Press, 2004, p. 29.

[207] M. Schwartz, Brazing: For the Engineering Technologist, London, UK: Chapman & Hall, 1995, p. 21.

[208] Ford GmbH, *Braze Speed Comparison - Laser vs. Plasmatron Brazing,* Cologne: Ford, 2013.

[209] J. K. Tatman, "Development of new weld heat input and dilution equations for gas tungsten arc welding - part 1," in *Proceedings of the ASME 2013 Pressure Vessels and Piping Conference*, Paris, France, 2013.

[210] R. S. Funderburk, "A look at heat input," *Welding Innovation,* no. XVI, No. 1, 1999.

[211] TWI Ltd, "Technical Knowledge," 14 11 2013. [Online]. Available: www.twi.co.uk/technical-knowledge/. [Accessed 14 07 2014].

[212] GalvInfo Center, "GalvInfo Center," [Online]. Available: http://galvinfo.com/ginotes/GalvInfoNote_2_8.pdf. [Accessed 16 01 2015].

[213] V. Nemchinsky, "Cathode erosion in a high-pressure high-current arc: calculations for tungsten cathode in a free-burning argon arc," IOP Publishing Ltd., Fort Lauderdale, USA, 2012.

[214] M. Tanaka, T. Ikeba, Y. Liu, S. Choi and T. Watanabe, "Investigation of Electrode Erosion Mechanism of Multi-Phase AC Arc by High-Speed Video Camera," Tokyo Institute of Technology, Tokyo, Japan, 2013.

[215] Linde, "Schutzgasschweißen und Formieren," Linde Gas, Unterschleißheim, 03 2004. [Online]. Available: http://www.mss-schweisstechnik.de/media/hpa/fach/Schutzgasschweiss_und_ Formieren_Linde.pdf. [Accessed 11 2012].

[216] U. Massari, Interviewee, *Advantages of the Castro glovebox.* [Interview]. 08 02 2013.

[217] R. Ghodssi, MEMS Materials and Processes Handbook, New York, USA: Springer, 2011.

[218] B. Kanegsberg and E. Kanesberg, Handbook for Critical Cleaning: Cleaning agents and systems, Band 2, Boca Raton, USA: Taylor & Francis Group, 2011.

[219] F. Thielmann, *Device for cleaning the gas nozzle of a welding torch,* USA: United States Patent, 1987.

[220] J. Hafner, *Device for cleaning a welding torch,* Germany: Deutsche Patentamt, 1987.

[221] G. Buerkner and W. Herber, *Methods for removing welding spatter and similar impurities of welding torches,* Germany, 2007.

[222] European Comitee for Standardization, *Paints and varnishes - Cross cut test,* Belgium, Bruessel: CEN, 2007.

[223] Toda, Kimio, Salazar, Abraham, Saito and Kozo, Automotive Painting Technology: A Monozukuri-Hitozukuri Perspective, Dordrecht: Springer Science+Business Media, 2013.

[224] J. W. Sutherland, "Automobile Assembly Painting: Energy and Environmental Impacts," [Online]. Available: http://www.me.mtu.edu/ ~jwsuther/erdm/lect36a.pdf. [Accessed 4 02 2015].

Appendix A – Publications

The following papers have been produced as a result of this work, some of which are in press at the time of writing.

1. ‘In situ low-cost and adaptable braze tool evaluation system with vision analysis’
   Matthias Hirsch, Johannes Dedenbach, Simon Lawes and Adam T. Clare
   Proceedings of the Institution of Mechanical Engineers, Part B: Journal of Engineering Manufacture, July 2, 2014

2. ‘Focused arc TIG brazing of Zinc coated steels’
   Matthias Hirsch, Johannes Dedenbach, Simon Lawes and Adam T. Clare
   Proceedings of the Institution of Mechanical Engineers, Part B: Journal of Engineering Manufacture, July 18, 2016

Appendix B – Rating of BIW Joining Methods

This appendix explain how the question was verified if Plasmatron brazing can be an upcoming high volume outer skin panel joining technique for steel vehicle bodies or if it would be better to concentrate on another joining technology.

The literature research from the current state of the art BIW joining methods (Chapter 2.3) identified and described twenty-one current and potential future BIW joining methods, which were benchmarked as contribution to this thesis to identify the joining methods with the highest potential for the future (12 years) of outer skin panel joining in high volume plants. To do this, eight benchmark factors were detected via the mind-map method as the best rating factors.
The following Table B.1 shows the outcome of the rating exercise. The rating assessment was performed based on the author's 20 years BIW experience plus details that the author has found during his literature research. Joining methods where the automotive industry already has experience were rated slightly higher than joining methods which would be relatively new for a bodyshop deployment.

Table B.1: Identification of high potential outer skin panel joining methods.

A

No.		BiW Joining Methods	Double sided access required	Vehicle weight effective	Cycle time influence	Sealer operation required	Joint aesthetic	Joint strength	Feasability for outer skin panel joining	Cost effective	Score summary	Top 3 Ranking
		Weighting factor: 1 = very poor, 10 = very good										
1	Adhes.	1K Structural adhesive bonding	8	3	2	10	8	2	2	5	40	
2		2K Structural adhesive bonding	8	3	2	10	8	1	1	5	38	
3	Mechanical	Self-piercing rivets	1	3	5	1	1	5	1	3	20	
4		RIVTAC® high-speed joining	7	3	5	1	1	5	1	3	26	
5		TOX® clinching	1	3	5	1	1	5	1	4	21	
6		Tog-L-Loc® clinching	1	3	5	1	1	5	1	4	21	
7		Hemming	2	3	5	4	6	6	4	4	34	
8	Welding	Resistance spot welding	4	3	5	3	6	8	7	8	44	
9		Resistance Projection welding	7	3	5	2	1	5	0	6	29	
10		Resistance Seam welding	7	4	6	3	5	7	6	4	42	
11		Ultrasonic spot welding	1	3	5	1	3	5	3	8	29	
12		Friction stir spot welding	1	3	5	1	3	5	3	2	23	
13		Laser beam welding	8	5	9	3	7	8	8	3	51	3
14		Gas metal arc welding	8	5	5	3	1	6	1	7	36	
15		Hybrid structural joining	5	3	3	9	5	7	4	3	39	
16	Brazing	Laser brazing	8	5	8	9	8	8	9	3	58	2
17		CMT brazing	8	5	6	7	3	7	3	7	46	
18		CMT braze+ (improved nozzle)	8	5	6	8	5	7	5	7	51	3
19		Force TIG brazing	8	5	6	7	4	7	2	7	46	
20		TopTig brazing	8	5	6	7	4	7	2	7	46	
21		Plasmatron brazing	8	5	6	9	8	8	8	8	60	1

=> Knock-out criteria. This process is not feasible for joining of outer skin panels.

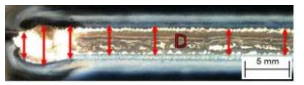
The outcome of this supporting BIW rating exercise is that two brazing methods are in the first two places: Laser brazing and Plasmatron brazing. Laser brazing is superior in terms of brazing speed but worse regarding the capital investment cost. Plasmatron brazing is good in investments but drops in process feasibility due to the robustness of the electrode lifetime. Both processes require single-sided access to the joint area only. On top, no additional sealer process is needed. Brazing delivers the best joint aesthetic due to a continuous smooth waterproof seam.

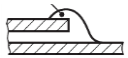
CMT braze+ has the third highest potential if this method could be improved further. The potential of this joining method is very high because this system is low-priced and does not require a tungsten

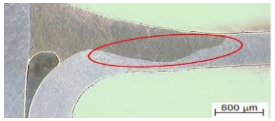
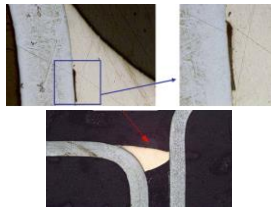
electrode, which means no electrode lifetime issues can occur. Unfortunately, the seam quality is still not good enough due to the high heat input in the brazing process, which often results in panel distortions and in an unsteady seam surface.

The 1K adhesive joining method was also rated highly. Some car manufacturers like BMW and Aston Martin use a roof to body adhesive process for their low volume models already. Unfortunately, there is no literature about a glued roof in a high volume plant (low cycle time) available. Therefore, it would be important to understand if an adhesive roof joining method would be a feasible method in a high volume plant. The following experiment should answer this question.

Appendix C – Braze Properties Report

Possible External and Internal Plasmatron Brazing Imperfections on Outer Skin Automotive Panels						
No.	**Defect**	**Defect Cause**	**Defect Severity**	**Corrective Action**	**Rework Action**	**Example Defect Image / Sketch**
External Brazing Imperfections (visual surface)						
1	**Incorrect Brazed Seam Width**	Wrong braze speed, filler wire speed or current setting.	If the seam width is to small it might be that the part has to be scrapped. The assessment result depends on the product development requirements. If the seam width is to wide it might be that this can be corrected with manual grinding.	Check, robot-/table and filler wire speed setting. Check current setting.	If the seam width is to small it might be that the part has to be scrapped. The assessment result depends on the product development requirements. If the seam width is to wide it might be that this can be corrected with manual grinding.	
2	**Incorrect Linearity** Braze does not follow the planned seam contour.	The cause is mostly an unstable robot arm or an unstable seam tracker. As well it could be a magnetic field disturbances due magnetized panel clamping or panels which was magnetized because of previous weld gun operations. For example could a bodyside be magnetized from previous spot weld operations. Check if the tactile finger is loose or worn off.	An uneven joint is not acceptable and cannot be reworked.	Use non-magnetic clamping units. Use path program options from your robot supplier. Use a mechanical seam tracker because these systems have no tracking delays.	Manual or robot re-brazing on short length only.	
3	**Surface Breaking Pores**	Braze gases escaping during solidification. To large gap between the panels. Dirty panels or filling wire. Incorrect shielding gas setting. To much water in the atmosphere or shielding gas. Often porosity is caused by getting the puddle too hot.	Unacceptable as the finished joint will not be aesthetically pleasing. Holes create potential weak spots in the joint. Potential risk for water intrusion into the vehicle.	Check the shielding gas setting. Check the gap width between the panels. Check the panel cleanliness. Check braze speed and braze current.	With PVC sealer or manual brazing for a small amount of holes but not at the start or end of the seam.	
4	**Surface roughness and/or texture.**	Lack of steady state condition being achieved. Unsteady braze speed or to fast braze speed. Robot related failures (programing, installation, etc.). Seam tracker failures. Electrode wear out.	Minor aesthetic defect of slight unevenness. Strength and functionality are normally not affected by this type of defect. However, these defects may act as stress concentrations.	Check, robot/table speed setting. Check filler wire speed setting and electrode quality.	Smooth grinding.	
5	**Edge notches** Notches at the passage to the parent metal, the rest of the seam surface is smooth.	Porous zinc surface. Elo-coated steel panels show less edge notches than hot dipped coated steel panels. Edge notches over longer distance can as well occur thru disturbance from magnetic fields, to high brazing speed or electrode wear out.	Medium aesthetic defect. Rework required.	Check if a different zinc coating (elo-zinc) improve the situation. Check, robot-/table and filler wire speed setting. Check current setting.	Smooth grinding.	
6	**Surface spatter** Drops of filler metal near to the brazed seam.	Filler metal being expelled during the brazing process due to excessive heating or gas pressures during the brazing process. As well material defects can lead in spatter.	Minor aesthetic defect. Rework required.		Smooth grinding.	
7	**Discontinuous Braze** Small lack of filler areas.	The gap between the panels was not parallel, to small or to large. Contaminated electrode or nozzle. Unsteady wire feed or braze speed. Seam tracker failure. Dust or corrosion particles on the panel surface. Dirty filler wire or old wire with corrosion spots. Defects on the wire feeder system. Defect on the robot or on the seam tracker. To high brazing speed.	Major aesthetic defect, which might influence the part/body rigidity. Rework required or even part/body scrapping.	Clean the panels before brazing. Check the gap size between the panels. Check the wire feeder, seam tracker and robot systems. Check the filler wire. Check the electrode and the nozzle. Reduce the brazing speed.	Repair with PVC sealer or manual brazing for small amount of seam interruptions only but not at the sensitive start or end of the seam.	
8	**Longer lack of filler adhesion** Joint is too thin and/or show discontinuous seam. Insufficient boundary diffusion layer between parent and filler materials.	Insufficient heating during brazing process causing lack of melting of filler material. Insufficient filler wire or the gap between the two panels is to large. The gaps should be maximum 0.3 mm. Better would be 0.2 mm. Magnetic fields can as well push the arc in one direction. Fluting wire due wire feeder issues. Electrode wear out. Misaligned electrode or guiding finger. Misalignment from the parts or braze path.	Major aesthetic defect, which effects the part/body rigidity. Rework required or even part/body scrapping. Additionally the seam might not provide a watertight connection.	Check if the wire flow smooth. If not check the wire feeder system. Check if the gap between the panels is correct. Check if the parts or the braze path have a misalignment.	Manual brazing or robot re-brazing, but only seam start or and is not effected.	

Possible External and Internal Plasmatron Brazing Imperfections on Outer Skin Automotive Panels						
No.	**Defect**	**Defect Cause**	**Defect Severity**	**Corrective Action**	**Rework Action**	**Example Defect Image / Sketch**
9	**To much filler** Filler metal has spilled over onto parent material solidifying as a bead or a thick layer.	Wrong wire speed or robot speed setting. Wire speed and robot speed are not matching.	Medium aesthetic defect, which requires rework.	Check the wire speed setting. Check if the wire flow smooth. If not check the wire feeder system. Check if the gap between the panels is correct. Check if the parts or the braze path have a misalignment.	Smooth grinding.	
10	**Melting of base material**	Excessive localised heating during the brazing process. To low brazing speed. To high current. The arc hits the panel surface. Misaligned electrode or guiding finger. Misalignment from the parts or braze path.	Joint hardening might effecting the part/body rigidity or create holes and/or distortion within the part/body. No re-work possible.	Increase brazing speed. Reduce current. Check if the arc hit the wire only. Check if the parts or the braze path have a misalignment.	Rework is not possible. Part/body has to be scrapped.	
11	**Imperfect seam start & end**	During brazing, a heat wave precedes the actual brazing process and pre warms the materials. In the beginning of a seam, this pre-warming has not yet occurred and so the chance of a brazing error increases. Towards the end of a braze, the heat caused by the braze has no material in front of it to dissipate into, and overheating of the joining materials can occur. This effect leads to localized melting of the materials being joined at the end of the seam. Not synchronized robot track program and brazing program. Current slope function is not correct; slope-up & slope-down. Pre- and/or post gas setting is not correct.	The seam quality in the beginning and end sections of the seam play an important role in creating the necessary torsional strength and rigidity of the entire vehicle. These type of defect need to be repaired or the part/body has to be scrapped.	Check if the wire flow smooth. If not check the wire feeder system. Check if the gap between the panels is correct. Check if the parts or the braze path setting have a misalignment. Check the brazing speed settings.	Part/body has to be scrapped. Manual or robot rework only on small defects possible.	
12	**Black soot**	Black soot caused by hydrocarbons released during the brazing process. White residue caused by release off zinc from zinc coated steel during the brazing process.	Might effect paint finish quality if not removed.	Incorrect gas setting. Dirty nozzle. To oily panel surface.	Cleaning with wire brush required. Paint ability of uncleaned panels have to tested before production release.	
13	**Sagging**	Wrong filler wire speed, braze speed or braze current setting. The gap between the panels might be to wide. The gap should be maximum 0.3 mm. Better would be 0.2 mm. Fluting wire due wire feeder issues. Electrode wear out. Misaligned electrode or guiding finger.	Unpleasant seam surface. Risk of base metal melting. Repair required.	Correction of wire speed, braze speed and/or braze current required. Check if the gap between the panels is correct.	Defect can be repaired by manual brazing or robot re-brazing.	
14	**Burn through**	Wrong braze speed or braze current setting. Wire feeder, seam tracker or robot failure.	This defect would result in both unacceptable aesthetic and mechanical strength. The part/body has to be scrapped.	Check wire feeder, seam tracker and robot.	No rework possible. Part/vehicle has to be scrapped.	

Possible External and Internal Plasmatron Brazing Imperfections on Outer Skin Automotive Panels						
No.	**Defect**	**Defect Cause**	**Defect Severity**	**Corrective Action**	**Rework Action**	**Example Defect Image / Sketch**
Internal Brazing Imperfections						
15	**Internal pores** Inside seam pores or bubbles.	Braze gases escaping during solidification. Unclean panels. Gas pockets caused by the wrong temperature or a dirty, contaminated braze. To much water in the atmosphere or shielding gas. Often porosity is caused by getting the puddle too hot.	This type of defect bears some danger for the construction. Bubbles located near the surface of the brazed seam can burst during heating inside the paint drying oven. Uncontrolled accumulation of internal bubbles in a brazed seam can also decrease the structural integrity of the seam.	Check the shielding gas setting. Check the gap width between the panels. Check the panel cleanliness. Check braze speed and braze current.	No rework possible. It might be that the part/body has to be scrapped. The assessment result depends on the product development requirements and the defect frequency.	
16	**Internal crack** Crack in the filler material, in the heat affected zone or in the parent material.	Cracks normally occur during the solidification process due inhomogeneous heat distribution in the joint. Makrocracking can be visible by the naked eyes while microcracking is only visible under microscope. Often cracks are only visible at the cut-out sections. When cracks are not visible on the seam surface it does not provide assurance that the braze is crack free. Cracks can happen anywhere along the joint, either in the filler metal zone, the heat affected zone or on both regions.	This defect can create some danger for the joint strength.	Check braze speed, braze current and gas setting. Check the zinc coat and filler wire quality.	No rework possible. It might be that the part/body has to be scrapped. The assessment result depends on the product development requirements and the defect frequency.	
17	**Melting of base material and/or alloying with the filler metal** Sometimes visible at the braze surface in the form of a blue coloured seam. Mostly, this imperfections can be detected after seam cutting only.	To much heat due to much electric power, to slow brazing speed, misalignment of filler wire or electrode tip.	Excessive melting of the base material and alloying with the filler metal can cause a change in microstructure and a loss of joint strength. Very danger because can often only be detected on cross section cuts. No rework possible.	Check braze speed, braze current and gas setting. Check electrode offset and panel alignment. Check seam tracker setting.	No rework possible. It might be that the part/body has to be scrapped. The assessment result depends on the product development requirements and the defect frequency.	
18	**Internal filling imperfections / insufficient adhesion** The filler metal has failed to flow through the required length of the joint. The seam lies outside of the intended area. Unsymmetrically seam adhesion of filler material, the so called 'wrong friends' because this failure is not detectable without cutting the seam.	Base material surfaces contaminated by oil and dirt can lead to inclusions in the brazed seam. The adhesion of filler material to base materials only occurs during specific conditions. The base material needs to be brought up to an adequate temperature to permit the capillary action between the filler material and the base material to take place. When using CuSi3 the required temperature is 950 °C. To low brazing temperature can occur to wrong gas setting, filler wire speed, braze speed or braze current setting. The gap between the panels might be to wide. The gap should be maximum 0.3 mm. Better would be 0.2 mm. Fluting wire due wire feeder issues. Electrode wear out. Misaligned electrode or guiding finger.	This defect type is very danger because it has an effect on the durability of the seam which can be determined in a very limited manner. The optical seam quality might not be effected by inconsistent centring of the braze along the length of the seam. As a result of this, this kind of failure is difficult to detect without cutting the brazed panels. Therefore this failure type is as well valid for internal defect classification.	Clean the panels before brazing. Check the gap between the panels. The panels should be free from scratches or other contaminations. Check braze speed, braze current and gas setting. Check electrode offset and panel alignment. Check seam tracker setting.	No rework possible. It might be that the part/body has to be scrapped. The assessment result depends on the product development requirements and the defect frequency.	
19	**Inclusions**	Base material surfaces contaminated by dirt can lead to inclusions in the brazed seam. These particles can lead to a decrease in joint strength. The surfaces of the base materials should also be kept clean to avoid contamination by dirt particles.	Inclusions can reduce the strength of a braze.	Clean the panels before brazing.	No rework possible. It might be that the part/body has to be scrapped. The assessment result depends on the product development requirements and the defect frequency.	

Appendix D – Adhesive Experiment

Tensile Strength Measurement

This appendix shows the tensile test results from the roof joining adhesive experiment. Two specimens could not be measured because they broke during the roof cutting phase for the specimen extraction. The specimens showed maximum tensile forces between 380 – 740 Newton.

Segment cut out position in mm from roof front	1st Vehicle		2nd Vehicle	
	Left Seam Tensile Force [N]	Right Seam Tensile Force [N]	Left Seam Tensile Force [N]	Right Seam Tensile Force [N]
20	380.4	428.4	555.7	476.4
200	733.2	597.1	721.6	497.6
400	434.5	477.4	452.3	specimen broke during the roof cutting phase
600	689.3	611.9	579.2	740.1
800	513.9	527.5	506.4	543.8
1000	463.9	475.9	634.7	698.1
1200	512.2	535.8	479.3	737.4
1400	486.3	521.2	547.9	704.1
1520	455.2	specimen broke during the roof cutting phase	466.7	567.4

Appendix E – Laser- vs. Plasmatron Brazing Tensile Strength Measurement

This appendix shows the input parameters and measurement from the Laser and Plasmatron brazed vehicle roof joint tensile strength experiment.

Plasmatron and laser brazing input parameters from the tensile strength experiments.

Parameters	Plasmatron Cell	Laser Cell
Gas Flow Rate (l/min)	8	n/a
Argon type	gas purity 4.6 (99,996 vol. %)	n/a
Ignition (A)	48	n/a
Main Current (A)	118	170
Laser Power (watts)		3,200
Wire Feed Speed (m/min)	1.3	4.4
Robot Speed (m/min)	1	3.9
Torch Angle in Y-direction (degrees)	20	18
Torch Angle in X-direction (degrees)	0	5
Cathode to Wire Gap out of joint (mm)		
Electrode to Wire Gap into joint (mm)	0.6	n/a
Electrode to Wire Offset (mm)	0	n/a
Wire Outlet to Electrode Distance(mm)	12	n/a
Wire Type	CuSi3, ø 1,6mm	CuSi3, ø 1,6mm
Nozzle Type	long-hole	n/a

Tensile strength – Laser vs. Plasmatron brazing

	Tensile Strength (kN)											
	Laser Brazing						Plasmatron Brazing					
Specimen No.	Vehicle #1		Vehicle #2		Vehicle #3		Vehicle #1		Vehicle #2		Vehicle #3	
	RHS	LHS	RHS	LHS	RHS	LHS	RHS	LHS	RHS	LHS	RHS	LHS
1	5.98	7.05	6.42	7.01	6.67	6.31	6.16	6.44	6.49	6.52	6.48	6.06
2	6.54	6.78	5.55	6.88	6.23	6.49	6.09	6.12	6.57	6.16	6.33	6.05
3	6.72	7.05	6.22	7.02	5.91	6.6	6.30	6.40	7.10	5.53	6.60	6.10
4	6.67	6.43	6.56	7.06	6.76	6.42	6.11	6.30	7.10	5.84	6.45	6.10
Max	6.72	7.05	6.56	7.06	6.76	6.60	6.30	6.44	7.10	6.52	6.60	6.10
Average	6.48	6.83	6.19	6.99	6.39	6.46	6.17	6.32	6.82	6.01	6.47	6.08
Min	5.98	6.43	5.55	6.88	5.91	6.31	6.09	6.12	6.49	5.53	6.33	6.05

Appendix F - Cost Comparison Laser vs. Plasmatron

Spare Part Cost (2013)					
No.	**Item**	**Qty.**	**Unit Cost** (US $)	**Plasmatron Brazing** (US $)	**Laser Brazing** (US $)
1	Electrode center ring	4	478	1,912	
2	Electrodes (9 regrindes)	500	92	46,000	
3	Stream nozzle	4	259	1,036	
4	Stream nozzle extension	4	188	752	
5	Oval nozzle	10	245	2,450	
6	Guiding skid	10	442	4,420	
7	Cross jet pipe	9	348		3,132
8	Guiding finger	20	28		560
9	Finger holder	81	302		24,462
10	Interface adapter	1	1033		1,033
11	Connector cable	3	226		678
12	Clamping device	35	85		2,968
	Total Spare Parts Cost for 100k Liftgates			56,570	32,833
	Spare part cost per liftgate [USD]			**0.57**	**0.33**

Variable Energy Cost (2013) - Consumptions per Brazed Liftgate					
No.	**Item**	**Unit**	**Unit Cost** (US $)	**Plasmatron Brazing**	**Laser Brazing**
1	Electricity				
2	Electricity Price	US $ / kWh	0.28		
3	Electricity Consumption Power Source	kWh		10	15
	Cycle time per Liftgate	min		1.56	1.01
	Electricity Consumption per Liftgate	kW		0.259	0.252
	Electricity Cost per Liftgate	[USD/unit]		0.073	0.070
5	Water				
6	Water price	US $ / litre	0.0003		
7	Water Consumption	l/min			20
8	Water Cost per Liftgate	[USD/unit]			0.006
9	Gas				
10	Gas Price	US $ / litre	0.02		
11	Gas Consumption	[l/min]		7	
12	Gas Price per Liftgate	[USD/unit]		0.22	
13	Filler Wire				
14	Filler Wire Price	US $ / meter	0.02		
15	Filler Wire Consumption	meter		1.1	1.1
16	Filler Wire Cost per Liftgate	[USD/unit]		0.02	0.02
Total Variable Energy Cost per Liftgate [USD]				**0.31**	**0.10**

Head Count Cost per Brazed Liftgate (2013)					
No.	**Item**	**Unit**	**Unit Cost** (US $)	**Plasmatron Brazing**	**Laser Brazing**
	Maintenance Personnel Wages				
1	Thailand	[US$ / hour]	18		
	China	[US$ / hour]	7.5		
	Germany	[US$ / hour]	56		
	Worktime per day	hrs		16	16
	Maintenance % from work time	%		13%	6%
	Maintenance hrs per day	hrs		2.1	1.0
	Workdays per year	hrs		250	250
	Maintenance hrs per year	hrs		520.0	240
	Maintenance personnal cost for 100k liftgates				
	Thailand	USD		9,510	4,389
	China	USD		3,884	1,793
	Germany	USD		29,030	13,398
	Maintenance personnal cost per liftgate				
	Thailand	USD		0.10	0.04
	China	USD			
	Germany	USD		0.29	0.13
	Operator Wages				
	Germany	[US$ / hour]	49		
	Braze time per liftgate	sec.		93.40	60.40
	Operator Wage per liftgate				
	Germany	USD		1.27	0.82
Total Head Count Cost per Liftgate - Germany [USD]				**1.56**	**0.96**

Total Variable Cost per Liftgate - Germany					
1	Spare Parts			0.57	0.33
2	Energy			0.31	0.10
3	Head Count			1.56	0.96
Total Varialbe Cost per Liftgate [USD]				**2.44**	**1.38**

Appendix G – Cause and Effect Diagram

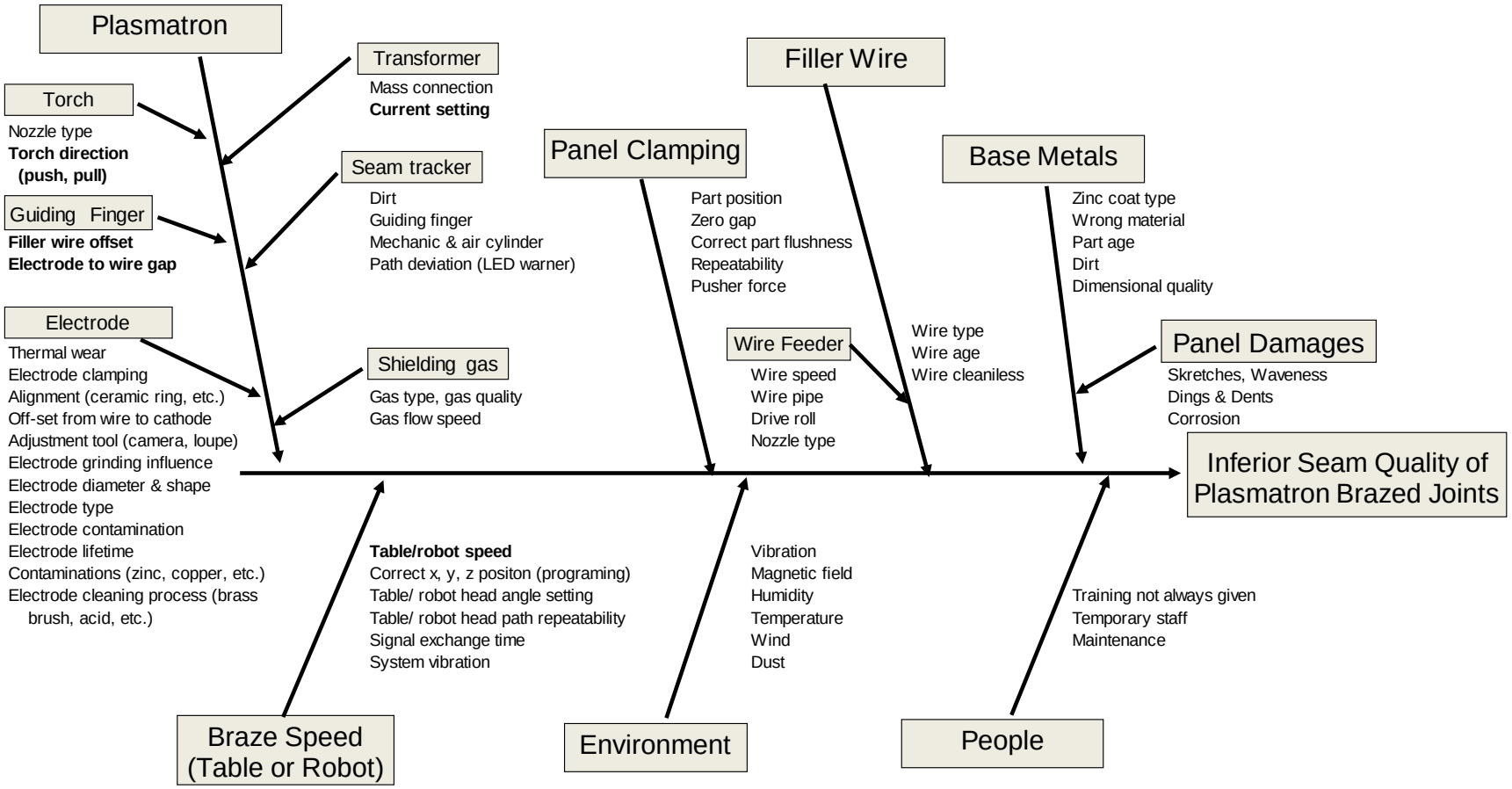


Figure Appendix E-1: Cause and effect diagram to identify all relevant factors, which can cause to inferior seam quality of Plasmatron brazed joints.

Appendix H – Experiment Decision Matrix

Experiment Decision Matrix of Proposed Plasmatron Related Experiments

Following experiements relates to the electrode service life enhancement as well as brazed seam quality control.

No.	Criteria	Experiem. Cost high = 1 low = 5	Experim. Relevance low =1 high-5	Experim. Time high = 1 low = 5	Combin-ability low = 1 high = 5	Liklihood of success low = 1 high = 5	Needed Resources a lot = 1 less = 5	Relev. for Plas. & Laser low = 1 high = 5	Weighting Summary	Experiment Status
	Criteria Relevance (1 = low, 5 = high important)	5	5	5	4	4	4	2		
1	Electrode lifetime; determine electrode service life criteria.									done
	Factor (1-5)	5	5	5	3	5	5	1		
	Score	25	25	25	12	20	20	2	**129**	
2	Electrode lifetime; Identify root causes.									done (Cause and Effect Diagram)
	Factor	5	5	5	3	5	5	1		
	Score	25	25	25	12	20	20	2	**129**	
3	Electrode lifetime; Visual assessment of the electrode by camera system.									done
	Factor	3	5	2	5	4	2	1		
	Score	15	25	10	20	16	8	2	**96**	
5	Electrode lifetime; Identify precise nature and composition of deposited material on the electrodes.									done
	Factor	4	4	3	4	4	3	1		
	Score	20	20	15	16	16	12	2	**101**	
6	Electrode lifetime; Simulate the influence of the ignition process (step brazes)									done
	Factor	4	5	3	3	4	3	1		
	Score	20	25	15	12	16	12	2	**102**	
7	Electrode size and tip shape influence. Influence of 4.0 mm vs. 6.4 mm diameter.									open
	Factor	4	3	3	3	3	3	1		
	Score	20	15	15	12	12	12	2	**88**	
8	Electrode lifetime; influence of the electrode tip surface roughness.									open
	Factor	3	2	1	2	2	2	1		
	Score	15	10	5	8	8	8	2	**56**	
9	Electrode lifetime; Electrode material influence. Test different electrode types.									done
	Factor	3	3	2	3	2	2	1		
	Score	15	15	10	12	8	8	2	**70**	
10	Influence of filler wire type, age and cleaniless.									open
	Factor	3	3	2	3	2	2	1		
	Score	15	15	10	12	8	8	2	**70**	
11	Influence of the Brazing current to the electrode lifetime, braze quality and Plasmatron set-up learnings.									done
	Factor	4	5	4	3	4	3	1		
	Score	20	25	20	12	16	12	2	**107**	
12	Influence of brazing speed to quality, etc.									done
	Factor	3	5	2	3	3	3	1		
	Score	15	25	10	12	12	12	2	**88**	
13	Torch position 'pushing - pulling' influence experiments. Influence to braze quality, electrode lifetime, brazing cell and set-up learnings.									done
	Factor	3	3	3	3	3	3	3		
	Score	15	15	15	12	12	12	6	**87**	
14	Torch position 'left - right side' influence experiments. Influence to braze quality, electrode lifetime, brazing cell and set-up learnings.									open
	Factor	3	3	3	3	1	3	2		
	Score	15	15	15	12	4	12	4	**77**	
15	Distance between filler wire and electrode tip. Influence to the panel quality, Plasmatron set-up and, electr. lifetime.									done
	Factor	3	5	3	3	5	3	1		
	Score	15	25	15	12	20	12	2	**101**	
16	Wire offset to the electrode tip. Influence to the panel quality, Plasm. set-up and, electr. lifetime.									done
	Factor	3	5	3	3	5	3	1		
	Score	15	25	15	12	20	12	2	**101**	

Experiment Decision Matrix of Proposed Plasmatron Related Experiments

Following experiements relates to the electrode service life enhancement as well as brazed seam quality control.

No.	Criteria	Experiem. Cost high = 1 low = 5	Experim. Relevance low =1 high-5	Experim. Time high = 1 low = 5	Combin-ability low = 1 high = 5	Liklihood of success low = 1 high = 5	Needed Resources a lot = 1 less = 5	Relev. for Plas. & Laser low = 1 high = 5	Weighting Summary	Experiment Status
	Criteria Relevance (1 = low, 5 = high important)	5	5	5	4	4	4	2		
17	Identify shielding gas related influence (pressure, gas type) to electrode lifetime, braze quality and Plasmatron cell set-up.									open
	Factor	2	3	2	2	2	2	2		
	Score	10	15	10	8	8	8	4	**63**	
18	Identify the shielding gas influence with help of an argon box.									done
	Factor	2	3	2	2	3	2	2		
	Score	10	15	10	8	12	8	4	**67**	
19	Develop and test different nozzle shields to float the braze seam with argon.									open
	Factor	2	3	2	2	3	3	2		
	Score	10	15	10	8	12	12	4	**71**	
20	Electrode lifetime; brazing wire material influence to the electrode lifetime.									open
	Factor	3	2	3	2	2	3	3		
	Score	15	10	15	8	8	12	6	**74**	
21	Electrode lifetime; zinc coating differences (magic zinc, galvanized, galvannealed, elo-zinc). Zinc evaporation differences due different zinc coatings.									open
	Factor	3	4	3	3	4	3	4		
	Score	15	20	15	12	16	12	8	**98**	
22	Seam Quality; corrosion test on brazed seam on different zinc coated steel panels.									done
		3	2	2	2	2	2	4		
	Score	15	10	10	8	8	8	8	**67**	
23	Black soat minimisations; panel cleaning before brazing.									done
		4	5	4	3	5	4	4		
	Score	20	25	20	12	20	16	8	**121**	
24	Black soat minimisations; usage of different zinc coating types.									open
		2	3	3	3	3	3	4		
	Score	10	15	15	12	12	12	8	**84**	
25	Black soot adhesion experiment on different zinc coated steel panels.									done
	Factor	3	5	3	5	4	3	4		
	Score	15	25	15	20	16	12	8	**111**	
26	Black soot; adhesion experiment from the different automotive coats to black soot.									done
	Factor	3	5	3	5	4	3	4		
	Score	15	25	15	20	16	12	8	**111**	
27	Electrode lifetime; Electrode cleaning in utrasonic bath.									done
	Factor	5	5	5	5	3	5	1		
	Score	25	25	25	20	12	20	2	**129**	
28	Electrode lifetime; electrode cleaning with acid.									done
	Factor	4	4	4	5	3	4	1		
	Score	20	20	20	20	12	16	2	**110**	
29	Electrode lifetime; electrode cleaning with dry ice grains.									open
	Factor	2	3	2	2	2	3	1		
	Score	10	15	10	8	8	12	2	**65**	
30	Electrode lifetime; electrode protect. with releasing agent (ceramic spray, etc.).									open
	Factor	4	4	2	3	1	3	1		
	Score	20	20	10	12	4	12	2	**80**	
31	Electrode lifetime; mechanical electrode cleaning device.									done
	Factor	3	5	3	4	4	3	1		
	Score	15	25	15	16	16	12	2	**101**	
32	Laser vs. Plasmatron; cost & quality.									done
	Factor	4	5	3	3	5	4	5		
	Score	20	25	15	12	20	16	10	**118**	
33	Brazing vs. Adhesive; quality.									done
	Factor	3	5	3	1	5	3	4		
	Score	15	25	15	4	20	12	8	**99**	
34	Joining of dissimilar material - Al alloy to zinced steel.									open
	Factor	2	3	2	1	1	2	2		
	Score	10	15	10	4	4	8	4	**55**	

Appendix I - Torch Tilting Experiment

This appendix shows the remaining input parameters from the torch tilting experiment.

Current Input	120 A
Brazing speed	1.2 m/min
Wire feeding speed	1.2 m/min
Brazing length	240 mm
Gas flow	8 l/min
Gas type	Argon 4.6
Electrode type	WL20, Ø 4.0 mm
Base material	Steel grade DC06, galvanized
Base metal thickness	0.8 mm
Filler material	$CuSi_3$, Ø 1.6 mm
Sparking duration	8 sec
Base panel cleanliness	Cleaned with alcohol before brazing

Appendix J - Surface Cleanliness Experiment

This appendix shows the remaining input parameters from the Surface Cleanliness Experiment.

Current Input	125 A
Brazing speed	1.2 m/min
Wire feeding speed	1.2 m/min
Brazing length	220 mm
Gas feed	8 l/min
Gas type	Argon 4.6
Electrode type	WL20, Ø 4.0 mm
Base material	Steel grade DC06, Galvannealed
Base metal thickness	0,8 mm
Filler material	$CuSi_3$, Ø 1.6 mm
Sparking duration	8 sec
Base panel cleanliness	Cleaned with alcohol before brazing

Appendix K - Electrode Offset Experiment

This appendix shows the remaining input parameters from the electrode tip offset experiment.

Current Input	120 A
Brazing speed	1.2 m/min
Wire feeding speed	1.2 m/min
Brazing length	240 mm
Gas feed	8 l/min
Gas type	Argon 4.6
Electrode type	WL20, Ø 4.0 mm
Base material	Steel grade DC06, Galvannealed
Base metal thickness	0,8 mm
Filler material	$CuSi_3$, Ø 1.6 mm
Sparking duration	8 sec
Base panel cleanliness	Cleaned with alcohol before brazing